JOURNAL OF

International Scientific Publications:

MATERIALS, METHODS & TECHNOLOGIES

Vol. 1

Published at:

http://www.science-journals.eu

Publishing by Info Invest Ltd

www.sciencebg.net

ISSN 1313-2539, 2007, Bulgaria

ISSN 1313-2539

ISSN 1313-2539

INVESTIGATION OF PROPERTIES OF HOLLOW AND LOW STRENGTH CONCRETE MASONRY UNITS WITH PUMICE AGGREGATE

Osman ÜNAL, Tayfun UYGUNOĞLU

Construction Department, Technical Education Faculty, Afyon Kocatepe University,

03200 Afyonkarahisar / Turkey

Abstract

Lightweight concretes can be produced by using different type of lightweight aggregates. The results of investigations on the suitability of using pumice aggregates from Isparta region in Turkey as fine and coarse materials in lightweight concrete masonry production are reported. In this study, pumice aggregate lightweight concrete (PLWC) samples were produced with different sizes of 0-4 mm as fine pumice aggregate (FPA), of 4/8 mm as middle pumice aggregate (MPA) and of 8/16 mm as coarse pumice aggregate (CPA). The pumice aggregates collected from the quarry were first crushed and screened in this study. In order to analyze the role of pumice aggregate ratio on the properties of lightweight concrete masonry for dry mix conditions, a series of preliminary trial batches were first carried out. Trial batches were cast into 100x100x100 mm cube samples with the cement content of 220 kg/m^3 in low water/cement ratio as 0,15. The specimens were analyzed to examine the compressive strength, water absorption and specific porosity of all series. According to the results of preliminary trial batches, it was decided to produce a full scale pumice aggregate masonry block (PAMB) units for the same mixture proportions of the best series in trials. PAMB units were analyzed to investigate their unit weight and the compressive strength for air dry condition at 28 days. The coefficient of thermal conductivity for the blocks was tested based on oven dry. According to experimental results, while dry unit weight has increased, compressive strength of 28 days samples has increased, too for the PLWC dry mix composition. Due to the low strength and thermal conductivity, pumice aggregate lightweight masonry units can be used in constructions for non-load bearing infill walls providing the high isolations.

Key words: *Pumice, lightweight aggregate, hollow blocks, property.*

1. INTRODUCTION

Compressed masonry blocks have traditionally been widely used as a construction material for both structural and non-structural walls. Masonry walls are primarily composed of masonry units (typically concrete blocks or clay bricks) and mortar. In addition to the various options available for masonry units with respect to material composition, further options relate to the geometry of the units and to their percentage of hollow volume. Furthermore, mortar can be composed of several materials and aggregate types and its workability may be adjusted by varying its water content. All these features naturally have a considerable effect on the mechanical characteristics of masonry walls [1].

The capacity of masonry in compression is strongly related to the compressive strength of the masonry units (stone, brick, and block), as well as mortar strength, bonding pattern and many other factors. Though other parameters, such as density, frost resistance and water absorption, may be specified in design, compressive strength has become a basic and universally accepted unit of measurement to specify the quality of masonry units. The relative ease of undertaking laboratory compressive strength testing has also contributed to its universality as an expression of material quality [2].

Masonry wall construction has a number of advantages the first of which is the fact that a single element can fulfill several functions including structure, fire protection, thermal and sound insulation,

ISSN 1313-2539

weather protection and sub-division of space. Masonry materials are available with properties capable of meeting these functions, requiring only to be supplemented in some cases by other materials for thermal insulation, damp-proof courses and the like. The second major advantage relates to the durability of the materials which, with appropriate selection, may be expected to remain serviceable for many decades, if not centuries, with relatively little maintenance. From the architectural point of view, masonry offers advantages in terms of great flexibility of plan form, spatial composition and appearance of external walls for which materials are available in a wide variety of colors and textures [5].

Concrete masonry blocks come in a much greater variety of sizes and formats (solid, cellular and hollow). Also, materials that used in making of masonry block such as aggregate are affected to physical and mechanical properties of blocks. In the production of masonry units, lightweight aggregates are used for reduce the unit weight of material [3].

Increasing utilization of lightweight materials in civil structuring applications is making pumice stone a very popular raw material as a lightweight rock. Due to its having a good ability for making the different products based on its physical, chemical and mechanical properties, the pumice aggregate finds a large using area in civil industry as a construction material. In order to design an initial stage of a building project, the construction material properties should be well evaluated. Therefore, the need arises to analyze the materials to be used in construction experimentally in detail [4].

In this study hollow and non-load bearing masonry units were designed with pumice lightweight aggregate. Physical and mechanical properties of masonry blocks were investigated.

2. EXPERIMENTAL STUDY

2.1. Materials

Isparta / Turkey region volcanic pumice was used for this study. Particle density and bulk density of pumice were 2.24 and 760 kg/m^3, respectively. Ordinary Portland cement (CEM I 42.5R) was used for the production of the LWC and blocks. Surface area by Blaine, specific gravity and 28 days compressive strength of cement were 386 m^2/kg, 3.07 and 48.5 N/mm^2, respectively. The chemical analyses of materials used in this study were determined in Acme Analytical Laboratories Ltd. in Canada and results were given in Table 1.

To define the optimal mix proportions and to obtain satisfactory mechanical properties of masonry units, the pumice LWA was divided into three different size ranges: smaller than 4 mm, 4 to 8 mm and 8 to 16 mm. The aggregates in these size ranges were combined in different proportions to obtain the optimum granulometry in five grading curves properly to TS 1114 EN 13055-1 [6] as Grade 1, Grade 2 and Grade 3, Grade 4 and Grade 5. Aggregate ratios in the mixes were designed that as fine aggregate (FA) has been reduced from 60 % to 40 % while that of medium aggregate (MA) was increased from 20 % to 40 % by a ratio of 5 %. Coarse aggregate (CA) was kept at a ratio of 20 %. Sieve analyses of pumice aggregates were given in Figure 1.

ISSN 1313-2539

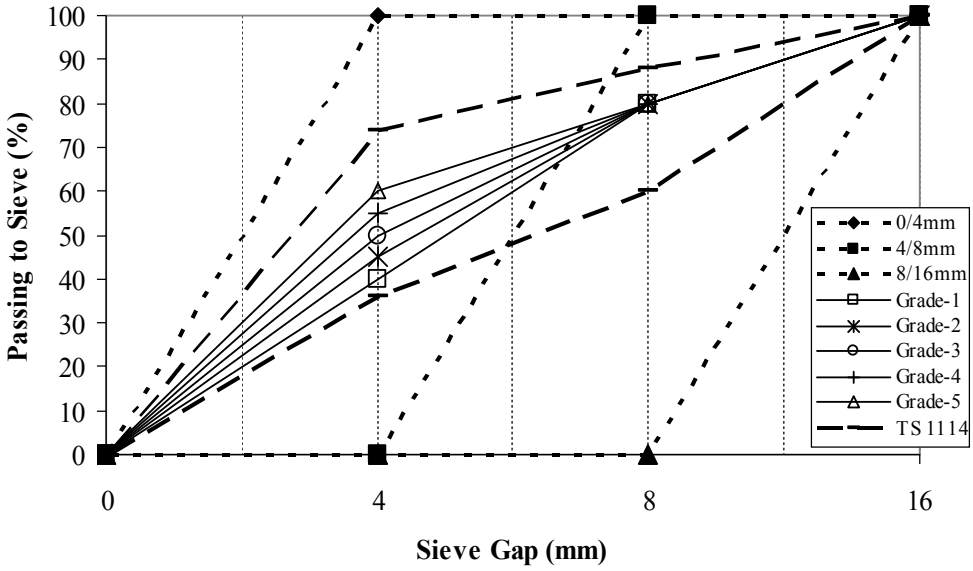

Figure 1. Sieve analyses of aggregates

Table 1. Chemical analysis of cement and pumice

COMPONENT (%)	SiO_2	Al_2O_3	Fe_2O_3	MgO	CaO	Na_2O	SO_3	K_2O	L.O.I.
Cement	19,3	5,57	3,46	0,86	63,56	0,13	2,91	0,80	2,78
Pumice	56,85	16,72	4,66	1,84	5,39	4,61	-	5,19	2,8

2.2. Mix Proportions and Test Program

Before production of masonry blocks, trial batches were produced for defining of optimum aggregate granulometry that supplying to the best properties on masonry units. The all mixtures were designed at 220 kg/m^3 cement content and at 0.15 actual water/cement ratios (w/c). The pumice aggregates were absorbed water in 30 min before adding the mix because of high porosity of aggregates [7]. In the trial batches, the prepared lightweight aggregate concrete (LWAC) as damped was filled in 100 x 100 x 100 mm cubic moulds by vibration-compression machine in 20 % compression ratio. The specimens immediately demoulded and cured in air (in laboratory condition) at 20±2 ^{o}C for 7, 28 and 56 days. On the trial specimens, compressive strength was defined according to TS EN 12390-3 [8] by 2000 kN compressive machine with a rate of loading controller. Unit weight (UW), specific porosity (SP) and water absorption (WA) were calculated aged in 7 and 28 days specimens according to Archimedes principle by the weight measurements of saturated specimens in air and in water, and the dry weight (oven drying at 105°C to constant weight). In the best granulometry, masonry blocks were produced in same cement content and w/c (Fig. 2). Three types of masonry blocks were designed as one-order hollow, two-order hollow and three-order hollow in size of 135 x 190 x 190 mm, 150 x 340 x 190 mm and 190 x 340 x 190 mm, respectively. Also, the production method was same with trial batches.

ISSN 1313-2539

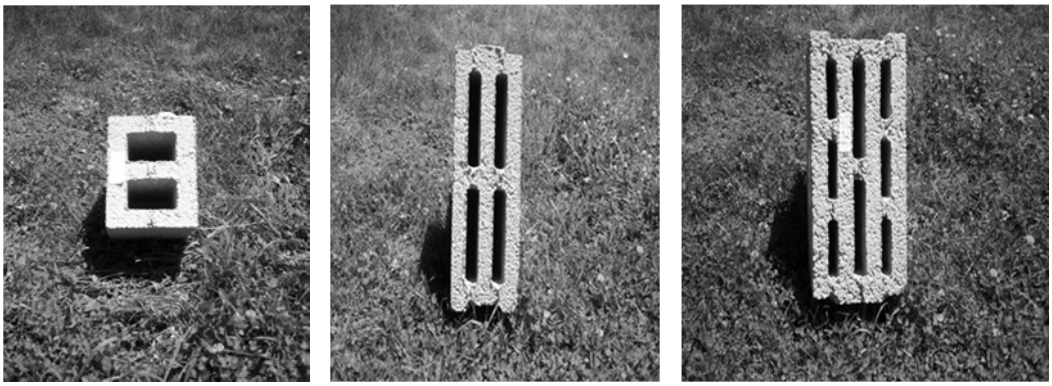

Figure 2 Masonry blocks produced with pumice LWA

Also, compressive strength and unit weight are defined on the masonry blocks. The thermal conductivity of masonry blocks was determined by the ‘‘hot box method” according to ASTM C1363 [9] on the aged 28 days specimens. For the all tests, arithmetic average of three specimens has been used.

3. RESULTS AND DISCUSSION

To investigate the influence of porous aggregate on the physical and mechanical properties of masonry units, natural lightweight aggregate as pumice has been used. Pumice lightweight aggregate concrete (PLWAC) was produced in low w/c ratio by vibration – compression method and they have been tested in 7, 28 and 56 ages.

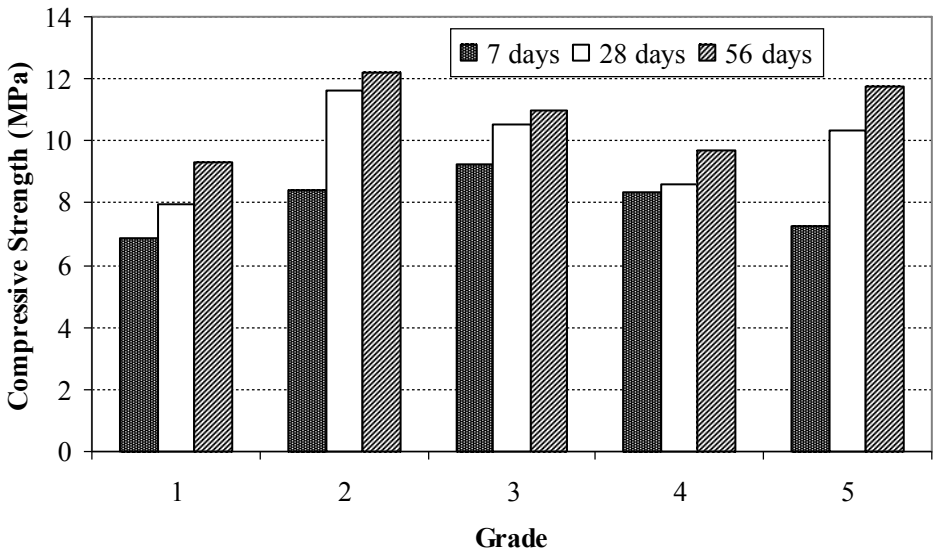

Figure 3 Compressive strength of PLWAC in different ages and gradations

Compressive strength of PLWAC was compared in Figure 3 depending on specimen age. Generally, the compressive strength of LWC has increased by rising of concrete age. Developing of strength in PLWAC was the highest in Grade-2 and Grade-5, Grade-1 and Grade-4, respectively. Of course, the

ISSN 1313-2539

strength development in lightweight concrete is limited by the inherent strength of aggregate [10]. The strength development was reduced by increasing of concrete ages from 28 to 56 days due to evaporation of free water that affect to hydration of cement. Besides, the highest compressive strength of PLWAC was obtained in Grade-2 as 12 N/mm^2. The compressive strength of PLWAC has changed between 7 - 12 N/mm^2 for 7 – 56 aged specimens.

Sari et. al. [11] investigated to the effects of gradation and admixture on the pumice LWAC. The specimens were cured at a temperature of 20-25 ^{o}C and a relative humidity of 50-55 %. Compressive strength of the specimens was determined as between 3.5 - 7 N/mm^2 for 28 and 56 ages. Babu et. al. [12] investigated to the performance of lightweight EPS aggregate concretes containing fly ash over a wide range of concrete densities of 500 - 2200 kg/m^3. The compressive strengths of the specimens have varied between 1.1 and 18.4 N/mm^2 for 28 ages.

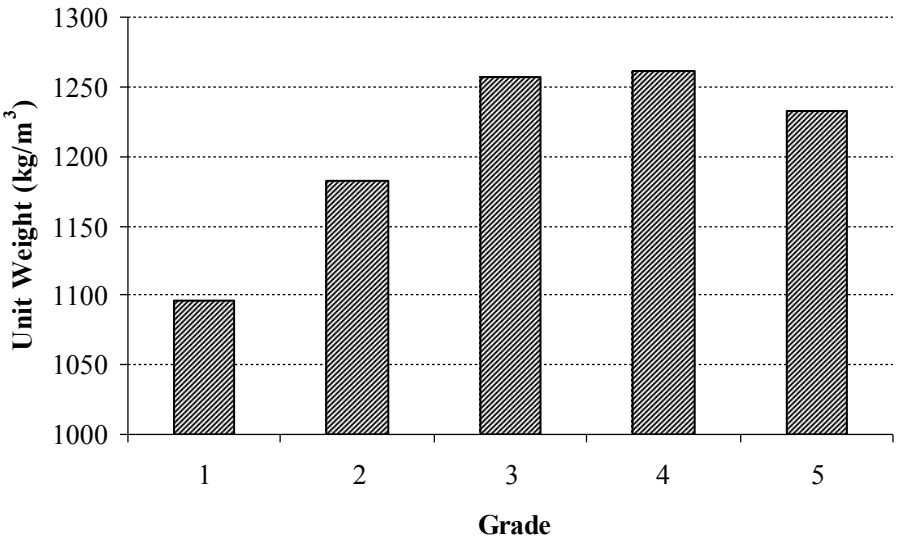

Figure 4. Unit weight of 28 aged PLWAC

As known from the literature, LWACs are categorized according to compressive strength and unit weight of them (Figure 4). Generally, the PLWAC for 28-56 days can be categorized as moderate strength LWC because of their strength in between 7 – 12 N/mm^2 and unit weight in between 1100 - 1260 kg/m^3. The grading effects to unit weight of LWAC as seen in Fig. 4. The lowest unit weight was obtained on the specimens that produced with Grade-1 while the highest unit weight was obtaining on the specimens produced with Grade – 4.

Figure 5 illustrates the specific porosity (sp) and water absorption (wa) of pumice LWAC. The specific porosity and water absorption of pumice LWAC have ranged between 15 % - 25 % and 12 % and 23 %, respectively. They have decreased until Grade-3 and then again increased by increasing of surface area of aggregate depending on fine material and in cubic meter. Pumice LWAC has higher "sp" and "wa" value than normal strength concrete due to properties of aggregate such as pore structure. The specific porosity and water absorption of LWC depends upon the raw material used for making them.

Even tough the lowest porosity and water absorption were obtained in the specimens that produced with Grade-3, the highest compressive strength and improper unit weight was obtained on the specimens produced with Grade-2. Hence, masonry units in this study were produced in Grade-2. Geometrical, physical and mechanical properties of three type's masonry blocks are presented in Table

ISSN 1313-2539

2. Compressive strength of masonry units is different depending on hollow ratio on surface or totally surface area, and it has changed between 3.77 – 5.11 N/mm^2. In the same cement and w/c ratios, three-order hollow masonry blocks more proper than other units due to strength and thermal conductivity.

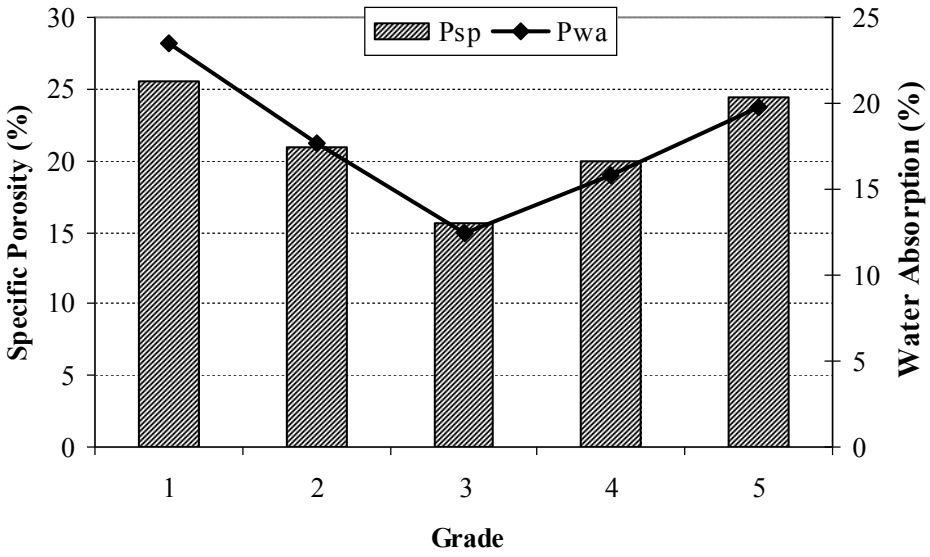

Figure 5. Specific porosity (sp) and water absorption (wa) of 28 aged PLWAC

Table 2. Properties of Masonry Blocks

Property	Masonry Block Type		
	135x190x190	150x340x190	190x340x190
Total surface area (cm^2)	256,5	570	710,64
Total hollow surface area (cm^2)	75	150,12	169,96
Total full surface area (cm^2)	181,5	419,88	540,68
Hollow ratio on surface (%)	29,24	26,34	23,92
Fullness ratio on surface (%)	70,76	73,66	76,08
Total volume (cm^3)	4874	10944	13502
Total hollow volume (cm^3)	1350	2732	3059
Total fullness volume (cm^3)	3524	8212	10443
Volumetric hollow ratio (%)	27,70	24,96	22,66
Volumetric fullness ratio (%)	72,30	75,04	77,34
Block weight (kg)	4,06	9,31	12,07
Dry unit weight (kg/m^3)	833	851	894
Masonry number in 1 m^2	28	13,5	13,5
Compressive strength (N/mm^2)	3.77	3.66	5.11
Thermal conductivity (W/mK)	0.237	0.214	0.203

ISSN 1313-2539

Thermal conductivity is depends upon the pore structure of the lightweight aggregates, density of concrete and the cement paste matrix [13]. Other words, the thermal conductivity is increases with increasing of density of concrete. Also, according to Kim et al. [14], aggregate volume fraction and moisture condition of concrete are revealed as mainly affecting factors on the thermal conductivity of concrete. The thermal conductivity of masonry units has decreased by increasing of volumetric hollow ratio and thermal conductivity of masonry blocks has ranged between 0.203 - 0.237 W/mK.

Al-Jabri et. al. [15] studied to block element for hot climate region. The blocks were produced from two indigenous materials: vermiculite (VerBlock) and polystyrene beads (PolyBlock1) which were used as lightweight aggregates with different proportions in the mix. The mechanical properties of the two types of blocks were compared and compressive strength of these blocks has changed between 2.2-15 N/mm^2.

Uysal et.al. [13] a study has conducted on thermal conductivity coefficients of concretes made up of mixtures of pumice aggregate (PA) and normal aggregate, and they were reported that when 25%, 50%, 75%, and 100% PA ratios were used in place of normal aggregate by volume, PA decreased the density and thermal conductivity of concretes up to 40% and 46%, respectively.

As seen, the masonry blocks produced with pumice aggregate has lower thermal conductivity than normal concrete and brick used in constructions.

4. ACKNOWLEDGEMENT

Authors thank to The Scientific & Technological Research Council of Turkey (TUBİTAK) for financial support throughout this study by project of 104.M.391.

REFERENCES

[1] C. Dymiotis, B. M. Gutlederer, Allowing for uncertainties in the modelling of masonry compressive Strength, Construction and Building Materials 16 (2002) 443–452.

[2] J.C. Morel, A. Pkla, P. Walker, Compressive strength testing of compressed earth blocks, Construction and Building Materials 21 (2007) 303–309.

[3] O. Ünal, T. Uygunoğlu, A. Yildiz, Investigation of properties of low-strength lightweight concrete for thermal insulation, Building and Environment 42 (2007) 584–590.

[4] L. Gündüz, İ. Uğur, The effects of different fine and coarse pumice aggregate/cement ratios on the structural concrete properties without using any admixtures, Cement and Concrete Research 2005;35: 1859-1864.

[5] E.A.W. Hendry, Masonry walls: materials and construction, Construction and Building Materials 15 (2001) 323-330.

[6] TS 1114 EN 13055-1, Lightweight aggregates – Part 1: Lightweight aggregates for concrete, mortar and grout, Turkish Standard Institute, Ankara, 2004 (in Turkish).

[7] Lo, T.Y., Cui, H.Z., Li, Z.G., Influence of aggregate pre-wetting and fly ash on mechanical properties of lightweight concrete, Waste Management. Vol. 24, 2004. pp 333–338.

[8] TS EN 12390-3, Testing hardened concrete - Part 3: Compressive strength of test specimens, Turkish Standard Institute, Ankara, 2003 (in Turkish).

[9] ASTM C1363-97, Standart test method for the thermal performance of building assemblies by means of hot box apparatus, American Society of Test Materials.

ISSN 1313-2539

[10] Al-Khaiat, H., Haque, M.N., Effect of initial curing on early strength and physical properties of a lightweight concrete, Cement and Concrete Research, Vol. 28, 1998. pp 859-866.

[11] Sari, D., Paşamehmetoğlu, A.G., The effects of gradation and admixture on the pumice lightweight aggregate concrete, Cement and Concrete Research. Vol. 35, 2005. pp 936-942.

[12] Babu, K.G., Babu, D.S., Performance of fly ash concretes containing lightweight EPS aggregates, Cement & Concrete Composites. Vol. 26, 2004. pp 605-611.

[13] Uysal, H., Demirboğa, R., Şahin, R., Gül, R., The effects of different cement dosages, slumps, and pumice aggregate ratios on the thermal conductivity and density of concrete, Cement and Concrete Research. Vol. 34, 2004. pp 845–848.

[14] Kim, K.H., Jeon, S.E., Kim, J.K., Yang, S., An experimental study on thermal conductivity of concrete, Cement and Concrete Research. Vol. 33, 2003, pp 363–371.

[15] Al-Jabri, K.S., Hago, A.W., Al-Nuaimi, A.S., Al-Saidy, A.H., Concrete blocks for thermal insulation in hot climate, Cement and Concrete Research Vol. 35, 2005; 1472–9.

ISSN 1313-2539

THE SORPTION OF WATER VAPOUR OF ELM WOOD CHEMICALLY MODIFIED WITH ACETIC OR MALEIC ANHYDRIDE

Antonios Papadopoulos, Ioannis Takos and Dimitrios Emmanouloudis

Technological Educational Institute of Kavala,

Department of Forestry and Management of Natural Environment,

66100, Drama, Greece. E-mail antonios1974@hotmail.com, antpap@teikav.edu.gr

Abstract

Elm wood was esterified with acetic and maleic anhydride and studied for moisture adsorption behaviour. The sorption isotherms for untreated and chemically modified wood were analysed using the Hailwood-Horrobin model. The experimental analysis of the sorption isotherms showed that esterification affects total, polymolecular, and monomol-ecular sorption. Acetic anhydride treatment was found more effective in reducing the hygroscopicity of wood compared to maleic anhydride treatment at comparable weight percentage gain.

Key words: *Chemical modification, Acetic anhydride, Maleic anhydride, Sorption, Hailwood-Horrobin model*

1. INTRODUCTION

The fibrous nature of wood has made it one of the most appropriate and versatile raw materials for a variety of uses. However, two properties restrict its much wider use: dimensional changes when subjected to fluctuating humidity, and susceptibility to biodegradation by microorganisms. The varying moisture content of wood results in dimensional and conformational instability, which can compromise the performance of other materials combined with wood, such as adhesives and surface coatings. Until relatively recently, these shortcomings were addressed by impregnating wood with appropriate hydrophobes (Stamm 1964; Kumar 1994). It has now been demonstrated that wood may be modified chemically so that selected properties are enhanced in a more or less permanent fashion (Rowell 1983, Hill and Papadopoulos, 2002).

It has been shown that the dimensional stability of wood can be effectively improved by esterification with anhydrides (Rowell *et al*. 1988, Papadopoulos and Hill, 2003). There is limited work reported on the water vapour sorptive properties of such modified woods. A number of authors have investigated the sorption isotherms of acetylated wood specimens at only one level of substitution (Risi and Arseneau 1957; Spalt 1958; Popper and Bariska 1972; Yasuda *et al*. 1995).

In this study, water adsorption behaviour of one widely used Greek hardwood, namely elm (*Ulmus montana)*, esterified by acetic and maleic anhydride was investigated. Esterified wood was analysed by FTIR spectroscopic technique to study the changes in spectral intensity of hydroxyl groups of cell wall polymers during the reaction with anhydrides. Adsorption isotherms were obtained to assess the hygroscopicity of esterified wood, using the Hailwood-Horrobin sorption theory.

2. EXPERIMENTAL

Wood modification reactions

Sapwood samples of dimension 20 mm x 20 mm x 5 mm (radial x tangential x longitudinal) were cut from freshly-felled kiln-dried elm (*Ulmus Montana*). Samples were carefully smoothed with

ISSN 1313-2539

sandpaper to remove loosely adhering fibres, then placed in a Soxhlet extractor for solvent extraction using toluene/methanol/acetone (4:1:1 by volume) for 8 h. and subsequently dried in an oven for 8 h at 105oC. Samples were removed from the oven, transferred to a vacuum desiccator and allowed to cool to ambient temperature over silica gel. Prior to reaction, each sample was weighed on a four-figure balance. Samples (thirty replicates) were then vacuum impregnated with pyridine (dried over KOH) for 1 h, then transferred to a flask containing pyridine set in an oil bath at 100oC. Samples were allowed to equilibrate in the hot pyridine for one hour. After heating for 1 h, the sample batch was transferred to a round-bottom flask containing a one molar solution of the anhydride (acetic or maleic) in pyridine set in an oil bath at 100oC. At the end of the reaction period (5 hours), the flask was removed from the oil bath, the hot reagent decanted off, and ice cold acetone added to quench the reaction. Samples were kept in the acetone for 1 h, before being transferred to the Soxhlet apparatus for solvent extraction, as previously detailed. Samples were then oven dried at 105oC for 8 h and weight gain due to reaction recorded.

Infra-red (IR) Analysis

For Infra-red (IR) analysis, the treated samples were ground up by using a microdismembrator (20.000 rpm for 6 min). The fibre flour was then mixed with oven- dry potassium bromide (KBr) powder (the fibre flour/KBr ratio was 1:100) and placed in a vibratory ball mill capsule. The mixture was ground for about 2 min. The ground mixture was then transferred to a press and the bolts of press screwed down. The bolts were tightened with a spanner to press the disk. After a few minutes, the bolts were loosen and removed. The press was placed directly into a sample beam of a Mattson FTIR spectrometer, Nicolet 750, series II.

Determination of moisture adsorption isotherms

Test samples were kept above saturated solutions of various salts in containers stored in a controlled temperature room set at 20oC (variation +/- 1oC). Six salts were chosen and these are listed in Table 1, along with the RH of the atmosphere above each saturated solution at 20oC (according to Kaye and Laby 1973). They were chosen on the basis of giving minimum RH variation with changes in the temperature (Stamm 1964). Data published by Kaye and Laby (1973) show the equilibrium RH above saturated solutions of these salts to be insensitive to any variation in temperature expected in the controlled temperature room (a variation around 20oC of +/-5oC, causing a maximum variation of +/- 1% RH). Excess salt was always present within each solution to ensure saturation was maintained. The solution and air in the container were agitated by bubbling air through the solution. The oven-dry wood samples were placed in the containers above saturated salt solutions. They were left to equilibrate for 4 weeks and then weighed once a week, using a four-place analytical balance, until it became obvious that no significant weight change had occurred since the last weight was recorded (and equilibrium moisture content (EMC) had been attained). After the adsorption equilibrium was attained, samples were weighed, and the moisture content was calculated on the oven dried weight basis.

Table 1. Saturated salt solutions used and their resultant relative humidities at 20 0C.

Salt	RH (%)
Potassium nitrate (KNO3)	93
Sodium chloride (NaCl)	76
Sodium dichromate (Na2Cr2O7)	55
Potassium carbonate (K2CO3)	44
Potassium acetate (CH3COOK)	23
Lithium chloride (LiCl)	12

ISSN 1313-2539

3. RESULTS AND DISCUSSION

Infra-red (IR) Analysis

Esterification of wood was established by infra-red spectroscopy (Fig. 1). Infra-red spectra confirmed the occurrence of wood-anhydride reaction. The strong vibrational absorbance obtained in the region of 1736 and 1730cm-1 (C=O) was a distinct pattern present in modified samples, which indicates ester bond formation. As expected, such absorption was not present in unmodified wood.

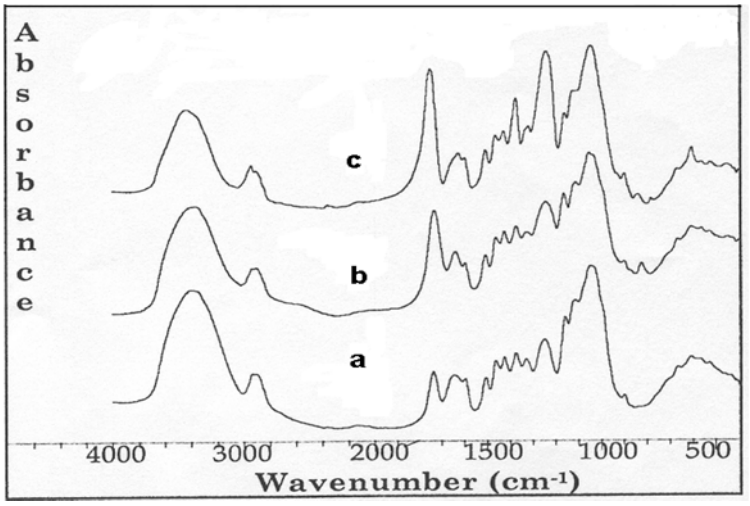

Fig. 1. FTIR spectra of esterified and control wood: (a) control, (b) modified with maleic anhydride and (c) modified with acetic anhydride.

Moisture adsorption isotherms

Isotherm fitting

To the experimental mean (average values obtained from two replicate samples) moisture contents at each RH values, the Hailwood-Horrobin (1946) adsorption equation was applied. The adsorption equation is defined as follows:

$$h/M = A + Bh - Ch2, \quad (1)$$

where:

$$A = \frac{W}{18}\left[\frac{1}{K_2(K_1+1)}\right] \quad (2)$$

$$B = \left(\frac{W}{1{,}800}\right)\left[\frac{K_1-1}{K_1+1}\right] \quad (3)$$

ISSN 1313-2539

$$C = \left(\frac{W}{180{,}000}\right)\left[\frac{K_1 K_2}{K_1 + 1}\right] \quad (4)$$

h (%) is RH, M (%) is moisture content, $K1$ is the equilibrium constant where the hydrate is formed from dissolved water and dry wood, $K2$ is the equilibrium constant between dissolved water and water vapour and W is the molecular weight of dry wood polymer per mole of water sorption sites. The H-H model divides total moisture sorbed into its monomolecular and polymolecular components. The equation for the model is as follows:

$$M = Mh + Md = \frac{1{,}800}{W}\left(\frac{K_1 K_2 h}{100 + K_1 K_2 h}\right) + \frac{1{,}800}{W}\left(\frac{K_2 h}{100 - K_2 h}\right) \quad (5)$$

where:

M is the wood moisture content in equilibrium with h, Mh is the moisture content relating to the hydrate water (monomolecular sorption), and Md is the moisture content relating to the dissolved water (polymolecular sorption).

From Equation 1 it can be seen that the H-H theory predicts a parabolic relationship between the ratio h/M and h. The constants A, B and C are obtained from the fitting parameters of a second-order polynomial. From these parameters the values of $K1$, $K2$ and W can be calculated as follows:

$$K_1 = 1 + \frac{B^2 + \sqrt{B^2 + 4AC}}{2AC} \quad (6)$$

$$K_2 = \frac{200C}{B + \sqrt{B^2 + 4AC}} \quad (7)$$

$$W = 1800\left(\frac{4AC + B^2 + B\sqrt{B^2 + 4AC}}{B + \sqrt{B^2 + 4AC}}\right) \quad (8)$$

The values of A, B, C, coefficient of determination (R2), $K1$, $K2$ and W of various modified woods are presented in Table 2. The degree of fit, as measured by the coefficient of determination (R2) is remarkably high, considering the complexity of the matrix of data, where wood samples were chemically modified at several levels of reaction with different anhydrides. The R2 values range from 0.844 to 0.981, indicating good fit to the experimental results. R2 is a statistical measure of the proportion of variation that can be explained by the regression line (*i.e.* for unmodified control maple wood, the regression line accounted for 98.1% of variation); the lower the R2 value, the lower the proportion of total variation accounted for the fitted regression line. The physical constants $K1$, $K2$, W obtained were found to be in good agreement with those previously reported by Spalt (1958) and Wangaard and Granados (1967) for unmodified wood, and by Spalt (1958) for acetylated wood. For the modified wood, the W values increase as the WPG increases, indicating that a proportion of sites are made unavailable for water sorption.

ISSN 1313-2539

Table 2. Fitted and physical constants calculated for the Hailwood –Horrobin adsorption isotherms.

Reagent	WPG	A	B	C	K1	K2	Wo	R2
Elm wood								
Control	0	3,58	10,78	10,27	4,95	0,76	292,0	0.981
Acetic	14.1	8,21	12,95	14,64	3,06	0,76	458,3	0.884
Maleic	15.9	5,99	12,47	12,84	3,75	0,75	387,3	0.844

As defined above, the constant *K2* expresses the activity of dissolved water per unit relative vapour pressure. According to Okoh and Skaar (1980), its value should be unity if it has the same activity as liquid water. The *K2* values vary approximately between 0.75 and 0.76, indicating that the dissolved water shows a lower activity than the liquid water. This suggests that the freedom of motion of water in the cell wall micropores (dissolved water) is not the same as that in liquid water.

Adsorption isotherms are shown in Fig. 2. Equilibrium moisture content of modified wood was reduced at all relative humidities compared to the control, indicating a reduction in the hygroscopicity of wood. The adsorbed water was then separated into hydrate water relating to monomolecular sorption and into dissolved water relating to polymolecular sorption, using the Equation (5). The isotherms for monomolecular and polymolecular adsorption are plotted in Figures 3, indicating a reduction in the hygroscopicity of wood at both the monomolecular and the polymolecular level.

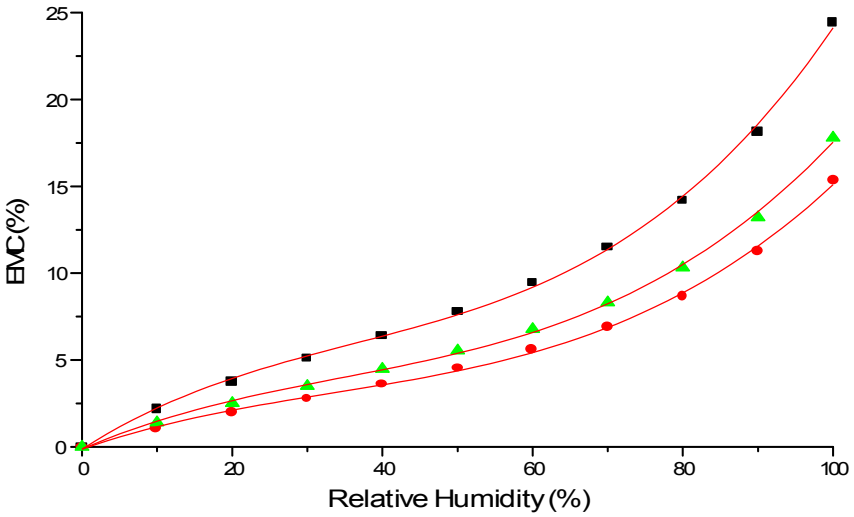

Fig. 2. Adsorption isotherms for unmodified (■), modified with acetic (●) and maleic (▲) anhydride elm wood.

ISSN 1313-2539

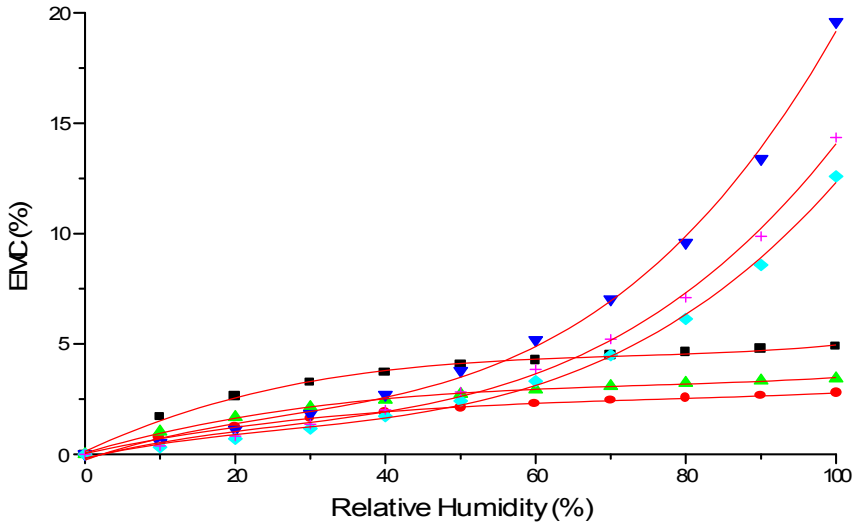

Fig. 3. Polymolecular adsorption isotherms for unmodified (▼), modified with acetic (♦), maleic (+) anhydride elm wood and monomolecular adsorption isotherms for unmodified (■), modified with acetic (●), maleic (▲) anhydride elm wood.

Acetic anhydride treatment was found to be more effective in reducing the hygroscopicity of wood, compared to maleic anhydride treatment at comparable weight percentage gain, at the total, monomolecular, and polymolecular levels, as it can been seen in Fig. 2 and 3. This is perhaps illustrated more clearly in Table 3, which presents the reduction in the hygroscopicity at saturation. It can be seen that the esterification with acetic anhydride to elm wood reduced total sorption by 38%, polymolecular sorption by 35.8%, and monomolecular sorption by 44% at saturation, whereas the corresponding reduction due to maleic anhydride was lower for both total, monomolecular and polymolecular level. The better performance of wood modified with acetic anhydride may be attributed to the smaller anhydride molecule, since it was known that the micropore network geometry controls the accessibility of molecules to the cell wall interior (Hill and Papadopoulos, 2001). It is resonable therefore to expect that different sized molecules would have different accessibility to the cell wall.

Table 3. Reduction in the hygroscopicity (%) at saturation of maple and elm wood as a result of esterification with acetic and maleic anhydride.

Reagent	**WPG**	**Reduction in Hygroscopicity (%)**		
		Total	Polymolecular	Monomolecular
Elm wood				
Acetic	15.3	38	35.8	44
Maleic	16.3	27.1	26.1	29.8

ISSN 1313-2539

The efficacy of modified wood with different anhydrides in reducing hygroscopicity has been the subject of many studies. A comprehensive investigation into the effect of molecular size of the substituent group of softwood modified with linear chain carboxylic acid anhydrides, namely acetic, propionic, butyric, valeric, hexanoic, upon the sorption of water vapour has been performed (Papadopoulos and Hill, 2003). Analysis of the sorption isotherms, using the Hailwood-Horrobin model, at comparable weight percentage gain, revealed that the five anhydrides used show similar effectiveness in total, polymolecular and monomolecular sorption, despite the substantial differences in the proportion of hydroxyl groups reacted. It was concluded that the reduction in total, polymolecular, and monomolecular sorption produced by the linear chain anhydrides is primarily determined by the volume of adduct deposited in the cell wall (bulking), rather than by the number of hydroxyl groups which have been substituted. The sorption properties of modified white fir with acetic and phthalic anhydride were measured by fitting isotherms to sorption data using the BET and Hailwood–Horrobin models (Popper and Bariska, 1972). It was found that the reaction with acetic anhydride significantly reduced monomolecular adsorption, as the hydrophilic hydroxyl groups were replaced. In contrast, wood modified with phthalic anhydride gave monomolecular adsorption isotherms similar to untreated wood. This was attributed to the hydrophilic acid introduced during reaction with phthalic anhydride. Similar observation was also made by Chauhan *et al*. (2001) in rubber wood. In this case, not much difference was observed in the behaviour of maleic and phthalic anhydride treated wood.

4. CONCLUSIONS

1. Water vapour sorption isotherms for untreated and chemically modified wood were analysed using the Hailwood-Horrobin model. The experimental analysis of the sorption isotherms showed that esterification affects the total, polymolecular, and monomolecular sorption.
2. Acetic anhydride treatment was found to be more effective in reducing the hygroscopicity of wood, compared to maleic anhydride treatment at comparable weight percentage gain.

REFERENCES

Chauhan, S. S., Aggrawal, P., Karmarkar, A., and Pandey, K. K. (2001). "Moisture adsorption behaviour of esterified rubber wood (*Hevea brasiliensis)*," *Holz als Roh-und Werkstoff* 59, 250-253.

Hailwood, A. J., and Horrobin, S. (1946). "Absorption of water by polymers: Analysis in terms of a simple model," *Trans. Faraday Soc*. 42 B, 84-92; 93-102.

Hill C.A.S and A.N. Papadopoulos (2001). A review of methods used to determine the size of the cell wall microvoids of wood. *Journal of the Institute of Wood Science* 15(6):337-345.

Hill, C. A. S., and Papadopoulos, A. N. (2002). "The pyridine catalysed acylation of sapwood and phenolic model compounds with carboxylic acid anhydrides. Determination of activation energies and entropy of activation," *Holzforschung* 56, 150-156.

Hill, C. A. S., Jones, D. (1996). "The dimensional stabilisation of Corsican pine sapwood by reaction with carboxylic acid anhydrides. The effect of chain length," *Holzforschung* 50, 457-462.

Kaye, G. W. C., and Laby, T. H. (1966). *Tables of physical and chemical constants and some mathematical functions*. Longmans, London.

Kumar, S. (1994). "Chemical modification of wood," *Wood and Fiber Sci*. 26, 270-280.

ISSN 1313-2539

Okoh, K. I. A., and Skaar, C. (1980). "Moisture sorption isotherms of the wood and inner bark of the southern U.S. hardwoods," *Wood and Fiber Sci.* 12, 98-111.

Papadopoulos, A. N., and Hill, C. A. S. (2003). "The sorption of water vapour by anhydride modified softwood," *Wood Sci. Technol*. 37, 221-231.

Popper, R., and Bariska, M. (1972). "Acylation of wood. Part I: The sorption behaviour of water vapour," *Holz als roh-und Werkstoff* 30, 289-294.

Risi, J., and Arseneau, D. F. (1957). "Dimensional stabilisation of wood. Part I: Acetylation," *Forest Prod J.* 7, 210-213.

Rowell, R. M. (1983). "Chemical modification of wood," *For. Prod. Abstr*. 6, 366-382.

Rowell, R. M., Youngquist, J. A., and Montrey, H. M. (1988). "Chemical modification: adding value through new FPL composite technology," *Forest Prod. J*. 38, 67-70.

Spalt, H. A. (1958). "The fundamentals of water vapour sorption by wood." *Forest Prod. J.* 8, 258-295.

Stamm, A. J. (1964). *Wood and Cellulose Science*, Ronald Press Co., New York.

Wangaard, F. F., and Granados, L. A. (1967). "The effect of extractives on water-vapour sorption by wood," *Wood Sci. Technol*. 1, 253-277.

Yasuda, R., Minato, K., and Norimoto, M. (1995). "Moisture adsorption thermodynamics of chemically modified wood," *Holzforshung* 49, 548-554.

ISSN 1313-2539

ACRYLIC ACID GRAFTED PDMS PRELIMINARY ACTIVATED BY AR+ BEAM PLASMA AND CELL OBSERVATION

A.Kostadinova* I.Keranov N.Zaekov*

*Institute of Biophysics, BAS, 1113 Sofia, Bulgaria

Department of Polymer Engineering, University of Chemical Technology and Metallurgy (UCTM), 8 Kliment Ohridski Blvd., 1756 Sofia, Bulgaria

Abstract

Plasma based Ar+ beam performed in RF (13.56 MHz) low-pressure (200 mTorr) glow discharge (at 100 W, 1200 W and 2500 W) with a serial capacitance was employed for surface modification of poly(dimethylsiloxane) (PDMS) aimedat improvement of its interactions with living cells. The presence of a serial capacitance ensures arise of an ion-flowinside the plasma volume directed toward the treated sample and the vary of the discharge power ensures varied density of the ion-flowThe initial adhesion of human fibroblast cells was studied on the described above plasma based Ar+beam modified and acrylic acid (AA) grafted or not fibronectin (FN) pre-coated or bare surfaces.

The cell response seems to be related with the peculiar structure and wettability of the modified PDMS surface layerafter plasma based Ar+ beam treatment followed or not by AA grafting.

Key words: *Biomaterials; Surface treatment of PDMS; Plasma based Ar+ beam; Acrylic acid grafting; Fibroblast cells*

1. Introduction

Cold plasma obtained in low-pressure glow discharge has been often used to activate polymer surface, including siloxane membranes [1–4], for further grafting of suitable monomers like AA HEMA, etc. aimed at improvement of its interactionwith living cells. On the other hand, ion-beam without following grafting [5,6] is known as other possible way to improve the bio-contact properties of poly(hydroxymethylsiloxane) (PHMS), this effect being confirmed also at poly(dimethylsiloxane) (PDMS) [7,8].We employed plasma based Ar+ beam performed in RF (13.56 MHz) low-pressure(200 mTorr) glow discharge (at 100 W, 1200 W and 2500 W) with a serial capacitance for surface modification of PDMS trying to combine some advantages of both: ion-beam and plasma treatment,namely the durability of the modifying effect of the ion-beam with the simplicity of the plasma as compared to ion-beam equipment. The presence of a serial capacitance ensures arise of an ion-flow inside the plasma volume directed toward the treated sample (Fig. 1) and the discharge power vary ensures varied ion-flow density [9]. Our investigation includes an optimization of the treatment conditions as well as a preparing of AA grafted surfaces with different grafting densities.

Therefore, the discharge power as well as the duration of the plasma based Ar+ beam treatment and the AA grafting were varied. On the other hand, the grafting of AA opens a way to a following biofunctionalization quoted also as improving the cellular interactions of the modified surfaces [10]. Therefore we are going to continue our investigation with immobilization of proteins to the AA grafted PDMS surface. Such ‘‘step’’ modification offers a possibility to obtain three types of modified PDMS surfaces: plasma based Ar+ beam treated,AA grafted and protein immobilized and to compare their chemical composition, surface energy and cellular response. In this paper we describe

ISSN 1313-2539

the preparation, characterization and initial cell adhesion of plasma based Ar+ beam treated and AA grafted PDMS surfaces.

2. Experimental

Samples preparation PDMS thin films (thickness of 50–70 lm) were deposited on pre-lyophilized cover glasses (15 · 15 mm) by spinning of Silopren LSR 2070 (FDA, GE Bayer Silicones) precursor polymer solution in toluene (3% v/v) and cured in a conventiona lway.

2.2. *Plasma based Ar+ beam treatment*

The samples were treated in plasma based Ar+ beam performed in RF (13.56 MHz) low-pressure (200 mTorr) glow discharge with a serial capacitance . In order to optimize the operation conditions were varied both: discharge power –100 W, 1200 W and 2500 W and treatment duration – 1 min, 5 min and 10 min. Six inch wafer sputtering inspection deposition system Genus

2.3. Acrylic acid grafting

Acrylic acid grafting was performed on plasma based Ar+ beam treated samples kept for 10 min in air. To obtain different grafting density the samples were immersed in water solution (50% v/v) of acrylic acid (Merck) at 80 _C for 3 h, 6 h or 12 h. The grafted samples were taken out of the flasks and washed by Soxhlet extraction with ethanol

for 24 h and then rinsed three times with de-ionized water to remove any adsorbed homopolymers. The surface carboxylic groups density was evaluated from the uptake of Toluidine Blue O as described by Sano et al. [11].

2.5. Cells culture

Human fibroblasts were prepared from fresh skin biopsy and used up to the 9th passage. The cells were grown in Dulbecco_s Minimal Essential

Medium (DMEM) containing 10% fetal bovine serum (FBS) (Sigma Chemicals Co., St. Louis, MO) in a humidified incubator with 5% CO2. For the experiments, the cells were harvested from nearly confluent cultures with 0.05% trypsin/ 0.6 mM EDTA (Sigma)/.

2.6. Overall cell morphology

Approximately 5 · 105 cells per well were incubated in serum-free medium (DMEM) for the times indicated in six-well polystyrene plates (Falcon Becton Dickinson, USA) containing PDMS samples. Half of them were pre-coated with 20 mg/ml FN (30 min in PBS). At the end of the incubation the samples were studied and photographed in an inverted phase contrast microscope (Axiovert, Zeiss, Germany).

2.7. *Fibronectin preparation*

Human plasma FN was prepared by affinity chromatography on gelatin–Sepharose 4B [20] and further purified on heparin–Sepharose 4B.FN was eluted with 0.5 M NaCl, 50 mM Tris pH 7.3 and lyophilized. For the experiments, FNwas dissolved in distilled water at concentration 1 mgml_1 and stored at 4 _C for up to 1 week. Working dilutions were done in PBS. Surfaces were pre-coated with FN by incubation with 20 lgml_1 for 30 min at 37 _C. Then the samples were washed three times with PBS and the cells added.

3. Results and discussion

3.1 Cellular interaction

As optimal operation conditions for plasma based Ar+ beam modification of PDMS surface could be accepted the discharge power of 1200 W and treatment duration of 1 min because of the almost completed surface compositional changes after a treatment under these conditions. The following AA grafting was performed on activated under such conditions samples and in the comparative study of the initial cell adhesion were involved these samples together with non-modified PDMS and acrylic

ISSN 1313-2539

acid grafted one with the highest grafting density, namely the sample at which the AA grafting durability was 12 h.

The initial cell adhesion on non-treated, plasma based Ar+ beam modified and AA grafted PDMS surfaces was studied using human fibroblast model, as it was previously described [20]. The cells were added in serum-free medium and incubated for 2 h on bare or FN pre-coated surfaces. Than the samples were viewed and photographed under phase contrast (20x). The pictures are shown in Fig. 1. It is evident, that the initial cell adhesion on the plasma based Ar+ beam modified PDMS surface (Fig. 4(c) and (d)) is significantly improved on both: fibronectin precoated (Fig. 7(d)) and bare (without FN precoating) surface (Fig. 1(c)). While the acrylic acid grafted surface demonstrates improved initial cell interaction on FN precoated (Fig. 1(f)), but not on bare (without FN precoating) (Fig. 1(e)) sample. Let us discuss the correlation between the biologicalresponse and the modification induced by plasma based Ar+ beam followed or not by AA grafting. Let us first consider the modification of the surface chemical composition, as determined from XPS spectra in our previous investigation. The irradiation effects have been seen to involve the formation of an altered surface layer formed by SiOxCyHz phase, whose detailed composition and chemical structure depend

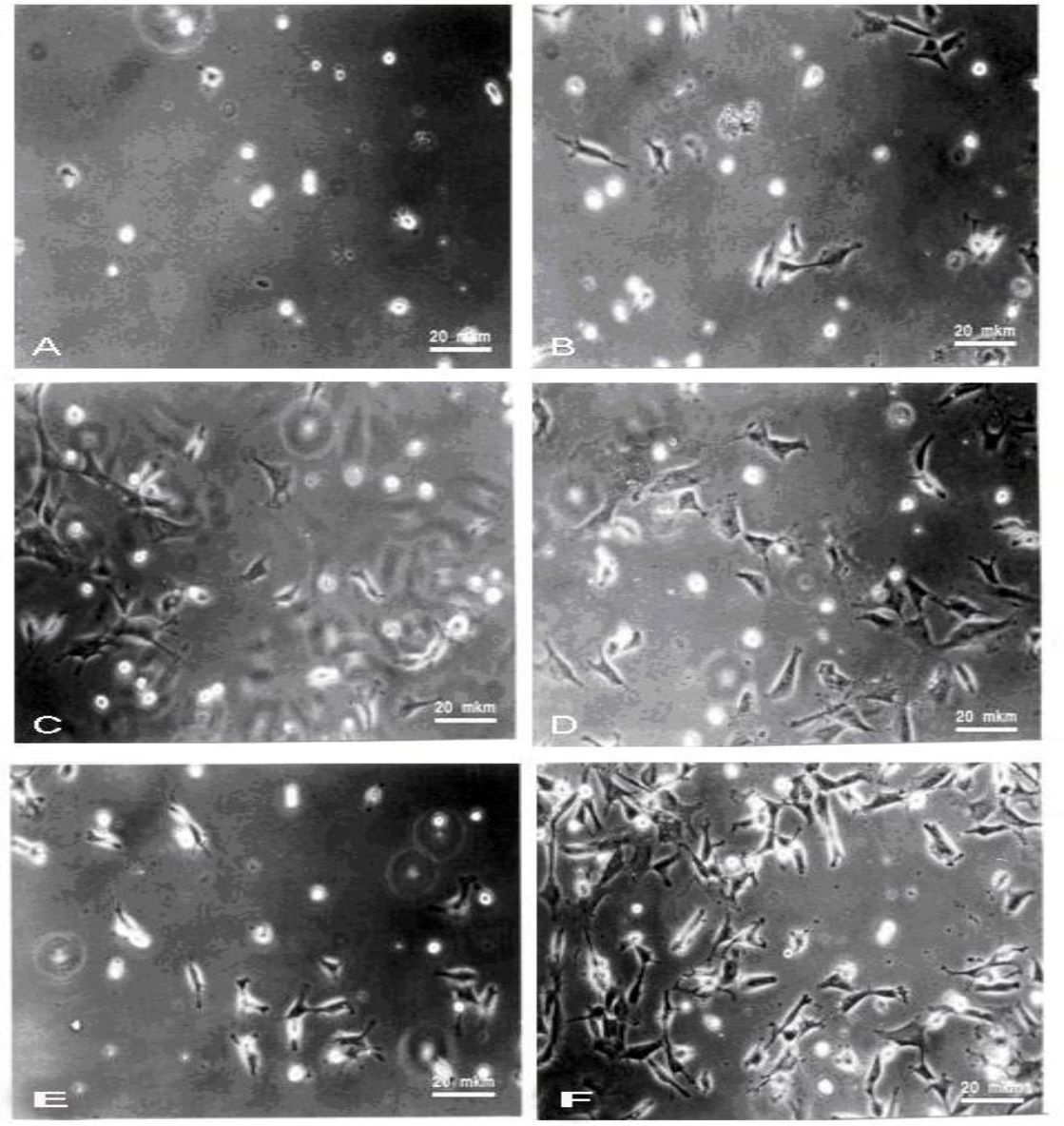

ISSN 1313-2539

on the operation conditions of the treatment. In our previous investigation(12), the analysis of the Si 2p XPS peak shows the evolution of the Si component assigned to SiOx clusters, that closely follows the C 1s peak decrease. Such plasma based Ar+ beam treatment induces change in the PDMS surface chemical composition obviously corresponding to a sharp decrease in its hydrophobic character Poly(acrylic) acid characterizes with lower owns hydrophilicity as compared to high power plasma.

Table 1

Contact angle, surface energy and polarity of various surfaces

Sample	θ_{H2O}	θ_{CH2I2}	γ_s (mJm^{-2})	γ_s^d(mJm^{-2})	γ_s^d (mJm_2)	Polarity, p	-COOH (nmol/m^2)
PDMS, control (non-treated PDMS)	101	70	22.9	21.8	1.1	0.05	
PDMS, treated by plasma based Ar+ beam at 1200 W/1 min	60	49	45.6	28.1	17.5	0.38	
PDMS, treated by plasma based Ar+ beam at 1200 W/1 min and AA grafted 3h	62	56	42.6	24.4	18.2	0.43	1.2
6 h	66	54	40.6	21.4	14.7	0.36	4.9
12 h	73	55	36.26	2 6.9	10.3	0.28	6.3

Treated PDMS and therefore the increase of the AA grafting density leads to less pronounced hydrophilicity of the AA grafted surface – the water contact angle reach up to 73 (see Table 1) and this value is closed to the water contact angle value (70) of AA coated surfaces prepared earlier by photopolymerization [13]. The cell response seems to be related to the peculiar structure and wettability of the plasma based Ar+ beam modified and AA grafted surfaces. A more detail study of the cellular interaction continues with the study of the extra cellular matrix formation and this cellular response will be compared to that of further protein immobilized PDMS surfaces.

ISSN 1313-2539

4. Conclusion

A partially mineralized surface layer, similar to that obtained after a conventional ion-beam is the result from plasma based Ar+ beam assisted surface modification of PDMS,. This modification is almost completed after a treatment for 1 min at 2500 W.

Both, plasma based Ar+ beam treatment itself and following acrylic acid grafting turn the strong hydrophobic PDMS surface into a hydrophilic one with significantly improved cellular interactions. The plasma based Ar+ beam modified surfaces Fig. 1. Initial cell adhesion of human fibroblasts to non-modified PDMS (a, b), or treated by plasma based Ar+ beam performed at 1200 W/1 min (c, d) and AA grafted for 12 h (e, f) in absence (a, c, e) and in presence (b, d, f) of pre-coated fibronectin without grafted AA are to be preferable regarding the initial cell adhesion because the last one is good even in absence of precoated fibronectin.The cell response seems to be related with the peculiar structure and wettability of the modified PDMS surface after plasma based Ar+ beam modification followed or not by AA grafting.

REFERENCES

[1] C.M. Chan, T.-M. Ko, H. Hiraoka, Surf. Sci. Rep. 24(1996) 1.

[2] F. Abbasi, A. Mirzadeh, A.-A. Katbab, Polym. Int. 50(2001) 1279.

[3] P.K. Chu, J.Y. Chen, L.P. Wang, N. Huang, Mater. Sci.Eng. R36 (2002) 143.

[4] Sh.-D. Lee, G.-H. Hsiue, Ch.-Y. Kao, J. Polym. Sci., A:Polym. Chem. 34 (1996) 141.

[5] C. Satriano, E. Conte, G. Marletta, Langmuir 17 (2001)2243.

[6] C. Satriano, S. Carpazza, S. Guglielmino, G. Marletta,Langmuir 18 (2002) 9469.

[7] T. Vladkova, I. Keranov, G. Altankov, in: Proc. 4th Int.Conf. Chem. Soc. of the South-Eastern European Countries(ICOSECS 4), 18–21 July 2004, Belgrad, Serbia,p. 629.

[8] T. Vladkova, I. Keranov, P. Dineff, G. Altankov, in: Proc.XVIIIth Congress of Chemists and Technologists ofMacedonia, Ohrid, 21–25 September 2004, p. 16.

[9] R. Hippler, S. Pfau, M. Schmidt, K. Schoenbach (Eds.),Low Temperature Plasma Physics. Fundamental Aspectsand Applications, Willey-VCH, Berlin, New York, Chichester,Brisbane, Toronto, 2000.

[10] Ch. Baquey, F. Palumbo, M.C. Porte-Durrieu, G. Legeau,A. Tressaud, R. d_Agostino, Nucl. Instr. and Meth. B 151(1999) 255.

[11] S. Sano, K. Kato, Y. Ikada, Biomaterials 14 (11) (1993) 817.

[12] T.G.Vladkova at all Nucl Instr and Meth. in Phys..Res .B236 (2005) 552-562

[13] C.-G. Goelander, S.-E. Jonsson, T. Vladkova, P. Stenius Colloids Surf. 21(1986)149

ISSN 1313-2539

TEMPERATURE SCHEMES WITH FUZZY MODEL PREDICTIVE CONTROL FOR POLYMER REACTOR

Vassiliy A. Chitanov

Technical University-Branch Plovdiv

Abstract

Two temperature schemes with fuzzy-neural model predictive control are presented. These schemes are applied over polymer reactor for control of the temperature of the reaction mixture. Such fuzzy-neural hybrid structure could be used successfully for model predictive control and optimization of polymerization processes. A few graphical examples for control of reaction mixture temperature with different references are presented.

Key words: *temperature control, polymer reactor, fuzzy-neural MPC*

1. INTRODUCTION

Batch reactors are frequently used to manufacture products with high quality in polymer industry. Their flexibility make their use attractive for application in reactors working with MMA. However, in order to improve the quality of the products and to ensure uniform production from one batch to another, it is necessary to improve the automation of these reactors. Several industrial heating/cooling configurations are used for their thermal control. This paper offer two temperature schemes applied over polymer reactor for control of the temperature of the reaction mixture.

In the last 10 years the leading edge process technology impacts on all sectors of the manufacturing and processing industries. As companies strive to reduce processing costs in response to global competitive pressures, attention moves towards sustainable manufacturing practices, which will realise the production of consistently high quality product at reduced costs. Areas targeted by end-user companies to achieve such objectives include the application of advanced process technologies, e.g. process modelling, new control algorithms, on-line optimisation, multivariate statistical process control, neural networks, fuzzy logic, knowledge integration, etc. However, the achievement of substantial improvements can not be accomplished through the application of one technology alone.

Over the last years the Model Predictive Control (MPC) is basic technology for obtaining the concrete purposes in linear and nonlinear control. The construction of new and adaptive nonlinear methods for identification makes possible the realization of different schemes for control. It is state of the art during the last decades finding new adaptive algorithms for control and using them for decision of complex nonlinear tasks. In this work are shown results of program realization of one contemporary algorithm for control based on hybrid model predictive control, consist of neural-fuzzy system for control and nonlinear mechanistic model. The applied algorithm is developed for optimization and control of the work of temperature mixture of batch polymerization reactor. The temperature control is realized with two temperature schemes.

2. THE POLYMER REACTION PROCESS

The batch polymerization process studied is a pilot scale polymerization reactor installed at the Chemical Process Research Engineering Institute (CPERI), Aristotle University of Thessaloniki, Greece and is shown schematically with its temperature control system on Fig.1. The reaction is the free-radical solution polymerization of methyl methacrylate (MMA) with a water solvent and benzol

ISSN 1313-2539

peroxide initiator. The jacketed reactor is provided with a stirrer to ensure thorough mixing of the reactants. Heating and cooling of the reaction mixture is achieved by circulating water at an appropriate temperature through the reactor jacket. A cascade control system consisting of a primary and two secondary PID controllers controls the reactor temperature. The reactor temperature is fed back to the master controller, whose output is taken as the set point of the two slave controllers. The manipulated variables for the two slave controllers are the hot and cold water flow rates. The hot and cold water streams are mixed before entering the reactor jacket and provide heating and cooling for the reactor. The jacket outlet temperature is then fed back to the two slave controllers. A detailed dynamic mathematical model of the reactor covering reaction kinetics and heat and mass balances has been developed and comprehensively validate against the pilot plant. Based upon this model, a rigorous simulation program is used to generate polymerization data under different batch operating conditions**.**

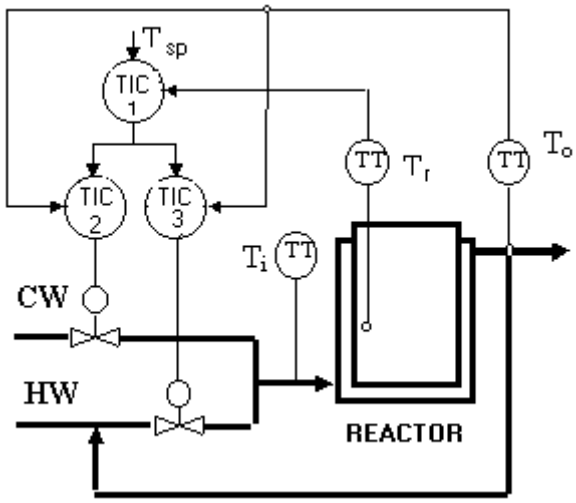

Fig.1. Reactor temperature control system

The on-line measured process variables are reactor temperature, jacket inlet temperature, jacket outlet temperature, monomer conversion and coolant flow rate. Polymer property variables are number average molecular weight (M_n) and weight average molecular weight (M_w). They are in practice not measured directly through the batch, but require estimation from the on-line process measurements. The evolution of the polymer properties during the course of polymerization are mainly determined by the batch recipe, i.e. the reactor temperature set point, and the initial initiator weight. Different batch recipes will lead to different polymer growth profiles coupled with different heat generation profiles. For the presented paper are used two temperature schemes for experiments. To the first one the main PID controller is removed and the predictive fuzzy-neural controller gives signals to the slave two PI controllers for the hot and cold water. On the second scheme the main and the two slave controllers are removed and the predictive fuzzy-neural model control directly the valves for hot and cold water.

ISSN 1313-2539

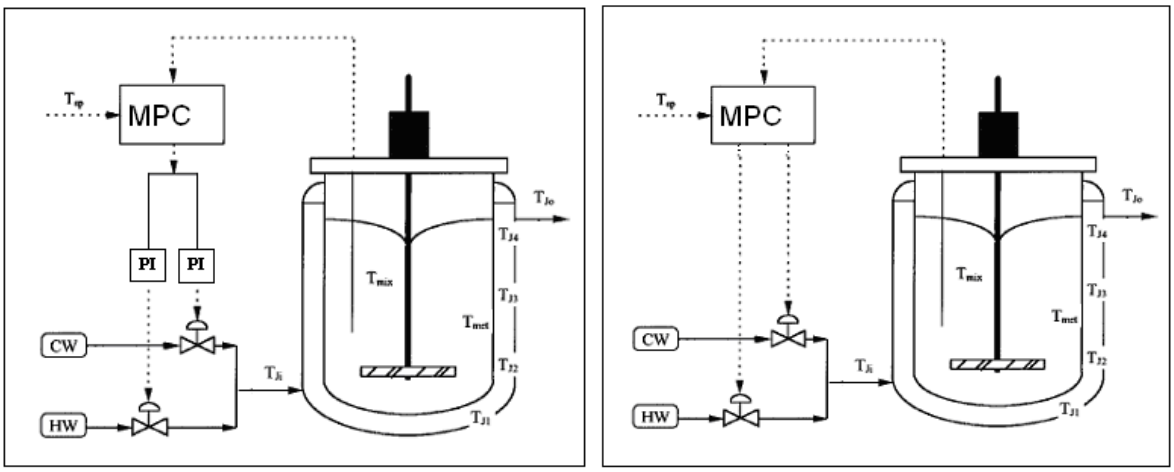

Fig.2. The implemented reactor temperature control systems.

Rigorous analytical kinetic model have been developed for modelling the Conversion, Zero Moment of Live Radical Chains [Kmol], First Moment of Live Radical Chains [Kmol], Second Moment of Live Radical Chains [Kmol], Zero Moment of Dead Polymer Chains [Kmol], First Moment of Dead Polymer Chains [Kmol], First Moment of Dead Polymer Chains [Kmol], Second Moment of Dead Polymer Chains [Kmol], Temperature of Mixture [K], Temperature of Metal [k],Temperature of jacket's First part [k], Temperature of jacket's Second part [k], Temperature of jacket's Third part [k], Temperature of jacket's Fourth part [k], Measured Temperature of Mixture [k], Measured Temperature of Jacket Outlet [k], Measured Temperature of Jacket Inlet [K], Jacket's Metal Temperature [K], Variable losses form jacket's metal to environment. Using this inputs and outputs the temperature setpoint can be used in SISO configuration as an output for controlling the temperature of the reactor mixture. The signals from the predictive controller for the Hot Water Flow Rate and Cold Water Flow Rate through the reactor jacket can be used as output parameters in SIMO configuration. Again the controlled parameter is the Temperature of the mixture of the polymer reactor.

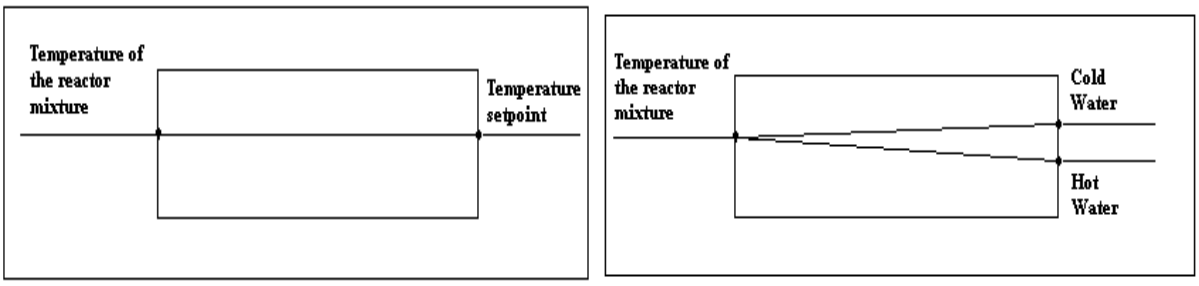

Fig.3. Control configurations

3. CONTROL SYSTEM STRUCTURE

Fuzzy model based predictive control (FMPC) is basically a type of model-based predictive control, where the model for predictions is a fuzzy model. Fig.3 represents the structure of the control

ISSN 1313-2539

configuration studied in this paper. The structure consists of three main parts. The first one is an internal precise analytical model (*software sensor*) of the process, which predicts the effects of the control actions and calculates the process output. The second one is a dynamic *fuzzy model*, which calculates the predictions of the process outputs and works as a predictive model. The third one is a controller, which optimizes the process and works as a *predictive controller*.

The software sensor give information for the parameters of the polymer process and can be used as mechanistic model giving information for control input and output parameters and also as control object(polymer reactor). In the case of the described polymer reactor such controlled variables are hot water signal Fhw, cold water signal Fcw and the temperature of the reactor mixture Tmix. Basically such a model is a state model or a static regressive model, developed by kinematics and mass balance equations of the process. The predictive fuzzy model is developed by the Takagi-Sugeno fuzzy technique and can be taken as a collection of many linear models. On the other hand this fuzzy model can be used in optimization procedure, calculating some derivatives for a gradient optimization.

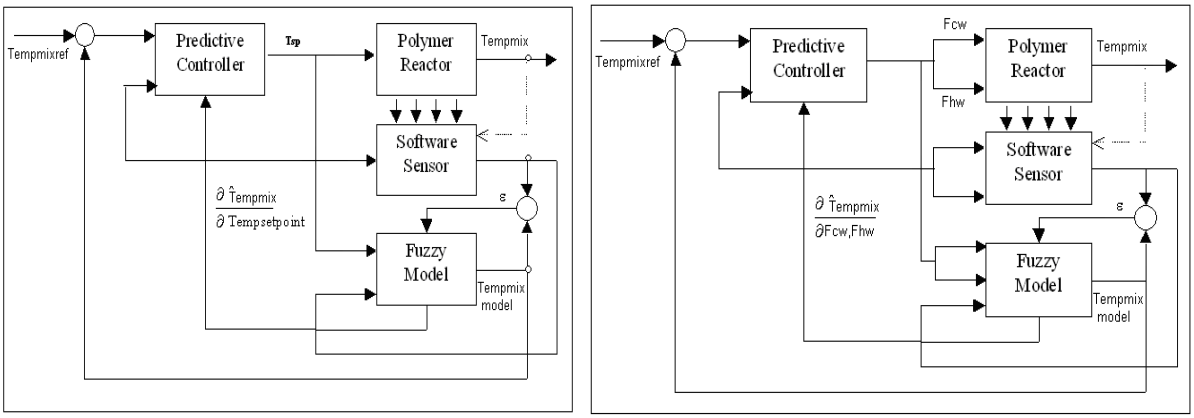

Fig.4. The functional structure of the control configurations.

This algorithm can be tunned adaptively according to the process changes, the description and optimization task.

4. FUZZY MODEL PREDICTIVE CONTROL

The general model predictive control (MPC) strategy is based on three main concepts. The first one is explicit use of a model to predict the process output at the future discrete time instants, over a defined *prediction horizon*. The second one is computation of the future control actions over a *control horizon* equal to or smaller than the prediction horizon, by minimizing a given objective function at the same time instants. And the third one is the *receding horizon* strategy. Only the first control action in the sequence is applied, the horizons are moved towards the future and optimization procedure is repeated. The control variable is manipulated only within the control horizon and remains constant afterwards.

The idea behind generalized predictive control (GPC) is based on circumstance to minimize at each step a criterion suitable for polymerization processes of the following type:

$$J(k,u(k)) = w\sum_{i=N_1}^{N_2}(r(k+i)-\hat{y}(k+i))^2 + \rho_1\sum_{i=1}^{Nu}\Delta u_1(k+i-1)^2 + \rho_2\sum_{i=1}^{Nu}\Delta u_2(k+i-1)^2 \qquad (1)$$

ISSN 1313-2539

where y is the controlled polymer parameter – temperature of the mixture, u_1 is the control action for hot water and u_2 is the control action for cold water; w is positive weighting factors; r is the reference for temperature mixture, which correspond to the controlled parameters.

Such a criterion represents a SIMO type controller, but for an easier implementation in the case of polymerization quality control, it can be divided in two different sections, which correspond to the each output parameter separately. Bellow, for the sake of simplicity the optimization task is described only for one section. The second one will have the same interpretation. In this case, it is used the criterion for classical GPC:

$$J[k,u(k)] = \sum_{i=N_1}^{N_2}[r(k+i) - \hat{y}(k+i)]^2 + \rho_1 \sum_{i=1}^{N_u} \Delta u_1(k+i-1)^2 \quad (2)$$

The tuning parameters of the predictive controller are N_1, N_2, N_u and ρ. N_1 is the minimum cost horizon, N_2 is the prediction (or maximum cost) horizon, and N_u is the (maximum) control horizon. ρ_1 is a weighting factor penalizing changes in the control actions. For a non-linear system, the optimisation problem must be solved at each sample k resulting in a sequence of future control actions. From this sequence only the first component, $u_1(k)$, is then applied to the process. The idea of the *receding horizon* is that at each sample the control signal is determined to achieve a desired behaviour in the following N_2 (*predictive horizon*) time steps. Another important attribute is the notion of a control horizon, which is smaller than the prediction horizon. The objective is here that only the first N_u future control actions are determined. From that point on, the control action is assumed constant. A long horizon allows a more active control signal, therefore enabling a higher performance, while a short horizon generally makes the control system more robust. As the computational burden increases dramatically with the length of this horizon, it is typically kept it as short as possible.

5. GRAPHICAL RESULTS

The presented simulation results are for two control structures. First four results are taken under SISO structure. The figures shows the reference signal, the input signal from the predictive controller(temperature setpoints Tsp for PI controllers) and the output signal for temperature of the reaction mixture. The next one are for SIMO structure. The data are received for one constant with time reference(70^0C) and two step modified references between 70-80^oC for reactor mixture temperature. For each output result for reaction mixture are shown the control signals for hot and cold water respectively for the second case in mA.

5.1 *Results for SISO Structure*

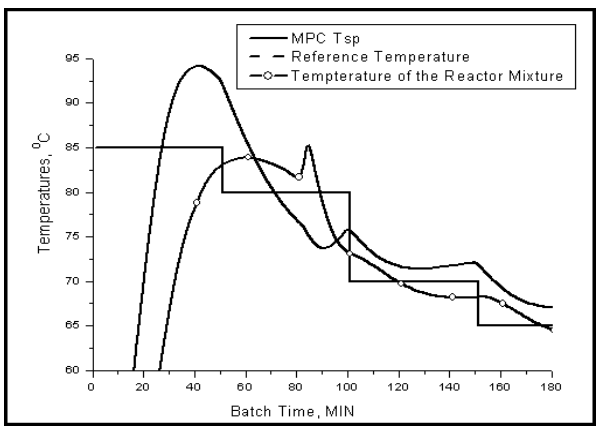

Fig.5. Step changing temperature reference.

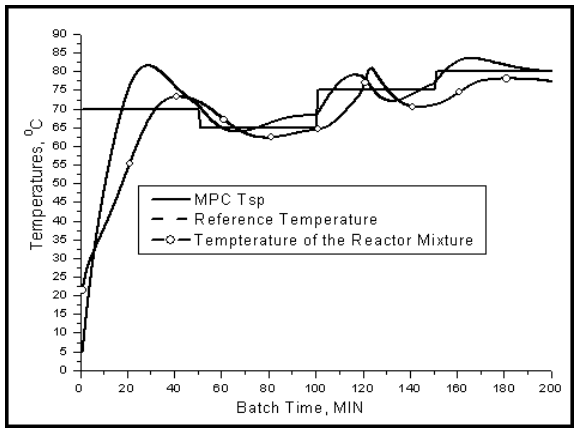

Fig.6. Step changing temperature reference.

ISSN 1313-2539

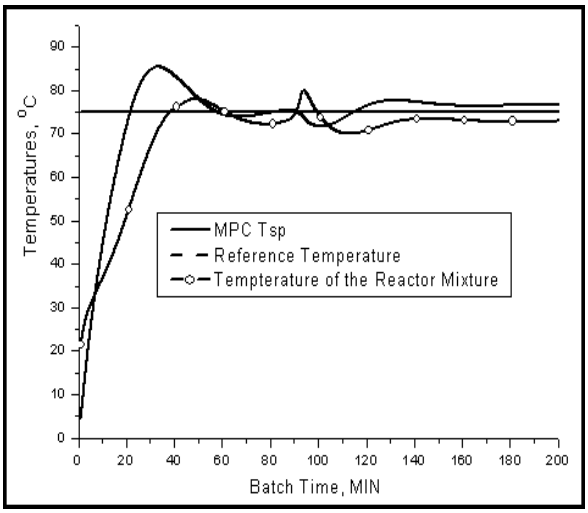

Fig.7. Constant temperature reference.

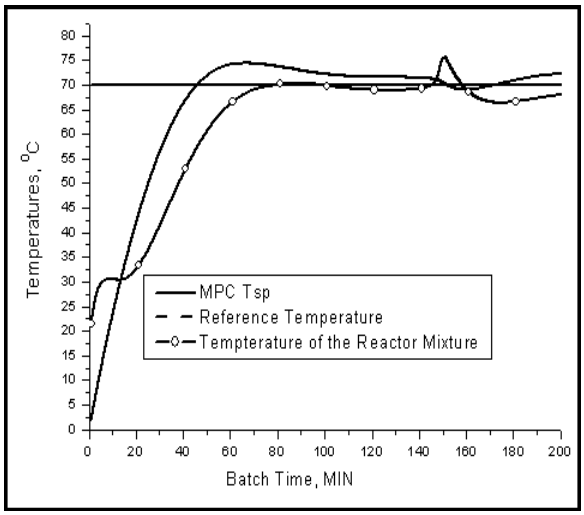

Fig.8. Constant temperature reference.

5.2. *Results for SIMO Structure*

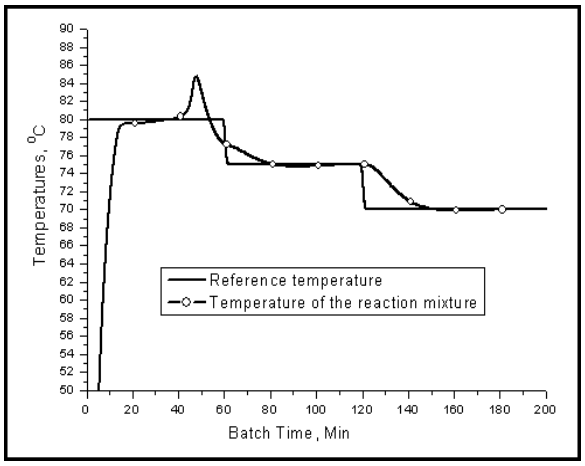

Fig.9. Step changing temperature reference.

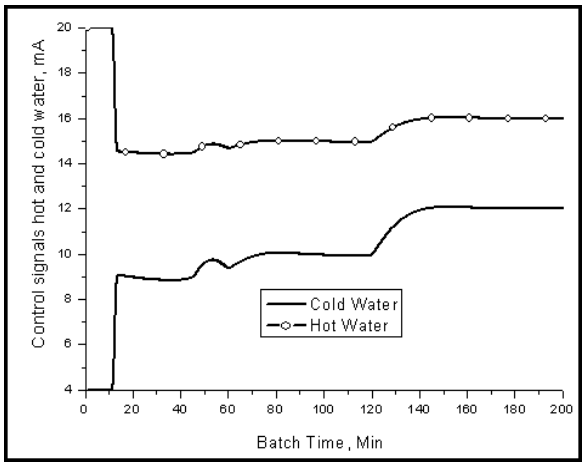

Fig.10. Control inputs of the polymer reactor.

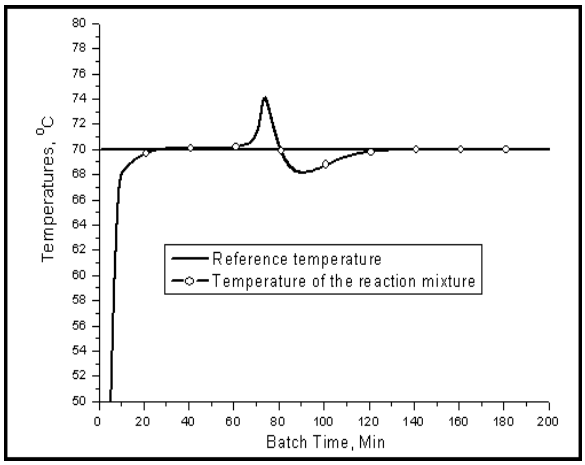

Fig.11. Constant temperature reference.

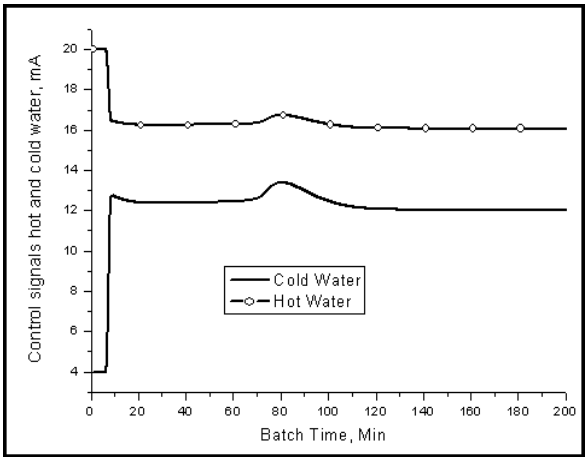

Fig.12. Control inputs of the polymer reactor.

ISSN 1313-2539

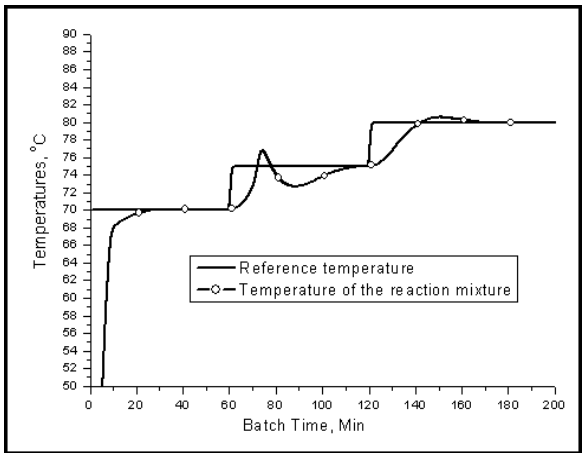

Fig.13. Step changing temperature reference.

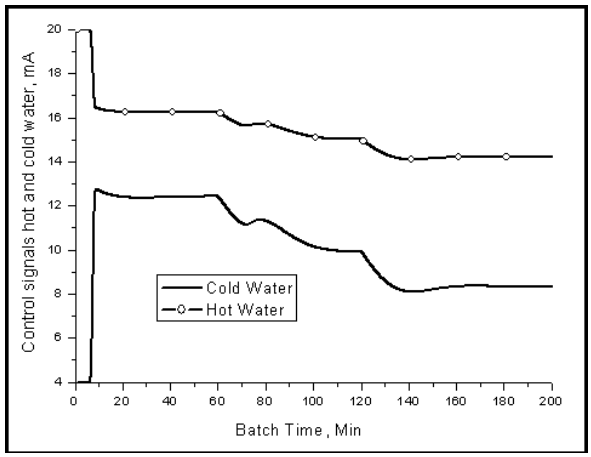

Fig.14. Control inputs of the polymer reactor.

6. CONCLUSIONS

Two different control schemes for temperature mixture control of polymer reactor are presented. The results with different set points show, that this control structures are applicable for objects with strong nonlinear character. MPC directly control the process temperature without middle PID control, which proof the advantage of using predictive controller. Comparing the two schemes we can see, that better results are received with the SIMO structure and the controller succeed to outwork the temperature reference. The future research work have to continue in direction of reduction the control time.

REFERENCES

1. V.Chitanov. Fuzzy Model Predicitve Control for temperature mixture of polymer reactor. Journal of the Technical University at Plovdiv. Vol.13, 2006 Anniversary Scientific Conference.

2. V. Chitanov, M. Petrov, M. Kiparissides. Model Predictive Control for polymer reactors, CEEPUS Cz-103 International Summer School, AAACTA, 2003.

3. V. Chitanov, M. Petrov, M. Kiparissides. Neural-Fuzzy Modeling of Polymer Quality in Batch Polymerization Reactors. Second international conference on intelligent systems, IEEE, Vol. 3, June 2004, 67-72.

4. M. Petrov, C. Kiparissides. Fuzzy model predictive control of molecular weight properties for batch polymerization reactors.

5. C. Kiparissides, P.Seferlis, P. Mourikas and Morris. Online optimizing control of molecular weight properties in batch free-radical polymerization reactors 2002 .

ISSN 1313-2539

CEREAL BREEDING AT THE INSTITUTE OF AGRICULTURE "OBRAZTSOV CHIFLIK"- RUSE, BULGARIA: I. OAT SITUATION AND PERSPECTIVES

Galina Panayotova

Institute of Agriculture and Seed Science "Obraztcov chiflik" – Ruse, Bulgaria

Abstract

Oat breeding program in Bulgaria is mainly carried out at the Institute of Agriculture and Seed Science "Obraztsov Chiflik"- Ruse. The program is focused on improving agronomically important traits in oat: yield potential, grain quality, tolerance to environmental and biotic stress and disease resistance, as well as milling, feed and hay end-use quality in both naked and hulled oat varieties. The aims of the breeding are the development of spring and winter oat varieties suitable for the environmental conditions of Bulgaria for growers, food processors and animal production systems.In view of the importance of oat germplasm for the success of the breeding the Institute has a large breeding collection included local varieties and populations, foreign varieties from the various public and private breeding programs, advanced test lines. Oat varieties development is carrying out through hybridization, advancing early generations in bulked and pedigree nurseries, followed by performance testing of selected lines. Thus, there is a need for the breeding of lines and varieties suitable for growing in many different environments throughout the country, climatic conditions in Obraztcov Chiflik are extreme with cold temperatures during the winter months and drought during the summer. The Institute of Agriculture and Seed Science "Obraztcov Chiflik" - Ruse develops and releases improved common and naked spring and winter oat varieties for the farmers and the food industry.

Key words: *cereal, oat, breeding, variety, quality, yield*

1. INTRODUCTION

Oat is one of small grains that have gained in importance in recent years, particularly with the availability of new varieties (Kirilov, 2004; Peltonen-Sainio, 1992) (figure 1). Oat is the fourth most important grain crop in Bulgaria. The oat acreage harvested for grain in 2006 is estimated to be 41 000 acres, down about 15% from 2005.

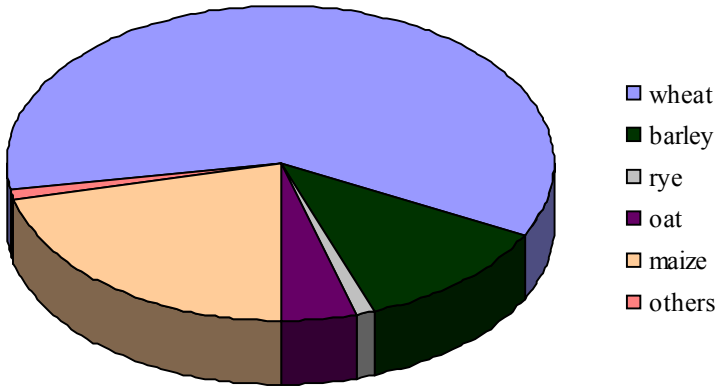

Fugure 1. Cultivated area of small grains, 2005, Bulgaria

ISSN 1313-2539

(Source: Agro statistic – BANSIK-86/2005, Ministry of Agriculture and Forestry, Bulgaria)

The privatization of agriculture in recent years has brought an increase in consumer demands for oats with enhanced quality and broader adaptability and in widening of areas (figure 2).

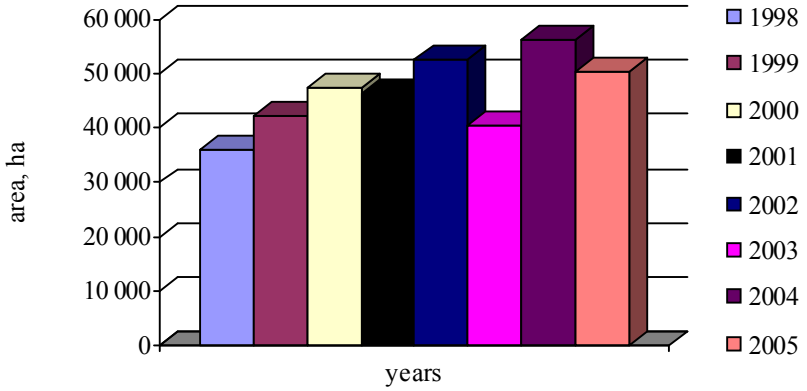

Fugure 2. Cultivated area of oat in Bulgaria

(Source: Agro statistic – BANSIK-86/2005, Ministry of Agriculture and Forestry, Bulgaria)

Short variety strength of oat in the country does not meet the market demands of forage oat varieties as well as varieties for production of baby and dietetic foods. The emphasis of the breeding is to develop new varieties of spring and winter oat with different tendencies for using, well-adapted to the environmental conditions (Panayotova, 2002). Climatic conditions in Obraztsov chiflik, near the town of Ruse are extreme in relation to temperature during winter months and drought during summer. There are natural conditions and opportunities for selection of forms, suitable for growing throughout the country.

2. OBJECTIVES

Current breeding objectives include:

2.1 Developing improved varieties and germplasm for forage grain - high yielding, dwarf, resistant to freezing, disease resistance and high grain quality

2.2 Developing improved varieties and germplasm for green mass – long-stemmed, well leafy, high high content of protein in green mass, disease resistance, suitable for joint growing with winter beans

2.3 Developing improved spring varieties and germplasm for production of baby and dietetic foods - naked grain and grain with easily dividing hulls, combining high grain yield, disease resistance, high grain protein content and balanced amino acids profile, fibers, fats and end-use quality.

2.4 High-temperature, drought, and winter freeze stress tolerance

2.5 Value adding to improve the marketability of oats

ISSN 1313-2539

3. MATERIALS AND METHODS

Breeding has three major components:

- variability,
- selection and
- testing.

3.1 Variability

The importance of oat germplasm for the success of the breeding program and for the status of ecological conditions has become more greatly appreciated. The "Obraztsov chiflik" institute disposes with a large collection that includes local and foreign oat varieties and populations, test lines, samples obtained by the National Collection of the USA, Canada and Europe, including the European Collection of sources of stability to oat diseases. The gradual study of these collected materials has revealed their potential as initial breeding materials and genetic resources (Panayotova and Mincheva, 2003). Preliminary research on large part of the collection materials was made with a view of combining the most valuable traits of the best Bulgarian and foreign oat varieties. The genetic diversity contained within this collection acts as a valuable resource for the breeding. In order to get higher percentage of seeds, different hybridization methods and techniques of pollination were tested – mechanically and chemically. By using the mutagenesis method in applied independent and combined treatment with gamma rays (Co_{60}) (Panayotova, 1995), ethyl methane sulphonate /EMS/, sodium azide (SA) and the selection assessment of mutagenic generations, lines with improved agronomic characteristics of plant and grain were isolated and used as an initial material in the selection of some valuable qualities as: productivity, dwarfness and resistance to crown rust.

3.2 Selection

Approach:

3.2.1 Development of new cultivars

In conformity with the breeding tasks set, genetic studies on the inheritance of traits, connected with grain yield and quality through hybridization in diallel crossing schedule Method II, Model I (Griffing, 1956a; Griffing, 1956b) were made (Panayotova, 2005; Panayotova and Tsenov, 2005; Panayotova and Tsenov, 2006). The evaluation of parental materials and their progenies, made in the initial stages of breeding is considerably important for a proper strategy of subsequent selection (Machan, 1989). The most frequent genetic methods, enabling this evaluation are represented by analysis of general and specific combining abilities (Caierro et al., 2001; De Koeyer, et al., 1998; Doehlert, et al., 2001). The analysis of experimental results was done on the basis of following schema:

$$x_{IJK} = \mu + g_I + g_J + s_{IJ} + e_{IJK}$$

x_{IJK} - *value of a feature selected in the cross i x j in k - th replication*

μ - *average value of the total set of crosses*

g_I - *general combining ability (GCA)of the i - th parent*

g_J - *general combining ability (GCA) of the j - th parent*

s_{IJ} - *specific combining ability (SCA) of the cross i x j*

e_{IJK} - *error*

ISSN 1313-2539

One of the main objectives of oat breeding program is using method of recurrent selection as an effective breeding procedure to produce improved oat germplasm with higher grain yield potential (Holland et al. 2002; Stuthman et al. 1992). A recurrent selection program for adaptation to diverse environments was successful in improving mean oat (Avena sativa L.) grain yield within and across testing environments.

Evaluation of winter hardiness and drought resistance of selection oat samples that are of interest for solving the breeding tasks was made (Pavlova et al., 2001; Pavlova and Panayotova, 2005, 2006). The genetic control on the character of oat development was studied in order to establish those genes that control winter and spring type of development. Investigated sources of winter genotypes in 24 spring oat varieties give an opportunity of increasing the effectiveness of the selection (unpublished data).

3.2.2. Selection of resistance to crown rust

Virulence diversity of pathogen populations in Bulgaria is studied (Momchilova, 2000). Comparison is made between efficacy of the Pc genes in Bulgaria and other parts of the world – Europe, Middle East and North America. Resistance of collection and selection materials to crown rust is studied and sources of resistance to pathogen are detached.

Stages of immune selection:

- Hybridization
- Backcross of F_1 with the recurrent parent
- Selection upon an infectious background

Including the method of intercrossing hybridization in the selection work aims to enrich the genome of common oat Avena sativa L. with genes, determining higher winter hardiness, resistance to diseases, higher quality of grain and green mass.

The working program includes all sections of selection work with winter and spring oat:

- Maintenance, enrichment and examination of the working collection,
- Hybridization in different crossing schemes and including of the initial hybrid generations in the breeding process;
- Continuing work with the hybrid generations; evaluation of yield (Panayotova, 2004), yield stability, grain quality, drought and winter freeze stress tolerance of advanced breeding lines,
- Testing

3.3 Testing

The breeding lines obtained are tested in hybrid nurseries, control testing, competition variety strain testing and propagation of perspective varieties by using the apprehended agricultural practices (Savova et al., 2005). Needed phenological observations and biometric analyses are made annually. Evaluation of winter hardiness of the hybrid generations is conducted under laboratory conditions by gradual freezing to –15^{o}C; in green house sowing; freezing in environmental test chambers and in field provocative experiments by creating snowlessness under roof structure.

Evaluation of technological qualities of oat is conducted according the quality breeding of the grain in relation to quality of oat products (Savova et al., 2005).

4. NAKED OAT

Recently, breeding efforts focused toward development of naked oat varieties, distinguished for its high content of protein, as well as for its balanced of amino acids profile, beta – glucan content and

ISSN 1313-2539

fats (Panayotova and Tsenov, 2004; Panayotova and Tsenov, 2007). Oat based foods have long been recognized for their health benefits, and it is now generally accepted knowledge that oats make a significant contribution to human health. Except as highly energetic supplement to the food rations of animals, grain of the hulless grain oat finds application in human food (Panayotova and Petkova, 2005). In recent years, we have concentrated on the development of hull-less or naked oat cultivars. This novel oat sheds its fibrous hulls during the harvesting process, thus the hull-less oat grain is higher in protein and energy content relative to its hulled, or covered, counterpart.

5. RESEARCH FACILITIES

Oat breeding research at the Institute relies on various field, greenhouse and laboratory facilities - for technological evaluation of grain, pathology and physiology laboratories, a biochemical laboratory for the relevant analyses - to accomplish the program objectives.

6. PARTNERSHIP

A critical component of this effort is the partnership that exists between the Dobrudja Agriculture Institute-General Toshevo, Institute of Agriculture – Karnobat, Agricultural University – Plovdiv, Bc Institute for Breeding and Production of Field Crops – Zagreb, Croatia. Oat breeding program rely on its associations with other European researchers and on funding from National Centre of Agrarian Sciences, Ministry of Agriculture and Forestry.

7. RESULTS

Promising yield grain potential was demonstrated in some of cultivars and breeding lines of oat breeding program in Bulgaria. Breeding efforts have resulted in developing and releasing of common and naked spring and winter varieties (Radkov et al., 1997; Staneva, 1990) and advanced breeding lines (Panayotova and Mlinar, 2005) that are also being handled through the State Variety Testing release system.

7.1 New varieties and germplasm releases:

Winter oat – Ruse 8; Jubilee 4

Spring oat – Prista 2

Spring forage oat SL-30 (Aleksi 1)

Spring naked oat N-2-7

Spring naked oat G-6

8. FURTHER RESEARCH

Further research is aimed at:

- Developing breeding strategies to improve the efficiency of selection
- Grain yield and quality maintenance under drought stress
- Understanding genetic control of early vigor
- Applying new technologies in order to enhance the efficiency of oat breeding research besides conventional breeding

ISSN 1313-2539

ACKNOWLEDGEMENTS

We express our sincere thanks to Dr. James B. Holland, North Carolina State Univ., USA and to Dr. Harold Bockelman, National Small Grains Collection, Aberdeen ID, USA for their important contributions.

REFERENCES:

1. Caierro, E., M. de Carvalho, M. T. Pacheco, C. Lonrecetti, V. Marchioro, J. G. Silva (2001) Indirect selection in oat to improve grain yield, *Sci. J. Agr. Center*. 31: 231-236

2. De Koeyer, D.L., D.D. Stuthman (1998) Continued response through seven cycles of recurrent selection for grain yield in oat, Avena sativa L., *Euphytica*. 1: 67 - 72

3. Doehlert, D.C., M.S. McMullen, J.J. Hammond (2001) Genotypic and environmental effects on grain yield and quality of oat grown in North Dakota, *Crop Sci.* 41: 1066-1072

4. Griffing, B. (1956a) A generalized treatment of the use of diallel crosses in quantitative inheritance, *Heredity.* 10: 31–50

5. Griffing, B. (1956b) Concept of general and specific combining ability in relation to diallel crossing system, *Australian J. of Biol. Sci.,* 9: 463 – 493

6. Holland, J.B. et al. (2002) *Euphytica* 126: 265–274

7. Kirilov, A. (2004) Fodder oats in Europe, In: *Fodder oats: a world overview*; Ed. Suttie J.M. and S.G. Reynolds, FAO. 179-196

8. Machan, F. (1989). Evaluation of combining ability of oat varieties, *Scient. agr. bohemoslov*, 2, 91-97

9. Momchilova, P. (2000) PhD Thesis, IASS, Ruse, 136 pp (in Bulgarian)

10. Panayotova G., D. Petkova (2005) Development of high quality oat varieties for human consumption, *Proc. of Jubilee conference: 50 years ICC* –1955 – 2005, "Cereals – the future challenge", Vienna, Austria, 1: 145

11. Panayotova, G. (1995) Effects of treatment with gamma rays (Co_{60}) on the productivity of M_1 generations of oats (Avena sativa L.), *Proc. Sci. Conf. of IASS*, 1: 46-50.

12. Panayotova, G. (2002) Oat breeding program at the Institute of Agriculture, Ruse, Bulgaria, *Oat Newsletter* 48; http://wheat.pw.usda.gov/ggpages/oatnewsletter/v48/

13. Panayotova, G. (2004) Evaluation of Grain Yield Potential of Oat Germplasm in Bulgaria, *Agrifood Research Reports, MTT, Finland*, 51: 157. www.mtt.fi/met/pdf/met51.pdf

14. Panayotova, G. (2005) *Combining ability of spring oat samples (Avena sativa L.) concerning grain yield and quality*, PhD Thesis,

15. Panayotova, G., N. Tsenov (2004) Combining ability for β-glucan content of oat (*Avena sativa* L.) grain, *Field Crops Studies*, 1, 3: 378-382.

16. Panayotova, G., N. Tsenov (2007) Combining ability of naked spring oat varieties (*Avena sativa* L.) for grain number per panicle, *Field Crops Studies* (in press)

17. Panayotova, G., R. Mincheva (2003) New oat germplasm sources for breeding, *Proc. Int. Sci. Conf. of Ruse University*, 40: 106-109.

18. Panayotova, G.; R. Mlinar (2005) Biological and economical properties of spring oat (Avena satuva L.) varieties and perspective breeding lines. *Plant Science*. 42, 2: 165-168 (in Bulgarian)

ISSN 1313-2539

19. Pavlova, S., G. Panayotova (2005) Ecological stress of spring oat varieties and breeding lines (Avena sativa L.), Union of Scientists - Ruse, 5: 44-47.

20. Pavlova, S., G. Panayotova (2006) Biological traits of spring oat seeds samples, obtained under conditions of ecological stress, Journal of Central European Agriculture, 7, 1: 198 *www.agr.hr/jcea/issues/jcea7-1/*

21. Pavlova, S., G. Panayotova, A. Prodanova, L. Nikolova (2001) Drought resistance of oat cultivars and breeding lines from the Institute of Agriculture and Seed Science "Obraztcov Chiflik", Ruse, *Union of Scientist of Bulgaria*, 3, 56-60 (in Bulgarian)

22. Peltonen-Sainio, P. (1992) The Achievements of Oat Breeding, In: Slafer, G.A.(Editor), *Genetic improvement of field crops,* Marsell Dekker, Inc., NY, 69-94

23. Radkov, P., G. Panayotova, S. Pavlova, P. Momchilova (1997) Prista 2 – new spring oat variety, *Plant Sci.,* 1, 43-46 (in Bulgarian)

24. Savova, T., G. Panayotova, T. Georgieva, (2007) Estimation of the oat source material according the quality breeding of the grain, *Field Crops Studies* (in press)

25. Savova, T., P. Penchev, V. Koteva, B. Zarkov, S. Stankov, D. Atanasova, N. Antonova, T. Georgieva, G. Panayotova, H. Krysteva, J. Karadjova, N. Bakardjieva, V. Vencislavov (2005) Oat Growing Technologies, Sofia, ISBN 954-749-056-7, pp. 62

26. Staneva, B.I. (1990) Spring oat variety Obrazcov chiflik 4, *Proc. of IASS "Obrazcov chiflik"-Ruse Conference*. 1: 110-117 (in Bulgarian)

27. Stuthman, D.D. et al. (1992) *Proc. of 4th Intern. Oat Conference* Adelaide, South Australia. 1: 70-76

International Scientific Publications: Materials, Methods and Technology, Vol. 1
ISSN 1313-2539

EMOTIVE PRODUCT DESIGN BY SWARM INTELLIGENCE MODELLING

Alexander Nikov[1], Arvind Mohais[1], Selahattin Nesil[2]

[1]Department of Mathematics and Computer Science, University of the West Indies, St. Augustine, Trinidad and Tobago (W.I.), E-Mail: {anikov, amohais}@fsa.uwi.tt

[2]Department of Electronics Engineering, Fatih University, 34500 Istanbul, Turkey, E-Mail: snesil@fatih.edu.tr

Abstract

The purpose of this paper is to apply swarm intelligence in Kansei engineering and explore ways to integrate it into an industrial product development process. For connecting customer emotional needs mathematically to product design properties a particle swarm optimization (PSO)-based approach is proposed. Using PSO, together with the Huffman algorithm, a generic factor was extracted, and used to define product design features. Emotional customer needs are derived bottom-up using Kansei words. PSO approach is illustrated and validated by a case study for pen design. Participants' emotional responses for 13 different pens with 3 design properties were collected for 12 Kansei words measured in 5-point semantic differential scale. Experimental work in implementing the proposed approach was able to suggest credible design attributes of a pen that would be considered optimal by all of those surveyed. The advantages and further developments of approach proposed are discussed.

Key words: *emotive design, integrating feelings in design process, swarm intelligence, particle swarm optimization*

INTRODUCTION

Tendencies in product development of today make it likely that many future products will be functionally equivalent and therefore hard to distinguish between for customers [15]. They will decide by highly subjective criteria which product to purchase. One goal for product development in this context is to be able to capture the customer's considerations and feelings regarding products and translate these emotional aspects into concrete design characteristics.

Emotive/affective design attempts to define the subjective emotional relationships between consumers and products and to explore the affective properties that products intend to communicate through their physical attributes [1], [2]. It aims to deliver artifacts capable of eliciting maximum physio-psychological pleasure from consumers, targeting all of their senses. Saul Carliner [1] defined the affective design as the third level of a three-part model of information design. The systematic framework [2] conceptualizes customer affective needs in product design.

The aesthetic intelligence [10] acknowledges that we possess an innate, sometimes subconscious, ability to perceive a wide range of qualities in products that shape our responses to them. These qualities can be purposefully discussed and provide engineering designers a way of structuring the complex field of aesthetic response. A process of designing for the senses can be viewed as a means of providing products with which customers can feel a greater degree of empathy.

The approach [5] is based on respect for the user of electronic products. It uses bodily skills to make electronic interaction more tangible, and, as humans are emotional beings, to make interaction a more fun and beautiful experience. It focuses on those neglected aspects of human-product interaction: perceptual-motor and emotional skills. To get to new innovative products, the interaction problem is dealt with on the level of creating a context for experience allowing for rich aesthetics of interaction.

A number of different methods, such as Quality Function Deployment, Semantical Environment Description, Conjoint Analysis and Kansei Engineering are used in emotive product design. Kansei Engineering helps to identify customer needs, their importance and the technical responses as well as

ISSN 1313-2539

to conduct benchmarking and to connect the customer needs mathematically to the technical responses [4], [15]. It is applied in many studies on a macro level, a micro level and for verifying purpose. Statistical methods like regression analysis, general linear model, qualification theory type 1, as well other methods like genetic algorithms, fuzzy sets and rough sets are used to give a mathematical connection between customer emotions mapped through Kansei words and the product properties [9], [15]. But there are no applications of swarm intelligence methods in Kansei Engineering for emotive product design. Therefore we propose to use swarm intelligence to analyzing customers' emotional responses with regard to products, and to try to propose design properties that embody those responses.

The term *swarm intelligence* is used in artificial intelligence and evolutionary computation research to mean a variety of things. In this paper it will be used in the context of Particle Swarm Optimization, which is an evolutionary algorithm based on observed social interactions in nature that can be mimiced in order to solve optimization problems [6], [7]. We propose to employ swarm intelligence to aggregate emotional design keywords and to suggest product design properties.

DESCRIPTION OF APPROACH FOR SWARM-OPTIMIZATION-BASED EMOTIVE DESIGN

An approach is proposed, which suggests product design properties based on emotive responses. It uses a combination of Kansei techniques and an evolutionary optimization algorithm called Particle Swarm Optimization. The overall process involves designing a survey to collect data on customers' emotional responses to various aspects of a product and then using the swarm intelligence technique to analyze the collected data in such a way as to propose product design suggestions.

Emotive design steps

Figure 1 shows at a high-level, the set of steps that are proposed for determining desirable design properties of a product. An illustration of these steps will be presented in a case study.

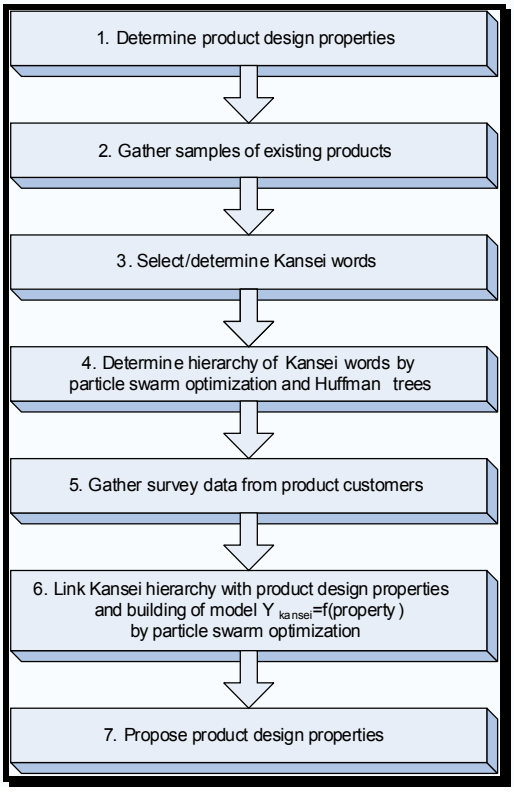

Figure 1. Emotive design steps

ISSN 1313-2539

Particle swarm optimization algorithm

In this subsection, a general description of the Particle Swarm Optimization (PSO) algorithm will be given using terms of a general optimization function. At a later point in the paper, the PSO algorithm will be used twice, first, in step 4 of Figure 1, where the optimization task will consist of building a binary tree using the Huffman algorithm [5] that minimizes a weight function, and second, in step 6 of Figure 1, where it will consist of fitting a number of binary design parameters to the output of the selected tree from step 4.

Particle swarm optimization (PSO) is an algorithm that is inspired by social interactions of insects, animals, and even human beings [6], [7]. Given the problem of finding a minimiser of the optimization function $f: R^n \to R$, (where R is the set of real numbers) the PSO algorithm works on a set of candidate solutions called *particles*, "flying" them through the solution space R^n for a certain number of generations until a solution is found, or time constraints force the termination of the algorithm. Each particle $P = (x, v, p_b, f_x, f_{pb})$ consists of a position vector $x \in R^n$, a velocity vector $v \in R^n$, a previous best position $p_b \in R^n$), a fitness value $f_x = f(x)$) and a previous best fitness value $f_{pb} = f(p_b)$.

The set of particles used by the algorithm called population $POP = (P_0, \dots, P_{m-1})$ is represented by a vector of m particles. They exchange information with others in the population, and it is thus that evolution of the candidate solutions takes place. The manner in which information is exchanged between particles is constrained by *neighborhoods*. Each particle P has a *neighbourhood,* which is a subset of the population $N(P) \subseteq POP$ and each element of $N(P)$ is called a *neighbor* of P. The neighbors in $N(P)$ are not determined based on their positions in the search space; they can be completely arbitrary. All of the neighborhoods taken together, i.e. $N = \{N(P_0), \dots, N(P_{m-1})\}$ can be represented by a directed graph $G_N = (V, E)$, where $V = \{0,1, \dots, m-1\}$ and $E = \{(i,j) | P_j \in N(P_i)\}$. This graph is called a *neighborhood graph* or a *neighborhood structure.*

At each iteration of the PSO algorithm, each particle has its position updated in two steps. First a new velocity vector is computed by among other things, consulting with neighbors to determine their best positions encountered thus far in the run of the algorithm, as well as using the particle's own previous best experience. And then the position vector is updated by adding the newly calculated velocity vector to the current position. These steps are summarized by the following equations, specific formulae for the velocity update equation will be consider below.

$$v' = update - velocity(x, v, p_b, N(P))$$

$$x' = x + v'$$

A pseudocode description of the basic PSO algorithm is given in Figure 2 and that of the subroutine `find_neighborhood_best_index()` is given in Figure 3. In Figure 2, K_1 and K_2 are called *individual* and *social* constants; they are parameters of the algorithm and represent the degrees of importance allocated to each of the individual and social influences, respectively.

Velocity update equation

The velocity update equation is a very important aspect of the algorithm. The most basic formula used is $v' = v + \phi_1(p_b - x) + \phi_2(p_* - x)$. Modified versions are common. Clerc and Kennedy [2] introduced the *constriction factor* χ making the equation $v' = \chi(v + \phi_1(p_b - x) + \phi_2(p_* - x))$. Regarding this equation, typical values used in experimental work are χ =0.729 and ϕ_1, $\phi_2 \sim$ U(0,2.05). Mendes altered the equation so that the particle is influenced by all of its neighbors, not just the best one [11], [12], [13]. This scheme, called the *Fully Informed Particle Swarm* (FIPS) operates as follows. For a particle P letting $\phi_k \sim U\left(0, \frac{\phi_{max}}{|N(P)|}\right)$ for all $k \in N(P)$, and letting $P_{fips} = \frac{\sum_{k \in N} W(k)\phi_k k.p\_b}{\sum_{k \in N} W(k)\phi_k}$, the velocity update equation becomes $v' = \chi(v + \phi(p_{fips} - x))$. ϕ_{max} is usually

ISSN 1313-2539

set to 4.1 and χ to 0.729. $W(k)$ is a weighting function that scales the contribution of the neighbor k. It may be desired to weight neighbors' contributions in proportion to their fitnesses, or their distances from the current particle. Alternatively, with $W(k)$=1 $\forall k \in N(P)$, all neighbors contribute equally to the velocity update equation; in this case, $P_{fips} = \frac{\sum_{k \in N} \phi_k k.p_b}{\phi}$, where $\phi = \sum_{k \in N} \phi_k$.

```
set t=0
initialize_population(m,n,x_max)
initialize_neighborhoods(m)

  while ( NOT termination-condition ) {
     for (i=1; i <= m; i++){
        * = find_neighborhood_best_index(N(i))

              for (d=1; d <= n; d++){
           φ1 = K1 · random(0,1)
           φ2 = K2 · random(0,1)

           for particle Pi:
               v_d = update − velocity(v_d, p_bd, p_*d, φ1, φ2)

           enforce_maximum_velocity(P_i, v_d, v_max)

           P_i.x_d = P_i.x_d + P_i.v_d
        }

        P_i.f_x = f(P_i.x)
        if (P_i.f_x < p_i.f_pb){
           P_i.p_b = p_i.x
           P_i.f_pb = P_i.f_x
        }
     }
  }
```

Figure 2. Pseudocode for the PSO algorithm

```
find_neighborhood_best_index(N){
  set idx = α, for some α ∈ N
  for each j ∈ (N − {α})
    if (P_j.f_pb < P_idx.f_pb))
      idx = j
  return idx
}
```

Figure 3. Pseudocode for finding the neighborhood best index

In [8], it was concluded, counter-intuitively, that weighting neighbors' contributions based on fitness does not help the algorithm. In this paper FIPS with equal weighting is used for all experimental work.

ISSN 1313-2539

Neighborhood Structures

PSOs typically use one of two neighborhood configurations. The first is called the *ring topology* (cf.

Figure **4**a. In this structure, particles are arranged in a circular manner and each is connected to the two particles on its left and right. The second commonly used structure is called the *global topology* (cf.

Figure **4**b. Here each particle is connected to all other particles in the population. It is commonly accepted that the global neighborhood leads to too much information being exchanged too quickly, resulting in the premature convergence of the algorithm. Nevertheless, this is a commonly used structure by researchers who are focused on other aspects of the PSO algorithm. In this paper a different type of neighborhood is used: *random* neighborhoods. These are directed, randomly generated graphs Two parameters affect the nature of the neighborhood graph structure used: the neighborhood size *n* and the uniform out-degree of the graph *k*. *n* is the number of nodes in the graph and hence the number of particles in the swarm. *k* is the number of neighbors that each particle influences.

Figure **4**c shows an example of a graph with 12 nodes and with a uniform out-degree of 2.

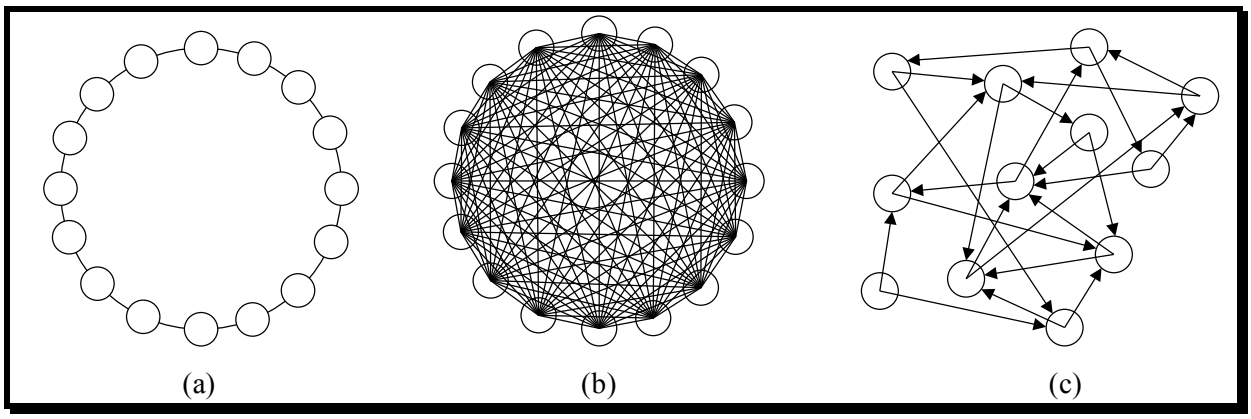

Figure 4. The ring structure, the global structure and a randomly generated structure.

Neighborhood dynamism

Randomized neighborhood re-structuring was introduced in [14]. Under this approach, given values for the *n* and *k* graph parameters, the neighborhood graph is subjected to massive perturbations from time to time, according to a *dynamism probability,* p_{dyn}. This drastic change is called *re-structuring* and involves generating an entirely new random graph, but with the same *n* and *k* values. At the end of each iteration, this operation is performed with probability p_{dyn}. It is possible to use a fixed value of p_{dyn} for the entire run of the algorithm, or a time varying value may be used. For example, using a linearly decreasing dynamism probability from p_{dyn} = 1.0 down to 0.0 over the duration of the run may be used. This means that at the first iteration p_{dyn} = 1.0, and at each iteration, it is decremented by $\frac{1.0}{\text{max-iterations}}$, where max-iterations is the maximum number of iterations that would be executed by the algorithm; this is equal to the maximum number of function divided by the population size. In this way, as the algorithm progresses, the probability of a total re-structuring operation becomes less and less.

Specific PSO adaptations for emotive product design

In this subsection, specific models will be given for the types of optimization functions that will be considered for the Emotive Product Design task being considered.

ISSN 1313-2539

Evolving a binary tree using the Huffman algorithm

Step 4 of Figure 1 represents the creation of a hierarchy of the Kansei words used in the study. This is done by evolving a tree using the Huffman algorithm [5], by means of a PSO. Each particle of the PSO is *n*-dimensional, where *n* is the number of Kansei words used in the survey. Each dimension represents a weight assigned to the corresponding questionnaire item.

The weights embodied by each particle are then used to create the tree. Each weight is used to create a leaf node of the eventual tree, and as is usual in such a construction, higher level nodes are created by selecting the two with the smallest weights and aggregating them into a new node whose weight is the sum of the weights of the two children.

In order to evaluate a particle in the PSO, the data vectors (assume there are *l* of them) of the Kansei survey are introduced as inputs at the leaf level of the Huffman tree corresponding to the particle's weights, and a fitness value is computed using the following formula:

$$fitness(tree_x) = \sum_{i=1}^{l}\sum_{j=1}^{n} data_{ij} * pathlength(leafnode_j)$$

The weights of the nodes are not directly used in the computation, instead for each leaf node of the tree, the path length from it to the root is calculated and multiplied by the input value form the survey data corresponding to that node, this computed value is then added to a cumulative sum. After all of the survey vectors have been processed, the cumulative sum serves at the fitness value of the particle.

Fitting binary design parameters to the tree output.

For step 6 in Figure 1, a PSO is again used, this time to fit the product design properties (see step) to the output of the tree from step 4. Here, categorical design properties are converted into binary design properties. For example, if property *A* can have values of *a*, *b*, or *c*, then this will be converted into three binary properties A_a, A_b, and A_c, each of which can be *true* or *false* (*1* or *0*). Depending on which value *A* possesses, the corresponding binary property will be set to *true* and all others to *false*.

For the PSO used here each particle is *p*-dimensional, where p is the number of binary product design properties. Each dimension of a particle represents a weight associated with one of the binary properties. The fitness of a particle in this phase is calculated using the following formula:

$$fitness(x) = \sum_{i=1}^{l}\sum_{j=1}^{p} x_j \cdot bin\_data_{ij}$$

where *l* is the number of data vectors from the Kansei survey and bin_data_{ij} represents the binary properties derived from the categorical product design properties.

CASE STUDY

3.1 Kansei survey

To illustrate and validate the PSO approach for aggregating Kansei words and suggesting product design properties, a case study for design of pen for students of Fatih University, Istanbul was carried out. 13 pens of varying characteristics were presented to 23 students and they were asked to answer a questionnaire based on their feelings about each of the pens. This produced 299 data vectors which will be referred to as $data_{ij}$, where i is a vector index, and j is a questionnaire item index.

ISSN 1313-2539

The questionnaire consisted of 12 semantic differential Kansei words measured in 5-point scale (cf. Table 1), and 3 pen properties (cf.

Table *2*). The first 11 items were used to group the Kansei words by evolving a binary tree using PSO, and the last 3 items (13, 14 and 15) were used for fitting the design properties to the output of this tree. The 13 pens used in the case study are shown in Figure 5.

3.2 PSO parameter values

FIPS-based PSOs with dynamic neighborhood re-structuring for a maximum of 120000 function evaluations were used. As a preliminary step, the neighborhood parameters were kept fixed at n = 30 and k = 4. These values were shown in other applications to produce high-performance PSO results.

The number of data vectors l=299 and the number of questionnaire items considered n=11 (corresponding to questionnaire items 1-11). Hence the optimization function for step 4 of Figure 1 becomes:

Table 1 - Scaled questionnaire items**.**

Questionnaire item number	**Questions**		
1.	Unimposing	1-2-3-4-5	Imposing
2.	Straight	1-2-3-4-5	Curved
3.	Cool Feel	1-2-3-4-5	Warm Feel
4.	Conservative	1-2-3-4-5	Modern
5.	Ugly	1-2-3-4-5	Beautiful
6.	Unpleasant	1-2-3-4-5	Pleasant
7.	Low quality	1-2-3-4-5	High quality
8.	Feminine	1-2-3-4-5	Masculine
9.	Hard to write	1-2-3-4-5	Easy to write
10.	Bad Design	1-2-3-4-5	Good Design
11.	Thin	1-2-3-4-5	Thick
12.	Unfit for FU students	1-2-3-4-5	Fit for FU students

Table 2 - Categorized product properties.

Questionnaire item number	**Product property**	**Product property values**
13.	Pen length	[1] short [2] average [3] long
14.	Pen volume	[1] thin [2] average [3] fat
15.	Pen color	[1] mixed color [1] white [2] blue [3] green [4] yellow

ISSN 1313-2539

Figure 5. Sample of pens used in the case study

$$fitness(tree_x) = \sum_{i=1}^{299}\sum_{j=1}^{11} data_{ij} * pathlength(leafnode_j)$$

There were 3 categorical design properties (questionnaire items 13, 14 and 15), with 3, 3 and 5 categories respectively, yielding 11 binary design properties. Thus the optimization function for step 6 of Figure 1 becomes:

$$fitness(x) = \sum_{i=1}^{299}\sum_{j=1}^{11} x_j \cdot bin\_data_{ij}$$

The desired fitting is illustrated in Figure 6 .

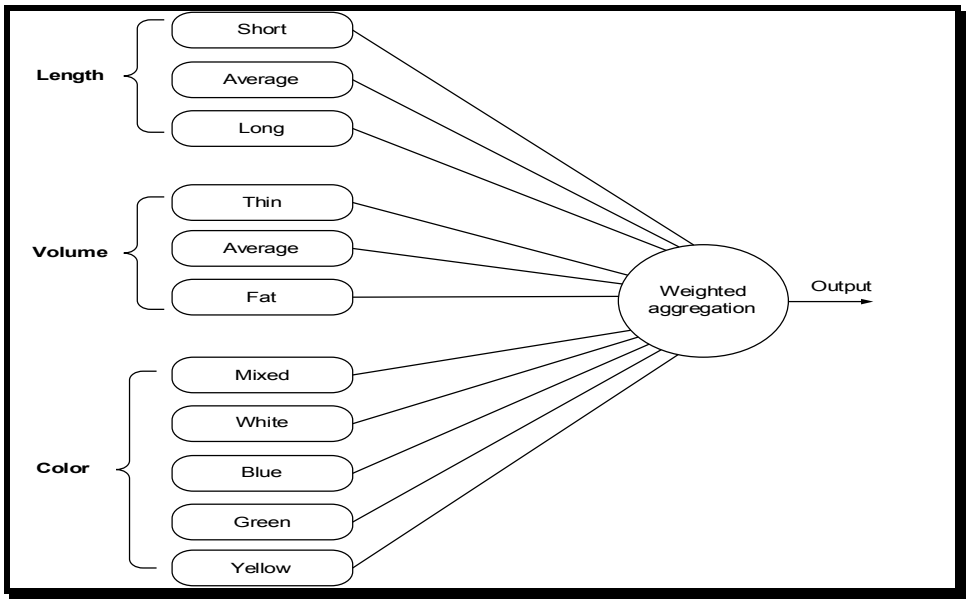

Figure 6. Linking binary design properties to the Huffman tree output

ISSN 1313-2539

3.3 Case study results

The best result obtained by the PSO algorithm using the specified configuration is the tree shown in Figure 7, where the circled numbers are the weights of the question items q_i.

The fitting of the binary design properties to the output of the tree in Figure 7 yielded the results shown in

Table *3*. Based on these results the most important Kanseis for Fatih University students seemed to be long pens with average volume and blue color. This fits also with the logo color of university. Those considered of students to be of less importance is thin pen with average length and white color.

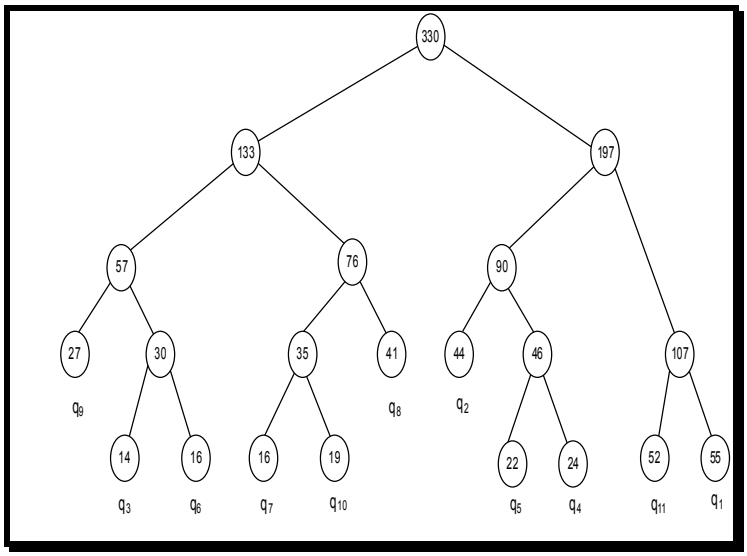

Figure 7. The optimal binary tree

Table 3 Design properties results

Length	Value	Volume	Value	Color	Value	MSE
short	1.4416	thin	0.1451	mixed colors	1.1949	0.0283
average	1.4287	**average**	**0.1581**	white	0.9520	
long	**1.5257**	fat	0.1483	**blue**	**1.1968**	
				green	1.1504	
				yellow	1.1074	

CONCLUSIONS

A particle-swarm-optimization-(PSO)-based approach for emotive product design was proposed. The most popular swarm intelligence method, the particle swarm optimization algorithm, was used to model the relationship between Kansei words and product design properties. It is a simple, feasible and versatile approach determining the combination of product properties that could results in designs taking into account customer emotions. A model evolved by the particle swarm predicts the desired values of product design properties. Depending on these values relevant product designs can be proposed.

ISSN 1313-2539

For illustrating and validating the PSO-based approach a case study of pens for Fatih University was carried out. Relevant Kansei words, three product design properties and sample pens were defined. Based on data gathered from Fatih University students and using the approach, a relevant pen design was determined. The proposed approach can be used for emotive product design.

Some **advantages** of the approach proposed are:

- Particle swarm optimization is a very flexible evolutionary computation method that can be adapted to different optimization tasks and as was done in this paper, it can be re-used in different phases to help solve a problem.
- The use of binary trees built using the Huffman algorithm, provided a standard method of aggregating Kansei words based on numeric weights, without having to consider the semantics of the words themselves.

This work is preliminary and there is room for **further developments**, such as:

- Modified trees using 3, 4 or more children could be considered. Variable numbers of children could also be considered.
- PSO neighborhood and dynamism parameters such as the number of nodes, the uniform-out degree and the dynamism probability could be investigated with a view to improving the optimization of both phases of the approach.
- Attempts could be made to fit the binary design parameters to nodes in the tree, other than the root node.
- Emotional PSOs [3], which presents a modification of the PSO algorithm introducing some psychology factor of emotion into the algorithm may be considered for use in this application.

REFERENCES

[1] Carliner S. (2000) Physical, Cognitive, and Affective: A Three-Part Framework for Information Design. http://saulcarliner.home.att.net/id/newmodel.htm (visited 16 May 2007).

[2] Clerc M. and Kennedy J. (2002) The Particle Swarm - Explosion, Stability, and Convergence in a Multidimensional Complex Space. *IEEE Transactions on Evolutionary Computation*, 6(1), 58-73.

[3] Ge Y. and Rubo Z. (2005) An Emotional Particle Swarm Optimization Algorithm. In Proceedings of the International Conference on Advances in Natural Computation (China), Springer Berlin / Heidelberg, pp. 553-561.

[4] Grimsæth K. (2005) Kansei Engineering. Linking emotions and product features. Undergraduate Thesis, Norwegian University of Science and Technology (NTNU) http://design.ntnu.no/forskning/artikler/2005/artikkel_Kansei_Engineering_K_Grimsath.pdf (visited 16 May 2007).

[5] Huffman D.A. (1952) A method for the construction of minimum redundancy codes, *Proc. IRE*, vol. 40, pp.1098-1101.

[6] Kennedy J. and Eberhart R. (1995) Particle swarm optimization. *In Proceedings of the IEEE International Conference on Neural Networks*, IEEE Press, pp.1942-1948.

ISSN 1313-2539

[7] Kennedy J., Eberhart R. and Shi Y. (2001) *Swarm Intelligence*, Morgan Kaufmann, San Francisco.

[8] Khalid H. M. and Helander M. G. (2004) A framework for affective customer needs in product design. *Theoretical Issues in Ergonomics Science*, 5(1), 27-42.

[9] Lee S. H., Harada A. and Stappers P. J. (2000) Pleasure with Products: Design based on Kansei. In Chapter 16 of *Pleasure with Products: beyond usability*, by W. S. Green (Ed.), Taylor and Francis, pp. 219-230.

[10] MacDonald A. S. (2001) Aesthetic intelligence: optimizing user-centred design. *Journal of Engineering Design*, 12(1), 37-45.

[11] Mendes R., Kennedy J. and Neves J. (2003) Watch thy neighbor or how the swarm can learn from its environment. In *Proceedings of the Swarm Intelligence Symposium*, IEEE Press, pp.88-94.

[12] Mendes R. (2004) *Population Topologies and Their Influence in Particle Swarm Performance*, PhD thesis, Universidade do Minho, Braga, Portugal.

[13] Mendes R., Kennedy J. and Neves J. (2004) The fully informed particle swarm: Simpler, maybe better. *Transactions on Evolutionary Computation*, 8(3), 204-210.

[14] Mohais A., Mendes R., Ward C. and Posthoff C. (2005) Neighborhood Re-structuring in Particle Swarm Optimization. In *Proceedings of the Australian Conference on Artificial Intelligence*, Springer, Berlin, pp.776-785.

[15] Schütte S. (2002) *Designing Feelings into Products: Integrating Kansei Engineering Methodology in Product Development*, PhD Thesis, Linköping University.

ISSN 1313-2539

DESIGNING OF THE ROAD NETWORK IN WOOD OF THE SECOND GROUP

Jane Iv. Bavbel, Petr Al. Lyshchik

Belarussian state technological university, Department of Technology and machines of logging and forestry, Sverdlova str. 13a, 220050, Minsk, Belarus. E-mail: jane18@mail.ru.

Abstract

Road location is the "foundation" of any road. A road constructed in a poor location can fail and cause serious environmental damage, as well as add financial strain from continuous and costly maintenance problems. A road location must be accomplished on the ground, regardless of the procedures used for road construction control (whether direct location or survey) to assure a road can be properly constructed to meet management and environmental objectives. In either method, the goal is to get a road from one point to another in the most efficient manner, with the least amount of earth movement and the least amount of follow-up maintenance and environmental damage, given slope, topography, and ground stability, as well as the operating constraints of the vehicle, such as turning radius and grade.

The purpose of planning roads for timber exploitation is to try to achieve the combination of road cost and extraction cost (and sometimes road haulage cost as well) which gives the lowest overall cost of moving timber. There may, of course, be other purposes for roads through woodlands, such as general management, access for sporting and to property beyond the forest edge. Such needs may generally be accommodated within the road system designed for timber extraction.

Keywords: *forest roads, location, forest network, road density*

1. INTRODUCTION AND SCOPE RESEARCH

In Belarus, nearly 38 percent of the country is forested and hosts numerous beautiful and multifunctional natural resources.

Most forests - 9,4 million ha - and a volume amounting to almost 1433,9 million m^3 of standing trees, of which about 90 percent have a productive function, are located in the northern, north-eastern and south-eastern parts of the country, in remote areas with fairly high and steep lands. Because of the fact that these areas are far from rural or industrial centers and because road infrastructures are seriously lacking, access and penetration into forests is not easy and makes exploitation and silvicultural activities difficult [1].

We have actually altogether 14 852 km of roads network, with an average density of 2,2 m/ha, of which 65 percent constitutes high forests and the rest coppice. Around 10 862 km are macadam coated and allow annual circulation of transportation means, whereas the other part has a seasonal function, more especially from May to October.

As far as the technical situation is concerned, only 30 percent of the road network is in good condition, while the other part requires numerous and sometimes major management works.

The lack of a road network, the difficulty encountered when attempting to carry out silvicultural works or exploitation cuttings in old forests, explains the inadequate level of working methods and sometimes the use of a technology ecologically damaging and ill-adapted to the prevailing conditions of Belarusian forest lands.

The experience gained to-date by many countries and the results obtained have confirmed the importance and functions of an optimum density road network for forest management and scientific

ISSN 1313-2539

treatment, through the practice of intensive and nature-oriented silviculture. In addition, a good forest road network makes possible the utilization of modern exploitation and transportation methods [2].

As far as Belarusian forests are concerned, the studies carried out indicate primarily the urgency of setting up an adequate road infrastructure which will permit to harmonize ecological, technical, economic and social factors.

These studies draw attention to the following facts: 71 percent of forests have to be very well served and need a good road network; in high forests the road network has to increased to 4,3 m/ha; considering the actual state of our forests, manual unloading proved more effective on average distances (hand rolling) of 100-120 m; tractors on distances of 250-300 m; skylines on distances of 400-600 m.

The main trends and prospects still to be attained are: estimate of ecological data for each sector of the forest economy, where their environmental function occupies the first rank; the extension of the road network in the form of main roadways taking the exact shape of the valley and with short roads within plots; wood unloading according to simple or combined technological schemes, in the first place manual rolling downhill, tractors, skylines, etc.; a higher mechanization level in road works; optimum values and economic efficiency of road density and unloading distances; positive contribution of the road exploitation for tourism, leisure and restful activities, etc.

In short, these trends are among our most ambitious objectives in forestry and for their accomplishment funds, working means and technical assistance are sought from foreign organizations. In this manner, we would accomplish the extension of a properly designed and profitable road network capable of fulfilling its complex role with a special care for environment and nature.

2. THE PROBLEM OF BUILDING FOREST ROAD NETWORK

Belarus, a small country situated in the Europe, counts shading and forests among its most splendid and multifunctional natural resources.

Forests are mainly situated in the central, northern and southeastern parts of the country, in hilly lands and present a rough configuration. At the same time, most particular is the fact that they stretch onto lands considered "remote", far from rural or industrial inhabited areas. The distance worsens even more the lack of road infrastructure, essential to forest accessibility and to entrance into these forests. Because they cover various functions, priority must be given to adequate installations also matching the requirements of silviculture [1].

Actually, a 14 852 km long road network has been implemented with the aim to serve forest natural resources in our country. Out of 14 852 km of roads (total length), 73 percent are macadamized roads and permit the transportation of wood all year round, whilst the other part fulfils seasonal functions, mainly during the period May-October. As far as the technical situation is concerned, about 3 989 km, or 27 percent, are in a good condition, whilst the other part requires a lot of management work.

Compared to the total forest area, the road density index is very low, only 2.15 m/ha and in the case of productive forests 4.3 m/ha. These are mean values for this specific country whereas many particular economies have a higher density, thus rendering possible the access to mature forest, the application of appropriate techniques and technologies in silvicultural work, and distant transport of main and secondary forest products in close and distant areas. Table 1 gives the actual state of the road network, at the national level together with a few of its most typical characteristics.

ISSN 1313-2539

Table 1 - Typical characteristics of the forest road network.

Total Length (km)	Total Area (1000ha)	Road Density (m/ha)	Whole-year road network				Technical state of the road network			
			Macadam		Without macadam		Good		Bad	
			%	km	%	km	%	km	%	km
14 852	6921,89	2,15	73	10 862	27	3990	27	3989	73	10 863

From the data given in the table, concurrently to the low road network density, the value of other pertinent indexes is not satisfactory and limits activities in many forests, such as the introduction of silvicultural works, or does not allow particular forests to be multifunctional.

The serious technical situation of 73 percent of the road estate, the fact that only 73 percent of the existing roads are in a unsatisfactory condition, which prevents the all-year-round circulation of transport means, are more important than the savings generated by 10 percent of the high forests with a 13.5 million m3 volume of standing trees, without a single linear metre of roads suitable for motor vehicles. All this requires appropriate and efficient care, attention and investments with regard to road infrastructures.

Together with the lack of a road network, the difficulty of practicing fellings in old forests has also imposed an inadequate level of mechanization in the technological process and sometimes the use of technologies prejudicial to the environment and not well adapted to our forest lands, which are predominant on very hilly areas.

It is known that the extension of the road network in forested areas dates back to the first decades of this century. Nevertheless, the existing results, gained from experience in many countries, have certified the importance and the role it plays as a basic constituent and a permanent element in the modern forest exploitation system and transportation process. In the meantime, it allows operations related to forest management and scientific processing of wood, as well as the practical operation of an intensive and naturalistic silvicultural programme [3].

Nowadays, the experience gained in many countries has demonstrated the validity of these methods. The positive results deriving from a good road infrastructure and the profitable solutions that follow show how important this extension is for the present forest economy.

The extension of a road network depends on several factors and their study looks into their ecological, technical and economic effects on nature

A particular attention is devoted to the extension of a road network in high forested areas. About 87 percent of our forests are situated on hilly or plain lands starting with a 67 percent and more gradient, forested with coniferous trees (particularly shrinkage fir-wood), which are the dominant species in our country.

This difficult basic factor, up to a certain point, had exerted its influence on road infrastructure limitation in the forests and, when carried out, has caused heavy expenses.

Considering the ecological aspect - although it is commonly said that "road is a necessary damage, but the lesser" opinions about the extension of the road network in forests are situated at different levels but with a result which proves positive, rational and effective [4].

The construction of road infrastructures has positive effects on silvicultural works, as well as on exploitation, fellings, in view of agricultural activities, land reform or soil protection against erosion,

ISSN 1313-2539

avalanche control, etc. As far as the ecological aspect is concerned, negative aspects exist nonetheless regarding the protection of landscape or forest biotypes especially in the case of our forests.

A road network subject to extension works with a high density, where motor circulation prevails, always brings about negative and immediate effects on the forest environment.

On the contrary, a concrete extension of the road network, where data resulting from an ecological observation of each forest management aspect are well taken into account, allow such a forest, such a road, to fulfil each their environmental role and functions.

Regarding the technical aspect, the extension of the road network in our forests showed demands concerning their management and scientific usage, particularly for productive forests presenting long-term installation projects.

As there is a majority of old forests, cuttings, which are considered indispensable to silvicultural activities, were used as a continuous and complementary wood provision source that averages 0,05 million m^3.

Considering the motorway a basic component of forest management works and a component of the modern transportation system in forested areas, and at the same time, technological solutions for two other phases of the complex exploitation process, the extension of a road network combined with the other available methods of unloading and transportation of felled trees, on storage or loading areas, near motorways (Figure 1).

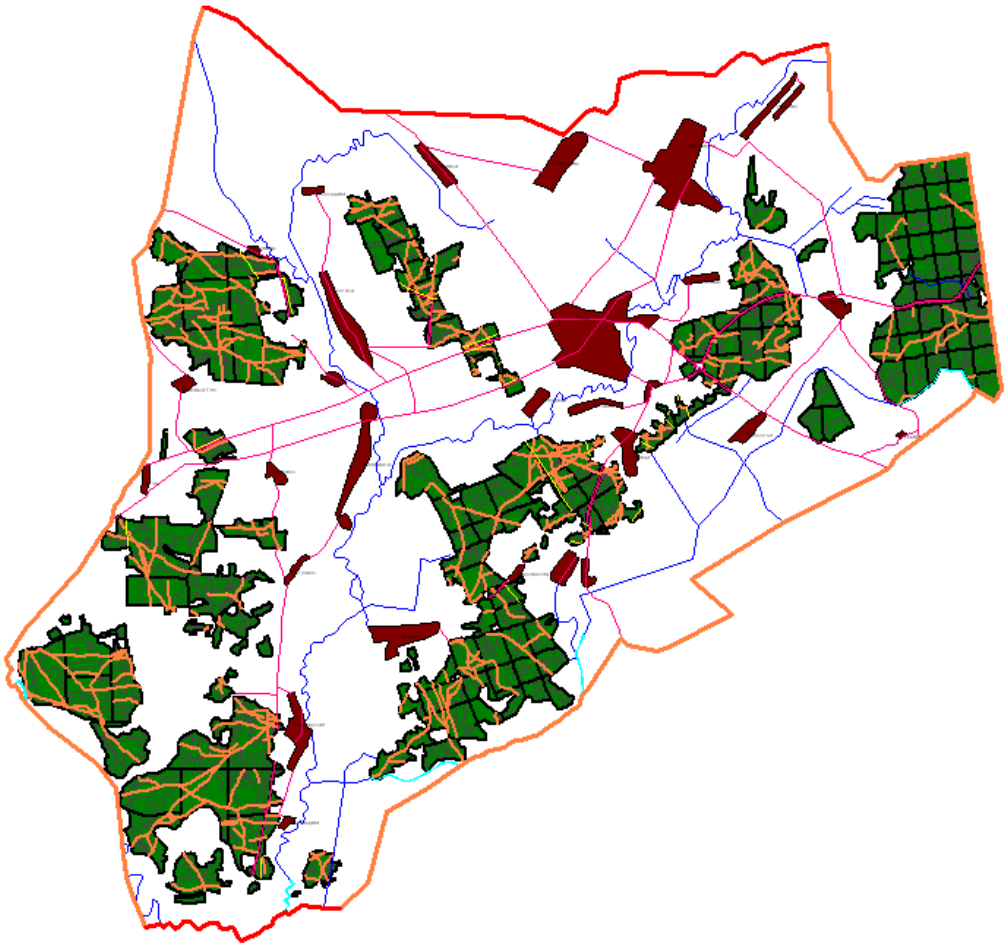

Figure 1. Forest road network

ISSN 1313-2539

Even though, in high forests, the road density is higher than somewhere else when compared to the average index value for the country, around 2,2 m/ha refers to the optimum average values that can be applied. Through the experience acquired by many European countries, it arises that the situation is not as expected and that it would have been desirable to emphasize intensive silvicultural practices.

Methods consisting in using manual or mechanical hauling for tree-length logs and mules for small-size logs have a large application in the international transportation fields. This technical solution said "in between" illustrates, with the help of internal transportation technological schemes, the repercussions of works carried out as far their efficiency is concerned.

At the same time, as it is impossible to build motor roads and, due to the limited number of mechanical equipment used to extract wood from our forests situated at a cross-country altitude, the only technically sound solution is the extension of the road network in the form of main roadways, positioned according to valleys and hollows with short access roads (Figure 1). The accumulation of fellings in their vicinity, especially down the slope is also very important. Wood hauling on long distances between wide spaces and motorways having mean values ranging from 100 to 120 m for manual hauling, 250 to 300 m for mechanical hauling (tractors) and 400 to 600 linear metres for skylines are the results of these solutions [5].

The road network under consideration with an optimum density of high technical characteristics and excellent structures, provided profitable returns for all types of works. They aim at easing man's access to sites, work technologies and extend their field of activities to environmental effects and repercussions on the protection of nature.

In spite of the results achieved during the construction of the road infrastructure, relatively high building costs, annual maintenance, recurrent repair costs have been experienced of average values twice as high as in some other European countries. Strongly marked slopes and abrupt shapes in forested areas, the regulations applying to silvicultural methods through selective cuttings (at two or three different stages of evolution) have to be considered separately.

The organization and positioning of road networks with a high coefficient together with what follows are a few of the results achieved so far:

- earthworks as part of the accomplishment of the main road network;
- numerous constructive works such as support walls, small bridges, piping, etc.;
- considerable annual maintenance works, especially during winter months;
- large amounts of recurrent repairs, often reaching 60 percent of the entire structure;
- structures made of paving blocks or gravel, to allow all-year-round circulation of motor vehicles;
- all this resulting in heavy expenses.

As far as the above-mentioned expenses are concerned, if we refer to Prof. N. P. Vyrko's point of view [6] concerning the classification of forests according to the functions fulfilled by motorways in about 70 percent of our forests, we can understand the delay in setting road infrastructures in these areas. Consequently, we retain that our forested zones are well served and we insist on the necessity to enlarge the road network to 2,6-4,3 m/ha.

The accomplishment of a satisfactory road network, which will allow intensive silvicultural activities, obviously belongs to the future. Nevertheless, a project financed by the Department of Forestry has been launched which anticipates the restoration of 13 900 km of the road network in forests.

The economic influence of wood extraction on factors such as the reciprocal indirect dependence between road density and hauling distances determinates the configuration of the road network extension. This operation in the case of specific data, situations or factors (forest, land, transportation facilities, technologies and working regulations, road classification, etc.) allows an estimation of

ISSN 1313-2539

optimum values for the two indexes (density of road network/hauling distance) which will permit the extraction of each unity (m^3) of wood with lower expenses.

Basing our argument on the above-mentioned laws and with the yielding capacity of forest road works in mind, during the last few years, studies have been carried out regarding the problems concerning access to the forests and extension of the road networks in our forest management. General information, not yet in final form, is given in Table 2.

Table 2 - Belarusian forest

Struc-ture	The basic breeds								Bu-shes	Total
	pine	spruce	oak	birch	alder black	aspen	Other	Total		
Surface, (10^6ha)	3474,6	676,02	240,91	1540,07	578,6	147,42	230,3	6888,34	33,41	6921,9
Volume, (10^6m^3)	695,2	149,54	37,79	233,83	92,95	26,07	30,45	1265,9	0,73	1266,62
Average stock, (m^3/ha)	200	221	157	152	161	177	132	-	22	-

In the course of the last few decades, experience has shown that, due to the low value of motorway density, wood had to be hauled on longer distances within plots. At the beginning, manual hauling on long distances, due to the lack of mechanization, was commonly done, whereas the gradual increase of technology relations between the extension of the road network and the hauling methods have become more efficient, leading to a 10-15 percent decrease of total costs for each unity of wood (m^3).

The increase of economic efficiency of the road network as a consequence of the cost of wood extraction affects the level of works carried out and their construction which, in our country, has been and is still very low.

The positive effects which result from the increase of technology in wood extraction, together with a denser road network, will be higher if they lead to a major level of mechanization of construction works. In Albania, apart from a few tractors of bulldozer type, used to dig land and a few other means to transport materials, the technology indispensable to carry out specific tasks such as digging machines, superchargers, stone crushers, road rollers, transportation means, etc., is seriously lacking and it is highly recommended to consider the results obtained with such developed technology in some countries throughout the world.

The extension of the road infrastructure in mountain forested areas in Belarus is considered a solution that not only provides assistance in settling natural forest balance but, as these forests, typical of Belarus, are situated near rural centers, this assistance takes on double value, as it warrants social and economic development [6].

The solutions to this situation, i.e. connection between rural communities and motorways, easy motor circulation for the local population, delivery of farming products, exploitation of local mineral resources, etc., are all included in this context.

Access road by motor vehicles, especially the ones that go alongside and the ones that enter forests, apart from the important role they play in ensuring a proper service to the forest, allow and promote tourism, recreation and restful activities which go hand in hand with these developments.

ISSN 1313-2539

Numerous examples illustrate the complex role of forest roads in our country. They can be found in the following regions: Brest, Vitebsk, Gomel, Grodno, Minsk, Mogilev, etc.

3. MODEL OF SEARCH OF OPTIMUM PARAMETERS OF WOOD-TRANSPORT NETWORKS FOR ACCOMMODATION IN LARGE FOREST M_S

3.1 The purposes

Any wood-transport network (WTN) is created for achievement *of the basic purpose - maintenance transport development of large forests*. For such complex T - systems as the WTN the purposes which it is difficult to formulate, describe and plan ways of their achievement are peculiar some. Other difficulty consists in that, modern opportunities of the system analysis do not allow to express the purpose in a quantitative kind [7].

Therefore the purposes of creation the WTN we shall describe only at the qualitative level, the received results will be used for definition of the general directions on search of optimum parameters the WTN and a choice of optimum variants of its accommodation on a degree of preferability.

The purposes are formed under influence external and internal, in relation to the WTN, factors. Set of the purposes are united by one initial purpose which can be broken into set of more private, but also more simple and concretized purposes. Such splitting is connected with construction of *"a tree of the purposes"*. Thus the condition is provided: the purposes of the bottom levels should form a set, sufficient for achievement of the general purpose [8].

The formulation of the purposes - process exclusively creative and informal; it concerns to the theory of decision-making and in a strong degree depends both on intuition and art of the researcher, and from features most T - systems. In view of this we develop "a tree of the purposes" FG (fig. 3) for the decision of a problem of predesign synthesis the WTN.

<table>
<tr><td colspan="2">Maintenance of transport development of large forests and preservation of an environment</td></tr>
<tr><td rowspan="2">1.1. To choose optimum forest-transport process</td><td>1.1.1. To choose structure of process</td></tr>
<tr><td>1.1.2. To choose an optimum complex of machines</td></tr>
<tr><td rowspan="3">1.2. To place an optimum wood-transport network</td><td>1.2.1.1. To choose plans of development of cuttings area
1.2.1.1. To define stocks of a wood and operational conditions
1.2.1.2. To break economic sections into cuttings area</td></tr>
<tr><td>1.2.2. To choose the plan of development of large forests
1.2.2.1. To choose optimum structure the WTN
1.2.2.2. To choose an optimum configuration the WTN</td></tr>
<tr><td>1.2.3. To choose sequence of accommodation the WTN
1.2.3.4. To define volumes of freight traffics and volumes of passenger traffic</td></tr>
<tr><td rowspan="2">1.3. To provide preservation and reproduction of the forest environment</td><td>1.3.1. To execute the technological device of large forests
1.3.1.1. To break a large forest into economic sections</td></tr>
<tr><td>1.3.2. To choose ways of restoration of cuttings area</td></tr>
<tr><td colspan="2">1.4. To establish rational sequence of development of cuttings area</td></tr>
</table>

Figure 3. "A tree of the purposes"

ISSN 1313-2539

The most adequate display of a configuration and structure the WTN is the description of spatial connections of its components in the form of graph-tree G_s (X, L) where the set of tops X includes: sources X_i of formation of transport streams in size q_i, stations of an adjunction of network X_v and forks of ways X_s, and set of edges L - transport ways in length l_{ij}, connecting tops i and j [9].

The station of adjunction X_v refers to *as a root* which the fragments of a network named by *"branches"* graph G_s adjoin. Obviously, any two tops of a graph are connected by unique transport connection, and forks of network X_s for freight traffics are only transit points (fig. 4).

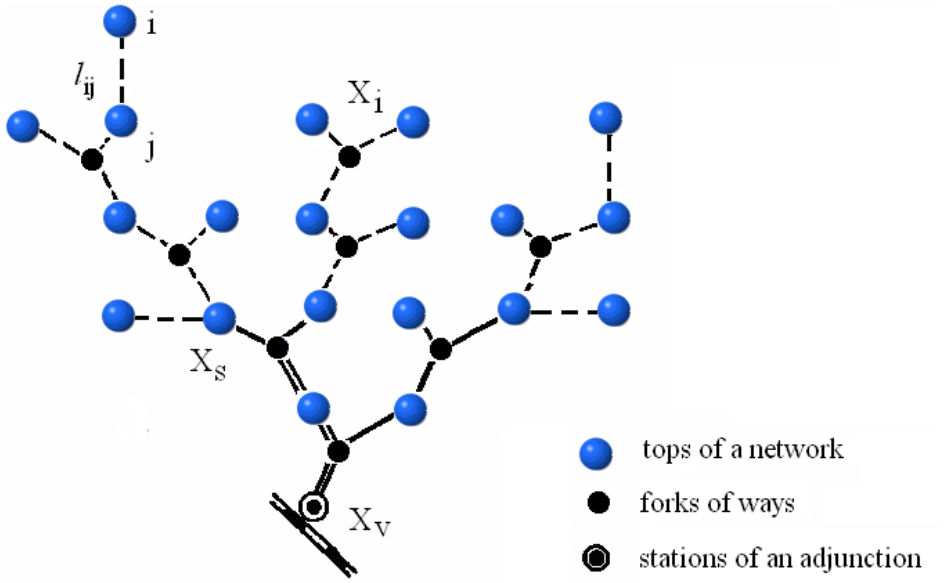

Figure 4. Graph of spatial connections G_s (X, L) the WTN

Change of a spatial arrangement of tops X_i and X_s at constant position of station of adjunction X_v conducts to change of a configuration of a network, and change of sizes of transport streams q_i, concentrated in points X_i, the WTN leads to change of throughputs q_{ij} transport connections l_{ij} and therefore, structures C_s, configurations K_s and density.

Basically the WTN is estimated by two is functional-structural properties: configuration K_s, as a parameter for an estimation of a spatial arrangement of wood-transport ways and trajectories of moving of transport streams of wood raw material and not forest loads, structure C_s presented by set of ways of various categories on all sites of a network and types of transport units.

Additional parameters for the WTN are: amount of the centers of formation of transport streams N_i of forks of ways N_s and stations of adjunction N_a in a large forest and specialization of a network.

For optimization of parameters the WTN we have started drawing up of mathematical models after performance of researches of the abstract networks representing various combinations of the treelike graph.

ISSN 1313-2539

3.2 Statement of a problem

Results of research of abstract models the WTN have allowed to draw the important conclusion: predesign synthesis optimum on a configuration and structure real the WTN will be connected with the decision of two mathematical problems:

1) Search of the shortest connecting network (SCN);
2) Search locally-optimum the WTN by addition of forks of ways and definition of their coordinates.

Let's carry out the formal description of a problem. Let in some limited area on a plane are set:

1) final set a load of forming tops $X_i \subset \{X_i, x, y, q_i\}$, including N_i the centers X_i stocks of wood, not forest loads and volumes of passenger traffic;

2) final set of root tops $X_v \subset \{X_v, x, y, Q_a\}$; containing N_a points of adjunction X_v of forest road.

Everyone X_i top of a network possesses the capacity equal to volume q_i of wood raw material concentrated to it; and capacity X_k tops - to volume q_k a transport stream. In X_v to top the station of an adjunction (a drain for a network), an accepting transport stream in volume Q_a equal to annual volume of manufacture of the bottom forest warehouse is located.

Here x, y - coordinates of tops of a network.

To receive representation about the difficulties arising at drawing up of mathematical model we shall note two features connected with predesign synthesis locally-optimum WTN.

The first feature - the sketch of a network represents R_s - a tier structural tree in the form of graph G_s with root tops X_v. The given graph are formed by introduction in SCN a new subset of forks of ways X_s $\{X_s, x, y\}$ with zero stocks of transport streams ($Q_s = 0$) in them. The concept the WTN in the form of (R_s) a tier tree is entered by us for the first time, meaning, that *r* tier of graph G_s edges l^{r}_{ij} having q_r a settlement turnover of goods make all.

The second feature. Simple connection of top X_i, X_j, transport connection l^{r}_{ij} does not allow to estimate cost of way C_{ij} since are unknown a category *r* and throughput q_{ij} ways.

The above described features do not allow to execute predesign synthesis the WTN known methods [9]. The following approach for the decision of a problem.

Therefore is supposed:

1 stage - to construct SCN with use of Prim's algorithm [10] in the form of graph G_p;

2 stage - at known configurations K_p, column G_p and costs of unit of length of ways C^{r}_{ij} (at $r = 1$) to conduct search minimal "Steiner's multitier tree " (SMT) by optimum accommodation of forks of ways X_s. It provides a finding the WTN with locally-optimum parameters and reception of the sketch in the form of graph G_s close to optimum $G_{s\ opt}$.

The mathematical description of network model M_s with N_i the centers of stocks of transport streams in size q_i, with N_a stations of an adjunction (with volumes of manufacture Q_a) and with N_s forks of transport ways is executed.

Criterion function - a minimum of expenses for transport development of large forests:

$$\min F(G_s) = \sum_{r}^{R} \sum_{i \neq j} C_{ij}^{r} \cdot l_{ij}^{r} \cdot q_{ij}^{r}$$

ISSN 1313-2539

4. RESULTS AND DISCUSSION

Models of optimization the WTN are developed on the basis of the executed parametrical description of systems cooperating among themselves "an environment - a wood-transport network - the environment of functioning". It has allowed for each model will make the list of considered factors, to execute the plan of transformation of the entrance information and interaction of factors in model, to prove criteria of an optimality and to define parameters for optimization.

Function of the purpose and mathematical model the WTN in the form of the graph including forks of ways are made and allowing to enter predesign search of their optimum configurations and structures. Are offered new mathematical model for the decision of problems of optimum accommodation of cuttings area in an economic section and model for definition of rational sequence of development of cuttings area in a section.

5. CONCLUSIONS

By results of modelling the WTN is obviously possible to conclude:

1. Results of research of developments a WTN arising at transport development of large forests, have allowed to develop hierarchical system of modelling the WTN in structure of:

- the basic models of optimizations located at hierarchical levels of decomposition the WTN (T-systems) both providing predesign synthesis and a substantiation of parameters: the WTN - for transport development of large forests; fragments the WTN - for accommodation in economic sections; temporary technological the WTN on cuttings area.

- the auxiliary models located at levels of a partition of structural structure the WTN and providing modelling of accommodation a section and cuttings area in large forests, optimization of structure of logging process and sequence of development of cuttings area, modelling of transport streams. Use of the given models allows to increase a degree of completeness of initial data for designing the WTN, than effective predesign synthesis of networks is provided.

2. At modelling the WTN new reserves of improvement of their configurations and structures - application of plans of connection of wood-transport ways with optimization of coordinates of forks of ways are revealed at existing classification of forest roads.

3. For the further increase of efficiency of search of optimum parameters the WTN complicating and excluding accommodation on them of wood-transport ways of sites of the forest and not forest grounds, situational model the technique of an estimation and modelling are developed for allocation of such sites on cards-plans of large forests and forest exploitation a section.

ACKNOWLEDGEMENTS

The Authors wish to thank Mr. Nikolay Pavl. Vyrko for his valuable help in the analytical work. Thanks are also due to Mr. Michail Naskovets for his assistance in interpreting the model, and for helping to create the forest roads network.

REFERENCES

1. Bavbel J.I. (2007). Optimization of transport-technological plans of development of wood raw material base in woods of the second group. *Works BSTU. Forest and woodworking industry*. Vol.15. pp. 100-103.

ISSN 1313-2539

2. Anderson, A.E., and Nelson, J.D. (2004). Projecting vector-based road networks with a shortest path algorithm. *Can. J. For*. Res. 34: 1444-1457.

3. Hillier, F.S., and Lieberman, G.J. (2001). Introduction to operations research. 7th ed. McGraw-Hill, New York.

4. Moore, G.D. (1994). Resource road rehabilitation handbook: planning and implementation guidelines (interim methods). Watershed Restoration Technical Circular 3. British Columbia Ministry of Environment, Lands and Parks and British Columbia Ministry of Forests, Victoria, B.C.

5. Nelson, J. (2003). Forest Planning Studio - ATLAS program reference manual. Version 6. Faculty of Forestry, The University of British Columbia, Vancouver.

6. Vyrko N.P., Lyshchik P.A. (2004) Designing of forest roads. Belarussian state technological university, Minsk., 2004. - pp. 307.

7. Sessions, J., and Sessions, J.B. (1988). SNAP-A Scheduling and network analysis program for tactical harvest planning. In *Proceedings of the International Mountain Logging and Pacific Northwest Skyline Symposium, Portland*, Ore., 12-16 December 1988. College of Forest Resources, University of Washington, Seattle, Wash. pp. 71-75.

8. Walbridge, TA. (1991). The paper location of forest roads. Virginia Polytechnic Institute and State University, Blacksburg, Va.

9. Chenge S.K. (1972). The generation of minimal trees with Steiner topology. *Journal of ACM*, Vol.19. - pp. 699-720.

10. Komlos M.T., Shing H.T. (1985). Probabilistic Partitioning Algorithms for the Rectilinear Steiner Problem. *Networks*, vol. 15. - pp. 113-123.

ISSN 1313-2539

DETERMINATION OF THE COMPOSITE MATERIAL ELASTIC CONSTANTS BY HARMONICAL AND MODAL ANALYSIS

Arcady N. Soloviev[1] and Igor V. Baranov[2]

[1] Southern Federal University, Department of Mathematical Modeling,

344006 Rostov-on-Don, Russia. E-mail: soloviev@math.rsu

[2] Don State Technical University, Department of Aviation Engineering, Gagarin pl. 1,

344010 Rostov-on-Don, Russia

Abstract

The value of all composite elastic modules has the crucial influence on the aviation load-bearing structures dynamic behaviour. Numerous experimental techniques are used to characterize the elastic properties of polymeric composite materials. There are exist the large group of static tests, acoustic methods based on longitudinal, lateral or shear surface sound wavespeed measurements and also on vibrating surfaces amplitude measurements. However, a preparation of specimens for static test with shape required by standards not always possible from already manufactured piece. In this study an acoustic method is developed using the measure of all specimen's eigenfrequencies in a certain frequency range. Small rectangular composite specimen is excited by bonded piezoelectric actuator and the frequency response is measured by piezoelectric sensor. Preliminary performed finite-element (FE) analyses serve to think the vibration natural modes of linked mechanical system - specimen and piezoelectric element. In this FE analysis used the rough estimations of all elastic constants obtained from other independents (as a rule static) experiments. Further the amelioration of initial elastic modules was performed. Thereby the target nonlinear functional dependent on all quest modules was minimized by genetic and (or) Levenberg-Marquardt algorithm.

Keywords: *polymeric composite, elastic module, acoustic measurements, eigenmodes, finite element method*

1. INTRODUCTION

The dynamic behavior of carrier composite structures in particular passed through significant elastic strains essentially depends on all material elastic constants (Hoskin et al., 1986). Therefore the problem of a ready components material elastic constant monitoring has the large importance, especially, in aircraft manufacture. Despite of a series of the standards, designed and used for trial of composite materials, the problem of polymeric composite elastic constants identification has not lost urgency. It is stipulated both development of new materials, and use of composite workpieces, which shape does not allow to make samples of a standard configuration. Besides the actually used standards provide an excise of samples from the specially prepared plates, the technique of which manufacture (pull-up of winding, conditions of a curing) can not match to the work piece.

Among sources of rough errors and bad reproducibility of composite elastic modules determination results in static tests (Jianmey et al., 2002; Kuraishi et al., 2002; Jenkins, 2002; Tomblin et al., 2001; Van Paepegem et al., 2006) is the nonuniformity of stress distribution in a working area of specimen, stipulated by the testing scheme (Jianmey et al., 2002; Shevtsov et al., 2006), or numerical instability of a calculation method at experimental data handling, and also the geometrical errors of samples preparation and grabbing of a testing machine.

ISSN 1313-2539

One of utilized techniques of elastic properties investigation is the comparative analysis of a surface displacement field (Hoskin et al., 1986; Jenkins, 2002), eigenfrequencies and natural modes derived from experimental data and numerical simulations (Cugnoni et al., 2004; Lee et al., 2006), and employment of calculated results elaboration by iterative methods (Araújo et al., 2002; Lauwagiea et al., 2003; Lee et al., 2006), genetic algorithms (GA) (Cugnoni et al., 2004), etc.

In the present article experimental dynamic techniques for specimens cut out from a ready workpiece (polymeric composite spar of the helicopter main rotor blade) is considered. These techniques complement the early designed by authors' FE-based means (Shevtsov et al., 2006) for orthotropic composite static tests. The offered dynamic tests include an evaluation of specimen's amplitude-frequency response, determination of fundamental frequencies and vibration modes of specimens both in natural experiments and numerical FE - simulations.

The identification process consists of several stages. In series of static tests are determined all allowable modules. Further a complete matrix of elastic constant is constructed, but some modules specified by approximated values (in particular, interlaminar shear modules). A series of dynamic tests executed in which the periodical excitation in samples and the frequency response is recorded by means of piezoelectric actuators and sensors. Then on basis of early defined modules of composite and experimentally founded eigenfrequencies by means of FE modelling the vibration natural modes, and also the boundaries of the damping factors variation are identified. By combination of FE modeling, GA, and Levenberg-Marquardt method the specification of composite mechanical properties is evaluated.

2. IDENTIFICATION OF PIEZOELECTRIC ELEMENTS PROPERTIES

The identification of piezoelectric elements properties is indispensable for an adequate numerical modeling of a compound structure including a composite specimen with sensor and actuator. With this purpose for polarized on width piezoelectric rectangular plate ($14.6 \times 6.8 \times 0.28$ mm) the frequency response of impedance is measured (see Figure 1).

The mathematical description of dynamic problem is carried out within the framework of the linear theory of electroelasticity. This boundary value problem for electro elastic body $\underline{x} \in V_P$ consists of the differential equations (Parton et al., 1988)

$$\sigma_{ij,j} = \rho \ddot{u}_i \ (-\rho\omega^2 u_i), \quad i = 1,2,3, \tag{1}$$

$$D_{i,i} = 0, \tag{2}$$

constitutive equations

$$\sigma_{ij} = c_{ijkl} u_{k,l} + e_{ijk} \varphi_{,k}, \quad D_i = e_{ijk} u_{j,k} - \varepsilon_{ij} \varphi_{,j}, \tag{3}$$

ISSN 1313-2539

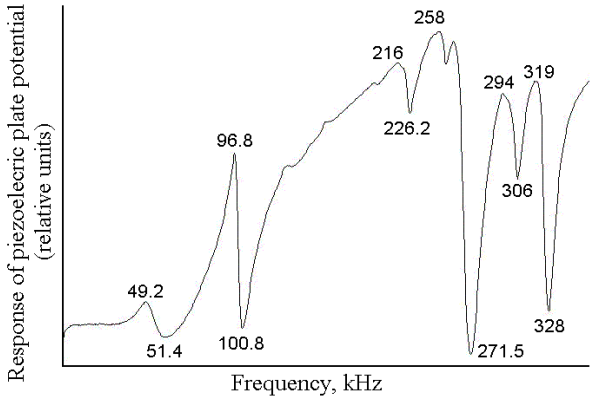

Figure 1. The frequency response of piezoelectric plate potential (experimental data)

mechanical boundary conditions

$$t_i = \sigma_{ij} n_j \mid_S = 0 \,, \tag{4}$$

and electrical boundary conditions on $S = \bigcup_{m=1}^{M} S_{E_m} \cup S_D$

$$\varphi \mid_{S_{E_m}} = \varphi_m^0 = const \,, \qquad D_n \mid_{S_D} = D_i n_i \mid_{S_D} = D_n^e \quad (=0) \,, \tag{5}$$

where: ρ=7910 kg/m^3 – material density, σ_{ij} – elements of stress tensor, u_i, $u_{i,k}$ – components of displacements and deformations respectively, D – electrostatic displacement, c_{ijkl} – stiffness matrix, e_{ijk} – piezoelectric constants tensor, ε_{ij} – electric permeability tensor, t_i – normal stress vector on i – boundary, n_i – boundary unit normal vector, φ – electric potential, S_{Em}, S_D –coated by electrodes and free boundaries respectively, and m – boundary number.

The unknown potential on m – electrode was determined from equation

$$\int_{E_m} \dot{D}_n dS = I_m \,, \tag{6}$$

where I_m – electric current in external circuit.

The FE - simulation of piezoelectric elements was performed in software ACELAN (Belokon et al., 2004). The FE - meshing is shown in a Figure 2. The properties of piezoelectric plate can be determined on basis of frequency response (see Figure 1) and method combining FE and genetic algorithms (Acopyan et al., 2006; Baranov et al., 2006). However applyings this procedure needs identification of oscillations modes, which one will match to splash on the frequency response curve (Figure 1). The used piezoelectric ceramics composition has matched to properties represented in Table 1.

ISSN 1313-2539

Table 1 - Properties of sensor and actuator piezoelectric material.

Stiffness matrix, GPa					
c_{11}	c_{12}	c_{13}	c_{33}	c_{44}	c_{66}
109	61	54	93	24	$(c_{11}- c_{12})/2$
Piezoelectric and dielectric constants					
e_{31}, $N/(V \cdot m)$	e_{33}, $N/(V \cdot m)$	e_{15}, $N/(V \cdot m)$	$\varepsilon_{11}/\varepsilon_0$	$\varepsilon_{33}/\varepsilon_0$	
-4.9	14.9	10.6	820	840	

The results of the harmonic analysis in ACELAN are shown in a Figure 3, on which the dependence of admittance amplitude on excitation frequency is figured. Some unconformity between the graphs of a Figure 1 and Figure 3 in the frequencies range 40 - 50 kHz, in which one there are some flexural modes (second flexural mode of a plate along a short edge and first flexural mode in a plane along the longest edge), is stipulated by their excitation at the irregularity of the geometrical shape, polarization and specimen's electrode coating. In numerical experiment at the perfect prism geometry these modes are not piezoelectric.

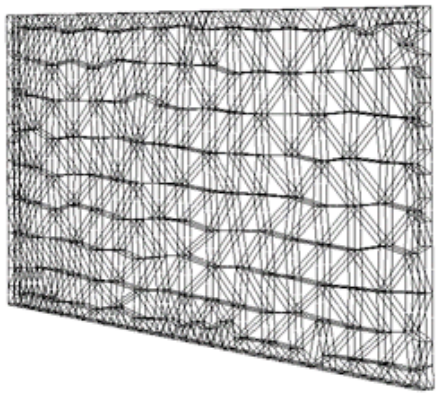

Figure 2. The finite element meshing of piezoelectric plate

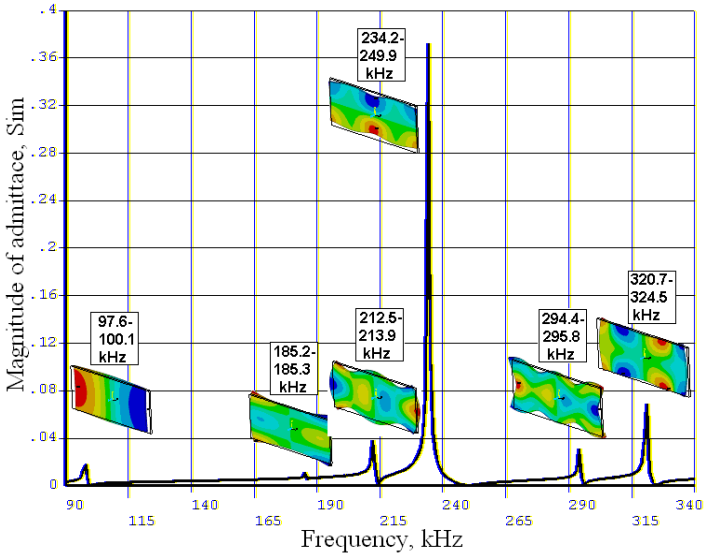

Figure 3. The frequency response of piezoelectric plate's admittance (FEM - simulation results)

The graphic portrait of displacements amplitude on six foremost oscillations modes are linked with correspondent splashes on the frequency response curve (see Figure 3). The results of the modal analysis have allowed to identify piezoelectric oscillations modes and to receive improved values of elastic and piezoelectric modules, which one will be utilized further in a problem of composite elastic modules identification.

ISSN 1313-2539

3. EXPERIMENTAL SETUP, SPECIMENS AND RESULTS OF MEASUREMENTS

The installation for dynamic tests of mechanically coupled piezoceramic plates and polymeric composite specimen include the ultrasound generator, digital frequency meter, oscilloscope, digital voltmeter, optical meter of the surface point displacement amplitude and specimen header. In experiment the different schemes of piezoelectric elements connection utilized (see. Figure 4). The inset (a) corresponds to the connection «actuator - sensor», (b) - «actuator - passive element», (c) - «two parallel actuators», (d) - «bimorph actuator».

The polymeric composite material utilized for a specimen's excision is the multilayered laminate obtained by spool of unidirectional tape (prepreg) with a further curing of epoxy resin matrix at heating up in a mold tool. This material used at production of spar for the helicopter main rotor blade. The shape of the sample - parallelepiped ($25.0 \times 14.5 \times 5.5$ - sizes in mm). Unidirectional fiberglass tapes are parallel to major plane of specimen and are located under angles $\pm 30^0$ to a direction of the greater edge (Figure 5, a). At centre of the major plane, are symmetrically attached the piezoelectric plates. The used connection circuits allow exciting symmetric, flexural and other oscillations modes with different efficiency.

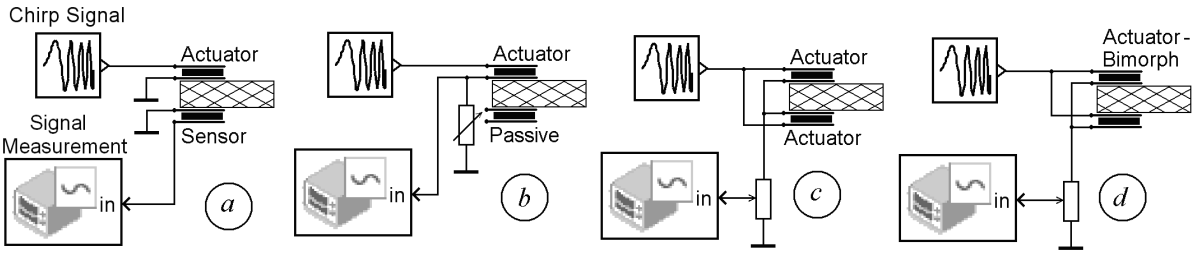

Figure 4. Electrical circuits for specimen's excitation on different oscillation natural modes

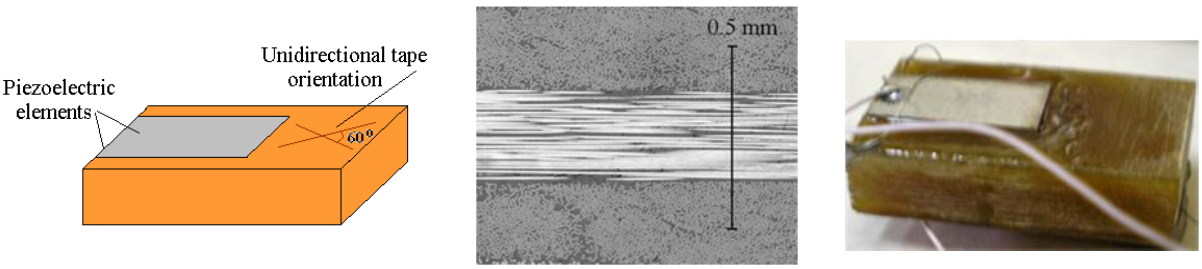

a) b) c)

Figure 5. Composite specimen for determination of elastic constant by dynamic test:
a – schematic view; b – magnified transversal cross-section normal to largest plane;
c – snapshot of specimen with installed piezoelectric elements

The Figure 6 depicts a frequency response of a sample oscillations obtained by optical meter of displacements, and Figure 7 - frequency response of potential on sensor's contact, when the

ISSN 1313-2539

oscillations are excited by actuator. The obtained information on eigenfrequencies will be utilized by identification of oscillations modes corresponding to peaks of frequency response.

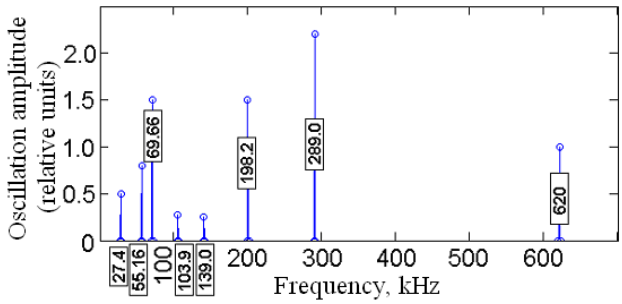

Figure 6. Frequency response of polymeric composite specimen
(experimental data obtained by displacements optical meter)

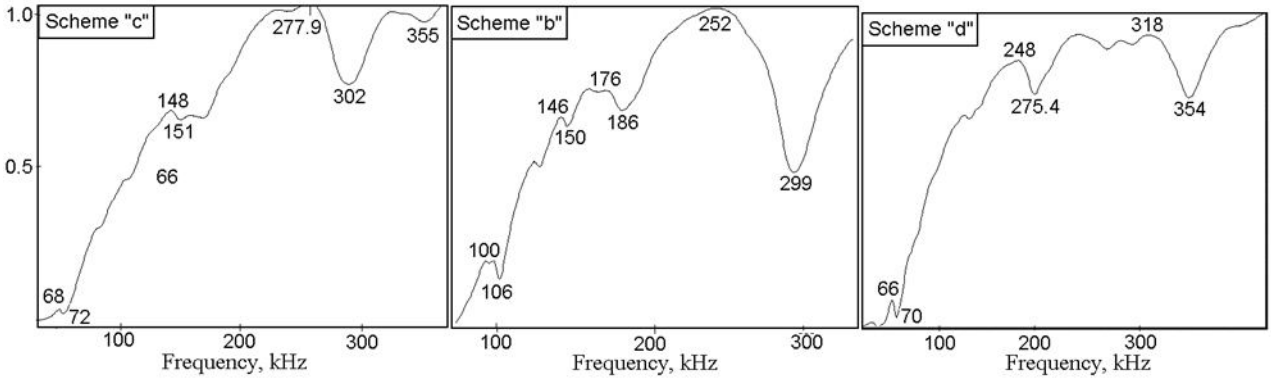

Figure 7. Frequency response of polymeric composite specimen
(experimental data – explanation in text)

4. FINITE ELEMENT MODELS AND SPECIMEN'S NATURAL MODES IDENTIFICATION

The problem description includes relations (1) - (5) for an electroelastic body, and for $\underline{x} \in V_E$ - elastic body: the equations of motion (1), constitutive relations

$$\sigma_{ij} = c^{(E)}{}_{ijkl} u_{k,l} \quad i = 1,2,3 \tag{7}$$

and mechanical boundary conditions (acting forces):

$$t_i = \sigma_{ij} n_j \big|_S = p_i \tag{8}$$

The components of an elastic tensor in two index matrix notations $C = ((c^{(E)}{}_{rt})), \; r,t = 1,2,...,6$ have values determined in static tests (Shevtsov et al., 2006) (see Figure 8, b).

The simulation of specimen (Figure 8,a) oscillations was carried out in ACELAN taking into account a damping, both in elastic, and in electroelastic bodies. The purpose of this simulation was the identification of specimen's eigenfrequencies obtained in experiment, and oscillations modes, correspondent to them.

ISSN 1313-2539

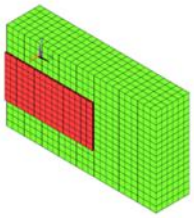

a)

$$C = \begin{pmatrix} 8.378\cdot10^{10} & 3.939\cdot10^{10} & 3.357\cdot10^{10} & & & \\ 3.939\cdot10^{10} & 3.348\cdot10^{10} & 1.899\cdot10^{10} & & 0 & \\ 3.357\cdot10^{10} & 1.899\cdot10^{10} & 2.414\cdot10^{10} & & & \\ & & & 5\cdot10^{9} & 0 & 0 \\ & 0 & & 0 & 1.3\cdot10^{10} & 0 \\ & & & 0 & 0 & 1.5\cdot10^{10} \end{pmatrix}$$

b)

Figure 8. FE – model of specimen with attached piezoelectric elements (a) and stiffness matrix for used orthotropic composite material (b)

Vibration modes forced by piezoelectric actuator were selected in numerical experiment (harmonic analysis). The numerical calculation results of admittance frequency response (Figure 9, a) and of displacement module of a point on the sample upper surface (Figure 9, b) are submitted.

In the Table 2 the results of the modal analysis are presented. The cells of this table contain frequencies of a resonance and anti-resonance, image of the oscillations modes, and numbers of the circuits (Figure 4), which excite the given oscillations mode. The data of the table specify, that use of the different commutation allow exciting founded by numerical simulation the majority of oscillations modes in a wide frequency range. Note, that at a spectrum there are frequencies with small factor of electromechanical linking (No. 3 and 4 in Table 2), which experimental detection needs more sensitive instrumentation, than that was used in the conducted experiments.

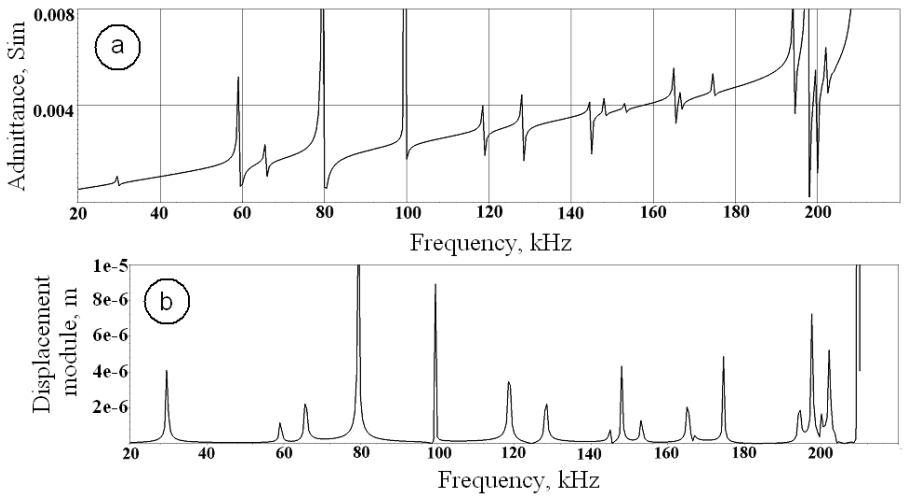

Figure 9. Frequency response of admittance (a) and the surface point's displacement modulus for studied polymeric composite specimen (simulation results)

Table 2 - The natural modes of composite specimen's oscillation (simulation results).

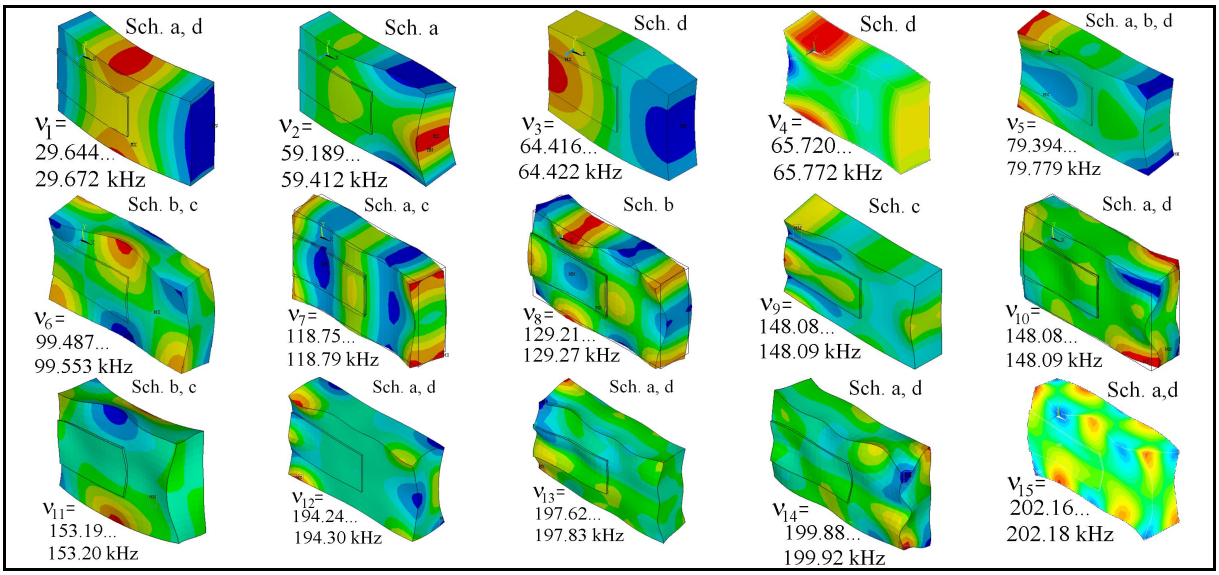

5. PROCEDURE OF EFFECTIVE ELASTIC MODULES IMPROVEMENT

Elastic constants used in FE analysis are obtained in static tests. Their precision is not identical, in particular it concerns to interlaminar shear modules (Chan et al., 2006; Jenkins, 2002). The improvement of these modules can be carried out by minimization of some nonquadratic functional of a discrepancy between measured and calculated magnitudes. As basic experimental information we used a spectrum of eigenfrequencies and frequency response of potential on piezoelectric plate (Figure 7). The values of surface points displacement was used in (Baranov et al., 2006; Hurley et al., 2001) for determination of elastic modules. Unfortunately, for a specimen with used shape the exactitude of displacement measurements inaccessible to the available instrumentation was required. Therefore problem of nine modules C_{ij} $i, j = 1,2,...6$ improvement is formulated as minimization of an objective function

$$G(c_{11},c_{12},c_{13},c_{22},c_{23},c_{33},c_{44},c_{55},c_{66}) = \sum_{i=1}^{n} k_i \left(\frac{\omega_i - \psi_i}{\psi_i} \right)^2 + \sum_{i=1}^{n} \sum_{k=1}^{m} h_{ik} (a_{ik} - u_{ik})^2 \qquad (10)$$

where $\psi_1,...,\psi_n$ - set of measured, and $\omega_1,...,\omega_n$ - set of the FE - simulated eigenfrequencies; k_i and h_{ik} - weighting coefficients; a_{ik} - displacement of k - point, obtained from numerical experiment on the i – natural form; u_{ik} - displacement in the same point obtained as a result of measure. Usage of second summand in (9) eliminates an "intermixing" of eigenfrequencies at consecution of minimization epochs. For this purpose on a specimen's surface the set of reference points was selected (see Table 2). These points should be placed near minimum and maximum of oscillations on all observable modes. Thus to maximum amplitude corresponded values $u_{ik} = \pm 1$ (sign there corresponds to a phase shift on π), and to minimum amplitude – the values $u_{ik} = 0$. All these points should be accessible to optical amplitude measurement. The minimization of a functional (9) was performed by GA using the "strong selection", the "elite" strategy, Gray's codes and procedure of improvement (searching in narrow area by Levenberg-Marquardt method). The obtained experimental results and

ISSN 1313-2539

numerical calculations for fiberglass reinforced orthotropic composite have shown a good efficiency and reliability of proposed identification method.

ACKNOWLEDGMENTS

We would like to thank the Russian Foundation for Basic Research for their financial support by Grants 05-01-0690, 06-01-08041, 07-08-12193, 07-08-13589.

REFERENCES

1. Acopyan V.A., Soloviev A.N., Shevtsov S.N. Full Set Compatible Constants Determination of Piezoceramic Material (2006) *Manual of Instrument Production* (Moskow), No.1, pp. 31-37.

2. Araújo A.L., Mota Soares C.M., Herskovits J., and Pedersen P. Development of a finite element model for the identification of mechanical and piezoelectric properties through gradient optimization and experimental vibration data (2002) *Composite Structures*, Vol. 58, pp. 307–318.

3. Baranov I.V., Vatulyan A.O., Soloviev A.N. On one genetic algorithm and its application to inverse problems for identification in elastic bodies (2006) *Computational Technologies*, Vol. 11, No.3, pp. 14-26, Novosibirsk.

4. Belokon A.V., Soloviev A.N., The new schemes of piezoelectric devices finite element dynamic analysis (2005) *Applied Mathematics and Mechanics*, Vol. 66, Issue 3, pp. 491-501, Moskow.

5. Chan A., Liu X.L., Chiu W.K. Viscoelastic interlaminar shear modulus of fibre reinforced composites (2006) *Composite Structures*, Vol. 75, pp. 185–191.

6. Cugnoni J., Gmur Th., Schorderet A. Identification by modal analysis of composite structures modelled with FSDT and HSDT laminated shell finite elements (2004) *Composites*: Part A, Vol. 35, pp. 977–987.

7. Hoskin B.C., Baker A.A. Composite Materials for Aircraft Structures, AIAA Education Serie, 237 p., N.-Y. 1986.

8. Hurley D.C., Tewary V.K., and Richards A.J., Surface acoustic wave methods to determine the anisotropic elastic properties of thin films (2001) *Meas. Sci. Technol.* Vol. 12, pp. 1486–1494.

9. Jianmey He, Martin Chiang Y.M., et al. Application of the V-Notch Shear Test for Unidirectional Hybrid Composites (2002) *J. of Composite Materials*, 36, No.23, pp.2653-2666

10. Kuraishi A., Tsai S.W., and Wang J. Material Characterization of Glass, Carbon, and Hybrid-Fiber SCRIMP Panels (2002) Report SAND2002-3538, Stanford University, Department of Aeronautics and Astronautics, p.28.

11. Lauwagiea Y., Solb H., Roebbenc G., Heylena W., Shib, Y., and Van der Biestc, O., Mixed numerical–experimental identification of elastic properties of orthotropic metal plates (2003) *NDT&E International*, Vol. 36, pp. 487–495.

12. Lee C.R., and Kam T.Y. Identification of mechanical properties of elastically restrained laminated composite plates using vibration data (2006) Journal of Sound and Vibration, Vol. 295, Issues 3-5, No. 22, pp. 999-1016.

13. Manual on Experimental Methods for Mechanical Testing of Composites (2002) 2nd Ed., Editor C.H.Jenkins, Society for Experimental Mechanics, Fairmont Press Inc., 264 p., Indiana.

14. Parton V.Z., Kudryavtsev B.A. Electro-Magneto-Elasticity of Piezoelectric and Electroconducting Bodies (1988) Science publ., 472 p., Moskow.

ISSN 1313-2539

15. Shevtsov S.N., Soloviev A.N., and Pahanyan O.D. Polymeric Composite Shear Elastic Constants Determination on the Basis of Modified Technique (2006) Proc. of the 2nd Int. Conf. "From Scientific Computing to Computational Engineering", pp. 234-243, Athens.

16. Tomblin J.S., Yeow C.N., and Raju K.S., Material Qualification and Equivalency for Polymer Matrix Composite Material Systems (2001) Final Report DOT/FAA/AR-00/47, U.S. Department of Transportation, FAA, p.119, Washington.

17. Van Paepegem and oth., Modelling the nonlinear shear stress–strain response of glass fibre-reinforced composites (2006) *Composite Science and Technology*, Vol. 66, pp. 1455–1478.

ISSN 1313-2539

CONTROL OF COMPOSITE STRUCTURE DYNAMIC STATE ON BASIS OF NEURAL NETWORK APPROACH

Sergey N. Shevtsov [1], Vladimir A. Acopyan [2], Sergey A. Bragin [2]

[1] Laboratory of Mechanical Engineering & High Technology, South Center of Russian Academy, 344010, Rostov-on-Don, Russia

[2] Institute of Mechanics & Applied Mathematics, South Federal University, 344003, Rostov-on-Don, Russia, E-mail: aeroengdstu@list.ru

Abstract

The adaptive system of vibration damping for finite-element model of helicopter composite main rotor blade was designed. This control system include a neural network controller based on reference model, a bunch of distributed sensors measuring the local deformations in vibrating structure and piezoelectric power actuators acting on structure by local bending and twisting torques. The mentioned controller adjust a behavior of finite element model close to behavior of reference beam model that have a best parameters of structural damping, vibration stability and weight balancing. The control system model implemented in MATLAB Simulink© have shown an essential decrease of vibration level and suppression of rotor blade finite element model dangerous auto oscillations.

Key words: *smart structure, composite structure, active vibration damping, helicopter rotor blade, sensor, actuator, neural network*

1. INTRODUCTION

The most principal feature of the V/STOL (vertical or short takeoff and landing) flying vehicles future genetion is the refusal of a rigid passive carrying surface for the benefit of “active”, “adaptive”, “morphing”, or “intelligent” structures (Sater et al., 1993). Last years this problem is a subject of intensive researches of the leading air corporations and scientific schools. The properties of a wing activity are most evidently appear at flying insects having an exclusive maneuverability, which is achieved because of ability to adaptive change of geometry and distributed mechanical properties of the morphing wings. It is expected that the ability of the helicopter main rotor blade to controlled change of twist and local stiffness during a part of a rotor cycle revolution, will allow to improve the flight performance, controllability in critical situations, to lower of the noise and vibrations level, the load of all rotor design, to improve a survivability at local damages of blade's hollow sections (Rodgers et al., 1998: Hodges et al., 2003). The design concept and technical realization of a control system for active composite carrying structure is considered in the present article.

It is known that the forward flight almost always produce the vibrations of the completely balanced helicopter rotor. It is known also (Johnson, 1994), that on the hub of the main rotor with k - blades there are forces acting in a plane of rotation and in a plane of thrust with frequencies $kn\omega,(n=1,2,...)$, where n - number of a harmonic, ω - frequency of the rotor rotation. Besides, the flap movements of the blade create the Coriolis forces with harmonics of the following order, creating a complex interference picture of acting forces. In practice a movement of the blade relative to the horizontal hinge and its rotation in the axial hinge cause also the periodic forces, which amplitudes are appreciable up to tenth harmonics anyway. In flight the distribution of loading forces along the blade periodically varies, and these variable loadings can cause a resonance on one of eigenfrequencies of the blade.

ISSN 1313-2539

Traditionally for damping of resonant vibrations amplitude use constructive measures, for example, selection of the certain relations between own first flexural and torsional vibrations frequencies. However, at occurrence of such resonances the exciting forces are counterbalanced only by aerodynamic and structural damping of the blade material.

For reduction of a vibrations level aspire to increase of the blades material structural damping, to increase of number of blades, their trailer speed (Leishman, 1990).

The vibro-isolation of the rotor from airframe theoretically also it is possible to supply at small blades weight relative to a fuselage weight by way of the hub manufacturing as a dynamic damper adjusted on required frequency. Such means is not applied in practice because of the large overall dimensions and weight of similar dampers. Besides they are completely inefficient for suppression noise created by blades.

The rotor blade of the modern helicopter is made of composite materials, has essentially major structural damping versus metallic blade, and because of the greater flexibility can undergo a major strain. The blade of the middle-sized helicopter has close to a rectangular plane form, span length 7…8,5 m, chord 0,5 … 0,65 m, and twist ranging from +4 6 up to -1,5.. 2,5 degrees. The basic load-bearing element of the blade - spar, is made or level-by-level packing of reinforcing fiber glass fabric, or spiral winding by unidirectional fiber glass tape, stacked on epoxy resin symmetrical to an axis of the spar. Root parts of the spar usually strengthen by packets of a titanium foil and fiber glass fabric. The maximum centrifugal forces and tensile stresses have the order consequently of 20 … 25 ton and 80 … 100 MPa.

The known experimental architectures of the geometry and vibrations intelligent control (Jin et al., 2005; Gardonio et al., 2005; Seong et al., 2005) include a group of a strain gages and power piezoelectric actuators bonded on a surface of controlled structure, or embedded between layers of composite material. The intelligent control system treats the information from sensors and hand out signals in a real-time. These signals drive the actuators which change the dynamic stress-strain state and damp the load-carrying structure vibrations (Figure 1). Because of it a rotor disbalance, noise and total vibrations level decreases, and prevent occurrence of critical modes. Successes in development of similar systems (Li et al., 2006; Salman, 2005; Rajasekaran, 2002; Valoor et al., 2001) are achieved, basically, on the neural network-based approach.

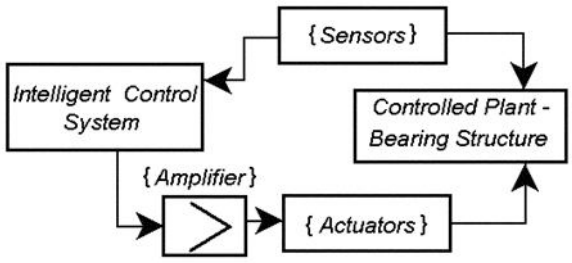

Figure 1. Concept of intelligent control of bearing structure's dynamics

Unfortunately, the lack of suitable mathematical foundations does not allow to a priori selecting the most effective architecture of neural network. Its design is yielded on the basis of the exhausting information on dynamic of a controllable mechanical system and, mostly, error method.

2. THE NEURAL NETWORK – BASED ARCHITECTURE OF STRUCTURE'S VIBRATION DAMPING

The architecture of a control system closest to the purposes of the present work contains two neural networks: networks - identifier and networks – controller (Valoor et al., 2001) (see figure 2). It is

ISSN 1313-2539

evident (in any case, while we do not have the sufficient information to consider differently) each network should have a number of hidden layers depending on complexity of a structure dynamic state. In dynamics operation of network quantized, i.e. the acting signals are treated not continuously, and in discrete instants. Thus the continuous time t is substituted by discrete time t_k:

$$t \to t_k = k \times \Delta t \to k\,.$$

The input signal of network – identifier is the signals from all sensors $\{V_s(t-\Delta t)\}$ and voltages from the controller to actuators $\{V_{ac}(t)\}$. An output of the identifier - new predicted signals from sensors $\{\overline{V}_s(t)\}$. The input signal of network – controller can be signals from sensors $\{V_s(t-\Delta t)\}$ and actuators $\{V_s(t-\Delta t)\}$ at preceding sample time. From an output the new signals $\{V_{ac}(t)\}$ operate on actuators.

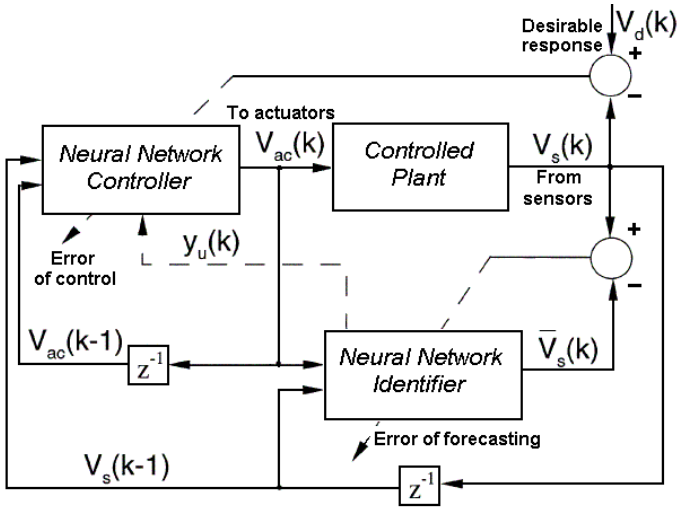

Figure 2. Neural network architecture of system for structure's vibration adaptive control (after Valoor et al., 2001)

The devices indicated in a Figure 2 by blocks z^{-1}, memorize of signal at preceding sample time. Selected signals of errors of a system's dynamic state forecasting are

$$E = 0.5\sum_{k=1}^{N_s}\left(\overline{V}_{sk} - V_{sk}\right)^2 = 0.5\sum_{k=1}^{N_s}{\delta_{sk}}^2$$

and control signal

$$E_c = 0.5\sum_{k=1}^{N_s}\left(V_{dk} - V_{sk}\right)^2 = 0.5\sum_{k=1}^{N_s}{\delta_{ck}}^2\,,$$

where V_{dk} – desirable response and V_{sk} – registered response of systems by k-th sensor in each sample time are produced at network learning.

Feature of the given approach is that the investigated dynamic system should be completely defined; thus the selftuning control system will provide optimum control, if the exterior perturbations do not overstep the bounds of given amplitude and frequency ranges. However the contingencies are possible when the control is not defined. Just such situations introduce the greatest hazard, and for their

ISSN 1313-2539

elimination the systems of intelligent control are intended. This circumstance essentially restricts applying such approach for build-up of rotor blade dynamics intelligent control. On the other hand, at presence of a broad frequency spectrum of vibrations the scheme represented in Figure 2, apparently, can not provide satisfactory reaction rate, since it will utillize of registered parameters values only on two temporal layers - actual and preceding. Adequate restoring of the mechanical system dynamic state evolution needs increase of neural network inputs number, information contents about system in preceding instants and, naturally, number of temporal layers.

Our numerical simulations carried out with a neural network such type as depicted on a Figure 2 and controlling finite-element model of a beam have confirmed the basic result obtained in (Valoor et al., 2001) about efficiency of similar system for damping vibrations on two first eigenfrequencies. However, two and the triple increase of hidden layers, volume of learning sequenses did not result into an effective vibration damping of beam model at impulsive loadings.

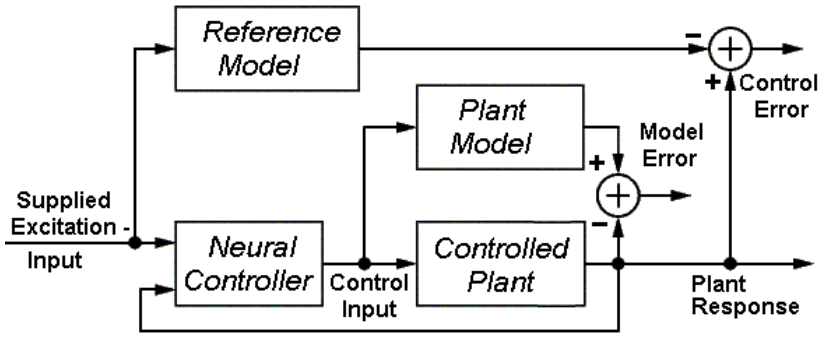

Figure 3. Architecture of control system based on reference model

For elimination of the marked limitation the control system architecture with use of master model (Model Reference Control) was designed (see Figure 3). According to (Hagan et al., 2002) in the beginning a model identification of a controllable mechanical system is yielded, then training of the neural network controller so that the output of controllable plant has match follows to an output of reference model. The structure of both neural networks contains a number of hidden layers, dependent by complication of controllable system - plant. The set of the controller input signals include: a delayed input of reference model; a delayed output of controller; a delayed output of a controllable system. The magnitude of delays can vary being increase with plant complication. The networks for mechanical systems simulation include two set of inputs: a delayed output of the controller; and delayed output of plant. The values of delays also are regulated in accordance with complication of controllable system behavior.

As reference model can be utilized an extreme simplified analytical or finite element model, maximum closest on dynamic responses to an actual controllable structure. An indispensable requirement superimposed on reference model, is it much improved behavior in critical situations (flutter, local damage etc.) at the expense of a heightened stiffness and structural (often nonlinear) damping.

Because of plant is a distributed mechanical system working in a frequency range cover to several first vibration modes, the considered architecture requires major volume of computations at stage of controller's learning and well balanced reference model. Furthermore that training teamwise with substantial mechanical system is represented difficultly implemented, adequate model of the plant – helicopter rotor blade required. The most perspective way is the making of blade finite element model and performing on it massive numerical simulations with the purpose of development of learning sequences.

ISSN 1313-2539

3. FINITE-ELEMENT (FE) MODEL OF PLANT – HELICOPTER MAIN ROTOR BLADE

3D models built by Catia v.5 on the basis of a full-scale blade design. For a guaranteed reliability of results the finite element analysis executed independently in ANSYS-10, Comsol Multiphysics 3.2, and ACELAN; all mathematical calculations - in MathCAD 11, MATLAB 7.3. That the properties of created 3D models were maximum close to dynamic responses of a full-scale blade the imported points of a blade spar cross-section optimally transformed to the spline representation specific to the used finite element program. The coordinates of spar sections were read as the text file by the program - converter translated points of sections to spline representation (rational curves Bezier and NURBS), ensuring thus minimization of splines coordinates deviation from a theoretical profile. The sketch of blade design and it finite-element model are demonstrated on Figures 4 and 5.

Along blade spar the cross-sections considering the hollow trailing sections the accurate (in geometrical sense) finite-element models were designed. On this basis the static characteristics and natural vibration modes were tested. However for major computational complexity of such models in the helicopter rotor blade at finite-element analysis some distinctive parts selected, which one modeled by relative simple geometry and homogeneous properties (Figure 5, a).

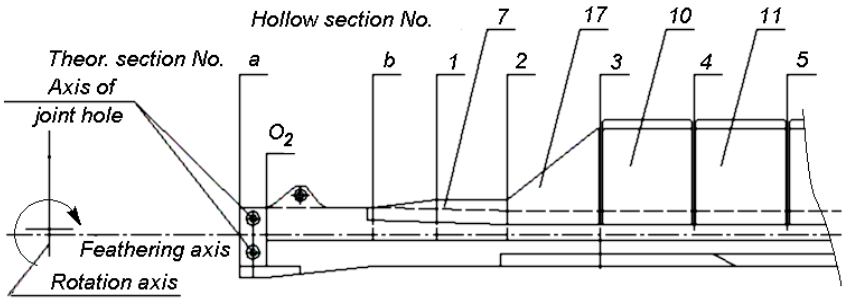

Figure 4. Piece of the modeled blade sketch

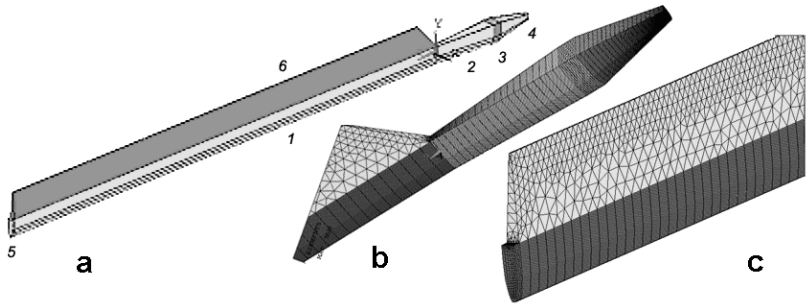

Figure 5. The simplified rotor blade finite-element model
a – full view; b – near root; c – near tip

In subdomains V_q, $q = 1,2,...6$ we have the equations of elastic body

$$\sigma_{ij,j} = \rho \ddot{u}_i \ (-\rho\omega^2 u_i), \quad \sigma_{ij} = c_{ijkl} u_{k,l} \quad i = 1,2,3$$

and boundary conditions on exterior boundaries $S = S_u \bigcup S_t$:

$$u_i|_{S_u} = u_i^0, \quad t_i = \sigma_{ij} n_j|_{S_t} = p_i,$$

ISSN 1313-2539

where u_i, n_i - components of displacement and normal vector respectively, σ_{ij}, c_{ijkl} - components of a stress tensor and elastic constants, ρ - density, ω - angular frequency.

The problem was raised in weak formulation, and its solution was searched in finite-element representation

$$\mathbf{u}(\mathbf{x},t)=\mathbf{N}_u^T(\mathbf{x})\cdot\mathbf{U}(t)\ ,$$

leaving to the differential equations for vector of nodal variables $\mathbf{a}=[\mathbf{U}]^T$

$$\mathbf{M}\cdot\ddot{\mathbf{a}}+\mathbf{C}\cdot\dot{\mathbf{a}}+\mathbf{K}\cdot\mathbf{a}=\mathbf{F}$$

where $\mathbf{M}$, $\mathbf{C}$, $\mathbf{K}$, $\mathbf{F}$ - matrices of masses, damping, stiffness and vector of nodal loadings respectively. At modal analysis achievement the generalized eigenvalues problem was considered

$$\mathbf{K}\cdot\mathbf{a}=\omega^2\mathbf{M}\cdot\mathbf{a}$$

The comparative calculations of eigenfrequencies and natural vibration modes were performed in finite-element packages ACELAN, ANSYS and Comsol Multiphysics. With respect to character of blade bracing in the elastomeric bearing box of rotor hub modal analysis is carried out and the first 7 eigenfrequencies and vibration modes (see Figure 6) are determined. On a presented investigation phase the influence of centrifugal forces was leave out of this study framework.

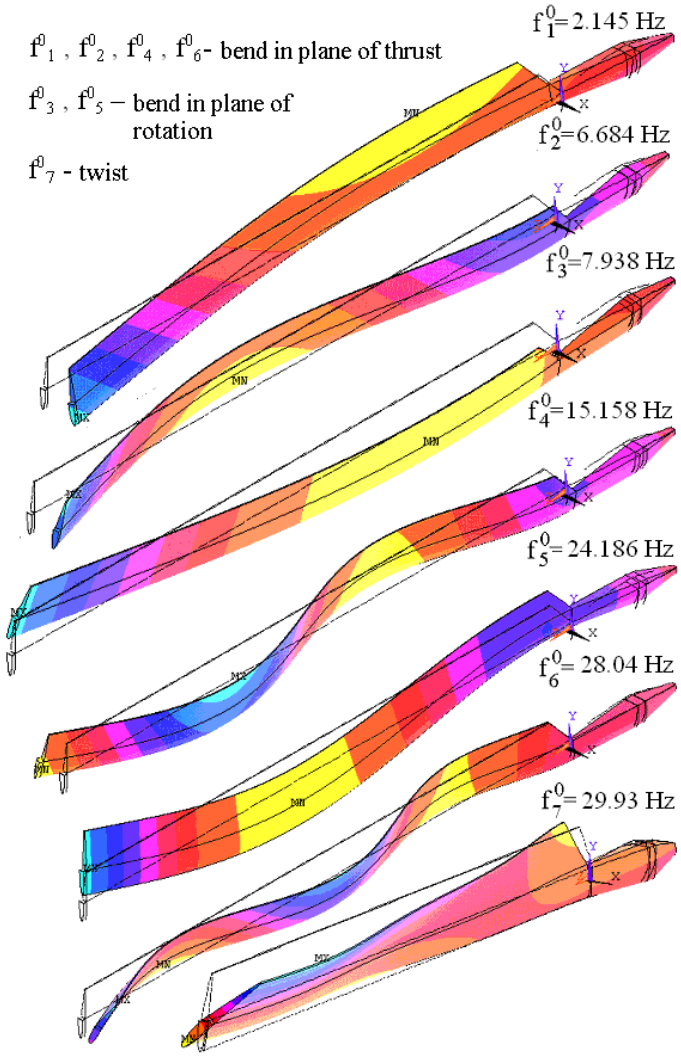

Figure 6. First vibration modes of model blade

ISSN 1313-2539

Obtained finite-element and beam models were utilized for modal and non-stationary analysis, showing the good agreement. The modal analysis (Figure 6) has revealed the allocation of eigenfrequencies and amplitudes distributions, thus, allowing a rational placement of actuators for extinguishing undesirable vibration modes, and also eliminate dangerous proximity of eigenfrequencies for flexural and torsional modes. For use as reference model obtained beam model was modified by increase of stiffness, viscous damping and translation of an axis of centers mass in flight direction.

4. CONTROL SYSTEM MODELING

The convenient tools for design and simulation of neural network-based dynamic systems in MATLAB and Comsol Multyphysics capabilities for export finite-element models in Simulink have predetermined a choice of these programs for making model of rotor blade dynamics control system. In numerical experiments have utilized from 2 up to 8 sensors and separately controllable actuators, placed on top and bottom surfaces along a reference beam and controllable plant. The neural network controller (No 3 on Figure 7) contained from 2 up to 5 hidden layers and up to 7 delays; the value of sample time 5 ms. An amount of nodes in finite-element models varied: for reference beam - 120…400, for plant - 14000…80000. All simulations were performed in 64-bit versions of the programs under Windows XP-64. Behavior of system inspected on time charts of flapping movement and angular displacements (angle of attack) of separate blade section. The case history of control system with neural network controller having 5 hidden layers and 5 delays is shown in a Figure 8.

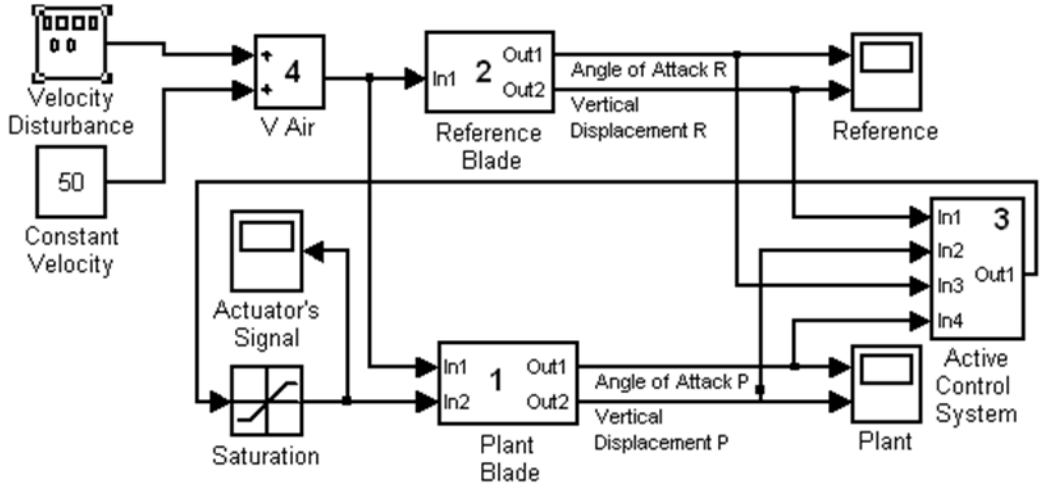

Figure 7. Simulink - model of neural network system for vibration damping of rotor blade finite element model

In lack of control signals at critical airflow velocity 60 m/s the vibratory instability - flutter of blade model arise. The frequency of elastic vibrations decrease, and the amplitude accrues sharply (see Fig.8, b, d) meanwhile the oscillations of reference beam is stable (see Fig. 8, a, c).
After run-up of the controller (Fig. 8, e, f) because of the expense of stiffness and structural damping the vibration amplitudes of a transverse displacement and angle of attack after short transient (3-4 periods) are drop down and stabilized - the flutter not arise. The duration of this transient is determined by an amount and power of used actuators. On the Simulink-model the ultimate actuators output was limited by saturation blocks.

.

ISSN 1313-2539

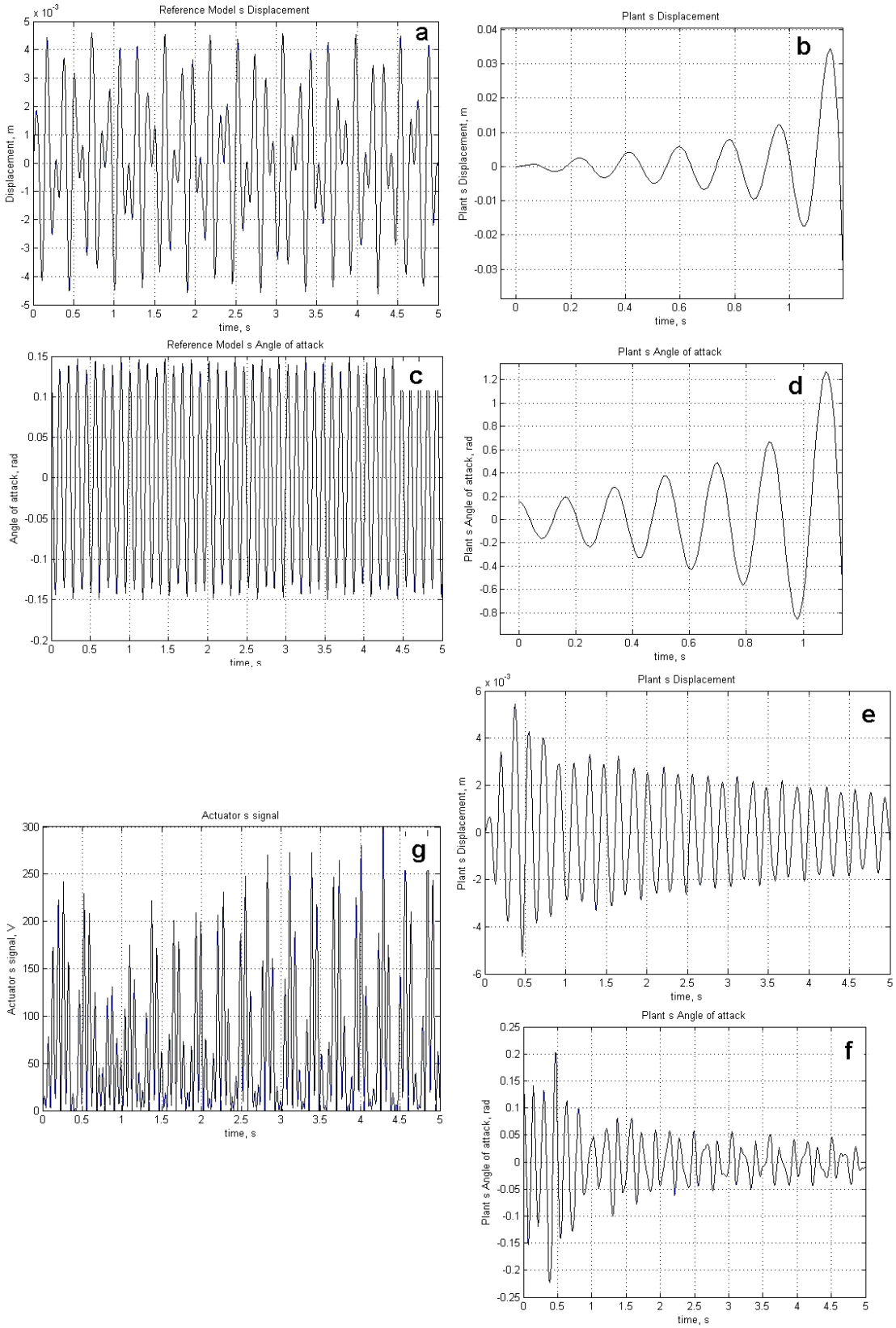

Figure 8. The time charts of displacement and angle of attack at airflow speed 60 m/sec:

ISSN 1313-2539

a, c - near reference plate tip;
b, d – near tip of the rotor blade unruled finite element model (shown on figure 5);
e, f - near tip of the rotor blade finite element model with active neural network controller;
g – electric potential on a piezoelectric actuator

5. CONCLUSIONS

The realization of proposed system has required considerable volume of computational operations at stage of the neural controller training for development about 10 thousand learning vectors. However experience of operation with created model and the first experimental results obtained on apparatus for study of composite plate auto-oscillations, have shown, that due to flexibility and speed of implementation in real time the architecture of control with reference model is represented as most perspective.

ACKNOWLEDGEMENTS

The authors wish to thank the Russian Foundation for Basic Research for her valuable help in projects 05-01-0690, 06-01-08041, 07-08-12193, and 07-08-13589.

REFERENCES

1. Sater J.M., Lesieutre G., Martin C. A Smarter Transition for Smarter Technologies (2006) *Aerospace America*, June, p.18-21

2. Rodgers, J.P., Hagood N.W. Development of an Integral Twist-Actuated Rotor Blade for Individual Blade Control (1998) Active Materials and Structures Laboratory Report #98-6, MIT, 56 p.

3. Hodges D.H.; and Bauchau O. A.: Multi-Body Approach to the Dynamic Analysis of Space Structures with Actuated Components (2003) Final Report: Grant F49620-01-1-0038, U.S. Air Force Office of Scientific Research, Dec. 2003

4. Johnson W. Helicopter Theory (1994) Dover publ, N.-Y., 1096 p.

5. Leishman J.G. Principles of Helicopter Aerodynamics (1999) Cambridge University Press, 496 p.

6. Jin-Chein Lin, M.H. Nien. Adaptive control of a composite cantilever beam with piezoelectric damping-modal actuators/sensors (2005) *Composite Structures*. No 70. pp.170–176

7. Gardonio P., Elliott S.J. Modal response of a beam with a sensor–actuator pair for the implementation of velocity feedback control (2005) *Journal of Sound and Vibration*. No 284. pp.1–22

8. Seong Hwan Moon, Joon Seok Hwang. Panel flutter suppression with an optimal controller based on the nonlinear model using piezoelectric materials (2005) *Composite Structures*. No.8 pp.371–379

9. Li Chuntuo, Tan Yonghong. Adaptive control of system with hysteresis using neural networks (2006) *Journal of Systems Engineering and Electronics*. Vol. I7. No 1. pp. 163 – 167.

10. Salman R. Neural networks of adaptive inverse control systems (2005) *Applied Mathematics and Computation*. No.163. pp.931–939

ISSN 1313-2539

11. Rajasekaran S., Vijayalakshmi G.A.P. Recurrent Neural Dynamics Models for Equilibrium and Eigen Value Problem (2002) *Mathematical and Computing Modelling*. No 35. pp.229-240

12. Valoor M.T., Chandrashekhara K., Agarwal S. Self-adaptive vibration control of smart composite beams using recurrent neural architecture (2001) *International Journal Solids and Structures*. No. 38. pp.7857-7874

13. Hagan M.T., Demuth H.B., and Beale M.H. Neural Network Design. Boston (2002), MA: PWS, 437 p.

ISSN 1313-2539

A FEW ASPECTS ABOUT ESTABLISHING THE STATUS OF THE GAS INSULATION INSIDE HIGH VOLTAGE EQUIPMENT

Alexandru S. Jude[1], Petru Ehegartner[1], Petru Andea[1] and Flaviu M. Frigura-Iliasa[1]

[1] Power Systems Department, Faculty of Electrical and Power Engineering, POLITEHNICA University of Timisoara, Romania, E-mail: flaviu.frigura@et.upt.ro

Abstract

SF_6 insulating installations are today the most performing technical solution applied to high voltage devices such as circuit-breakers and surge arresters. This gas is used due to a lot of excellent insulating properties. These properties are depending on many variables, one of them is electrodes' geometry and material. Capsulated SF_6 installations unlike open ones are submitted to various faults which are revealed only when all the equipment is completely or partially destroyed. This paper presents some aspects concerning fault location methods used in the diagnosis of capsulated SF_6 equipment (circuit breakers, surge arresters). These methods are applied in Romania and in other countries by both producers and users of this piece of equipment.

Key words: *high voltage equipment, gas insulation*

1. INTRODUCTION

Generally, in capsulated equipment each fault which appears is less visible than in open ones. Only when the entire compartment is open (and by doing that, it is totally or partially destroyed), all faults could be visible and located. In the case of insulation tests made by the producer or by the user of that equipment, each partial discharge have to be precisely located in order to reduce time or to reduce the costs of the maintenance.

Generally, when studding the dielectric breakthrough process, ideal electrode surfaces are taken in consideration. But many experimental results, different than theoretical ones, could be a consequence of microscopic asperities. These asperities are mostly undefined and could modify the dielectric breakthrough process by local increases of the electric field's intensity or by supplementary electrons emission which leads to an apparent dielectric rigidity decrease. In reality, only a few parameters are modified (the electric field, the initial electrons number). The individual asperities number will affect the dielectric rigidity empirically determined before.

We also notice all SF_6 equipment users' requests for having precise methods and test equipment adequate for continuous control of the insulation state [2], [3]. Such methods and test equipment will be presented in this paper.

2. FAULT LOCATION POSSIBILITIES INSIDE SF_6 CAPSULATED INSULATIONS

Insulation breakthrough appears as a consequence of an electrical discharge like a streamer or like an electrical arch. Breakthroughs during insulation test are most likely streamers and the others, appearing during long time service are electrical arches.

As we know, the appearance of the leader (as a preliminary phase of the breakthrough) is characterized by an intense light, heat, sound and ultrasound emission as well as SF_6 decomposition. These effects are normally limited to the fault area. Combined with these effects, an electromagnetic transitory phenomenon, consisting in traveling waves, over voltages or intense magnetic fields, occurs too.

ISSN 1313-2539

Each fault location device has to be able to memorize that fault, which mostly has a very short period of time, until the fault (the state) is registered by the operator or by a dispatcher. After that, the record could be erased on demand or automatically.

Figure 1 shows the main effects produced by electrical breakthrough, which could be used for fault location. "*S*" means an effect used for spark faults and "*A*" an effect used for arch faults.

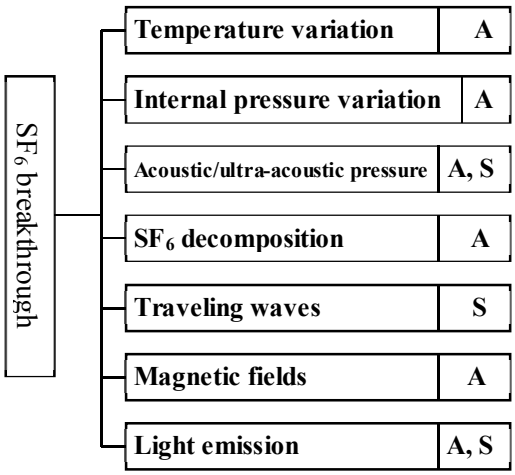

Figure 1. The effects of SF_6 breakthrough and their use for fault location

Fault location is based on the main effects of dielectric breakthrough and it could be:

- Fault location based on temperature increase is a function of the electric energy transformed in heat in the electrical arch canal. It could not be applied to insulation tests. But it could be used in detecting faults appearing in long service time by applying heat sensitive paint on capsulated devices.
- Pressure increase based fault location applied to separated capsules (with no gas exchange) is possible only in the case of an electrical arch.

  Pressure variation is given by equation (1):

$$P = k\,I\,t\,/\,V \tag{1}$$

  where I is the RMS value of the short-circuit current, t is the short-circuit time, V is the capsulated gas volume, and k is a constant depending on equipment' design. Pressure variation occurred in this case has the same order like gas pressure and it's bigger than temperature caused pressure variation. It could be measured by using a simple manometer.
- Fault location based on acoustic waves caused by the incident is possible both in case of sparks and electrical arch. Although it is difficult to separate sounds of an electrical arch fault from sounds of an electrical arch which appears on normal commutation.
- Gas analysis based fault location, on each compartment of the capsulated device is a cheap technical solution. A minimum amount of gas from the verified compartment is released by a valve in a glass tube containing a basic solution. In presence of acid decomposition residues, the solution is neutralized and changes color. For the whole capsulated device, this process could take a few hours, so its use is limited.

ISSN 1313-2539

- Traveling waves based fault location can be used only for a short amount of sections, only in specialized labs, because each impedance variation causes reflections and refractions which could complicate the process.
- Magnetic field based fault location is used when an internal breakthrough, followed by an electrical arch, occurs. This phenomenon produces a strong magnetic field which could be measured only on the exterior surface of the aluminum shield, as we notice on Figure 2. The experimental results [3] shown a radial component of the magnetic induction of about 3 mT for a fault current of 1 kA. This kind of magnetic fields could be measured by magnetic sensors placed on an adhesive tape fixes around the envelope. This deposit has to look like a heavy magnetic material and the distance between two separate tapes has to be at least 120 – 150 mm [3].

  The flexible magnetic sensors, (named from 1 to 8 in Figure 2) are initially de-magnetized and in normally service state of the equipment and their magnetic status is not affected by the current crossing the envelope. The reading of the measurements is done by using a flux-meter. I_k is the short-circuit current and B_r is the radial magnetic induction.

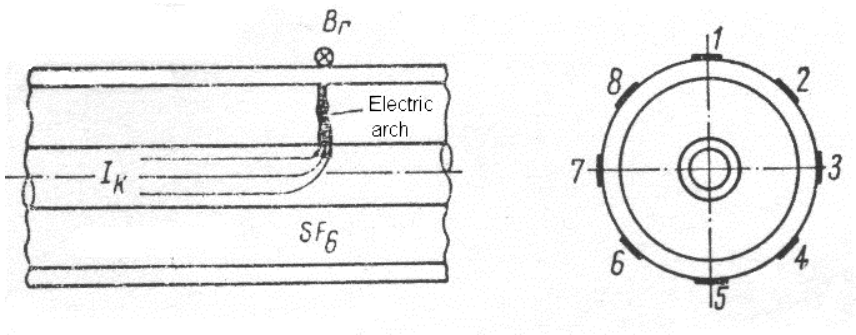

Figure 2. Magnetic field based fault location method applied to a capsulated bar system

- Light emission fault location allows detection of both sparks and electrical arch. Experiments shown that breakthroughs in SF_6 made light emissions in a specter between 330 and 655 nm [2]. We can also notice a weak continuous red specter and a spectral maximum between 330 and 470 nm (ultra-violet and blue). If every section of the capsulated device contains an optical sensor, each of them must be extremely sensitive, due to the geometry of that section (curves, angles, insulations, different layer).

  As we notice in Figure 3a, the light open angle of that device must be as large as possible due to its exocentric position. Light emission diodes, and photo-transistors are placed as sensors and the light is received by passing trough Plexiglas windows. The detection block may be realized, as we notice in Figure 3b, by using an integrated light sensor. This block contains also a pre-amplifier followed by a comparator block which gives de sensitivity limit of this device. The turn-off of that comparator acts an execution circuit which maintains the information for a local or remote control. In order to avoid any electromagnetic interferences caused by fault short-circuit currents, detectors' electric supply is made by using batteries, the whole device being made inside an electromagnetic shield.

  In Figure 3 a:

  - *1* are the optical sensors;
  - *2* are the tight insulating elements;

ISSN 1313-2539

- *3* is a middle insulating element.

In Figure 3 b, (which is the schema of the optical sensor):

- *1* is a threaded connection;
- *2* is a transparent section;
- *3* is a photo-diode (or a photo-transistor);
- *4* is a pre-amplifier;
- *5* is a comparator;
- *6* is a relay;
- *7* is a battery;
- *8* a signal output gate;
- *9* is an electromagnetic shield.
-

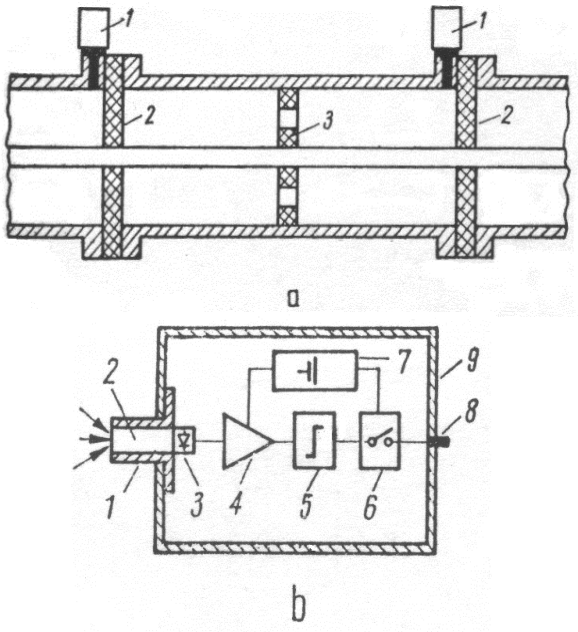

Figure 3. Light emission based fault location method applied to a capsulated SF_6 compartment

3. PREDICTIVE BREAKTHROUGH DETECTION POSSIBILITIES

This problem is more difficult to solve than fault location due to the lack of information about it. One way to do this is by using the partial discharges.

Each partial discharge detector must have these properties:

- to not modify the existing capsulated insulation (eventually to be placed outside that device);
- to be as compact as possible;
- to not be affected by external discharges or electromagnetic noises and to resist to extreme internal ones.

ISSN 1313-2539

Fault simulation in a capsulated insulation (having a nominal voltage of 77 kV) has lead to the results shown in Table 1. All the measurements were made by using an electrical fault detection equipment type ERA3. We can notice that no matter the detection method involved, that one has to be able to detect partial discharges on a level from 10 to 20 pC.

Table 1- Partial discharges level and repetition frequency made by artificial faults in a 77 kV capsulated insulation

Simulated fault	Apparent charge pC	Frequency Hz
Imperfect contact on current way	10 000	1 000
Contour discharge for a border insulating element	11 000	600
Presence of foreign elements:		
Grains of Copper	40	-
M10 screw	600	100
Border insulating element enclosures	2800	80

Between all preventive fault detection methods taken in consideration, the optical and the acoustical method are mostly used. The ultra-acoustic method was successfully applied by the biggest Romanian high-voltage circuit-breaker manufacturer, Electroputere S.A. Craiova [2] to detect any free particle inside that equipment. This company is making some researches in order to design and manufacture an industrial testing equipment based on this method.

An original electrical preventive fault detection method is described in [1]. This method is designated for fault detection on conic insulators or disc insulators. These faults could appear as pollution with SF_6 decomposition residues.

As we notice on Figure 4 a, on one exterior surface of the insulating element *1* (made of resin) which sustains the main conductor *2*, a conductive layer *3* was applied. This layer represents the electrode used to collect all the information about any possible faults in the insulating element. This information is then transmitted to the differential amplifier *4*. On the other entry of that amplifier, a signal from the capacitive sensor made through the insulation *5* between the electrode *6* and the earth-connected metal envelope *7* is received.

ISSN 1313-2539

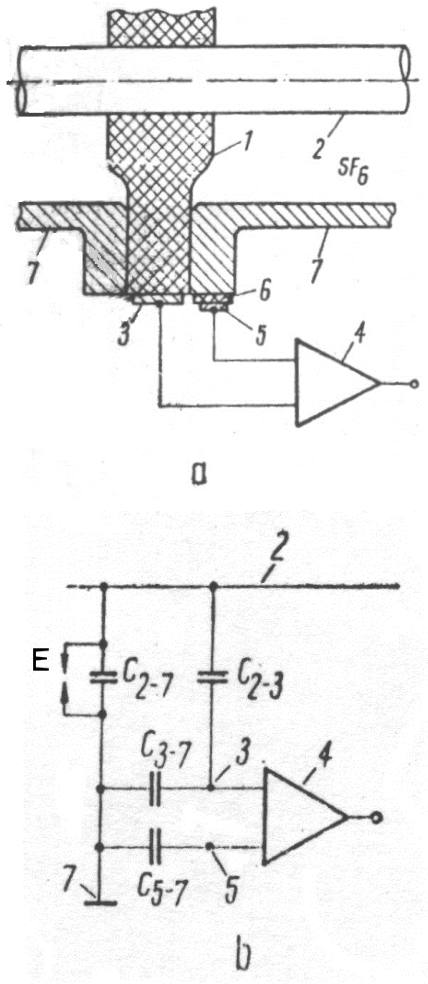

Figure 4. Partial discharges detection method applied to a capsulated SF_6 installation

This differential scheme assures a very high noise reduction as we observe in Figure 4 b. A 10 pC partial discharge could be easily detected using this equipment.

On this figure, *E* is an spark gap which simulate the partial discharges on the insulating element *1*.

$C_{2\text{-}7}$, $C_{2\text{-}3}$, $C_{3\text{-}7}$ and $C_{5\text{-}5}$ are the capacities existing between all these electrodes involved.

4. THE INFLUENCE OF THE ELECTRODES' ROUGHNESS ON SF_6 DIELECTRIC BEHAVIOR

Generally, when studding the dielectric breakthrough process, ideal electrode surfaces are taken in consideration. But many experimental results, different than theoretical ones, could be a consequence of microscopic asperities. These asperities are mostly undefined and could modify the dielectric breakthrough process by local increases of the electric field's intensity or by supplementary electrons emission which leads to an apparent dielectric rigidity decrease. In reality, only a few parameters are modified (the electric field, the initial electrons number). The individual asperities number will affect the dielectric rigidity empirically determined before. We will present separately the influence of the asperities and the influence of electrodes' material on supplementary electrons emission.

ISSN 1313-2539

The breakthrough fault could be stimulated when microscopic electrodes are present. The influence of the roughness of the electrodes must be taken in consideration after a massive maintenance operation when all contacts are cleaned, polished and covered.

On a technical electrode surface, depending on which treatment was applied on that surface, all asperities are distributed evenly (polished, sandblasted, cast) or periodically (turned, milled, planed) [1]. Even polished aluminum surfaces have roughness when looking on an electronic microscope. The maximum peak of that surface could be determined in a dielectric breakthrough. This microscopic fault, on a few square centimeters surface seems almost unidentifiable, because it could be detected only on a longitudinal palpation. That's why the maximum roughness R_{tmax}, taken from a standard profile is not representative for the entire electrode [2].

If measured values for the dielectric withstand-voltage are related to R_{tmax}, those results could heavily be used to other systems. It is more advantageous to describe the roughness of a certain electrode surface by using a standard well-defined method or (better) by using the medium roughness $\overline{R_t}$, measured from a roughness profile. A complete analysis is done when using both $\overline{R_t}$ and microscopic pictures taken from that profile. The electronic microscope pictures indicate even post-breakthrough geometrical variations of that superficial surface which normally don't affect the withstand-voltage, because simultaneously conductive deposits appear. The influence of electrode's roughness on the withstand-voltage could be easily and detailed studied by making measurements on aluminum electrodes characterized by a certain $\overline{R_t}$ combined with electronic microscope pictures.

As we know, when the medium roughness $\overline{R_t}$ increases, the dielectric rigidity E_{s063} decreases.
The relation between dielectric rigidity and gas pressure is given by (2):

$$E_{s063} = \left(\frac{E_{sT}}{p_{20}}\right)^{*} \cdot (10 \cdot p_{20})^{C} \qquad (2)$$

This linear family is limited on top by the interior dielectric rigidity, line 1, E_{si} (considered only for ideal electrodes) and on bottom by the technical dielectric rigidity line 6, E_{st}, for not treated surfaces. All the surfaces considered are also represented by lines. Some values for those parameters are given in Table 2 [2]:

By using this relation between the dielectric rigidity and the medium roughness, a roughness factor, depending on pressure, could be determined, as shown in relation (2):

$$e_r = \frac{E_s}{E_{si}} = \frac{(E_{st} / p_{20})^{*}}{(E_{sl} / p_{20})^{*}} p^{C-1} = f(\overline{R_t}) \le 1 \qquad (3)$$

These parameters are deductible from different other relations given in literature.

By knowing this roughness factor, for a given medium roughness $\overline{R_t}$, the requested dielectric rigidity could be easily determined:

$$E_s = e_r \cdot E_{si} \qquad (4)$$

The withstand-voltage, for a given electrodes system is given by:

$$U_s = E_{si} \cdot e_r \cdot e_h \cdot \eta_F \cdot d \qquad (5)$$

Where e_k is the curve coefficient, η_F is the homogeneity coefficient and d is the distance between the electrodes [3].

ISSN 1313-2539

Table 2 - Dielectric rigidity values for different surface treatments

Line nr.	$\left(\frac{E_{sT}}{p_{20}}\right)^{*}, in \frac{kV}{mm \cdot MPa}$	Treatment	$\overline{R_t}$ [μm]
1	89	-	(0)
2	84	Polished	0,085
3	81	Pulled	0,550
4	78	Sandblasted	5,0
5	71	Striated	36,0
6	65	none	(300)

These relations could be used for any type of voltage.

5. CONCLUSIONS

Fault detection and location in capsulated SF_6 installations could be easily made on new pieces of equipment as well as on existing service ones.

Fault location optical devices have a large perspective for the next future, due to their simplicity. They are compact, easy to use and very high noise resistant and could be applied both for fault risk detection and effective fault detection.

Dielectric rigidity for SF_6 insulations depends on different factors. One of them is roughness. Generally, we can say that when the medium roughness increases, the dielectric rigidity decreases. The electrodes material's influence on dielectric behavior is interesting only for "smaller asperities". We noticed that for normal SF_6 insulations, no important electrode material influence was detected.

REFERENCES

1. K. Abe and others, *Gas-insulated electric apparatus and method of detecting partial discharge therein*. U.S. registered patent no.4,277,746.

2. S.A. Boggs and others, (1982) Propositions pour ameliorer la fiabilité des postes blindés à très haute tension et faciliter les interventions. *CIGRE, 1982*, Rap. 23-10.

3. Ryan H.M., Spence G., (1975) Surface roughness determination. *ISH Zurich*, p. 17-22

4. Vatau D., Frigura F., (2003) *Elemente moderne de materiale si tehnologii pentru electrotehnica*, "Orizonturi Universitare" Publishing house, Timisoara, Romania

ISSN 1313-2539

WAYS OF RISING OF EFFICIENCY OF N-PARAFFIN DEHYDROGENATION REACTOR BLOCK FUNCTIONING WITH USE OF TECHNOLOGICAL MODELLING SYSTEM

Anatoly Kravtsov V., Emily Ivanchina D., Elena Ivashkina N., EgorYuriev M., Irena Shnidorova O.

Tomsk Polytechnic University, 634050, Lenin Street, 30, Tomsk, Russia

Abstract

In this article the applied using of technological modelling system of dehydrogenation process of n-paraffins has been examined. The products of this process are monoolefines, which are used to obtain synthetic detergents. In the basis of this system a formalized mechanism of hydrocarbons transformation on the Pt-catalyst surface lies. Using of the developed system allows to prolongate the catalyst durability due to optimisation of its usage mode and also to model different variants of plant reconstruction. After preliminary research of temperature influence, raw materials consumption and volume on the process efficiency, it was ascertained that one of the possible variants is switch into two-reactor scheme (it means using the second reserve reactor of paraffins dehydrogenation). Also the conditions of continuous functioning of two parallelly working reactors have been considered. Conformity of proposed variants of plant reconstruction has been economically proved. This helps to raise efficiency of synthetic detergents obtaining.

Key words: *mathematical modelling, dehydrogenation, reactor, catalyst, n-paraffin, n-olefines, efficiency,model, account*

1. INTRODUCTION

Last years development of the consumer market actively stimulates development of the industry, including petrochemical one. In particular, manufactures of synthetic detergents and their raw-material base - linear alkyl benzenes (LAB), linear alkyl benzene sulphanates (LABS) rapidly develop. Thus the volume of import of synthetic washing-up liquids remains high enough: More than 60 % of the Russian release of synthetic washing-up liquids are supervised by transnational corporations.

By expert estimations, the American company Procter&Gamble, German Henkel, etc. supervise about 80 % of the market of detergents [1].

The factor of updating of a fixed capital is for Russian manufacturers of household chemical goods in 4 times less than necessary. The reached level of capital investments mismatches real needs of a chemical complex. Especially depresses that fact, that raw branches till now do not perceive chemical manufacture as the integral part - the share of ready chemical production in total amounts of sales of the Russian oil and gas companies makes only 3 % whereas at foreign partners it comes up to 30 %.

Narrow segmentation and a stable demand earlier did not allow the domestic companies to be fixed for a long time in this sphere, and they gave a up the place in the market to foreign competitors. But the situation changes also those foreign technologies which contained growth of the domestic industry, now work for its blessing. A striking example of it is the enterprise of Open Company «Kirishinefteorgsintez » (Open Company " Kinef ") and a factory the "LAB-LABS" included in its structure. The complex LAB and LABS manufacturing includes a number of technological blocks:

1) Plant of separation of n-paraffins by adsorption on zeolites;

2) Plant of of n-monoolefines obtaining by means of n-paraffins dehydrogenation on Pt-catalyst ;

3) Block of benzene alkylation with obtained monoolefines with the use of HF-catalyst;

ISSN 1313-2539

4) Plant of LAB sulphidation and neutralization.

Such complex allows to receive about 180 tons of LAB with high ability to biological decomposition per day.

It is necessary to note, that for a petroleum-refining industry of all countries of the world last decade of XX century has passed under growing pressure of the ecological factor with accompanying toughening requirements of new technics to consumer properties of mineral oil [2] .

Ability for biological decomposition of synthetic detergents is the base criterion of quality of production which level, according to modern Russian ecological norms, should be not less than 88 %. The LAB obtained by Open Company " Kinef ", meets these requirements with a greater stock. The technology realized at this factory, allows to obtain the LAB with ability for biological decomposition up to 95 %.

Despite high quality, the domestic market of LAB is characterized by high deficiency of this production. Potential need of the domestic market in LAB is about 100 thousand tons per year.

Therefore increase of a production efficiency of alkyl benzenes is an important and actual problem.

The continuous monitoring of plants work with application of modern mathematical modelling methods is necessary for maintenance of optimum conditions of carrying out the processes.

The methodology of mathematical modelling developed by us for multicomponent catalytic processes of hydrocarbonic raw material processing is based on following concepts of the system analysis of chemical-technological processes:

1) Availability and reliability of the experimental data put in a basis of researches (on raw material, products and mode conditions of process);

2) Formalization of the mechanism of hydrocarbons transformation on the catalyst surface, based on association of components according to reactionary ability; drawing up of the transformation scheme of the incorporated components, finding out how reactionary ability of the hydrocarbons belonging to one gomological group depend on their physical and chemical properties;

3) An establishment of kinetic laws of processes of catalyst desactivation, based on the account of simultaneously proceeding reactions of coke formation, ageing and a poisoning with poisons of an active contact surface, and also influence of technological conditions of process and hydrocarbonic structure of processed raw material on speed of catalyst desactivation;

4) Construction of technological modelling system of process for monitoring and forecasting of work of plants, computer support and revealing of "narrow" places of manufacturing.

These concepts are most fully fulfilled on an example of catalytic reforming of gasolines [3-7].

At the same time, the developed methodology is applicable for a petrochemical complex of processes of LAB manufacturing processes, (fig 1) which capacities make 50 thousand tons of alkyl benzene.

ISSN 1313-2539

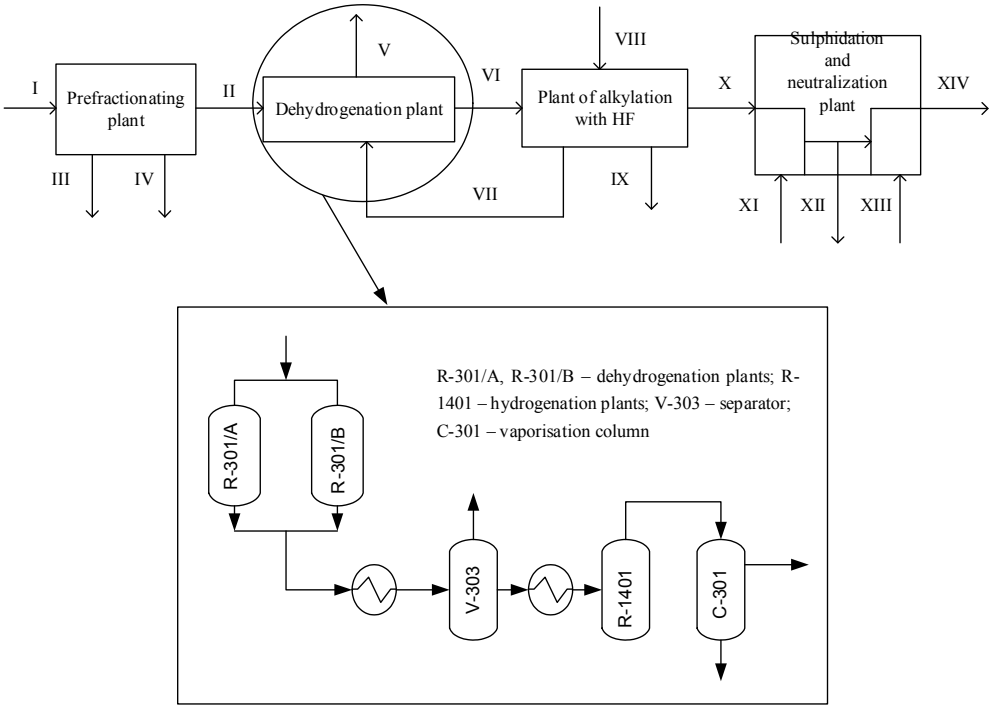

Fig. 1. Flowchart of lines of LAB, LABS production complex: I) n-paraffins from adsorption plant ; II) C_{10}–C_{13}n-paraffins; III) fraction of C_{14}–C_{17} n-paraffins; IV) fraction of C_{18} and higher n-paraffins; V) hydrogen containing gas; VI) mixture of n-paraffins and monoolefines; VII) recirculating n-paraffins; VIII) benzene from catalytic reforming plant; IX) heavy alkylate; X) LAB; XI) sulfur from an elemental sulfur set; XII) LABS; XIII) alkali; XIV) sodium salt of alkylbenzenesulphuric acid

One of possible ways of plant productivity increase is switching of a reserve reactor dehydrogenation reactor in parallel work with operating one.

2. SEARCHING OF HOW DOES CONCENTRATION OF OLEFINES DEPENDS ON TEMPERATURE, VOLUME AND EXPENDITURE OF RAW MATERIAL PASSED

The basic purpose of works at the present stage of researches is development of recommendations on technological parameters of carrying out of industrial dehydrogenation process with simultaneous work of two dehydrogenation reactors at the various expenditure of processed raw material and volumetric speed of raw materials supply (VSRMS).

Switching to parallel work of dehydrogenation reactors means decrease in raw material loading on one reactor from 75 m3 per hour to 37,5 m3 per hour, that will be reflected both on kinetic, and in a hydrodynamical operating mode of a reactor.

We have lead calculations of hydraulic resistance of the dehydrogenation catalyst layer at various loadings on raw material, tab. 1.

ISSN 1313-2539

Table 1 - Influence of the raw material supply on hydraulic resistance of the catalyst layer

Parameter	G_c=75 m^3/h *l*=7/1	G_c=37,5 m^3/h *l*=7/1	G_c=37,5 m^3/h *l*=8/1
VSRMS, h^{-1}	22	11,3	11,3
$\Delta P_{сл}$, kPa	18	4,9	5,4

**l* - molar ratio "hydrogen/raw material", $_{Gc}$ - raw material supply, $_{\Delta Pсл}$ - hydraulic resistance of the catalyst layer, VSRMS - volumetric speed of raw materials supply.

Decrease in hydraulic resistance of the catalyst layer will allow to lower diffusion complications during the target dehydrogenation reaction passing and to maintain the Pt-catalyst in softer hydraulic mode.

Change of volumetric speed of raw materials supply will affect a degree of grain use of the catalyst which can be evaluated through the factor of efficiency (fig. 2):

$$\varphi = l \cdot \sqrt{\frac{k}{D_{эфф}}} \quad (1);$$

$$\eta = \frac{3}{\varphi}\left(\frac{1}{th\varphi} - \frac{1}{\varphi}\right) \quad (2),$$

where *l* – a radius of the catalyst particle, m; *k* - a constant of speed of chemical reaction, s^{-1} ($l\ mol^{-1}\ s^{-1}$), $D_{эфф}$-effective factor of diffusion, m^2/s; φ-module of Tile; ŋ factor of efficiency of grain use of the catalyst.

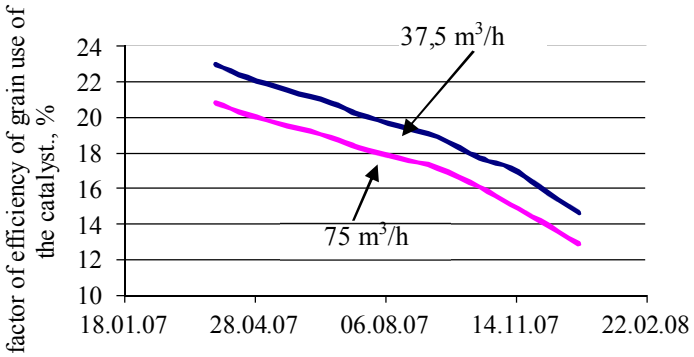

Figure 2. A degree of the catalyst use in dependence on loading on raw material and time of the catalyst operation

Change of temperature drop in a reactor depends on kinetics of the process, so, on type of the loaded catalyst and structure of raw material. With application of non-stationary mathematical model of process and calculation of its thermal balance it became possible to lead an estimation of change of temperature drop.

ISSN 1313-2539

The mathematical model of industrial dehydrogenation process, developed by the department of chemical technology of fuel of Tomsk polytechnical university is sensitive to a chemical compound of raw material processed on the plant [9]. The kinetic description put in a basis of technological modelling system, is developed taking into account various reactionary ability of paraffin hydrocarbons C9-C14 in dehydrogenation reactions. The hydro dynamical component of model allows to consider influence of the raw material expenditure passed through a reactor on parameters of process. The generalized mathematical description of process represents system of the following differential equations of material and thermal balances, eq. (3) - (4).

$$G\frac{\partial C_i}{\partial z}+G\frac{\partial C_i}{\partial V}=(1-\varepsilon)\sum_j w_j, \qquad (3)$$

s.c. z=0: C_i=0, гр.у. V=0: C_i=$C_{вх}$

$$G\frac{\partial T}{\partial z}+G\frac{\partial T}{\partial V}=-(1-\varepsilon)\frac{\sum_j \Delta H_j r_i}{c_p \rho}, \qquad (4)$$

s.c. z=0: T=T_0, гр.у.V=0: T=$T_{вх}$,

where C_i- concentration of i-th hydrocarbon, mol/m^3; U- linear speed of a stream, m/h; ε -pore volume of catalyst layer; r_i- speed of reaction, mol/m^3·h; $r_i=\sum_j W_j=\frac{dC_i}{dt}$; w_j–speed *of j-th* component in *i-th* reaction, mol/m^3·h; T – temperature of the process, K; ΔH_j- thermal effect of reaction, Joule/mol; c_p – thermal capacity of a mixture, Joule/mol·K; ρ -density of a mixture, kg/m^3; T_0- start temperature (temperature of an environment), K; $T_{вх}$- temperature of an input in a reactor, K; $C_{вх}$ –entrance concentration of hydrocarbon, mol/m^3.

Time of stay of reagents in the reactionary zone, depending on the hour expenditure of raw material G, volume of the catalyst V, in conditions of a stable loading of plant on raw material is replaced with « resulted time » or total volume of the processed raw material, $z=Gt$, m^3, t – time, hour.

Forecasting of a variant of double-reactor scheme of work of operating plant can be most effectively executed with application of the developed by authors kinetic model adequately describing real industrial paraffins dehydrogenation process [3].

Experimental researches allow to estimate only influence of change of volumetric speed of raw materials supply on process parameters.

At the same time it is necessary to consider a degree of dehydrogenation catalyst deactivation, that, in its turn, makes the contribution to change of a technological mode and, accordingly, qualitative and quantitative characteristics of a target product.

Experiments of such duration cannot be lead, since, the degree of the catalyst deactivation depends both on a temperature mode of catalyst operating, and on structure and volume of the raw material passed through the reactor.

ISSN 1313-2539

So, the estimation of the catalyst activity change lead on mathematical model, has shown, that for 3-6-day period of plant work (about 7, 2 thousand m3 of raw material passed) the catalyst activity concerning target paraffins dehydrogenation reaction will decrease on 0,04-0,11 %. Concerning collateral reactions of olefines dehydrogenation - on 0,01-0,02 %, paraffins hydrocracking - on 0,21-0,58 %, isoparaffins dehydrocyclization - on 0,07-0,21 %; the content of coke on the catalyst thus is estimated as 0,022 %, that practically does not influence a course of process.

On fig. 3-8 the results of calculations on model of concentration of olefines and diolefines in a product flow depending on temperature, the expenditure and volume of the raw material passed through a reactor are presented.

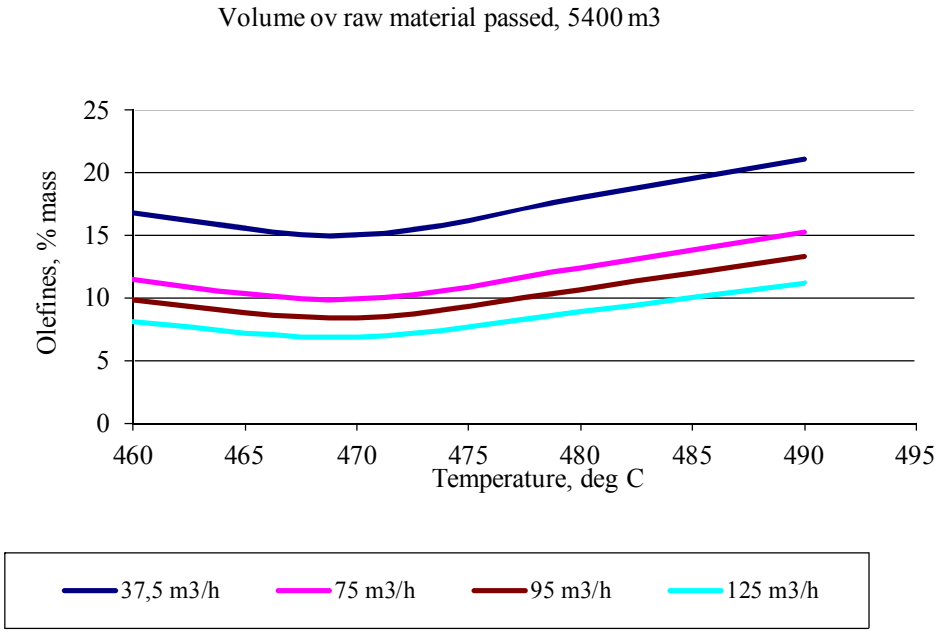

Figure 3. - Change of concentration of olefines depending on temperature and expenditure of raw material at 5 thousand m^3 of raw material passed (about 3 days of plant work)

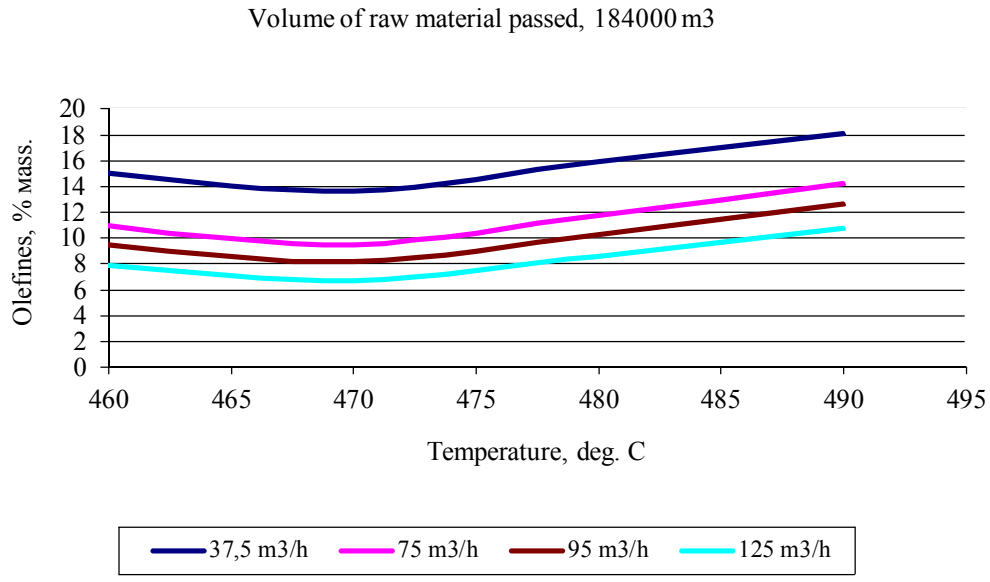

Figure 4. - Change of concentration of olefines depending on temperature and expenditure of raw material at 184 thousand m^3 of raw material passed (more than days of plant work)

ISSN 1313-2539

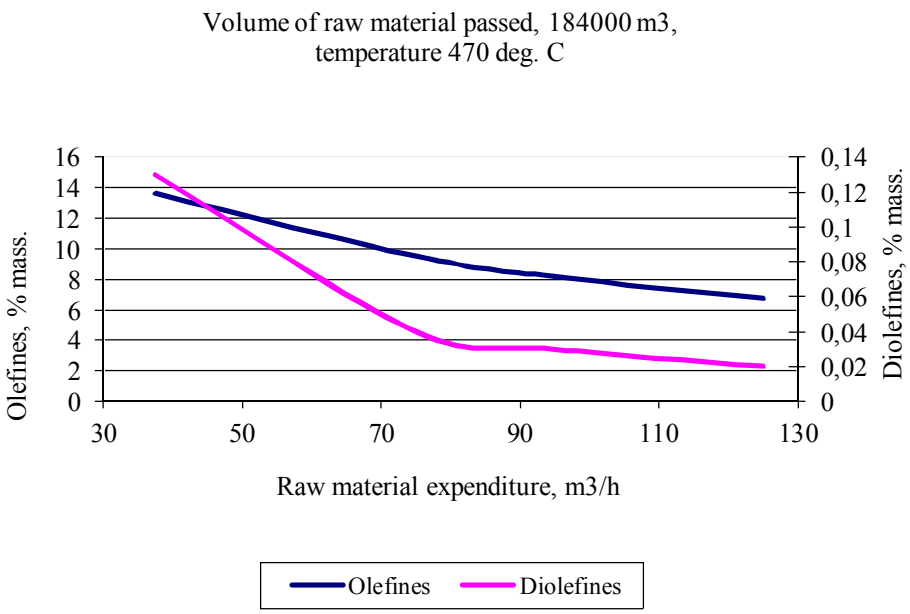

Figure 5 - Change of concentration of olefines and diolefines depending on temperature and the expenditure of raw material at 184 thousand m^3 of raw material passed (more than days of plant work)

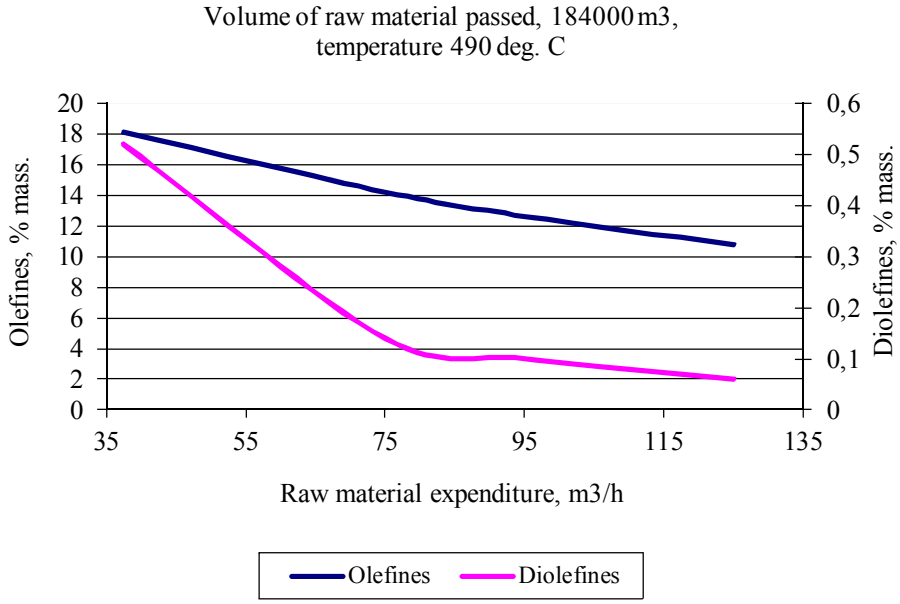

Figure 6- Change of concentration of olefines and diolefines depending on temperature and the expenditure of raw material at 184 thousand m^3 of raw material passed (more than days of plant work)

ISSN 1313-2539

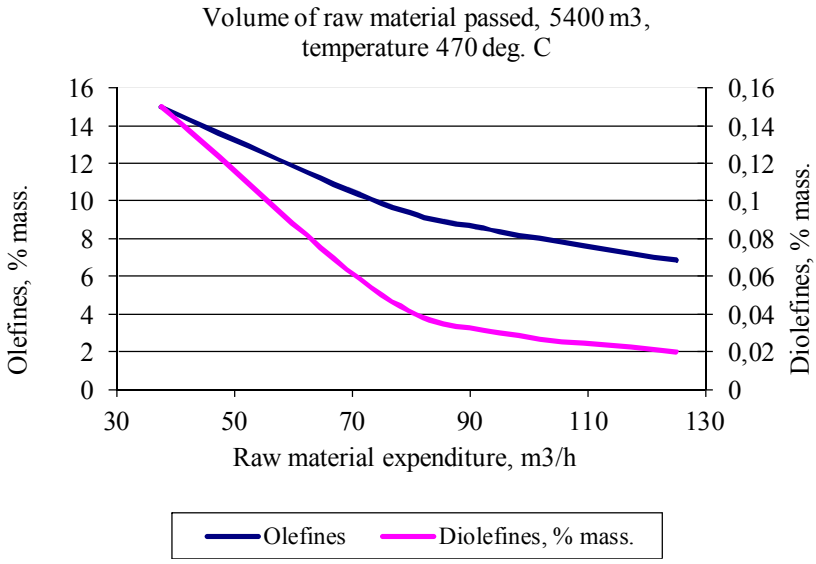

Figure 7- Change of concentration of olefines and diolefines depending on temperature and the expenditure of raw material at 5,4 thousand m^3 of raw material passed (about 3 days of plant work)

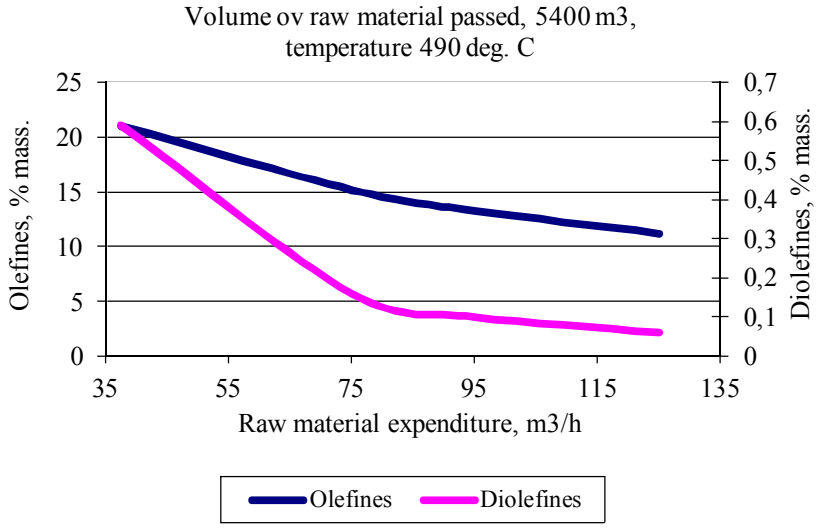

Figure 8- Change of concentration of olefines and diolefines depending on temperature and the expenditure of raw material at 5,4 thousand m^3 of raw material passed (about 3 days of plant work)

As it shown in fig. 3-8, with growth of temperature concentration target and by-products in mixture increases. At the same time it falls with increase of raw material expenditure and volume of raw material passed through dehydrogenation reactor (with strengthening of the catalyst), that does not contradict classical conceptions about heterogeneous catalysis. Inclusion of a reactor of diolefines by-products hydrogenation in the technological scheme allows to increase quantity target olefines, acting on a stage of benzene alkylation with monoolefines, tab. 2-3.

ISSN 1313-2539

Table 2

Concentration of target and by-products (without taking into account a stage of hydrogenation) at various temperature and raw material expenditure (molar ratio "hydrogen/hydrocarbons» =7/1, volume of the raw material passed-184 thousand m^3)

Products, % mass.	Temperature, °C	
	470	490
Raw material expenditure, 37,5 m^3/h		
Olefines	12,74	16,32
Diolefines	1,27	2,63
Aromatic hydrocarbons	0,34	0,4
Raw material expenditure,75 m^3/h		
Olefines	9,19	13,28
Diolefines	0,56	1,33
Aromatic hydrocarbons	0,29	0,38
Raw material expenditure, 95 m^3/h		
Olefines	7,96	11,93
Diolefines	0,4	1,01
Aromatic hydrocarbons	0,22	0,31
Raw material expenditure, 125 m3/h		
Olefines	6,62	10,31
Diolefines	0,27	0,72
Aromatic hydrocarbons	0,23	0,33

Table 3

Concentration of target and by-products (with taking into account a stage of hydrogenation) at various temperature and raw material expenditure (molar ratio "hydrogen/hydrocarbons» =7/1, volume of the raw
material passed-184 thousand m^3)

Products, % mass.	Temperature, °C	
	470	490
Raw material expenditure, 37,5 m3/h		
Olefines	13,62	18,1
Diolefines	0,13	0,52
Aromatic hydrocarbons	0,29	0,35
Raw material expenditure,75 m3/h		
Olefines	9,52	14,2
Diolefines	0,04	0,14
Aromatic hydrocarbons	0,24	0,33
Raw material expenditure,95 m3/h		
Olefines	8,17	12,61
Diolefines	0,03	0,1
Aromatic hydrocarbons	0,22	0,31
Raw material expenditure, 125 m3/h		
Olefines	6,73	10,76
Diolefines.	0,02	0,06
Aromatic hydrocarbons	0,19	0,28

ISSN 1313-2539

Simultaneous rise in temperature of process and increase in time of contact of reagents (increase of "rigidity" of process), undoubtedly, will lead to growth of by-products concentration and high coke accumulation. It will negatively influence quality of obtained production and will reduce durability of the catalyst.

Thus, executed with application of mathematical model researches about how does raw material expenditure influence parameters of n-paraffins dehydrogenation process have allowed to reveal following laws:

a) With increase of raw material expenditure and, hence, volumetric speed of raw materials supply (VSRMS) it is necessary to rise temperature for manufacturing of demanded quantity of a target product - olefin, but without changing a process "rigidity";

b) With rise in temperature and decrease of VSRMS concentration of olefines in a product mixture increases; that can be explained by thermodynamics of target dehydrogenation reaction. Calculations on model show increase in concentration of olefines, on average on 20 %, with decrease of VSRMS up to 10 h^{-1} and temperature 490 °C;

c) With rise in temperature and decrease of VSRMS, together with increase of target product increases the level of by-products - diolefines and aromatic hydrocarbons also; that is connected with increase in time of reagents contact;

d) Selectivity of process decreases with growth of conversion and increases with increase of raw material expenditure.

These laws correspond to theoretical conceptions and are experimentally proved.

Thus, for forecast estimations of work efficiency of parallel working reactors it is necessary to consider influence of several factors, in particular, operating parameters of the given process is not only time of reagents contact, but also temperature of industrial process carrying out.

With decrease in loading on raw material (from 75 till 37,5 m^3/h) the decrease in rate of rise of input temperature in a dehydrogenation reactor on the average on 20 °C is possible in view of equally set concentration of a target product (at carrying out forecast calculations on model 9,61 % mass.), fig. 9.

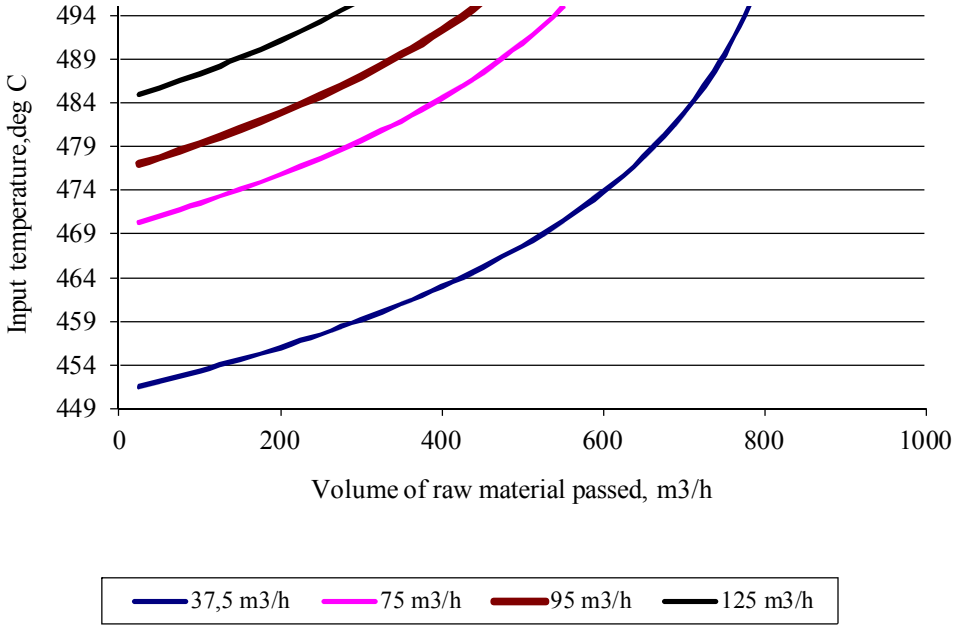

Figure 9. -Change of an input temperature in a dehydrogenation reactor at the various raw material expenditure

ISSN 1313-2539

Possible variant of decrease in rate of coke accumulation on the catalyst, and also growth of by-products concentration is the increase of molar ratio "hydrogen/raw material". Results of modelling researches are presented in tab. 4-5.

Table 4

Concentration of target and by-products (with taking into account a stage of hydrogenation) at various temperature and raw material expenditure (molar ratio "hydrogen/hydrocarbons» =8/1, volume of the raw material passed-184 thousand m^3)

Products, % мас.	Temperature, °C	
	470	490
Raw material expenditure, 37,5 m3/h		
Olefines	13,37	16,31
Diolefines	1,14	2,44
Aromatic hydrocarbons	0,34	0,41
Raw material expenditure, 75 m3/h		
Olefines	8,62	12,76
Diolefines	0,48	1,18
Aromatic hydrocarbons	0,28	0,38
Raw material expenditure, 95 m3/h		
Olefines	7,39	11,33
Diolefines	0,34	0,89
Aromatic hydrocarbons	0,25	0,35
Raw material expenditure, 125 m3/h		
Olefines	6,09	9,68
Diolefines	0,22	0,62
Aromatic hydrocarbons	0,22	0,31

Calculations on model show, that the thermodynamics of target reaction will not allow to raise essentially an output of a target product in a unit of time with decrease in loading on raw material. Undoubtedly, more economically justified and effective is the variant of simultaneous increase of raw material expenditure.

For achievement of the maximal economic benefit maintenance of raw material expenditure at level of 50 m^3/h (100 m^3/hour for both reactors) is expediently.

Thus, realization of following recommendations is necessary:

1) temperature of an input in a reactor 460-487 ˚C;

2) molar ratio «H2/hydrocarbons» 8/1.

Finally, the choice of any of variants of work is caused by indemnification of the costs connected with maintenance of the chosen technological mode, increase in an output of the LAB in a unit of time, tab. 6.

ISSN 1313-2539

Table 6

Variants of a technological mode at operation of the plant including two dehydrogenation reactors

Raw material expenditure, m^3/h	Input temperature, °C	Duration of the catalyst run, days	Average manufacturing of LAB, t/day.	By-products (diolefines) by the end of run, % mass.
Molar ratio 7/1				
75 (for 1 reactor)	470	263	190	0,84 on 263-th day
50 (100 for 2 reactors)	462	479	256	1 on 479-th day and 0,85 on 263-th day
37,5 (75 for 2 reactors)	456	611	201	1,21 on 611-th day and 1,02 on 263-th day
Molar ratio 8/1				
75 (for 1 reactor)	470	319	178	0,74 on 319-th day and 0,69 on 263-th day
50 (100 for 2 reactors)	462	604	245	0,92 on 604-th day 0,71 on 263-th day
37,5 (75 for 2 reactors)	456	833	187	1,03 on 833-th day on 0,74 on 263-th day

It is necessary to note, that the quantity of the LAB is estimated without taking into account loss of a target product as a result of ablation with polyalkylbenzenes (PAB). On average 8-10 % the LAB are carried away with PUB (by results of laboratory analyses).

Thus, economic benefit of realization of switching to parallel work of dehydrogenation reactors can be connected:

1) With increase in duration of plant work at one loading of the Pt-catalyst from 263 till 833 days (the greatest possible increase);

2) With increase in target product output in unit of time up to 201 th day of LAB. Simultaneous achievement of both parameters is obviously possible with increase in loading of raw material on 2 reactors till 100 m3/hour and increase of molar ratio «H2/hydrocarbons» up to 8/1 (increase in run till 604 day and daily average manufacturing of LAB up to 245 tones.

At the same time, the increase in loading on a hydrogenation reactor and, accordingly, on a reactor of hydrogenation, can cause decrease of conversion at diolefines hydrogenation. The rules of the enterprise provides a working temperature interval for this reactor 180-220 ◦C. Calculations on model have shown, that the increase in loading on raw material on a reactor from 75 till 100 m3/h (approximately from 56000 up to 75000 kg/hours) will not essentially affect conversion of diolefines at an intermediate stage of LAB manufacturing; target concentration of diolefines will not exceed 0,12 % mass during all run.

3. ORGANISATION OF CONTINUOUS PLANT WORK

One more effective variant of plant operation can become the organization of continuous work of reactors as at increase in loading till 100 m3/hour (50 m3/hour on one reactor), and at its preservation at a level of 75 m3/hour (37, 5 m3/hour on one reactor).

At carrying out forecast calculations the following prospective scheme of plant start-up has been chosen:

1) simultaneous start-up of dehydrogenation reactors at loading 50 m3/hour on one reactor (319 days);

2) a stop of one of reactors, for example, R-301/A, at achievement of input temperature in a reactor 487 °C; thus the second reactor R-301/B continues working at smooth rise of input temperature from 487 up to 491 °C and increase in loading of raw material at this reactor from 50 till 75 m3/h (a

ISSN 1313-2539

maximum of 30 day, a minimum of 2 weeks), depending on when will R-301/A be overloaded with fresh catalyst);

3) Switching off a reactor R-301/B; simultaneous inclusion in work of reactor R-301/A at loading of raw material 75 m3/hour with the fresh loaded catalyst with starting temperature of an input 470 °C (15 days);

4) inclusion of reactor R-301/B in work, increase in loading on raw material till 100 m3/h (50 m3/h on one reactor) (about 1 year), etc.

Results of calculation of a similar technological mode on model are shown on figures.12-13 (at loading of 50 m3/hour on one reactor).

Let's accept following designations of sites on a curve: 1, 3 - parallel inclusion of reactors, fig.10; 2 - monoreactor operating mode, fig. 11.

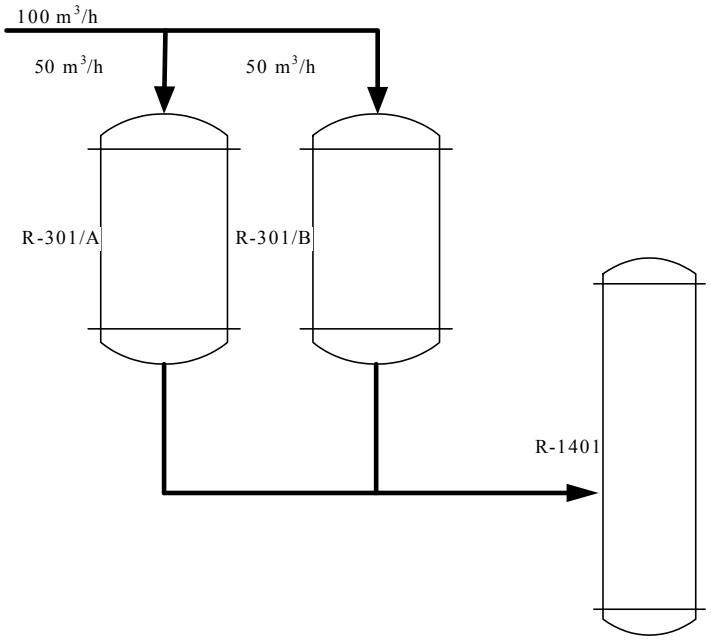

Figure 10. - parallel inclusion of dehydrogenation reactors

ISSN 1313-2539

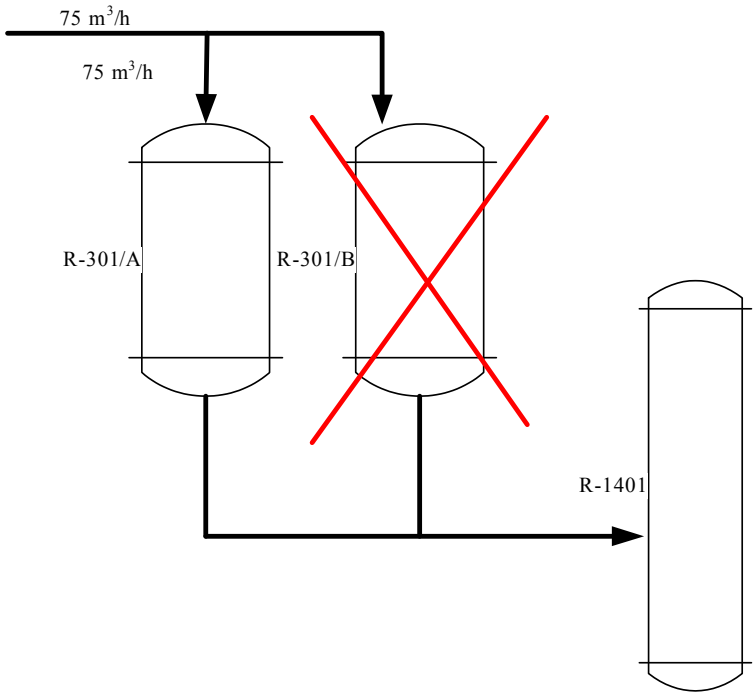

Figure 11- monoreactor operating mode

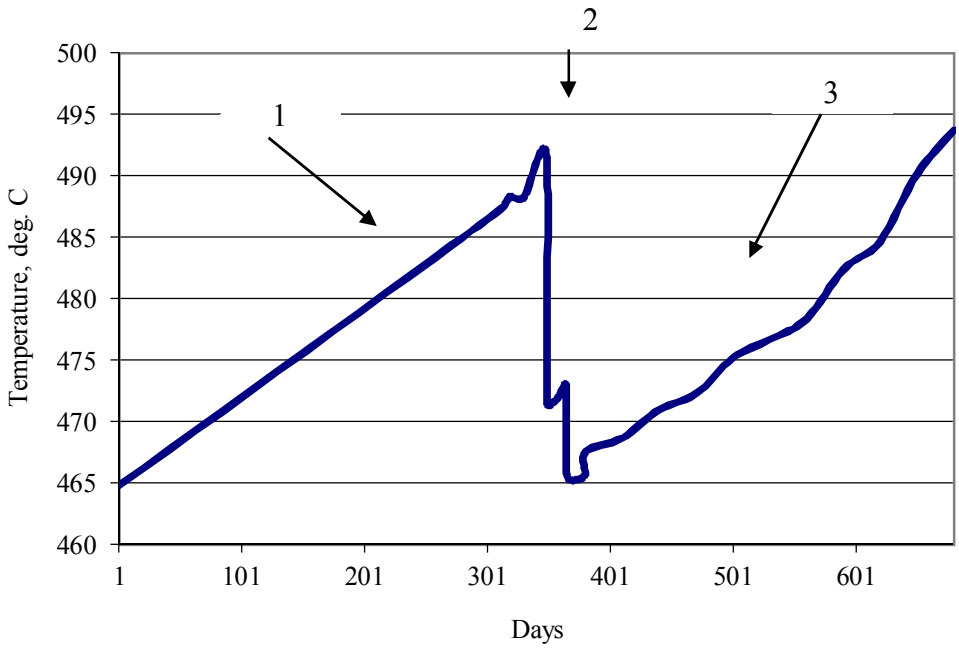

Figure 12. - Temperature of an input of raw material at the organization of continuous work of hydrogenation reactors

ISSN 1313-2539

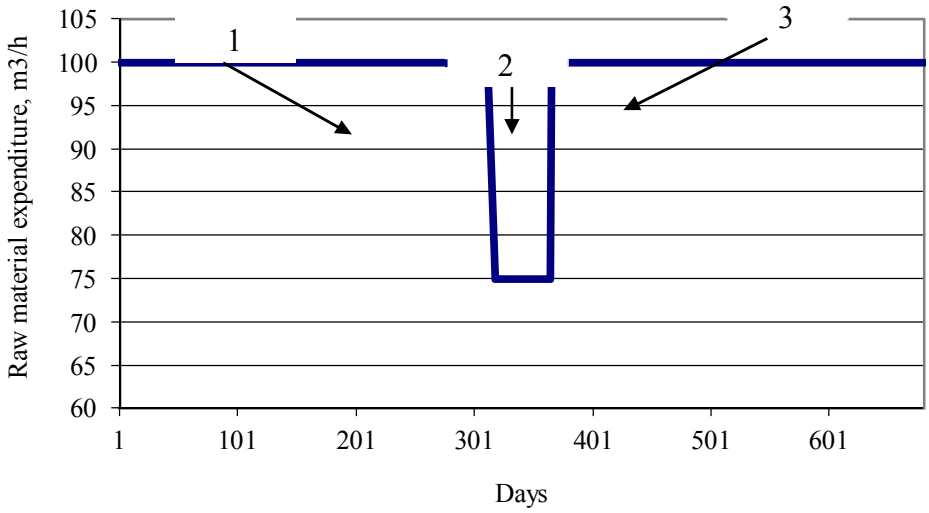

Figure 13. - Raw material expenditure at the organization of continuous work of hydrogenation reactors

If it is not possible to increase loading on raw material on both reactors till 100 m3/h, operating modes of plant and the basic parameters of efficiency at work on former loading (75 m3/hour) will look as follows, fig. 14 (at loading 37,5 m3/hour on one reactor).

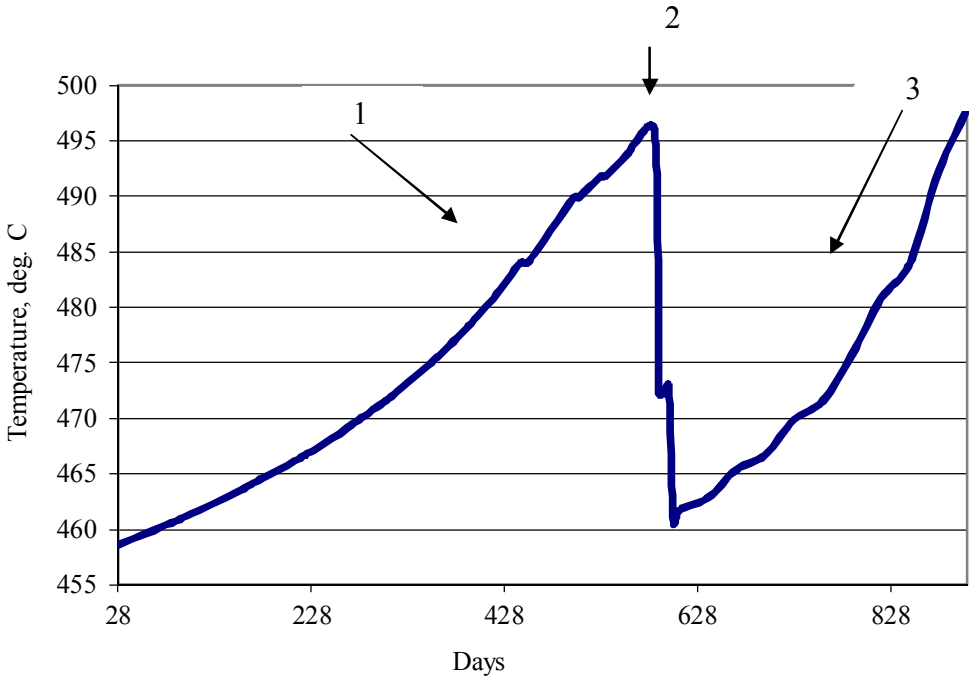

Figure 14. - Temperature of an input of raw material at the organization of continuous work of dehydrogenation reactors

ISSN 1313-2539

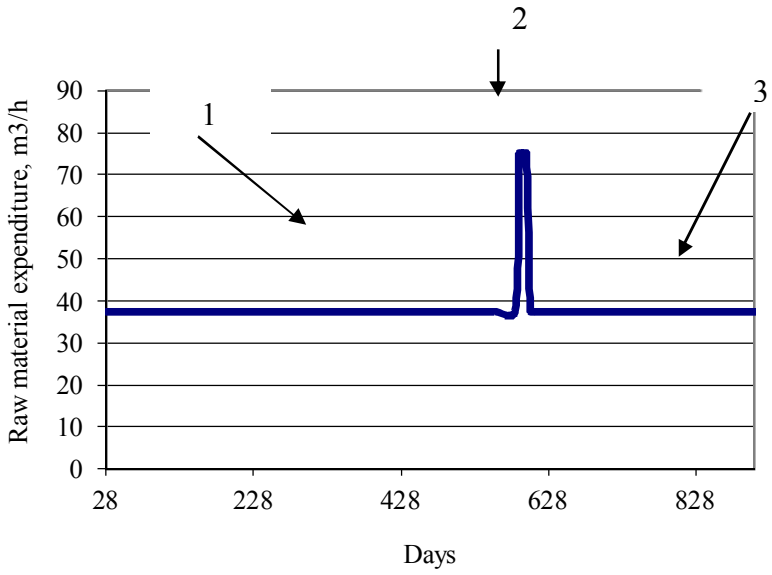

Figure 15. - Raw material expenditure at the organization of continuous work of dehydrogenation rea

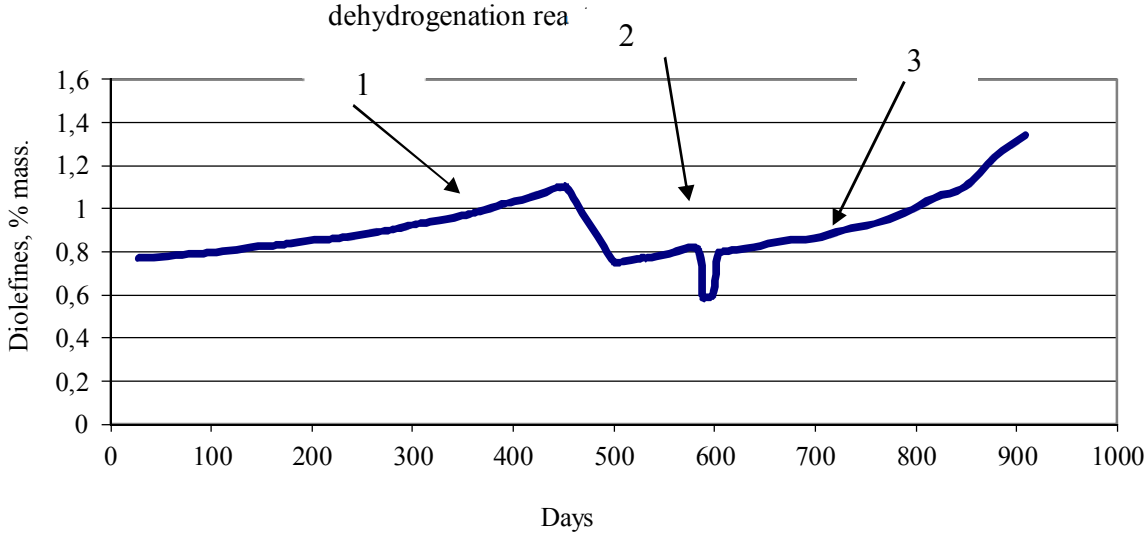

Figure 16. -Diolefines at the organization of continuous work of dehydrogenation reactors

Thus, simultaneous inclusion of two dehydrogenation reactors into work can be economically justified as from the point of view of increase in target product LAB manufacturing in a unit of time, especially with increase in "rigidity" of process, and with the organization of continuous plant work.

CONCLUSIONS

The researches carried out on mathematical model, have shown, that increase of economic efficiency linear alkyl benzenes obtaining plant work at its switching to parallel work of dehydrogenation reactors can be reached in some cases:

ISSN 1313-2539

□□At simultaneous increase in loading of raw material□up to 100 m3/h and hydrogencontaining gas expenditure the maximal effect connected both with increase of duration of catalyst run, and with increase in daily average LAB manufacturing will be reached;

□□ The organization of continuous work of reactors.

REFERENCES

1. http://www.business.dp.ua/cons/data/20070924_2.htm Inform analysis: Henkel and Procter and Gamble supervise half of Russian market of detergents // the Business world. All about the commodity markets.

2. V.E.Somov, I.A.Sadchikov, V.G.Shershun, L.V.Koreljakov Strategic priorities of the Russian oil refining enterprises. - M.: Neftechim, 2002. - 292 p.

3. Kostenko A.V. Perfection of a design and increase in dehydrogenation reactor block of catalytic reforming processes of hydrocarbonic raw material productivity. Diss. c.t.s., Tomsk, 2006.

4. Kostenko A.V., Kravtsov A.V., Ivanchina E.D., Estimation of technological parameters of Pt-catalysts for riforming procces with application of mathematical modelling method// Oil refining and petrochemistry. Scientific and technical achievements and the best practices, 2005.№12. p. 26-31.

5. Kravtsov A.V., Ivanchina E.D., Galushin S.A., Polubojartsev D.S.Experience in practical application of non-stationary kinetic model for increase of gasolines riforming process efficiency and forecasting // Oil refining and petrochemistry. Scientific and technical achievements and the best practices, 2004. - №10. - p. 8-9.

6. Kravtsov A.V., Ivanchina E.D., Averin S.N., Fedorov A.A., Krupenja L.V., Polubojartsev D.S.Activit and stability of platinum catalysts for riforming process // Chemistry and technology of fuels and oils. - 2004. - №3. - p. 40-42.

7. Kravtsov A.V., Ivanchina E.D.computer forecasting and optimization of of gasolines manufacturing process. Physico-chemical and technological bases. - Tomsk: STT: 2000. - 192 p.

8. Kravtsov A.V., Hadartsev A.C., Shatovkin A.A., Milishnikov A.V., Ivashkina E.N., Ivanchina E.D., Yuriev E.M.Computer modelling of high n-paraffins hydrogenation process on Pt-catalysts // Oil refining and petrochemistry. Scientific and technical achievements and advanced experience.-2007. - 5. - p. 35

ISSN 1313-2539

NICKEL AND COBALT-CONTAINING HETEROGENEOUS CATALYSTS CARBON DIOXIDE CONVERSION OF METHANE

Emin A. Majidov, Natalya K. Andrushenko,

Rovshan B. Akhverdiev, Afina A. Aliyeva, Sara K. Faradjeva, Tarana S. Latifova

Azerbaijan National Academy of Sciences Institute of Petrochemical Processes,

Baku, AZ1025, Khodjali ave. 30

Abstract

The valent and coordination condition of nickel and cobalt ions in contents of catalysts carbon dioxide conversion of methane is investigated. At rather low concentration (5 % mas.), as a result of chemical processes the phase of surface mixed spinel $NiAl_2O_4$ was formed, and at big quantities (10 and 15 %) - along with it surface phase of NiO was also formed. Processing of nickel-containing catalysts by methane results in practically complete reduction of Ni^{2+} nickel ions to Ni° (or Ni_n^o) and to covering of surface with coke precipitations. In CH_4 mediums + air; CH_4 + CO_2 the oxidation-reduction processes $Ni^{2+} \rightleftarrows Ni°$ with shift of balance the right in case of processing the catalyst by mix CH_4 + CO_2 proceed to. In this case on a surface of catalysts oxidizing [Ni^{2+} (T_d and O_h) in structure $NiAl_2O_4$] and reduced [NiO (or) Ni_n^o] forms of nickel coexist.

Processing cobalt-containing catalysts in the reactive medium practically does not affect a condition of ions Co^{2+} (T_d) and Co^{2+} (O_h). On a surface of cobalt oxide catalysts within the limits of concentration of cobalt 5 and 10 % mas., a phase normal spinel and $CoAl_2O_4$ and isolated surface ions Co^{2+} (O_h) are available

Key words: *carbon dioxide, methane, conversion*

Processing of methane as accessible, cheap and raw material having huge resources in useful chemical products is a problem of vital importance.

Research works on the given direction are carried out practically at all leading scientific research institutes [1-4]. The certain successes that allow to hope for the successful solution of this very actual problem have been achieved.

In IPCP of NAS of Azerbaijan nickel and cobalt-containing oxide catalysts of carbon dioxide conversion of methane, which have shown encouraging results have been developed.

With the purpose of definition of principle of effect of the developed catalysts, as well as for increase of their efficiency it is necessary to comprehensively investigate physical and chemical characteristics of catalysts, in particular, a power condition (valency and coordination) of nickel and cobalt ions on a surface of heterogeneous catalysts.

In order to study spectral characteristics of catalysts samples we selected the method of electronic spectroscopy diffusive reflections in UV and visible area as the most sensitive to a surface of solid bodies.

ISSN 1313-2539

TECHNIQUE OF EXPERIMENT

Catalysts for researches prepared a method of impregnation of microspherical γ-Al_2O_3 for 20 % aqueous solutions of nitrate salts of nickel or cobalt with the subsequent drying and impregnation at 600 °C [1].

Processing of catalysts initial reactant in various combinations was carried out in a flowing quartz reactor (V = 3 cm^3). Before experiment initial samples were warmed up in a current of nitrogen to temperature 700 °C, then via calibrated flowmeters this or that reactant, or mix (1 : 1 mole) was delivered.

Diffuse reflection electronic spectra (DRES) in the field of 50000-10000 sm^{-1} are recorded on spectrophotometer «SPECORD M 40».

OXIDE NICKEL-ALUMINIUM CATALYSTS

$Ni^{2+}(3d^8)$. The basic term of free d^8-ion ^3F, excited - ^3P, ^1D, ^1G, ^1S. In octahedral crystal field the term 3F is split on $^3A_{2g}$ (the basic condition, a configuration $t^6_{2g}\,e^2_g$), $^3T_{2g}$ and $^3T_{1g}$. As for all ions with the basic F-condition of free ion (^3F in Cr^{3+} and Ni^{2+}, ^4F in V^{3+} and Co^{2+}) there is only one term of the same multiplet ^3P (or ^4P), therefore, in a crystal field three transitions allowed on spin out in all cases are formed: two levels of the split term ^3F (or ^4F) [$^3A_{2g}\rightarrow{}^3T_{2g}$ and $^3A_{2g}\rightarrow{}^3T_{1g}$ (^3F)] and one more level formed from ^3P (or ^4P) [$^3A_{2g}\rightarrow{}^3T_{1g}$ (^3P)]. Weak, forbidden on spin, narrow strips are observed as a result of transitions with $^3A_{2g}$ on ^1E_g and $^1A_{1g}$ (from ^1D), weak wide strips – as a result of transitions to the other singlet levels (fall in UV-area).

In tetrahedral coordination the basic condition Ni^{2+} becomes $^3T_1$ and three transitions allowed on spin are allowed: $^3T_1\rightarrow{}^3T_2$, $^3T_1\rightarrow{}^3A_2$ and $^3T_1$ (F) $\rightarrow{}^3T_1$ (P), but shifted in long-wave area (since $D_{qtetr} = 4/9D_{qoct}$ and D_q M^{2+} $<D_q$ M^{3+}). Absence of symmetry center in tetrahedral positions removes forbidenness of transitions on parity that results in increase in intensity of absorption of ions of nickel in tetrahedron in comparison with octahedron.

Diffuse reflection spectra of NiO system (5 have been recorded and analysed; 10 and 15 % mas.) - γ-Al_2O_3 after processing in the reactive medium.

NiO (5 % mas.) - γ-Al_2O_3

Spectrum of sample with rather low contents of nickel (5 % mas.) is characterized by group of strips of absorption (s.a.) in the field of 13500, 15900, 17000, 27400 cm^{-1} to which it agrees [5, 6] can be interpreted as follows:

- the s.a. at 13500 and 27400 cm^{-1} are attributed to octahedrally coordinated ions Ni^{2+} (accordingly transitions $^3A_{2g}\rightarrow{}^3T_{2g}$ and $^3A_{2g}\rightarrow{}^3T_{1g}$ (P)) [7-10];
- the s.a. at 15900 and 27400 cm^{-1} are characteristic for ions Ni^{2+}, stabilized in fields tetrahedral coordination (transitions $^3T_1(F)\rightarrow{}^3T_1(P)$ and $^3T_1(F)\rightarrow{}^1T(D)$ respectively) [9, 10].

Thus, given oxide system contains octahedral and tetrahedrally co-ordinated ions Ni^{2+}. It is known, that in spinel $NiAl_2O_4$ which is mixed, there is a nickel both in O_h-, and at T_d-coordination. The formul of this spinel is possible to give as

$$Ni_{1/4}Al_{3/4}\,[Ni_{3/4}Al_{5/4}]\,O_4.$$

It is possible to assume, as in our conditions surface of mixed spinel $NiAl_2O_4$ is formed. This result will be coordinated to the data of other researchers of this system [7-11].

ISSN 1313-2539

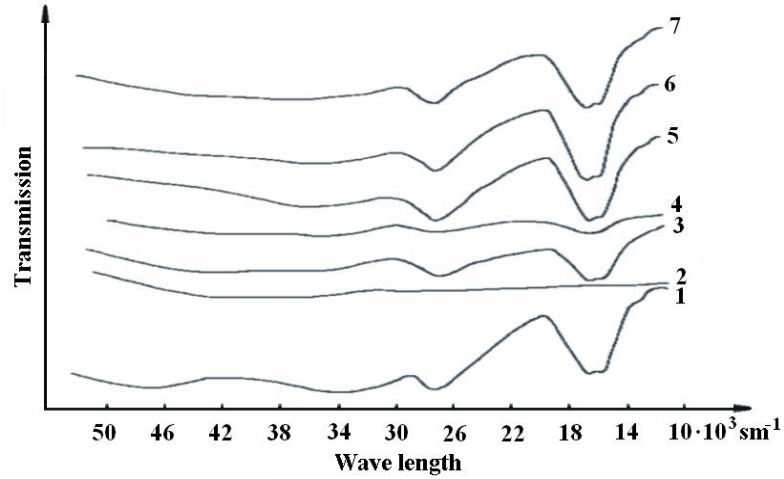

Fig. 1. Spectra diffuse reflection of NiO (5 % mas.) - γ-Al_2O_3 system after processing by initial reactants: 1 – fresh catalyst; 2 – after processing in CH_4; 3 – after processing in mix CH_4 + air; 4 – after processing in mix CH_4 + CO_2; 5 – after processing in CO_2; 6 – after processing by oxygen of air; 7 – after processing in mix CH_4 + CO^2 + air

Processing of the catalyst in methane results in essential changes in a spectrum, namely, the items from ions Ni^{2+} (T_d) and Ni^{2+} (O_h) completely disappear and the spectrum is characterized by the continuous unstructured absorption, covering all area (Fig. 1, c. 2). Probably, in this case processing of the catalyst by methane results practically in complete reduction of ions Ni^{2+} (in $NiAl_2O_4$) and occurrence in system of reduced particles Ni° or Ni_n^o. It, in turn, is accompanied by covering surface coke precipitations on reaction [2, 3]:

$$CH_4 + M \rightarrow M - C + 2H_2,$$

where: the M – nickel ions, with – a symbol of coke precipitations, which nature (amorphous carbon, graphite, metal carbide) remains not clear and demands additional researches.

At processing the catalyst in CH_4 medium + air is observed insignificant reduction of intensity of items from nickel ions (Fig. 1, c. 3), that can be connected to partial reduction of ions Ni^{2+}.

As against it processing in mix CH_4 + CO_2 results in sharp reduction of intensity of items from nickel ions with simultaneous change of painting of sample from blue to grey (Fig. 1, c. 4). It is possible to assume that this phenomenon is connected to occurrence in system of a significant amount of reduced particles Ni°.

Probably, in both cases oxidation-reduction processes $Ni^{2+} \rightleftharpoons$ Ni° with shift of balance to the right in case of processing the catalyst by mix CH_4 + CO_2 proceed.

Processing of the catalyst in the oxidizing medium (CO_2 and air) practically does not influence condition of nickel ions (Fig. 1, c. 5 and 6).

Finding out of influence of process carbon-dioxide conversion of methane on condition of surface nickel ions was of interest. The analysis of DRES spectra after processing the catalyst by a reactive mix (CH_4 + CO_2 + air) has shown air that in this case the condition of nickel ions practically does not vary (Fig. 1, c. 7). It is possible to assume that presence of significant amount of oxidizers at gas mix results in stabilization of surface condition of ions Ni^{2+} in composition of $NiAl_2O_4$ and fast burning probably formed surface coke precipitations.

NiO (10 % mas.) - γ-Al_2O_3

ISSN 1313-2539

Increase of concentration of nickel in system (10 and 15 % mas.) results in essential changes in ESDR. So, in both cases the s.a. are widely observed in the field of 18000-12000 cm^{-1} and very weak at 25600 cm^{-1} (fig. 1, cv. 2 and 3). The site and kind of s.a. are characteristic for the systems containing phase NiO [15]. The strips of absorption at 15900 and 27400 cm^{-1} are characteristic for ions Ni^{2+}, stabilized in fields tetrahedral coordination (transitions $^3T_1(F) \rightarrow {}^3T_1(P)$ and $^3T_1(F) \rightarrow {}^1T(D)$ respectively). On this background low-intensity a.b. from nickel spinel are observed. It follows from above-mentioned that at rather high concentration of nickel on surface phases of nickel spinel and NiO are formed. Probably, in case of superfluous quantity of nickel, there is a filling octahedral and tetrahedral vacancies γ-Al_2O_3, with formation of spinel and $NiAl_2O_4$, and the rest of nickel aggregates in phase NiO.

Processing of the catalyst by methane and mix $CH_4 + CO_2$ results practically in complete reduction of nickel ions to Ni° (or Ni_n^o) and to covering of surface coke precipitations. Black painting of sample, disappearance specifies it from spectra of items, characteristic for nickel ions and occurrence of the unstructured band covering all area (Fig. 2, c. 2 and 3). In case of processing of the catalyst by mix CH_4 + air essential reduction of intensity of items from nickel ions that specifies on partial (not complete as reduction of nickel ions is higher) (Fig. 2, c. 4), i.e. on the surface and oxidized forms of nickel coexist.

Spectra of the catalysts subjected to oxidizing processing in atmosphere CO_2 and air significantly differ from above-stated.

So, in both cases well resolved, intensive a.b. from nickel spinel (Fig. 2, c. 5 and 6) are observed. These spectra significantly differ also from a spectrum of initial sample. Most likely, as a result of oxidizing processing the most part of phase NiO, cooperating with γ-Al_2O_3, forms phase $NiAl_2O_4$ which becomes prevailing on the surface.

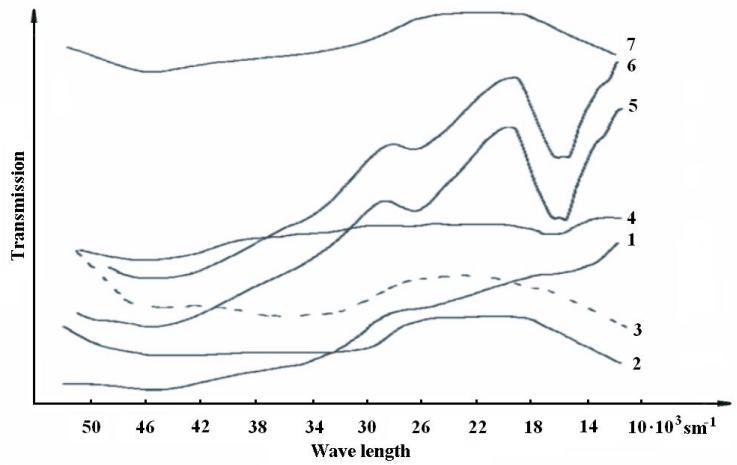

Fig. 2. Diffuse reflection spectra of NiO (10 % mas.) - γ-Al_2O_3 system after processing by initial reactants: 1 – the fresh catalyst; 2 – after processing in CH_4; 3 – after processing in mix $CH_4 + CO_2$; 4 – after processing in mix CH_4 + air; 5 – after processing in CO_2; 6 – after processing by air oxygen; 7 – after processing in mix $CH_4 + CO_2$ + air

The analysis of the spectral data shows that processing of the catalyst by initial reactants of carbon dioxide results conversion of methane in the course of three parallel reactions: reduction of nickel, formation of phase spinel $NiAl_2O_4$ and covering of surface coke precipitations. Occurrence in spectra, as against initial sample, of distinct items of average intensity from $NiAl_2O_4$ and non-uniform painting

ISSN 1313-2539

of sample (black coked and blue particles of the catalyst) specifies. In this case on the surface of oxidized and reduced forms of nickel coexist.

NiO (15 % mas.) - γ-Al_2O_3

Spectra of initial sample and that of processed in various oxidation-reduction mediums are identical to the spectra of NiO (10 % mas.) - γ-Al_2O_3 system (spectra are not given).

Thus, the spectral analysis of influence of separate components and the very reactive medium on a condition of surface ions Ni^{2+} has shown that irrespective of the contents of nickel, processing of catalysts by methane results practically in complete reduction of nickel ions Ni^{2+} to Ni° (or Ni_n^o) and to a covering of surface coke precipitations. As against it, oxidizers (CO_2 and air) differently affect the condition of nickel in samples with the various contents of nickel: in case when sample with the contents of nickel of 5 % mas. oxidizers practically do not affect and at rather high concentration of nickel (10 and 15 % mas.) create favorable conditions for process of formation and enrichment of surface by phase $NiAl_2O_4$. In CH_4 + air, CH_4 + CO_2 system oxidation-reduction processes with participation of nickel ions $Ni^{2+} \rightleftharpoons$ Ni° with shift of balance to the right in case of processing the catalyst by mix $CH_4 + CO_2$ proceed. In this case on a surface of catalysts oxidized [Ni^{2+} (T_d) and Ni^{2+} (O_h) in structure $NiAl_2O_4$] and reduced [Ni° (or Ni_n^o)] forms of nickel coexist.

At low concentration of nickel (5 % mas.) reactants carbon dioxide conversion of methane practically do not influence a condition of nickel ions, and at the large concentration (10 and 15 % mas.) three parallel reactions proceed: reduction of nickel, formation of phase spinel $NiAl_2O_4$ and covering of surface with coke precipitations. On the surface of the catalyst oxidized [Ni^{2+} (T_d) and Ni^{2+} (O_h) in structure $NiAl_2O_4$] and reduced [Ni° (or Ni_n^o)] forms of nickel coexist.

The reason for distinctions in behaviour of ions Ni^{2+} at processing in the reactive medium is probably connected with presence of phase NiO (phase $NiAl_2O_4$ is present in composition of all systems) in composition of catalysts with rather high contents of nickel (10 and 15 % mas.).

OXIDE-COBALT-ALUMINUM CATALYSTS

$Co^{2+}(3d^7)$. The electronic configuration $3d^7$ can be considered as a configuration with three holes in the filled d-environment. Therefore, the basic term of free ion with a d^7-configuration will be term ^4F and excited - ^4P, ^2G, ^2H, ^2D, ^2F.

The basic condition of d^7-ions in O_h-coordination term $^4T_{1g}$ [5, 6]. In spectra $Co^{2+}(O_h)$ two main areas of the absorption, corresponding quartet - quartet transitions have been observed: about 7000-10000 sm^{-1} – transition $^4T_{1g} \rightarrow {}^4T_{2g}$ (ε = 1-10 sm^{-1} ◁l/mole) and at 17000-20000 sm^{-1} – transition $^4T_{1g}$ (^4F) $\rightarrow {}^4T_{1g}$ (^4P), the most intensive (ε = 5-40 sm^{-1} ◁l/mole). There is one more transition allowed on spin, $^4T_{1g} \rightarrow {}^4A_{2g}$, but this transition is two-electronic, therefore, or is not observed or gives very weak strip. However, transition $^4T_{1g}$ (^4F) $\rightarrow {}^4T_{1g}$ (^4P) has the greatest intensity, and this strip of absorption is located in spectra Co^{2+} in octahedron and defines color of its compounds. From forbidden on spin quartet - duplet transitions it is necessary to note transition $^4T_{1g}$ (^4F) $\rightarrow {}^2T_{1g}$ which strongly mixes up with quartet transition $^4T_{1g}$ (^4P) on which it is imposed and it is expressed as shoulder on the short-wave side of strip of absorption [11-13].

In Table 1 the literary data on condition of nickel and cobalt ions are given in structure of various heterogeneous catalysts.

ISSN 1313-2539

Table 1. Position and reference of strips of absorption of Co^{2+} and Ni^{2+} ions in fields of octahedral and tetrahedral ions of symmetry

System	Symmetry of ion surrounding	Maximum of strips of absorption (cm^{-1})	Transition
1	2	3	4
$Ni(H_2O)_6^{2+}$	O_h	8475 13513 15385	$^3A_{2g}$ → $^3T_{2g}$ → $^3T_{1g}$ (F) → $^3T_{2g}$ (P)
Ni-MgO	O_h	8651-8598 (13736-13404) 14881-14706 24752-24510	$^3A_{2g}$ → $^3T_{2g}$ → $^3T_{1g}$ (F) → $^3T_{2g}$ (P)
Ni-ZnO	T_d	4598-4454 8439-8333 15456-15385 16181-16155	$^3T_1$ (F) → $^3T_2$ → $^3A_2$ → $^3T_1$ (P)
$Co(H_2O)_6^{2+}$	O_h	8000 16000 20200	$^4T_{1g}$ (F) → $^4T_{2g}$ → $^4A_{2g}$ → $^4T_{1g}$ (P)
Co-MgO	O_h	8496-8460 18692-17452 19608-19305	$^4T_{1g}$ (F) → $^4T_{2g}$ → $^4A_{2g}$ → $^4T_{1g}$ (P)
Co-ZnO	T_d	4167 7692-6173 17699	$^3A_{2g}$ → $^3T_2$ → $^3T_1$(F) → $^3T_1$ (P)

Position of the most intensive strip $^4T_{1g}$ (^4F) → $^4T_{1g}$ (^4P) defines pink or crimson color the majority of compounds of cobalt in octahedral coordination.

For Co^{2+} in a T_d-configuration the basic condition is $^4A_2$. Three areas of the transitions allowed on spin $^4A_2 \rightarrow {}^4T_2$, $^4A_2 {}^4T_1 \rightarrow$and $^4A_2 \rightarrow {}^4T_1$ (^4P) will consist each of 4-6 distinctly shown narrow strips obliged to back - orbital interaction, on which weaker duplet transitions can be imposed in part.

Distinctive feature of spectra Co^{2+} (T_d), described by absence of the center of symmetry, is very big intensity of strips of absorption. Force of oscillator in this case on some orders is more, than in case of octahedral coordination.

CoO (5 % mas.) - γ-Al_2O_3

Spectra of reflection of oxide systems are characterized by a.b. at 14000-20000 sm^{-1} (maxima at 15800, 17200 and 18400 sm^{-1}) from ions Co^{2+} (T_d) in the composition of normal spinel $CoAl_2O_4$ and weak bands, characteristic for isolated ions Co^{2+} (O_h), at 20900 and 24500 sm^{-1} (Fig. 3, c. 1).

Processing of catalysts in atmosphere CO_2, air, CH_4 + air and CH_4 + CO_2 + air does not affect the condition of ions of cobalt (Fig. 3, c. 2-5).

Influence of processing of catalysts by methane and mix CH_4 + CO_2 consists in some reduction of intensity of items from ions of cobalt that can be connected to partial their reduction to Co° (Fig. 3, c.6 and 7).

ISSN 1313-2539

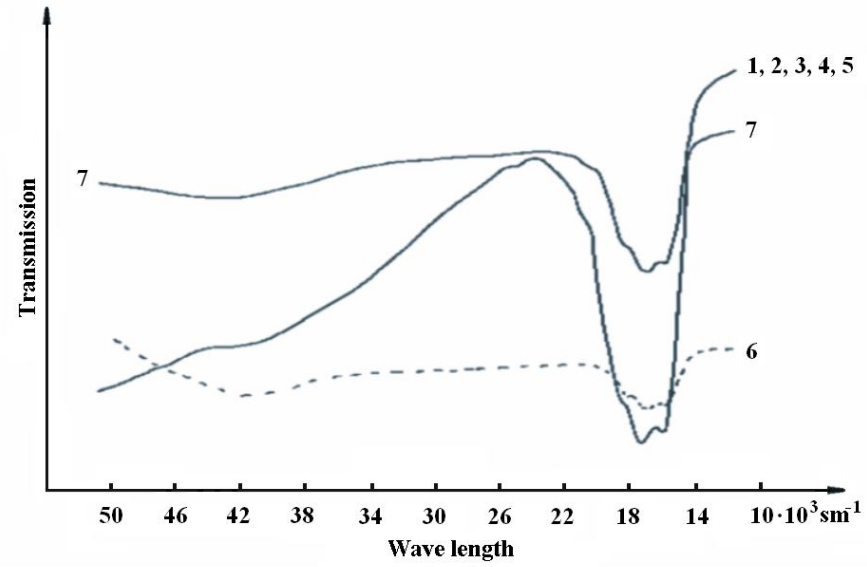

Fig. 3. Diffuse reflection spectra of CoO (5 % mas.) - γ-Al_2O_3 system after processing by initial reactants: 1 – fresh catalyst; 2 – after processing in CO_2; 3 – after processing by oxygen of air; 4 – after processing in mix CH_4 + air; 5 – after processing in mix CH_4 + CO_2 + air; 6 – after processing in CH_4; 7 – after processing in mix CH_4 + CO_2

CoO (10 % mas.) - γ-Al_2O_3

Spectra of initial sample and that of processed in various oxidation-reduction mediums are identical to spectra of CoO (5 % mas.) - γ-Al_2O_3 system (spectra are not given).

OXIDE NICKEL – COBALTALUMINA CATALYSTS

Binary oxide systems with various ratios of nickel (10 and 15 % mas.) and cobalt (5 and 10 % mas.) have black color, and spectra of diffuse reflections are characterized by the continuous unstructured absorption covering practically all spectral area (spectra are not given) that does not allow to interpret obtained data unequivocally.

Thus, on the basis of conducted spectral researches of valent and coordination condition of nickel and cobalt ions on a surface of γ-Al_2O_3 it is possible to draw some conclusions:

1) the surface phase composition of cobalt oxide catalysts significantly depends on concentration of an active component: at rather low concentration (5 % mas.), as a result of chemical processes the phase surface of mixed spinel $NiAl_2O_4$ is formed, and at big quantities (10 and 15 %) along with it surface phase of NiO is also formed;

2) on a surface of cobalt oxide catalysts within the limits of concentration of cobalt 5 and 10 % mas., a phase of normal spinel $CoAl_2O_4$ and isolated surface ions Co^{2+} (O_h);

3) processing of the catalyst by methane and mix CH_4 + CO_2 results practically in complete reduction of nickel ions to Ni° (or Ni_n^o) and to covering of surface coke precipitations (reduction of intensity of items from nickel ions with simultaneous change of painting of sample from blue to grey);

4) in case of processing the catalyst by mix CH_4 + air is observed essential reduction of intensity a.b. from ions of nickel that specifies partial restoration of ions of nickel, i.e. on a surface the superficial and oxidized forms of nickel coexist;

ISSN 1313-2539

5) processing of the catalyst in the oxidizing medium (CO_2 and air) practically does not influence condition of nickel ions;

6) it is revealed, that processing of catalysts by air, CO_2, and also mixes CH_4 + air and CH_4 + CO_2 + air does not influence a condition of ions of cobalt;

7) processing of catalysts by methane and mix CH_4 + CO_2 conducts to some reduction of intensity of strips of a.b. from ions of cobalt that can be connected with their partial restoration up to Co^o.

ACKNOWLEDGEMENTS

Authors express gratitude to academician M.I. Rustamov and professor V.S. Gadji-Kasumov for assistance at performance of tasks in view, fruitful and substantial advices during discussion of the basic results of the work.

REFERENCES

1. O.V. Krylov, Ros.chem.jour. V. 44. № 1. P. 19. (2000).
2. I.T. Bychkov, O.V. Krylov, V.N. Korchak, Kinetics and catalysis. V. 43. № 1. P.94. (2002).
3. C.J. Bradford M., M.F. Vannice, Catal. Rev.-Sci. Eng. V. 41. № 1. P. 1. (1999).
4. Y.-G. Chen., K. Tomishege., K. Fujimoto, Appl. Catal. A. V. 161. P. 11. (1997).
5. A.S. Marfunin. Introduction in physics of minerals. M.: Nedra. 328 p. (1974).
6. D.T. Sviridov., R.K. Sviridova., Y.F. Smirnov, Optical spectra of ions of transitive metals in crystals. M.: Science. 266p. (1976).
7. O.- Du Mont Schmits., H. Brokopt, Zannorg. allg. Chem. V. 7. P. 295. (1958).
8. D. Keinen, Monatsh. Chem. V.96. P.730. (1965).
9. H. Waklem, A. J. Chem. V. 36. P. 2117. (1962).
10. F. Pepe, M. Shiavello, G. Ferraris, J. Solid. Stade. Chem. V. 12. P. 63. (1975).
11. G.N. Asmolov, O.V. Krylov, Kinetika and catalysis. V. 12. P. 463. (1971).
12. M. Jacono, M. Shiavello, A. Chimino, J. Phys. Chem. V. 75. P. 1044. (1971).
13. W. Low, Phys. Rev. V. 10. P. 256. (1958).

ISSN 1313-2539

INVESTIGATION OF THE ASPHALTENE-RESIN-PARAFFIN DEPOSITS COMPOSITION OF THE IRELYAKH GOF (YAKUTIA) AND DEVELOPMENT OF PROCEDURES FOR THEIR ELIMINATION

Izabella K. Ivanova, ElenaYu. Shitz

Institute of Oil and Gas Problems SB RAS, Yakutsk, Russia E-mail: iva-izabella@yandex.ru

Abstract

The group composition of asphaltene-resin-paraffin deposits (ARPD) in the Irelyakh field and their solubility in the composite solvents on the hexane base with the additives consisting of nonionic surface-active substances (NSAS) and concentrates of aromatic hydrocarbons is determined. The results of the investigations show that the additives Neonol AF-9-10 and liquid products of pyrolysis (LPP) are most efficient. The use of these additives allows to increase the efficiency of ARPD breaking and dissolving by 1,3 – 1,6 times as compared with a base solvent. It is shown that the increase in the concentration of individual additives from 0,5 to 3% causes a decrease in the efficiency of detergent compounds.

Key words: *asphaltene-resin-paraffin deposits, oil well tubing, bottom hole zone, hydrocarbon solvent.*

1.INTRODUCTION

At present on the territory of Yakutia oil reservoirs of Talakansky, Sredne-Botuobinsky and Irelyakhsky fields of the Nepsko-Botuobinsky anteclise are in the experimental-industrial development. These gas and oil fields are situated in the zone of continuous distribution of permafrost rocks. That is why the regionally traced low reservoir temperatures (10 – 15 ^{o} C) and abnormally low reservoir pressures are characteristic of the producing horizons. Oils of the Nepsko-Botuobinsky anteclise are low-sulfur and have, mainly, methane composition (41-73%), the increased content of asphaltenes (to 11%) and resins (to 43%) [1]. During the operation of oil-producing wells at a temperature and pressure drop, followed by oil degassing, a sharp decrease in solubility of paraffin, asphaltenes and resin matters occurs. This phenomenon in combination with the rough surface of the walls of oil well tubing (OWT) brings about the intensive deposition of ARPD on the surface of the producing equipment and in the bottom hole zone (BHZ). As a result, a decrease in the liquid inflow to the bottom zone and an increase in hydraulic resistance of wells take place.

Negative consequences of ARPD formation set conditions for developing a great number of methods for combating this phenomenon: mechanical, thermal, physical, chemical and microbiological [2, 3]. However the use of the above methods depends on the conditions of a particular field. For example, application of the biotechnological methods is restricted by high reservoir pressures, gas factors, high hydrogen sulphide content in oil and temperature being higher than 40….50 ^{o} C. The magnetic treatment has its own requirements for the treated medium such as water hardness and mineralization of the produced water, gas factor (up to 200 m^3/m^3), etc. The electrical methods have a rather complex ground equipment used for the electric power supply in the underground heating installations. In this connection the intensive studies on breaking and removal of ARPD are carried out both in Russia and abroad [4]. As is known, hydrocarbon solvents are most efficient at removing ARPD [4, 5, 6, 7]. The main purpose of BHZ treatment with the use of solvents is breaking of water-oil emulsions in the bottom hole zone and ARPD removal. It is known that most of hydrocarbon solvents (casing-head gasoline, aromatic hydrocarbons, oil distillates, etc.) readily break water-oil emulsions as well as dissolve ARPD, formed in the oil well tubing, and do not evolve them after cooling of the solution.

ISSN 1313-2539

At present the main procedure for ARPD control in the Irelyakh field is the periodic treatment of the reservoir by the cold condensate. But as the practical experience shows this method turned out to be ineffective for combating the organic depositions. Therefore, the most appropriate procedure for controlling the ARPD formation in the conditions of abnormally low reservoir pressures and temperatures can be the application of composite solvents.

The purpose of the investigation is: on the basis of the investigation of the group composition of ARPD in the Irelyakh field to develop a composite solvent for cleaning the oil well tubing from paraffin deposits.

2. SUBJECTS AND METHODS OF INVESTIGATION

The subject of the investigation is ARPD of the oil of the Irelyakh field taken from the surface of the oil well tubing.

2.1. Determination of the ARPD group composition

The content of the main group components (hydrocarbon (HC) + hard paraffin, resins, asphaltenes and inorganic part) has been determined in the ARPD under study. Division of ARPD into group components is relevant and shows differences in solubility of these components in solvents used during the analysis of the residual oil products – the closest analogues of ARPD [8]. Therefore, investigations have been carried out with the use of the adsorption methods of analysis of the residual oil products by Marcusson [9]. The results are presented in Table 1.

2.2. Evaluation of the efficiency of hydrocarbon solutions at ARPD removing

Evaluation of the efficiency of the action of solvents with additives has been performed in static conditions by the methods of the RPO "Neftepromkhim" [10]. The ARPD sample is heated to the softening temperature, thoroughly mixed and shaped in the form of a cylinder 12 x 20 mm. Then it is cooled and placed into the previously weighed basket from the brass (steel) gauze with the size of a cell 1,5 x 1,5 mm. The dimensions of the basket are 70 x 15 x 15 mm. The basket with ARPD is weighed and placed in a glass hermetic cell where 100 mm of the solvent under study is poured. The experiment temperature is 10 ^{o} C. In 4 hours the basket with the residual non-destructed part of ARPD is taken out and dried to a constant weight. The destructed but undissolved part of ARPD, fallen from the basket in the cell, is filtrated, dried to a constant weight and weighed.

According to the above procedure the evaluation of the efficiency of the solvent is performed according to three indices:

- The ability of a solvent to break ARPD into smaller fragments. This is the dispersing ability of a solvent, which is evaluated by the percentage amount of ARPD remained on a filter. This index must be optimum as at a very high dispersing ability of a solvent there is the probability of forming the fragments of ARPD, which can plug the bottom hole zone.
- The ability of a solvent to form a real solution with the ARPD components. This is the dissolving capacity of a solvent, which is evaluated by the percentage amount of ARPD passing into the solution. The value of this index must be as large as possible.
- The ability of a solvent to dissolve and break components of ARPD simultaneously. This is the so-called detergent power of a solvent, which is evaluated by the difference between the ARPD taken for the analysis and the residual of ARPD in the basket in % mass. This index can be considered to be the universal one. The higher is its value, the higher is the efficiency of a solvent on the whole.

ISSN 1313-2539

3. RESULTS AND DISCUSSION

Table 1 shows the group composition of ARPD in the Irelyakh field.

Table 1 - The group composition of asphaltene-resin-paraffin deposits

The place of sampling	Mass composition, %			
	Asphaltenes	Silica resins	HC+hard paraffin	Mechanical admixtures
The Irelyakh field	7,6	15,1	72,9	4,4

One can see from Table 1 that ARPD is characterized by a high content of the paraffin HC. Paraffin type of deposits and, as a result, their low polarity indicate that the base of the composite for breaking the ARPD structure must consist of a low-boiling aliphatic HC, hexane being selected as such a hydrocarbon.

Evaluation of the efficiency of solvents has been carried out according to such complex of characteristics as dispersing, dissolving and detergent abilities of the base solvents (hexane) and hydrocarbon solutions consisting of hexane and the additive (mixture of additives of different functional purpose). Concentrates of aromatic HC – polyalkylbenzene resin (PABR) [11], liquid products of pyrolysis (LPP) [12], ethylbenzene cut (EBC) [13] and butylbenzene cut (BBC) [14] have been investigated as the additive for increasing the dissolving and solvation function of the base solvent. The NSAS, produced by the home industry and representing the oxyethylated alkylphenol – Neonol AF-9-10, has been studied as the additive having the detergent-dispersing properties.

First of all the efficiency of using the individual additives at their mass content in the base solvent being from 0,5 to 3% has been investigated. As the results obtained show, the LPP additives and Neonol AF-9-10 are the most efficient (Table 2).

Table 2 - Experimental data on ARPD solubility in the Irelyakh field

Additive		Dispersing ability, % mass.	ARPD residual in the basket, % mass.	Dissolving ability, % mass.	Detergent ability, % mass.
Components	Concentration in a solvent, % mass				
Base solvent: Hexane					
Hexane		14,68	3,41	81,91	96,59
PABR	0,5	15,68	4,01	80,31	95,99
	1	18,82	7,13	74,05	92,87
	3	12,89	21,54	65,57	78,46
EBC	0,5	13,92	4,85	81,23	95,15
	1	11,35	6,25	82,40	93,75
	3	11,52	11,19	77,29	88,81
BBC	0,5	14,16	6,13	79,71	93,87
	1	14,39	8,63	76,98	91,37
	3	11,60	24,21	64,19	75,79

ISSN 1313-2539

LPP	0,5	13,14	1,93	84,93	98,07
	1	11,89	8,00	80,11	92,00
	3	7,20	17,15	75,65	82,85
Neonol	0,5	20,03	2,59	77,38	97,41
	1	30,83	9,29	59,88	90,71
	3	55,38	14,87	29,75	85,13

The use of these additives allows to increase the efficiency of ARPD breaking and dissolving by 1,3 – 1,6 times as compared with the base solvent. The additive Neonol AF-9-10 has a higher dispersing ability in comparison with PABR, EBC, BBC and LPP. It is found out that the increase in the concentration of individual additives from 0,5 to 3% causes the increase in the efficiency of detergent compounds. In all probability, at the concentration of additives higher than 1,0% mass their absorption on the surface of ARPD occurs. The multimolecular layer formed in the conditions of the static regime prevents from further penetration of solvent molecules to ARPD, which is indicated by the general tendency for the decrease in the detergent ability of solvents regardless of the character of the additives being used.

Determination of the efficiency of the action of additive composites is of a great interest. In this connection the composite additives Neonol + PABR, Neonol + LPP, Neonol + EBC and Neonol + BBC with the total concentration in a base solvent being 0,5% have been studied (Table 3).

Table 3 – Experimental data on solubility of ARPD in the Irelyakh field

Additive		Dispersing ability, % mass.	ARPD residual in the basket, % mass.	Dissolving ability, % mass.	Detergent ability, % mass.
Components	Proportion of Components				
Base solvent: Hexane					
Hexane		14,68	3,41	81,91	96,59
Neonol:LPP	100:0	20,03	2,59	77,38	97,41
	90:10	14,28	14,31	71,41	85,69
	80:20	20,05	17,55	62,40	82,45
	70:30	14,11	15,71	70,18	84,29
	60:40	17,27	14,49	68,24	85,51
	50:50	21,07	13,71	65,22	86,29
	40:60	10,31	12,30	79,38	89,69
	30:70	6,48	18,32	75,20	81,68
	20:80	9,82	22,29	67,89	77,71
	10:90	10,47	11,35	78,18	88,65
	0:100	13,14	1,93	84,93	98,07
Neonol:EBC	100:0	20,03	2,59	77,38	97,41

ISSN 1313-2539

	90:10	40,62	10,99	48,39	89,01
	80:20	29,37	18,64	51,99	81,36
	70:30	29,59	14,19	56,22	85,81
	60:40	20,91	20,62	58,47	79,38
	50:50	24,71	14,00	61,29	86,00
	40:60	14,97	9,39	75,64	90,61
	30:70	14,37	16,04	69,59	83,96
	20:80	8,69	17,47	73,84	82,53
	10:90	14,07	13,08	72,85	86,92
	0:100	13,92	4,85	81,23	95,15
Neonol:BBC	100:0	20,03	2,59	77,38	97,41
	90:10	12,95	7,19	79,86	92,81
	80:20	13,38	11,75	74,87	88,25
	70:30	11,95	14,68	73,37	85,32
	60:40	10,76	15,12	74,12	84,88
	50:50	11,74	20,78	67,48	79,22
	40:60	9,41	13,72	76,87	86,28
	30:70	9,15	13,47	77,38	86,53
	20:80	9,72	15,29	74,99	84,71
	10:90	7,30	16,86	75,84	83,14
	0:100	14,16	6,13	79,71	93,87
Neonol:PABR	100:0	20,03	2,59	77,38	97,41
	90:10	20,47	14,99	64,54	85,01
	80:20	17,80	11,77	70,43	88,23
	70:30	13,65	15,79	70,56	84,21
	60:40	16,78	12,84	70,38	87,16
	50:50	16,68	21,53	61,79	78,47
	40:60	16,07	24,62	59,31	75,38
	30:70	11,54	18,00	70,46	82,00
	20:80	17,89	21,32	60,79	78,68
	10:90	10,07	12,11	77,82	87,89
	0:100	15,68	4,01	80,31	95,99

The experimental data show that the positive synergetic effect is not observed for the composites under study. The detergent ability of composite additives decreases as compared with the individually used additives.

ISSN 1313-2539

Therefore the hydrocarbon solvent with LPP at total concentration of 0,5% mass in a base solvent can be considered to be the most efficient for removing ARPD in the Irelyakh field. In comparison with the pure hexane this solvent has high detergent and dissolving ability. Evidently, the increase in the detergent ability occurs due to the fact that the LPP additive improves the solubility of resins, which cement separate crystals of paraffin, particles of asphaltenes and mechanical admixtures.

4. CONCLUSION

1. It is established that asphaltene-resin-paraffin deposits in the Irelyakh field are characterized by a high content of paraffin hydrocarbons.
2. It is shown that during breaking and dissolving the ARPD of the paraffin base the best effect is obtained at using the additive consisting of liquid products of pyrolysis with the total concentration in a base solvent being 0,5% mass.
3. With the increase in the total concentration of individual additives in a base solvent the efficiency of detergent compounds decreases.

The study is performed at the assistance of the Grant of the President of the Russian Federation – MK – 4561.2007.5.

REFERENCES

1. Каширцев В.А. Органическая геохимия нафтидов востока Сибирской платформы. РАН. Сиб. отд-ние. Объед. ин-т физико-техн. проблем Севера. Ин-т проблем нефти и газа; Отв. ред. А.Э. Конторович. - Якутск: ЯФ Изд-ва СО РАН, 2003. - 160 с.

2. Мазепа Б. Защита нефтепромыслового оборудования от парафиноотложений. -М.: Наука, 1966.

3. Бабалян Г. Борьба с отложениями парафина. – М.: Недра, 1972.

4. Разработка нефтяных месторождений: Издание в 4 т. / Под ред. Я.И.Хисамутдинова и Г.З. Ибрагимова. – М.: ВНИИОЭНГ, 1994. – Т.2: эксплуатация добывающих и нагнетательных скважин. -287 с.

5. Химические реагенты в добыче и транспорте нефти: Справочник / Д.Л. Рахманкулов, С.С. Злотский, В.И. Мархасин, О.В. Пешкин, В.Я. Щекотурова, Б.Н. Мастобаев. – М.: Химия, 1987. – 144 с.

6. Орлов Г.А., Кендис М.Ш., Глущенко В.Н. Применение обратных эмульсий в нефтедобыче. – М.: Недра, 1991. -224 с.

7. Мамедов Т.М. Добыча нефти с применением углеводородных растворителей. –М.: Недра, 1984. -152 с.

8. Особенности состава АСПО Западной Сибири: Науч. тр. «Проблемы химии нефти» / А.Н. Садыков, Р.Ш. Нигматуллина, Д.Ф. Фазлыев, Ф.Р. Фаррахова, Р.Г. Шакирзянов.- Новосибирск: Наука, 1992.- С.302-305.

9. Рыбак М.С. Анализ нефти и нефтепродуктов. – М.: ГНТИНГТЛ, 1962. – 888 с.

10. Эффективность применения растворителей асфальтосмолопарафиновых отложений в добыче нефти / Головко С.Н., Шамрай Ю.В., Гусев В.И., Люшин С.Ф. и др. – М., 1984. – 85 с. – (Обзор.информ. / ВНИИОЭНГ. Сер. «Нефтепромысловое дело»).

ISSN 1313-2539

11. Смола полиалкилбензольная. Технические условия. ТУ 38.102-96-83.

12. Жидкие продукты пиролиза. Технические условия. ТУ 38.402-62-144-93.

13. Этилбензольная фракция. Технические условия. ТУ 6-01-10-37-78.

14. Бутилбензольная фракция. Технические условия. ТУ 2414-175-00151727-2002.

ISSN 1313-2539

NEW TECHNIQUES FOR HIGH VOLTAGE EQUIPMENT MAINTENANCE

Alexandru S. Jude[1], Petru Ehegartner[1], Petru Andea[1] and Flaviu M. Frigura-Iliasa[1]

[1] Power Systems Department, Faculty of Electrical and Power Engineering, POLITEHNICA University of Timisoara, Romania, E-mail: flaviu.frigura@et.upt.ro

Abstract

This paper presents some basic theoretical aspects concerning the predictive maintenance applicable to high voltage switches as well as (on line and off-line) methods of monitoring and diagnosing the status of their main contacts. All principles are applicable to other many high voltage devices like surge-arresters, separators etc. Some fuzzy-logic algorithms are used to determine the key elements of the predictive maintenance. Those algorithms are implemented into powerful software tools for high voltage equipment maintenance. It is a clear example of implementing technology changes in order to obtain a higher efficiency of some existing equipment with low costs.

Key words: *high voltage equipment, maintenance*

1. INTRODUCTION

High voltage switching devices (and, generally, all high voltage equipment) are very expensive pieces of equipment. Their normal life is at least 30 years of continuous operating service. So, maintenance is crucial for those pieces of equipment, no mater their construction and destination.

The types of high voltage switching devices in service in the European Union (in 2002) are represented (as percentage) in Figure 1. Since then, no major improvements were carried out, so data are still valid. The situation in Romania is more or less similar.

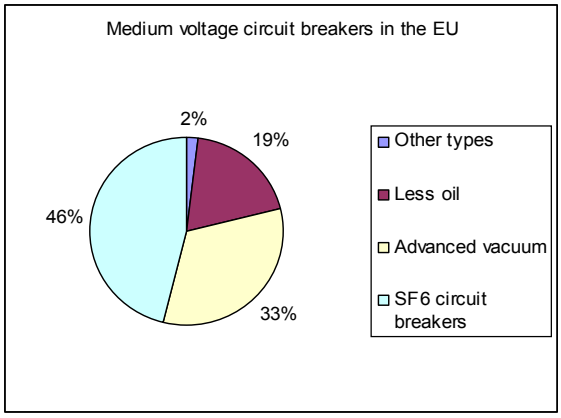

Figure 1. The main types of medium and high voltage European circuit breakers and their percentage in 2002

Monitoring high voltage equipments implies the following three main goals:

- optimizing the equipment maintenance;
- increasing its disposal;

ISSN 1313-2539

- ameliorating the knowledge concerning assembly functioning.

The present paper refers to the operations, which are necessary to ensure a normal work of the equipments in exploitation, which make up the maintenance of the product.

Maintenance can be:

- curative – detecting and connecting accidental faults;
- preventive – preventing faults throughout periodical interventions;
- predictive – forecasting faults and avoiding their apparition.

All these categories having as main goal amelioration of management and optimization of the use of equipments, goal realized through monitoring and diagnosing techniques.

Monitoring, as an action of measuring and automatic comparing of some peculiar parameters, having referential values of a process or equipment is based on (Pelinici) methods of diagnosis and analysis of appearing faults.

The choice of the number and types of sensors, their location and the establishment of the measuring schemes of the monitored parameters influence decisively the solution of this problem. More over, an adequate system of monitoring – diagnosing must have the following characteristics:

- to be capable of independent functioning;
- to be flexible, adjusting to the user's necessities;
- not to affect the response of the equipment or its reliability;
- to be capable of integration into the command and automation of the monitored installation work.

From the point of view of the resolution of the modeling problem of the monitored system, it can be approached either through optimizing the problem of monitoring – diagnosing following different criteria or through using artificial neuronic networks [2]

High voltage isolating switches (SIT) are the largest equipments of the transformers and it is their work that the continuity of electric power supply of the consumers depends on.

The main goals of the SIT predictive maintenance policy refer to:

- collecting, analyzing and interpreting the data of the important working characteristics of the equipment;
- elaborating the informational diagnosis concerning the SIT status to prevent the apparition of its faults;
- reducing the periods of unavailability in order to make work more effective.

The faults in SIT depend on:

- the type of construction,
- the voltage level of the installation,
- the location inside the diagram of primary commutation etc.

In [3] according to some research work done at S.C. Electrica S.A. – Sibiu Branch – there have been established the main sources of faults on SIT:

- an increase in the contact electric resistance corresponding to the close status of these equipment of maneuver – separation;
- breaking of the support isolators respectively acting ones;

ISSN 1313-2539

- other causes, whose importance is illustrated in Figure 2.

Among the causes of the increase, in the electric resistance the there have been mentioned [3], [4]:

- the decrease in the push force in the contact as a result of the fatigue of the springs used, function of the number of commutations made;
- the reduction of the real contact area, as a result of pollution oscillation and fatigue of the microscopic contact pins;
- the improper maintenance operations etc.

Their effect is an increase in the voltage drop on contacts, while functioning, above the admissible values [3].

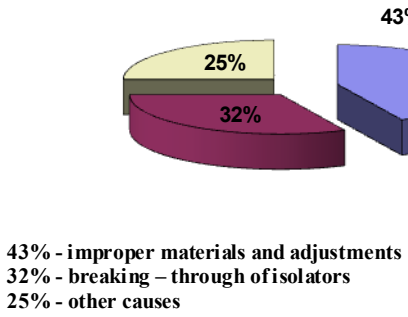

Figure2: The cause of faults in 110 kV exterior isolating switches

Any supplementary post-accident (curative) maintenance operation means supplementary costs and financial and operational losses for the electricity supplier or transporter. Predictive maintenance is, of course, more efficient.

2. TECHNICAL DIAGNOSIS OF ISOLATING SWITCH CONTACTS

Monitoring contact status in SIT is possible on line through the method of using optic fibers installed at the construction of the isolating switch and their connection to an interface for introducing, treating and interpreting data. It consists in analyzing the thermal images appeared and informing the decision staff on the evolution of the contact resistance R_c meant to prevent faults. Knowing the stationary supra-temperature of the contact, τ_c ($\tau_c = \theta_c - \theta_{amb}$) and the intensity of the permanent regime current, I, function of the nature of the superficial material of the contact pieces (copper or silver), there can be determined a voltage drop, U_c,

$$U_c = R_c \cdot I = \xi \cdot \tau^{1/2} \quad (1)$$

respectively, contact resistance, R_c

$$R_c = \xi \cdot I^{-1} \cdot \tau_c^{1/2} \quad (2)$$

which is steadily compared with the admissible limits.

ISSN 1313-2539

In table 1 [5] for couples of contact pieces of the same material (silver – silver or cooper – cooper) in a new status there have been raised the temperatures and critical voltage drops in contact (when plasticization of materials is possible) as well as the values of ξ factor:

Table 1 - Physical properties for contact materials

Material of contacts in the air in a new status	Critical temperature θ_{cr} [grd]	Critical voltage drops in contact U_{cr} [mV]	$\xi[V \cdot grd^{-1/2}]$
Silver–silver	180	93.6	$7.44 \cdot 10^{-3}$
Cooper-cooper	190	94	$7.40 \cdot 10^{-3}$

From relations (1) and, respectively, (2) there has been found out that the modification of the conduction status and increase of the contact surfaces, at work, through impurification with isolating pellicles, respectively, decrease in the pushing contact force, result in an increase of the contact temperature. Monitoring, either directly contact supra-temperature, or voltage drop in it, there can be appreciated with maximum economic efficiency, through predictive maintenance, the proper moment of maintaining works of the contact sub – assemblies of SIT.

Another way of diagnosing the status of the principal contacts of SIT which does not involve the thermal vision equipments, but which can be occasionally or periodically (off line) monitored is based on measuring the electric contact resistance of the equipment, according to the schema shown in Figure 3, [1].

According to this method, applicable to disconnecting the installation, where the checked isolating switch is found, a current of 100 – 1000 A is injected through it, both voltage drop U_2 between the equipment buses and current I through closed contacts of the maneuver / isolating switch apparatus being measured.

The CDR (Contact Disturbance Recorder) acquisition interface records, calculates, compares, transmits to the managing point and stores information obtained through the measurements done according to the schema in Figure 3, recording at the same time the number of commutations N made by the isolating switch between two successive acts of monitoring.

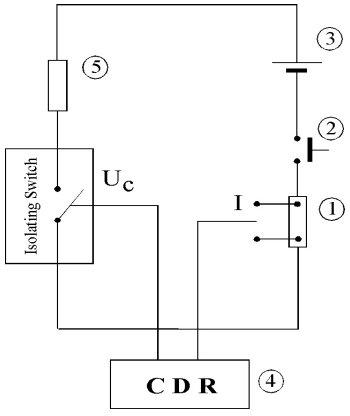

Figure 3. Block diagram of measuring and recording contact resistance

ISSN 1313-2539

The periodical determination of the resistance contact, which best characterizes the technical status of the commutation sub-assembly of the isolating switch and comparison of this parameter with pre – determined or referential values allows the quantitative appreciation of the current technical status of the equipment.

The best moment of the maintaining is established through fixing a percentage limit of value U_{cr} (Tab.1) which is compared with the current value of the contact voltage drop. U_{CN}, as a result of the measurement of the contact resistance R_{CN} (after N maneuvers with the isolating switch) and of current I recorded by CDR.

Algorithm of establishing the predictive maintenance period of the commutation sub-assembly of SIT could be implemented using FUZZY logic techniques.

The data obtained from the periodical measurements of the contact resistance after N maneuvers with isolating switch R_{NC} are used to calculate nominated error $\delta_j(N)$ versus the value of the same parameter established at the end of the latest revision, R_{CO}.

$$\delta_j(N) = 1 - \frac{R_{CO}}{R_{CN}} \tag{3}$$

as well as the variation of this value after N commutation cycles (between two consecutive measurements) $\varepsilon_j(N)$

$$\varepsilon_j(N) = \delta_j(N) - \delta_j(N-1) \tag{4}$$

Placing $\delta_j(N)$ and $\varepsilon_j(N)$ in fuzzy multitudes of Figure 3 and linking them to fuzzy values SP; MP; LP, we can pass to the calculation of the final functions of output to a fuzzy multitude:

$$\mu_j(SP) = \underset{x_i}{MAX}[MIN(\mu(x_i))] \tag{5}$$

$$\mu_j(MP) = \underset{x_i}{MAX}[MIN(\mu(x_i))] \tag{6}$$

$$\mu_j(LP) = \underset{x_i}{MAX}[MIN(\mu(x_i))] \tag{7}$$

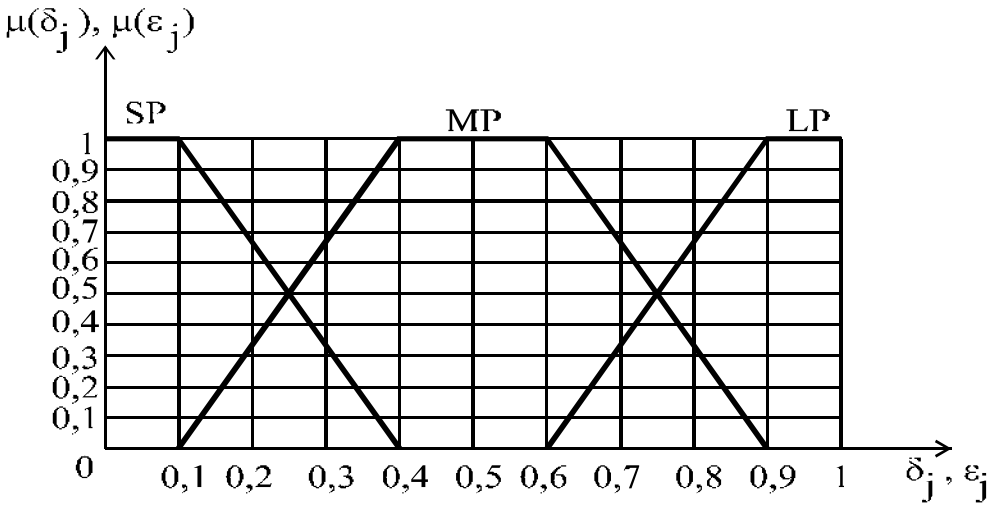

Figure 4: Fuzzy multitudes and belonging functions

ISSN 1313-2539

The calculation of functions $\mu_f(SP)$, $\mu_f(MP)$ and $\mu_f(LP)$ is realized on the basis of Table 2 and Table 3.

The following step consists of determining belonging function μ output from the algorithm presented in figure 4 in relations:

$$\mu_{output} = MAX\left[\mu_f(SP), \mu_f(MP), \mu_f(LP)\right] \quad (8)$$

Table 2 - Fuzzy rules

δ_j \ ε	SP	MP	LP
SP	SP	MP	MP
MP	MP	MP	LP
LP	LP	LP	LP

Through the conversion of the linguistic value of μ output into a clearly numerical value μ % (representing fatigue of SIT electric contacts in percentage) and comparing the latter with admissible fatigue of SIT electric contacts, μ_{adm}, there has been established the moment of the next diagnosis test and revision.

Table 3 - Decision table of fuzzy multitudes and belonging functions

x_i	Input	output		
	$(\delta_j, \varepsilon_j)$	$\mu(x_i, SP)$	$\mu(x_i, MP)$	$\mu(x_i, LP)$
x_1	(SP,SP)	1	0.5	0
x_2	(SP,MP)	0.5	1	0.5
x_3	(SP,LP)	0.5	1	0.5
x_4	(MP,SP)	0.5	1	0.5
x_5	(MP,MP)	0.5	1	0.5
x_6	(MP,LP)	0	0.5	1
x_7	(LP,SP)	0	0.5	1
x_8	(LP,MP)	0	0.5	1
x_9	(LP,LP)	0	0.5	1

A simple algorithm for calculating the predictive maintenance period of a SIT, based on this fuzzy-logic method is shown below:

ISSN 1313-2539

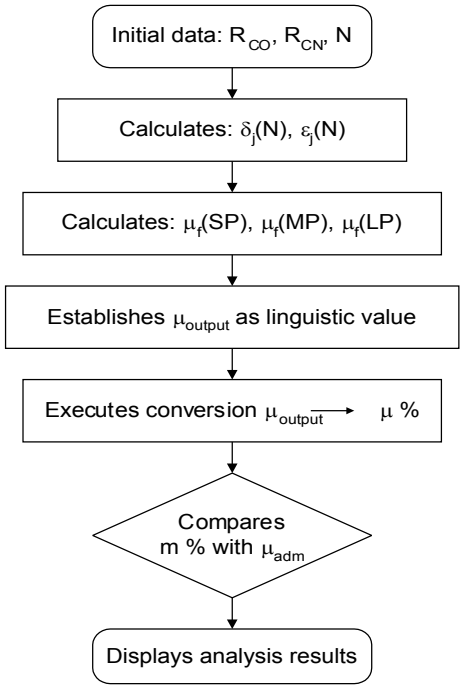

Figure 5. Block diagram of the algorithm used for establishing the period of predictive maintenance of SIT electric contacts

3. CONCLUSIONS

The methods presented in this paper allow high confidence diagnosis of the technical status of the commutation sub-assembly of high voltage isolating switches providing detailed information on: the electric contact resistance, the fatigue degree of main contacts and the best moment for predictive maintaining works with this equipment.

The monitoring off line system of contact resistance of the isolating switches found in high voltage stations presented in the paper allows the prevention exploiting of their breaking increasing the efficiency of the activity through the periods of unavailability, respectively increasing the reliability if these equipments.

Extending the application of the diagnosing methods, recommended for a large number of high voltage installations we could obtain data banks concerning the parameter we are intersected in – contact resistance – this allowing a report on the tested equipments at this data banks, thus ameliorating the knowledge about their work in order to optimally forecast the period of safe usage.

REFERENCES

1. Barkan, P., Deni, J. A., McCabe, A. K., Reckleff, J. G., Scherer, H. N., Woodward, R. C., (1988), *Méthodologie pour la surveillance de l'état des disjoncteurs des haute tension*, Rapport 13.04, CIGRE,.

2. Bouchon – Meunier, B., Nguyen H., (1996), „Les incertitudes dans systèmes intelligents" Presses Universitaires de France, Paris

3. Bourkes, P.D., Kayafs, F.A., Machias, A.V. (1988), „Specified current in emergency load switches", *IEEE Proced*., vol.135, Nr.4, p.330-333.

ISSN 1313-2539

4. Moldovan, L., Vasilievici, A., Suciu, I., Andea, P., Vătău, D., (1996), „Cercetări asistate de calculator privind ameliorarea unor contacte electrice de la echipamentele electrice", research contract. no.75/1994, UP Timişoara, FRE Sibiu, Timişoara.

5. Postolache, O., Poiată, T., Zaharia, Iustina (1998), „Utilizarea reţelelor neuronale artificiale în monitorizarea sistemelor de tip distribuit" *vol. SIAE, Galaţi*, , p.41-45.

6. Vătău, D., Şurianu, F., Moldovan, L., (1999), „Switch contacts state prediction of high voltages devices" *Proceeding of 19th International Conference on Electric Contact Phenomena,* Nuremberg

7. Vătău, D., (1998), „Asupra evaluării Fuzzy a duratelor de viaţă a întreruptoarelor de înaltă tensiune", vol.*SIAE, Galaţi*, 1998, p.416 – 420.

ISSN 1313-2539

INTENSIFICATION OF TRANFERRING THE KAZAKHSTAN'S HIGH-CONGEALED OIL: CHALLENGES AND ADVANCES

Tayhan P. Maimakov*, Galina I. Boiko*, Yerengaip M. Shaihutdinov**, Nina P. Lyubchenko*, Gulzhakhan Zh. Yeligbayeva**, Zhamal A. Konyrbayeva*,Rashida F.Mukhamedova

*High education institute «UNAT», Republic of Kazakhstan, 050013 Almaty, Satpaeva str., 22-b

** Kazakh national technical university, Republic of Kazakhstan, 050013 Almaty, Satpaeva str., 22

Abstract

It were investigated the rheological parameters of South-Turgay region waxy crude oils at presence of novel pour point depressant additive DP-43/2005. It has shown that additive improves pour point and rheological properties of crude oil mixture Kumkol-Akshabulak, inhibits wax deposition and can provide safe conditions of crude oil mixture transportation through pipeline at the cold season of year.

Key words: *oil, temperature of fluidity loss, rheology, viscosity, oligomer depressor dopants*

Improving low temperature properties of hydrocarbon fuel and lubricating oil is vital issue for Kazakhstan and a number of the north countries. This problem is increased for Kazakhstan, where the main part of oil produced is paraffinaceous i.e. basically consists of alkanes with normal and low-branched structures. These hydrocarbons have high congelation temperature. That causes worsening the properties of oil and oil refining products such as mobility, fluidity etc. Besides exploitation of oilfields containing high congealed oil is complicated by accumulation of hard deposits (asphalt-tar-paraffin deposits – ATPD) on inner walls of lifting columns that decreases in debit of oil wells and increases in exploitation costs.

Using reagents with integrated action is a prospective and economically sound way of preparing high congealed paraffinaceous oils for transferring through trunk pipelines. Introducing the small amount of reagents, as a rule - 0.01-0.1 wt. %, leads to significant decreasing temperature of congelation and improving fluidity at low temperatures and reaching inhibition of ATDP up to 60-85%. In contrast to the well-known methods this way provides the rational use of oil supplies and comprehensive improving the properties of various oil products.

Development of oil transfer preparation technology by treatment of oil with new reagents allows reaching a new technological level due to sufficient improvement of rheology parameters and prevention of paraffin and asphalt-tar deposits on surface of ground and under-ground equipment.

Authors of this communication have created a new generation of the condensation polyfunctional reagents with integrated action - DP-43/2005, DP-5/2007 and DP-58/2007 for intensifying the processes of producing and pipeline transferring the viscous and high congealed oils containing asphalt-tar-paraffin deposits and mineral salts [1-3].

The results of testing the new polymer additive – DP-43/2005 as a dope for highly paraffinaceous oil are presented. It has been shown that this additive improves the rheology and low temperature parameters and prevents the paraffin deposition on oil field equipment.

The technology for introduction of additives to oil based on the recommendations developed for the depressant dopants was used in the following way [4]. The dopant amount calculated (50-200 ppm) was added to mix of oils taken from the Kumkol and Akshabulak oil fields in a ratio of 60:40 vol.% and kept at temperature of 60 oC for 30 minutes. Rate of cooling corresponded to a regime earlier developed was the same for all experiments [5].

ISSN 1313-2539

Efficiency of paraffin deposition inhibition was evaluated according to the method of "cold finger"; temperature of fluidity loss was determined by ASTM D97 and ASTM D5853; effective viscosity and shift voltage was measured by the "Brookfield"rotary rheometer; kinematic viscosity was determined according to the GOST 33-2000 standards and the ASTM 445-96. Temperature of loss of oil mix fluidity was 12 oC and kinematic viscosity was 21 mm2/sec at 20oC.

The thixotropy oil properties were determined on a base of their viscosity characteristics by using the "Brookfield" rotary rheometer ("Euro Phisics" RHEO 2000). Values of shift voltage were determined on a base of on-line measurements of shift rate varying from 0 to 50 or 100 sec-1 at constant shift rate – 5 sec-1 under the thermal conditions from 15 to -5oC.

Using the DP-43/2005 depressant allowed significantly increasing the parameters of transferring oil, especially in a low temperatures range. Study showed that addition of dopant to oil mix lead to significant decrease in effective viscosity and shift voltage at experiment temperatures - 0 oC and -5 oC (Figures 1a and 1b).

For example, the effective viscosity of oil mix treated by 100 ppm of the DP-43/2005 at temperature is -5 oC and shift rate is 5 sec-1 was decreased by a factor of 35 and by 7 times for oil mix before heat treatment and after heat treatment respectively.

Under the same experiment conditions, shift voltage was decreased from 160 Pa for oil mix before heat treatment to 0.9 Pa after addition of 100 ppm of the DP-43/2005 into the Kumkol/Akshabulak (60: 40 vol.%) oil mix.

Ability of oil to transferring through the oil pipeline was studied by using a model pipeline designed to determination of static shift voltage in regimes simulating the real transfer conditions of the selected site of trunk oil pipeline such as oil temperature at the inlet and outlet, cooling rate, shift rate etc. Oil flow through the pipeline was simulated in dynamic reservoir by mixing during cooling. Injecting oil by pumps was simulated by pressing through nozzle, and pipeline break was simulated by oil cooling with using coiled pipes under static conditions.

The objective of studying the DP-43/2005 dope at the model pipeline is the test of its efficiency for transferring the Kumkol-Akshabulak oil mix (60:40%) through the industrial Karakain- Kumkol-Shymkent pipeline. In figure 2 the data on changing the static shift voltage depending on oil mix temperature after treating by heat and the DP-43/2005 dopant are presented. Pressure of restart at the corresponding temperature is calculated according to the formula:

$$P = \frac{\tau_{CTAT} \times 4L}{D} + \rho g \Delta h$$

where: P –pressure of restart;

L and D – length and diameter of pipeline section, respectively;

ρ - density of oil;

g – acceleration of gravity;

Δh – difference of heights for the certain part.

ISSN 1313-2539

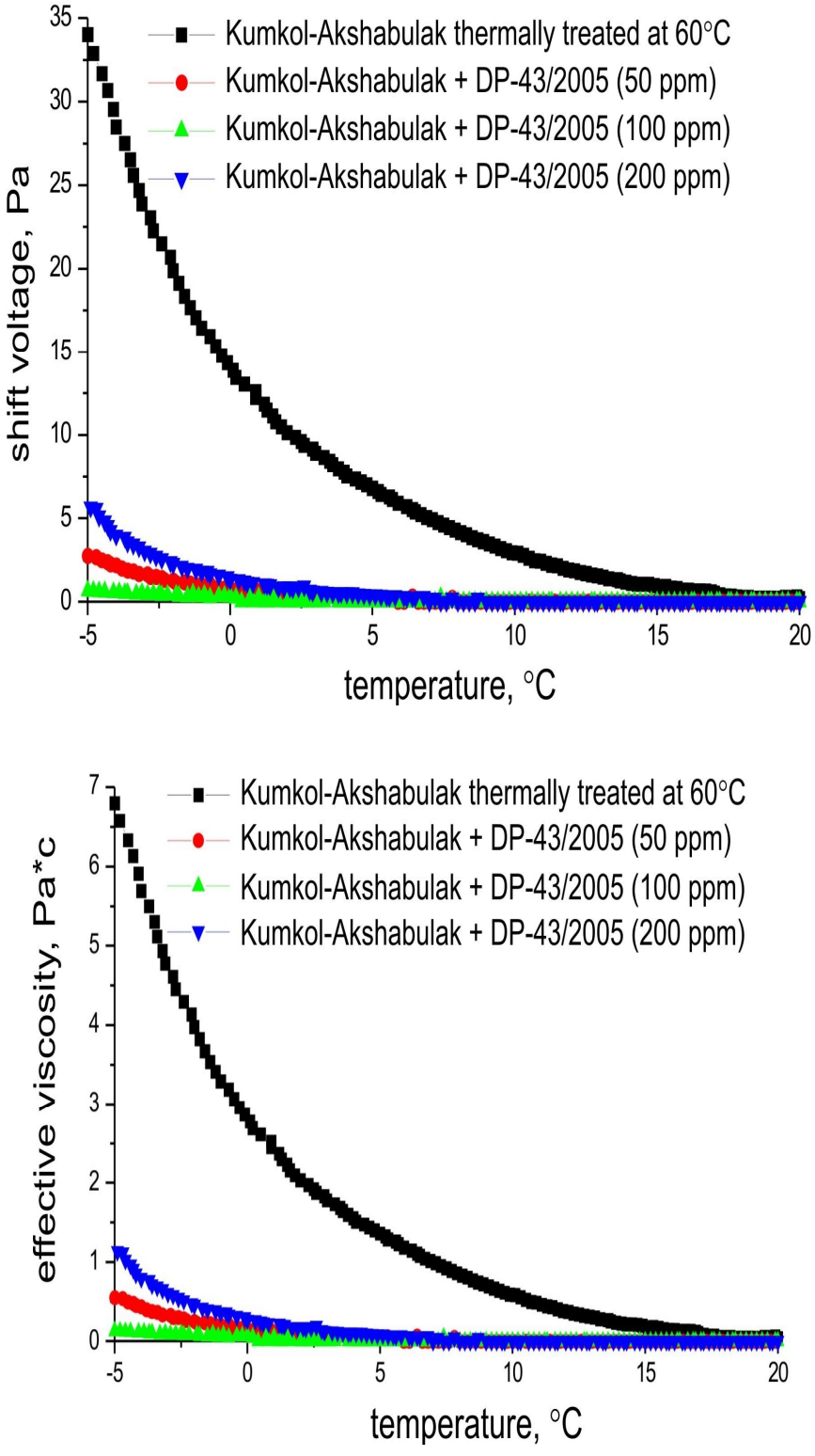

Fig. 1 Shift voltage (a) and effective viscosity (b) depending on temperature for the Kumkol/Akshabulak oil mix (60:40 vol.%) after treating by heat and the DP-43/2005 dopant, respectively.

ISSN 1313-2539

For the selected site of the Karakain- Kumkol-Shymkent pipeline, pressure allowing the safe restart is 6.2·106 Pa. The heights difference is about 169.8 м. The calculations show that the maximum static shift voltage should not exceed 4.2 Pa. It means that the safe restart of thermally treated oil mix must be carried out at temperature of 6 0C, and restart of oil mix treated by the dopant can be occurred at -10C.

The asphalt-tar-paraffin deposits (ATPD) formed in the pump-compressor- pipeline (PCT) and oil pipelines decrease in debit of oil wells and enhance the exploitation expenses. The numerous methods for the ATPD formation control in PCT and oil pipelines are known. The fuel, mechanical and chemical purification methods are widely used for oil production processes and transfer. The various special reagents and chemical and petrochemical wastes have been tested. But until now there is no certainty which reagent is more economically sound, provides the effective decreasing deposits and is optimal for the all oil fields.

Because of the new chemical reagents - DP-43/2005 and DP-44/2005 have been found to be high effective for the highly paraffinaceous and viscous oils, their testing as inhibitor for asphalt-tar-paraffin deposits attracted an attention. In laboratory scale, the inhibition effect of depressor dope on ATPD extraction has been studied by the “cold finger” method (T - 0 oC). The results presented in Table show inhibition degree reaches 60-67% after treating the Kumkol:Akshabulak oil mix by the DP-43/2005 dopant.

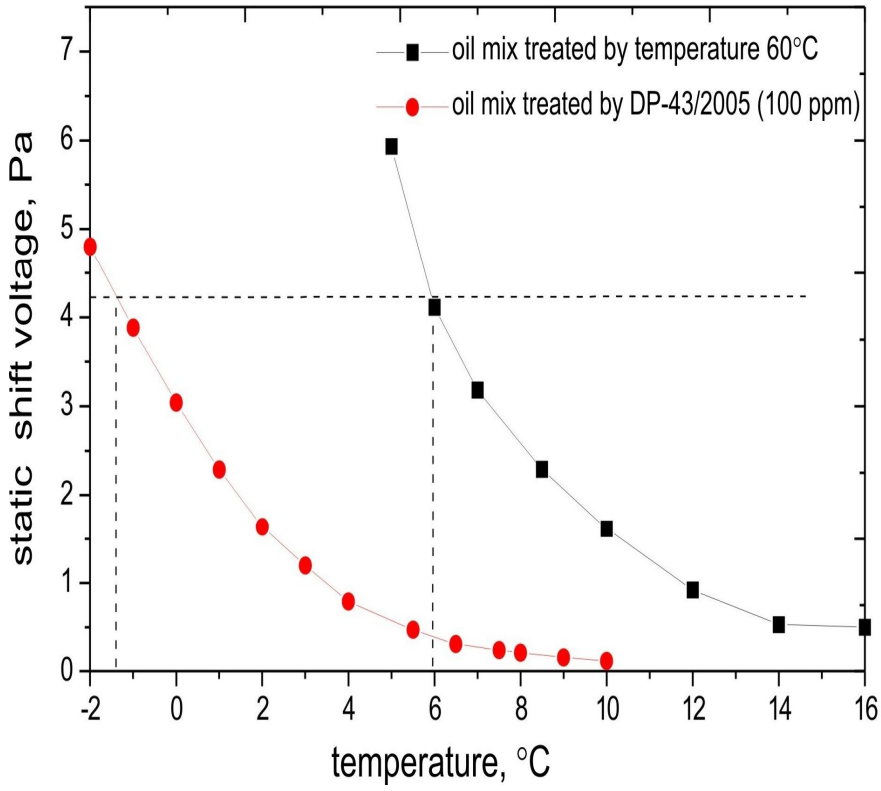

Fig. 2. The static shift voltage depending on temperature for the Kumkol/Akshabulak oil mix (60:40 vol.%) after treating by heat and the DP-43/2005 dopant, respectively.

ISSN 1313-2539

Table - Effect of DP-43/2005 dopant on inhibition of the paraffin deposition process

Duration, days	Non-treated oil mix			Oil mix treated by 100 ppm of DP-43/2005		
	m, g	Amount of ATPD from oil, %	Degree of inhibition, %	m, g	Amount of ATPD from oil, %	Degree of inhibition, %
1	9.2	4.5	0	3.6	1.8	60.9
3	9.2	4.5	0	3.0	1.5	67.4
5	9.2	4.5	0	3.1	1.5	66.3
10	9.2	4.5	0	3.2	1.6	65.2
20	9.2	4.5	0	3.1	1.5	66.3
30	9.2	4.5	0	3.3	1.6	64.1

Thus, the results obtained indicate that the new chemical reagent - DP-43/2005 shows both the high depressor activity concerning highly paraffinaceous oil as well as sufficient ability to ATPD inhibition. Application of the DP-43/2005 for the oil pipeline will allow transferring highly viscous oil in a cold season and significantly increasing reliability of pipeline start after a long transfer stoppage.

REFERENCES

1 Boiko G.I., Zhubanov B.A., Khutoryanskaya O.V., Pirogov A.G., Zakirova R.S.. New effective polymer reagents for the Kazakhstan's oil production and transferring highly paraffinaceous oil // Materials of the II International Symposium "Physics and Chemistry of carbon materials ". - Almaty, 2002. -P.45-502.

2 Boiko G.I., Shaihutdinov E.M., Khutoryanskaya O.V., Lyubchenko N.P., Maimakov T.P., Zhubanov B.A., Sayakhov S.K., Zakirova R.S.. On issue of regulation of rheological parameters of highly paraffinaceous oil // Materials Of the II Conference "Science for industry. Development of applied studies and their introduction into industry under modern conditions. Economy and experience. Practice and management. ". - Almaty, 2003. - P.67-71.

3 Boiko G.I., Lyubchenko N.P., Mukhamedova R.F., Maimakov T.P., Shaihutdinov E.M. Rheological properties of highly paraffinaceous oil, crystallization of n-paraffins in the presence of depressors // Proceed. Of the XYIII Mendeleev's Congress on General and Applied Chemistry - Moscow, 2007. - V3. - P.313

4 Zhubanov B.A., Boiko G.I., Khutoryanskaya O.V. Reological properties of oil from oilfield "Konys". Effect of thermal treatment and DU-ASB depressant concentration // Eurasian Chem. – Technolog. J. -2000. № 3-4, -P. 293-296.

5 Boiko G.I., Maimakov T.P. Lyubchenko N.P., Maimakov T.P., Sarmurzina R.G., Kozhabekov S.S., Didukh A.G., Shaihutdinov E.M. Rheological parameters of the South-Turgai bending oil in the presence of depressor additives,Vestnik of the KazNTU, №6, 2005. - P.49-53.

ISSN 1313-2539

CYLINDER WITH DIFFERENTIAL PISTON FOR MASS MEASUREMENTS

Ilare Bordeaşu

Universitatea "Politehnica" din Timişoara, Bvd. Mihai Viteazul, Nr.1, 300222, Timişoara, România

Anton Hadăr

Universitatea Politehnica Bucureşti, Splaiul Independenţei, nr.313, 060021, Bucureşti, România

Mircea O., Popoviciu

Academy of Romanian Scientists Timişoara Branch, Bvd. Mihai Viteazul, Nr.1, 300222, România

Victor Bălăşoiu

Universitatea "Politehnica" din Timişoara, Bvd. Mihai Viteazul, Nr.1, 300222, Timişoara, România

Abstract

The paper presents a cylinder with differential piston, adapted for measuring the weight of fixed objects such as: fuel tanks (regardless of their capacity), bunkers and silos for all kind of materials, or mobile objects such as: automobiles, trucks, locomotives and railway cars. Although, the cylinder with differential piston is used on a large scale in hydraulic drive or hydraulic control circuits, till now it was not used as constituent part for weight measurements devices. The novelty of the present paper is precisely the use of the device for such purposes. Based on a computation algorithm, the paper presents the general design (assembly), of the device used for weighing important masses (1…100 tones). The fundamental idea consist in the fact that, a mass over 10 tones may be weighted with a helicoidally spring subjected to an axial force between 0 and 3000 N, with a deflection of about 30 mm. Simultaneously with the mechanical part, the electronic recording system is also described. The great advantage of the presented device consist in the fact that it can be used in heavy polluted atmosphere or difficult topographic conditions as a result of both the small dimensions and the protection systems adopted.

Key words: *cylinder hydraulic with differential piston, hydrostatic pressure, measuring devices*

1. INTRODUCTION

In the technical literature, the cylinder with differential piston is mentioned in the schemes of hydraulic control or driving [1], [2], [3], [4], for various actuating systems (such as transport and hoisting devices, adjusting mechanisms for hydraulic turbines, actuating systems for lock gates, etc. The novelty of our studies was the use of differential pistons for measuring the weight of fixed objects, such as: fuel tanks (regardless of their capacity), bunkers and silos for all kind of materials or mobile ones, such as: automobiles, trucks, locomotives and railway cars. In this way a mass over 10 tones may be weighted with a helicoidally spring subjected to an axial force between 0 and 3000 N, with a deflection of about 30 mm. At the ground idea of the paper (for which it was obtained also the patent A00307/10.05.2006) there are the considerations regarding the devices having cylinders with differential pistons: simple and robust construction, great sensibility and precision. Such devices are not influenced by some corrosive environments in which there are used. Supplementary, the use of microelectronics allows obtaining a modern product, competitive and easy to employ. It is characterized by: low acquisition price (it is three times cheaper than similar other products) and favorable maintenance costs.

ISSN 1313-2539

2. DESCRIPTION OF THE SYSTEM

The weighing system has two components: a mechanical one, which includes the differential cylinder and an electronic one for the digital display of the measured mass.

2.1 The mechanical system

The assembly of the mechanical system is presented in Figure 1. It is composed from the cylindrical main part 1 continued by the cylindrical body 8, which separate the lower part, maintained under the oil pressure, from the upper one, where is formed a tight space under atmospheric pressure. In this tight space, the elements displaying the value of the measured mass are placed.

The piston 3, placed at the cylinder bottom is put in contact with the body that must be measured. Through the elastic membrane 4, a hydrostatic pressure is produced in the working fluid. Depending on the value of the measured mass this pressure ranges between 0 and 100 daN/cm^2. As a result of the communication orifices existing in the differential piston, the pressure will be equal on both sides of the piston. Because the working areas of the piston are different, the acting forces will be also different. As a result the piston rod will be pushed upward, into a translation motion. This translation will be converted into a rotation motion of the disk 9.

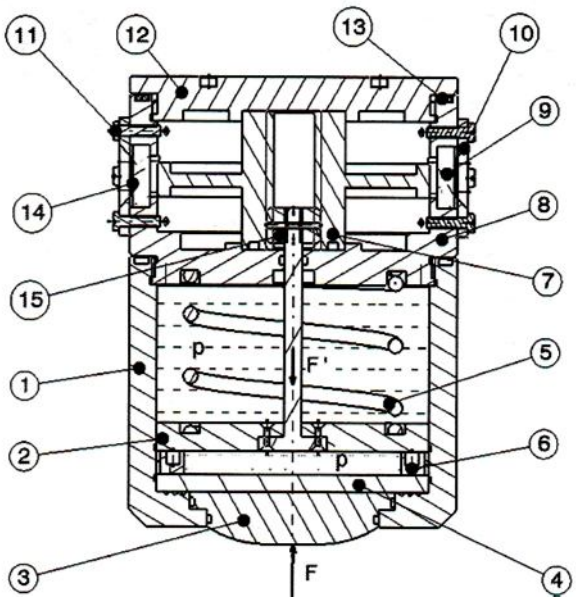

Figure1. The mechanical part of the device (axial cross section)

Considering that the hydrostatic pressure p has the maximum value (100 daN/cm^2), the force F acting on the inferior side of the piston will be [1], [5]:

$$F = S \cdot p = \frac{\pi \cdot D^2}{4} \cdot p \cong 5026 \text{ daN}$$

and the force F' acting on the upper side of the piston will be:

$$F' = S' \cdot p = \frac{\pi \cdot (D^2 - d^2)}{4} \cdot p \cong 5006 \text{ daN}$$

ISSN 1313-2539

The difference between the forces acting on the piston is:

$$F\text{-}F' = 20 \text{ daN}$$

The force acting on helicoidally spring being $F_{sp} = F\text{-}F'$, with a deflection of 30 mm the approximate constant of the spring will be:

$$k_{ap} = \frac{F - F'}{f} = \frac{200}{30} \cong 6.667 \text{ N/mm}$$

Choosing the following parameters for the hydraulic cylinder and the spring:

d_{sp} = 4.3 mm, the diameter of the spring wire,

D_{sp} = 60 mm, the wrapping diameter of the spring,

d = 5.05 mm, the piston rod diameter,

f = 30 mm, the spring deflection equal with the piston stroke,

p = 100 bar, the maximum pressure in the cylinder,

n = number of the spring whirl,

the actual constant of the spring becomes:

$$k = \frac{G \cdot d_{sp}^2}{8 \cdot n \cdot D_{sp}^3} = 6.648 \text{ N/mm}$$

Taking into account the actual parameters, the force developed by the spring is:

$$F_{sp} = k \cdot f = 199{,}44 \text{ N} \cong F\text{-}F'$$

and the force reduction of the device:

$$i = \frac{F}{F - F'} = \frac{50260}{199.44} = 252.00562$$

The stroke of the differential piston 2 is 30 mm and is put into correlation with the pitch of trapezoidal thread (Tr 18x30) of the nut 7 and the disc 9 so that at the end of the stroke, the indicatory disc rotates itself with 360º. This represents a good accuracy being 140 N for each degree.

The proposed solution offers the following advantages:

- allow the weighing of large and extra large masses in every place where such necessity occur, regardless if the objective is stationary or mobile;
- for mobile objects (cars, lorries, locomotives, railway cars, etc.) is sufficient a single device, over which every axle pass successively. Finally the total mass is computed by adding the successive values;
- for stationary objects, the measuring cylinders will be placed in those parts that sustain the objectives. The devices will remain there for the entire life of the objective.

In the figures 2 and 3 there are presented images of the cylinders and the complex device manufactured for the measurement of light vehicles masses. The assembly for measurements in the light variant comprises the following elements: the cylinder with differential piston 1, the central

ISSN 1313-2539

frame 2 and the access platforms 3. These platforms facilitate the mounting and descending of the vehicle wheel, on the central frame that include the cylinder with differential piston.

The central frame consists of two plates (the lower and the upper) pressed in heated conditions (deep drawing), between them being placed the cylinder 1. The upper plate sits on the cylinder (Figure 4) and transmitted the whole load towards the piston 3. It is important that the displacement of the two plates forming the central frame take place only on the vertical direction. To fulfill this condition, there were placed four plugs, for guiding and centering.

Figure 2. Cylinders with differential piston (measuring transducers)

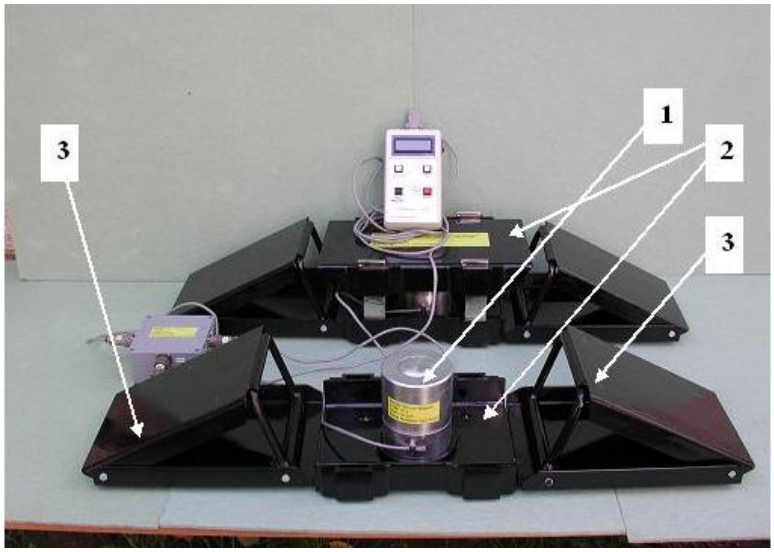

Figure 3. Prototype used for the mass measurement of light vehicles

For realizing a weighing, two such devices are needed so that the entire front axle, with both the left and right wheel, passes in a single movement, over the weighing cylinder. The operation will be

ISSN 1313-2539

repeated also for the rear axle (or rear axles, if the vehicle has multiple rear axles). The values read on the disk 7 will be totalized and the whole mass of the vehicle is found. It is possible to use a single device by passing successively the left wheels and the right ones (the errors are small but the weighing time is a little longer). For easing the handling and transportation of the frames the weighing device can be folded and dismounted.

The device for measuring very heavy masses, this is the case for lorry trailers, or lorry trailers combination, is similar to that presented in Figure 3 but between the two plates (the upper and the lower) of the frame 2, there were placed two differentials weighing cylinders. For this variant, the central frame must be longer, because here must be placed two weighing cylinders, but also because the rear part of a heavy lorry is provided with 2 axles. Because the mass is very great the load of each wheel is taken by two weighing cylinders.

For this variant, the two plates composing the central frame have a single degree movement (namely translation in the vertical direction), the oscillations and tilting are prevented by the tree pairs of plugs.

It must be mentioned that for weighing a heavy lorry, for the front axle, provided with a single axle, it is sometimes possible to use the light-weighing device, but for the rear axle in all cases it must be used the heavy weight device. Also in this case the central frame is composed from individual elements that can be assembled in the indicated place and the two frames may be folded and dismounted.

Fig. 4. The mass measuring of an automobile front axle

In order to maintain the alignment of the three elements, composing the frame, during the vehicle climbing, the lower plates are provided with elements preventing the plates to slide.

2.2 The electronic system for picking-up and displaying the measured values

Sometimes the reading of the measured values, mechanically displayed, encounter difficulties because the cylinder are placed in very low positions. For such situations it was conceived an electronic telemeter system for displaying the measured values. The electronic system maintains the high precision and the reading may be done easy at distances till 10 m, from the measuring cylinder.

The electronic system is composed from two devices:

ISSN 1313-2539

- the measuring device (two pieces)-MD;
- the displaying and control device-DCD.

The two MD are permanently in communication with the DCD through a RS 232 interface.

2.2.1 The measuring device MD

The measuring devices (Figure 5) are used for obtaining the mass of the vehicle on each wheel and to transmit this information to the displaying and control device.

The good working of the MD is supervised by a microcontroler. A piston that has a displacement proportional with the vehicle mass, play the role of transducer. This displacement is converted in voltage by a potentiometer transducer. At his turn the voltage is transmitted to an interface circuit. This circuit assures the calibration of the mass measuring transducer. The voltage is converted in a digital magnitude by the analogical/digital converter of the microcontroler. The digital magnitude processed by the microcontroler is transmitted through a RS232 interface.

The feeding of the measuring device is provided by five batteries of the type "AA". The other parts of the measuring device are:

- a supervision circuit of the fed voltage, which signalize through a led, the discharge of the batteries:
- an "ON/OFF" switch.

a) Measuring device of type 1 b) Measuring device of type 2 c) Measuring device of type 3

Figure 5 The electronic measuring devices (MD)

2.2.2. The displaying and control device-DCD

From a constructive point of view, this device is a portable console (Figure 6). This device displays the information obtained by the measuring devices upon a LCD with 2x16 characters.

ISSN 1313-2539

a) displaying and control device-DCD (front view) b) displaying and control device-DCD (rear view)

Figure 6 The displaying and control device-DCD

The displaying and control device-DCD has the following buttons:

- "ON/OFF";
- "RESET" for entering in the measuring menu;
- „MEASUREMENT" for performing a measurement;
- "M+" for adding the measured masses in order to obtain the vehicle mass;
- "STOP MEASUREMENT" to end the measurement process.

The feeding of the displaying and control device is done by five "AA" type batteries. The DCD contains also a circuit for signalizing discharge of the battery.

The running parameters of the electronic device are:

- Type of feeding: 5 "AA" type batteries;
- Number of measuring devices: 2;
- Maximum number of measurements for a vehicle: 8;
- Measurement precision for a measuring device: ± 25 kg;
- Displayed precision: ± 0.5%;
- The measuring unities: tons (T);
- The maximum measured mass for a single device: 10.0 tons;
- The dimensions of "DCD": (90x170x40) mm;
- The dimensions of "MD": Φ100 – 135 mm.

2.2.3 Description of the measuring process

For putting into operation the device, the DCD must be connected to the two MD with the proper cables. The button "ON/OFF" of the first „MD" is pushed in the position "ON". If the green led is continuously burning, the supplying voltage is in normal limits, if the led is intermittently burning, the supplying voltage is under the normal value and the battery must be replaced. The second "MD" must

ISSN 1313-2539

be proofed in the same way. The button ”ON/OFF” of the DCD is pushed in the position ‘ON’. On the LCD display the following messages appear (there are illustrated in the Figure 7):

- the message “DISCHARGED BATTERY”, if the voltage is under the normal value. If this message is seen, the batteries must be replaced and the procedure must be repeated (Figure 7a);
- the message “TRANSDUCER ERROR” appears if there is a communication lack between the transducers. If this message is seen, it means that there are transducers deficiencies or the connecting cable is damaged. At first, the connecting cable must be verified and if it is in order than all the transducers must be verified. After the defective part is repaired, the putting into function procedure must be repeated (Figure 7b);
- the message “READY FOR MEASUREMENTS” signifies that the installation is functioning (Figure 7c).

To obtain the vehicle mass, the following procedure must be applied:
The first axle of the vehicle is mounted on the two measuring devices and after that, the button „MEASURE” of the DCD is pushed. On the LCD display appears the message „THE MASS OF AXLE 1: xx.xT” on the first row, and the message „TOTAL MASS: zzz.zT” on the second row (Figure 8a). The figure 1 represents the axle number and is displayed intermittently and “xx.x” represents the mass of the axle. The device remains in measuring state for 50 ms. The measured value is displayed every 0.5 s. If the operator wants to memorize the measured value the button “+M” must be pushed. On the LCD appear the following messages, on the first row “THE AXLE MASS1: xx,xT” and on the second row “TOTAL MASS: zzz.zT” (Figure 3). The “TOTAL MASS” displayed value is equal with the measured value. The axle number “1” is continuously displayed, which means that the mass value is memorized.

a) ”DISCHARGED BATTERY” b) The message “TRANSDUCERS ERROR” c) The message “READY FOR MEASUREMENTS”

Figure 7 Messages displayed

ISSN 1313-2539

In order to fulfill the following measurement, the vehicle is mounted with the adequate axle on the two measuring devices and the button "MEASURE" of the DCD is pushed. On the LCD appears the message „THE MASS OF AXLE 2: yy.yT" on the first row, and the message „TOTAL MASS: www.wT" on the second row. The figure 2 represents the axle number and "yy,y" represents the measured axle mass. The axle figure is intermittently displayed. The device remains in measuring state for 50 ms. The measured value is displayed for 0.5 s. If the operator wants to memorize the measured value the button "+M" must be pushed. On the LCD display appear the following messages, on the first row "THE AXLE MASS2: xx,xT" and on the second row "TOTAL MASS: zzz,zT". The "TOTAL MASS" displayed value is equal with the current measured value added with the mass previously measured. The axle number "2" is continuously displayed, which means that the mass value is memorized. If the vehicle has only two axles and the measurement is finished, the button "STOP MEASUREMENTS" must be pushed. On the LCD appears the message: "AUTO MASS: aaa.aT". The DCD goes out from the measuring state and pushing any of the buttons 'MEASURE", "+M", "STOP MEASURING" remains without effect. In order to perform another cycle of measurements the button "RESET" must be pushed. On the LCD will appear the message "READY FOR MEASURE" and the procedure presented previously must be repeated.

If a vehicle has more than two axles, the measurement procedure for the other axles are similar as for the axle 2, the number of the axle being 3, 4 till 8. If the number of measurements goes beyond eight, on the display appears the message "ERROR: TO MANY MEASUREMENTS" (Figure 15). In this situation the "reset" button must be pushed, on the display appears the message "READY FOR MEASURE" and a new cycle of measurements can begin.

a) Display "TOTAL MASS": 0xx,xT' b) Display "ERROR TO MANY MEASUREMENTS"

Fig. 8 Messages displayed

ISSN 1313-2539

The homologation tests were accomplished in the following way:

- In traffic for a small weight vehicle (a DACIA car), as can be seen in Figure 16;
- By loading the devices with a 10 tons hydraulic press, available at the I. M. S. T. Faculty of the Bucharest Polytechnic University, considering that in the traffic loading the forces will be similar with those offered by the hydraulic press. Such a loading was necessary to see if heavy vehicles can be measured but also to verify if undesirable leakage may occur.

Each device was tested six times with different loadings and all the results were excellent.

The presented measuring system can be used for:

- **mobile objectives**: cars in traffic to see if it is loaded or empty, to verify the momentary mass, without deviating the vehicle from its moving direction, towards a weigh platform. The system allow the weighing of the vehicle in a short delay of time, just on the place were it was stopped;
- **fixed objectives (**bunkers, silos, tanks etc.). These objectives may be permanently observed and on there entire life. Sometimes this information is important for those, which administrate such objectives. Of course, the reduction of the content under an inferior limit may be announced by acoustic or optic means;
- **protection of fixed objectives** (protection against overloading). For example, the weight of lorries can be measured when acceding on some bridges. When the weight goes beyond some reference value, an optic or acoustic signal is released.

3. CONCLUSIONS

The presented system, which uses a differential hydraulic cylinder, is a new procedure in weighing systems. It allow to measure heavy and very heavy loads, easy, with high precision, from distances till 10 m, regardless if the objective is fixed or mobile.

REFERANCE

1. Bălăşoiu, V., Bordeaşu, I., Popoviciu, I., - Hydraulic Driving Systems for Asphalt Pouring Equipments, The Journal of the engeneering industries in Bulgaria, Machinebuilding and Electrical Engeneering, Nr.7-8, Sofia, 2006, ISSN 0025-455X, pp.3-6
2. Bălăşoiu, V, Rasga, C., Popoviciu, M, Bordeaşu, I.,- Experimental Results in the Analysis of Flow in a Sliding Control Valve, PNEU-HIDRO 2004, University of Miskoc, 2004, ISSN 1215-0851, p.55-60
3. Bălăşoiu, V., Popoviciu, M., Bordeaşu, I., - Mathematical model of the assembly cylinder-load for linear motor (Part I), The International Conference on ENERGY and ENVIRONMENT, Bucureşti 2005, Section S3, ISBN: 973-86948-5-x, pp.S3.13-S3.18
4. Bordeaşu, I., Bălăşoiu, V., Baciu, I. D., Bădărău, R., - About Braking of Big Masses, Acting by Liniar Hidrostatic Motors, Annals of the University of Petroşani, Mechanical Engineering, 2007, ISSN 1454-9166, pp. 59-64
5. Bordeaşu, I. Baciu, I.D., Hidraulica Aplicată -Hidrostatica– Noţiuni Teoretice şi aplicaţii, Editura Politehnica, Timişoara, 2002, ISBN: 973-8109-90-6, 120 pag.

International Scientific Publications: Materials, Methods and Technology, Vol. 1

ISSN 1313-2539

INVESTIGATION OF PROPERTIES OF HOLLOW AND LOW STRENGTH CONCRETE MASONRY UNITS WITH PUMICE AGGREGATE

Osman ÜNAL, Tayfun UYGUNOĞLU

Construction Department, Technical Education Faculty, Afyon Kocatepe University, 03200 Afyonkarahisar / Turkey

Abstract

Lightweight concretes can be produced by using different type of lightweight aggregates. The results of investigations on the suitability of using pumice aggregates from Isparta region in Turkey as fine and coarse materials in lightweight concrete masonry production are reported. In this study, pumice aggregate lightweight concrete (PLWC) samples were produced with different sizes of 0-4 mm as fine pumice aggregate (FPA), of 4/8 mm as middle pumice aggregate (MPA) and of 8/16 mm as coarse pumice aggregate (CPA). The pumice aggregates collected from the quarry were first crushed and screened in this study. In order to analyze the role of pumice aggregate ratio on the properties of lightweight concrete masonry for dry mix conditions, a series of preliminary trial batches were first carried out. Trial batches were cast into 100x100x100 mm cube samples with the cement content of 220 kg/m^3 in low water/cement ratio as 0,15. The specimens were analyzed to examine the compressive strength, water absorption and specific porosity of all series. According to the results of preliminary trial batches, it was decided to produce a full scale pumice aggregate masonry block (PAMB) units for the same mixture proportions of the best series in trials. PAMB units were analyzed to investigate their unit weight and the compressive strength for air dry condition at 28 days. The coefficient of thermal conductivity for the blocks was tested based on oven dry. According to experimental results, while dry unit weight has increased, compressive strength of 28 days samples has increased, too for the PLWC dry mix composition. Due to the low strength and thermal conductivity, pumice aggregate lightweight masonry units can be used in constructions for non-load bearing infill walls providing the high isolations.

Key words: *Pumice, lightweight aggregate, hollow blocks, property.*

1. INTRODUCTION

Compressed masonry blocks have traditionally been widely used as a construction material for both structural and non-structural walls. Masonry walls are primarily composed of masonry units (typically concrete blocks or clay bricks) and mortar. In addition to the various options available for masonry units with respect to material composition, further options relate to the geometry of the units and to their percentage of hollow volume. Furthermore, mortar can be composed of several materials and aggregate types and its workability may be adjusted by varying its water content. All these features naturally have a considerable effect on the mechanical characteristics of masonry walls [1].

The capacity of masonry in compression is strongly related to the compressive strength of the masonry units (stone, brick, and block), as well as mortar strength, bonding pattern and many other factors. Though other parameters, such as density, frost resistance and water absorption, may be specified in design, compressive strength has become a basic and universally accepted unit of measurement to specify the quality of masonry units. The relative ease of undertaking laboratory compressive strength testing has also contributed to its universality as an expression of material quality [2].

ISSN 1313-2539

Masonry wall construction has a number of advantages the first of which is the fact that a single element can fulfill several functions including structure, fire protection, thermal and sound insulation, weather protection and sub-division of space. Masonry materials are available with properties capable of meeting these functions, requiring only to be supplemented in some cases by other materials for thermal insulation, damp-proof courses and the like. The second major advantage relates to the durability of the materials which, with appropriate selection, may be expected to remain serviceable for many decades, if not centuries, with relatively little maintenance. From the architectural point of view, masonry offers advantages in terms of great flexibility of plan form, spatial composition and appearance of external walls for which materials are available in a wide variety of colors and textures [5].

Concrete masonry blocks come in a much greater variety of sizes and formats (solid, cellular and hollow). Also, materials that used in making of masonry block such as aggregate are affected to physical and mechanical properties of blocks. In the production of masonry units, lightweight aggregates are used for reduce the unit weight of material [3].

Increasing utilization of lightweight materials in civil structuring applications is making pumice stone a very popular raw material as a lightweight rock. Due to its having a good ability for making the different products based on its physical, chemical and mechanical properties, the pumice aggregate finds a large using area in civil industry as a construction material. In order to design an initial stage of a building project, the construction material properties should be well evaluated. Therefore, the need arises to analyze the materials to be used in construction experimentally in detail [4].

In this study hollow and non-load bearing masonry units were designed with pumice lightweight aggregate. Physical and mechanical properties of masonry blocks were investigated.

2. EXPERIMENTAL STUDY

2.1. Materials

Isparta / Turkey region volcanic pumice was used for this study. Particle density and bulk density of pumice were 2.24 and 760 kg/m^3, respectively. Ordinary Portland cement (CEM I 42.5R) was used for the production of the LWC and blocks. Surface area by Blaine, specific gravity and 28 days compressive strength of cement were 386 m^2/kg, 3.07 and 48.5 N/mm^2, respectively. The chemical analyses of materials used in this study were determined in Acme Analytical Laboratories Ltd. in Canada and results were given in Table 1.

To define the optimal mix proportions and to obtain satisfactory mechanical properties of masonry units, the pumice LWA was divided into three different size ranges: smaller than 4 mm, 4 to 8 mm and 8 to 16 mm. The aggregates in these size ranges were combined in different proportions to obtain the optimum granulometry in five grading curves properly to TS 1114 EN 13055-1 [6] as Grade 1, Grade 2 and Grade 3, Grade 4 and Grade 5. Aggregate ratios in the mixes were designed that as fine aggregate (FA) has been reduced from 60 % to 40 % while that of medium aggregate (MA) was increased from 20 % to 40 % by a ratio of 5 %. Coarse aggregate (CA) was kept at a ratio of 20 %. Sieve analyses of pumice aggregates were given in Figure 1.

ISSN 1313-2539

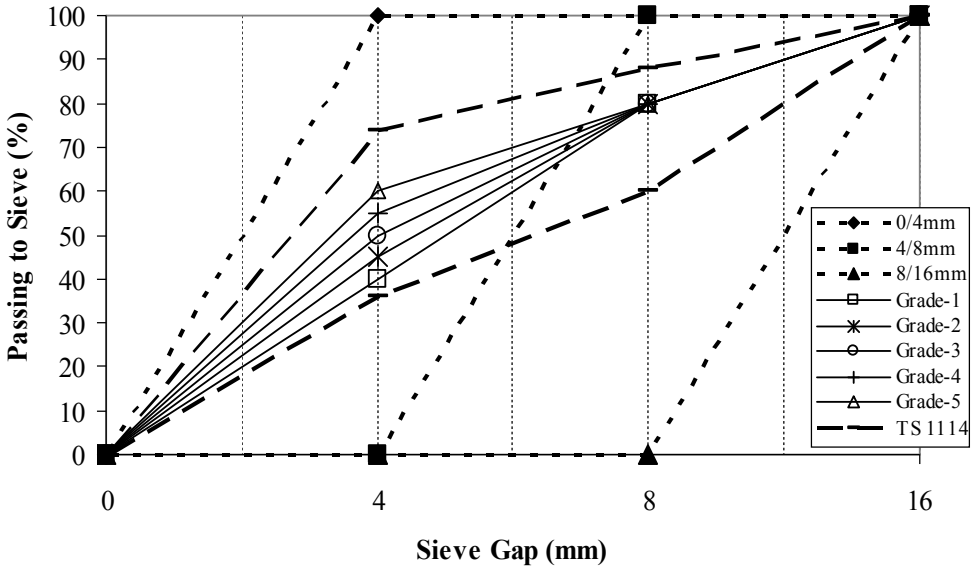

Figure 1. Sieve analyses of aggregates

Table 1. Chemical analysis of cement and pumice

COMPONENT (%)	SiO_2	Al_2O_3	Fe_2O_3	MgO	CaO	Na_2O	SO_3	K_2O	L.O.I.
Cement	19,3	5,57	3,46	0,86	63,56	0,13	2,91	0,80	2,78
Pumice	56,85	16,72	4,66	1,84	5,39	4,61	-	5,19	2,8

2.2. Mix Proportions and Test Program

Before production of masonry blocks, trial batches were produced for defining of optimum aggregate granulometry that supplying to the best properties on masonry units. The all mixtures were designed at 220 kg/m^3 cement content and at 0.15 actual water/cement ratios (w/c). The pumice aggregates were absorbed water in 30 min before adding the mix because of high porosity of aggregates [7]. In the trial batches, the prepared lightweight aggregate concrete (LWAC) as damped was filled in 100 x 100 x 100 mm cubic moulds by vibration-compression machine in 20 % compression ratio. The specimens immediately demoulded and cured in air (in laboratory condition) at 20±2 ^oC for 7, 28 and 56 days. On the trial specimens, compressive strength was defined according to TS EN 12390-3 [8] by 2000 kN compressive machine with a rate of loading controller. Unit weight (UW), specific porosity (SP) and water absorption (WA) were calculated aged in 7 and 28 days specimens according to Archimedes principle by the weight measurements of saturated specimens in air and in water, and the dry weight (oven drying at 105°C to constant weight). In the best granulometry, masonry blocks were produced in same cement content and w/c (Fig. 2). Three types of masonry blocks were designed as one-order hollow, two-order hollow and three-order hollow in size of 135 x 190 x 190 mm, 150 x 340 x 190 mm and 190 x 340 x 190 mm, respectively. Also, the production method was same with trial batches.

ISSN 1313-2539

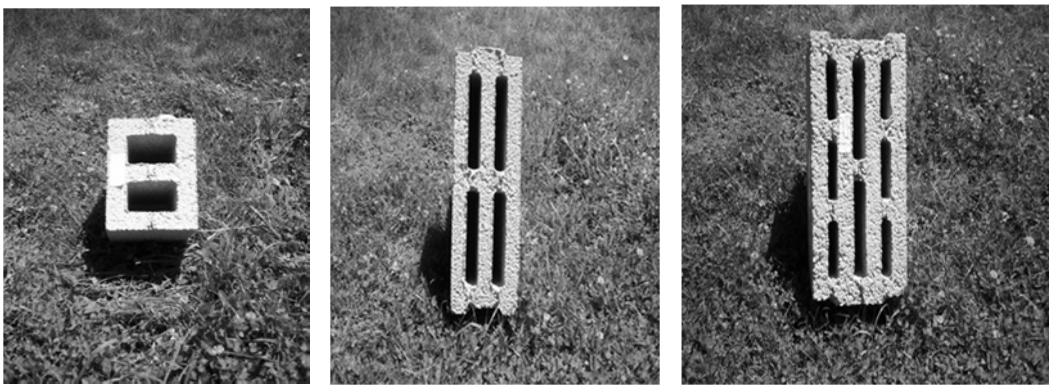

Figure 2 Masonry blocks produced with pumice LWA

Also, compressive strength and unit weight are defined on the masonry blocks. The thermal conductivity of masonry blocks was determined by the ‘‘hot box method” according to ASTM C1363 [9] on the aged 28 days specimens. For the all tests, arithmetic average of three specimens has been used.

3. RESULTS AND DISCUSSION

To investigate the influence of porous aggregate on the physical and mechanical properties of masonry units, natural lightweight aggregate as pumice has been used. Pumice lightweight aggregate concrete (PLWAC) was produced in low w/c ratio by vibration – compression method and they have been tested in 7, 28 and 56 ages.

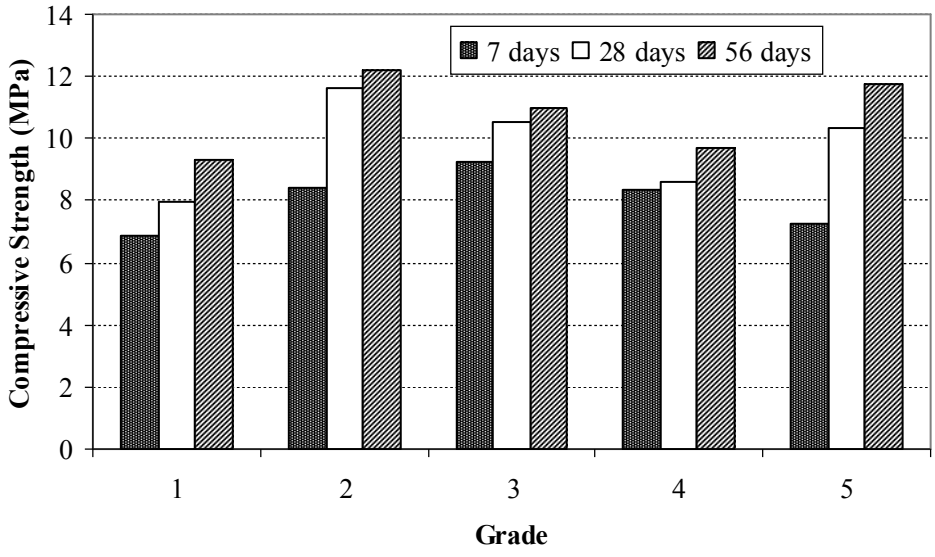

Figure 3 Compressive strength of PLWAC in different ages and gradations

Compressive strength of PLWAC was compared in Figure 3 depending on specimen age. Generally, the compressive strength of LWC has increased by rising of concrete age. Developing of strength in PLWAC was the highest in Grade-2 and Grade-5, Grade-1 and Grade-4, respectively. Of course, the

ISSN 1313-2539

strength development in lightweight concrete is limited by the inherent strength of aggregate [10]. The strength development was reduced by increasing of concrete ages from 28 to 56 days due to evaporation of free water that affect to hydration of cement. Besides, the highest compressive strength of PLWAC was obtained in Grade-2 as 12 N/mm^2. The compressive strength of PLWAC has changed between 7 - 12 N/mm^2 for 7 – 56 aged specimens.

Sari et. al. [11] investigated to the effects of gradation and admixture on the pumice LWAC. The specimens were cured at a temperature of 20-25 ^{o}C and a relative humidity of 50-55 %. Compressive strength of the specimens was determined as between 3.5 - 7 N/mm^2 for 28 and 56 ages. Babu et. al. [12] investigated to the performance of lightweight EPS aggregate concretes containing fly ash over a wide range of concrete densities of 500 - 2200 kg/m^3. The compressive strengths of the specimens have varied between 1.1 and 18.4 N/mm^2 for 28 ages.

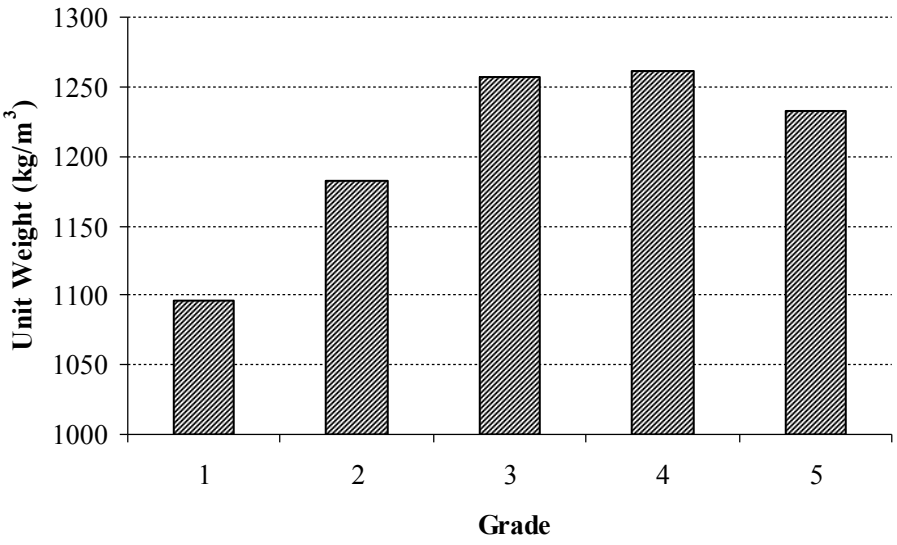

Figure 4. Unit weight of 28 aged PLWAC

As known from the literature, LWACs are categorized according to compressive strength and unit weight of them (Figure 4). Generally, the PLWAC for 28-56 days can be categorized as moderate strength LWC because of their strength in between 7 – 12 N/mm^2 and unit weight in between 1100 - 1260 kg/m^3. The grading effects to unit weight of LWAC as seen in Fig. 4. The lowest unit weight was obtained on the specimens that produced with Grade-1 while the highest unit weight was obtaining on the specimens produced with Grade – 4.

Figure 5 illustrates the specific porosity (sp) and water absorption (wa) of pumice LWAC. The specific porosity and water absorption of pumice LWAC have ranged between 15 % - 25 % and 12 % and 23 %, respectively. They have decreased until Grade-3 and then again increased by increasing of surface area of aggregate depending on fine material and in cubic meter. Pumice LWAC has higher "sp" and "wa" value than normal strength concrete due to properties of aggregate such as pore structure. The specific porosity and water absorption of LWC depends upon the raw material used for making them.

Even tough the lowest porosity and water absorption were obtained in the specimens that produced with Grade-3, the highest compressive strength and improper unit weight was obtained on the specimens produced with Grade-2. Hence, masonry units in this study were produced in Grade-2. Geometrical, physical and mechanical properties of three type's masonry blocks are presented in Table

ISSN 1313-2539

2. Compressive strength of masonry units is different depending on hollow ratio on surface or totally surface area, and it has changed between 3.77 – 5.11 N/mm^2. In the same cement and w/c ratios, three-order hollow masonry blocks more proper than other units due to strength and thermal conductivity.

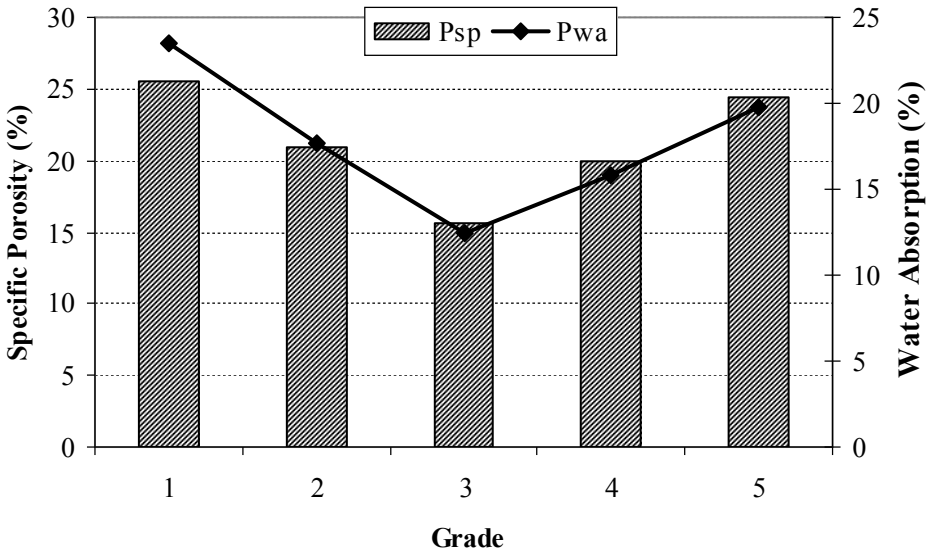

Figure 5. Specific porosity (sp) and water absorption (wa) of 28 aged PLWAC

Table 2. Properties of Masonry Blocks

Property	Masonry Block Type		
	135x190x190	150x340x190	190x340x190
Total surface area (cm^2)	256,5	570	710,64
Total hollow surface area (cm^2)	75	150,12	169,96
Total full surface area (cm^2)	181,5	419,88	540,68
Hollow ratio on surface (%)	29,24	26,34	23,92
Fullness ratio on surface (%)	70,76	73,66	76,08
Total volume (cm^3)	4874	10944	13502
Total hollow volume (cm^3)	1350	2732	3059
Total fullness volume (cm^3)	3524	8212	10443
Volumetric hollow ratio (%)	27,70	24,96	22,66
Volumetric fullness ratio (%)	72,30	75,04	77,34
Block weight (kg)	4,06	9,31	12,07
Dry unit weight (kg/m^3)	833	851	894
Masonry number in 1 m^2	28	13,5	13,5
Compressive strength (N/mm^2)	3.77	3.66	5.11
Thermal conductivity (W/mK)	0.237	0.214	0.203

ISSN 1313-2539

Thermal conductivity is depends upon the pore structure of the lightweight aggregates, density of concrete and the cement paste matrix [13]. Other words, the thermal conductivity is increases with increasing of density of concrete. Also, according to Kim et al. [14], aggregate volume fraction and moisture condition of concrete are revealed as mainly affecting factors on the thermal conductivity of concrete. The thermal conductivity of masonry units has decreased by increasing of volumetric hollow ratio and thermal conductivity of masonry blocks has ranged between 0.203 - 0.237 W/mK.

Al-Jabri et. al. [15] studied to block element for hot climate region. The blocks were produced from two indigenous materials: vermiculite (VerBlock) and polystyrene beads (PolyBlock1) which were used as lightweight aggregates with different proportions in the mix. The mechanical properties of the two types of blocks were compared and compressive strength of these blocks has changed between 2.2-15 N/mm^2.

Uysal et.al. [13] a study has conducted on thermal conductivity coefficients of concretes made up of mixtures of pumice aggregate (PA) and normal aggregate, and they were reported that when 25%, 50%, 75%, and 100% PA ratios were used in place of normal aggregate by volume, PA decreased the density and thermal conductivity of concretes up to 40% and 46%, respectively.

As seen, the masonry blocks produced with pumice aggregate has lower thermal conductivity than normal concrete and brick used in constructions.

4. ACKNOWLEDGEMENT

Authors thank to The Scientific & Technological Research Council of Turkey (TUBİTAK) for financial support throughout this study by project of 104.M.391.

REFERENCES

[1] C. Dymiotis, B. M. Gutlederer, Allowing for uncertainties in the modelling of masonry compressive Strength, Construction and Building Materials 16 (2002) 443–452.

[2] J.C. Morel, A. Pkla, P. Walker, Compressive strength testing of compressed earth blocks, Construction and Building Materials 21 (2007) 303–309.

[3] O. Ünal, T. Uygunoğlu, A. Yildiz, Investigation of properties of low-strength lightweight concrete for thermal insulation, Building and Environment 42 (2007) 584–590.

[4] L. Gündüz, İ. Uğur, The effects of different fine and coarse pumice aggregate/cement ratios on the structural concrete properties without using any admixtures, Cement and Concrete Research 2005;35: 1859-1864.

[5] E.A.W. Hendry, Masonry walls: materials and construction, Construction and Building Materials 15 (2001) 323-330.

[6] TS 1114 EN 13055-1, Lightweight aggregates – Part 1: Lightweight aggregates for concrete, mortar and grout, Turkish Standard Institute, Ankara, 2004 (in Turkish).

[7] Lo, T.Y., Cui, H.Z., Li, Z.G., Influence of aggregate pre-wetting and fly ash on mechanical properties of lightweight concrete, Waste Management. Vol. 24, 2004. pp 333–338.

[8] TS EN 12390-3, Testing hardened concrete - Part 3: Compressive strength of test specimens, Turkish Standard Institute, Ankara, 2003 (in Turkish).

[9] ASTM C1363-97, Standart test method for the thermal performance of building assemblies by means of hot box apparatus, American Society of Test Materials.

ISSN 1313-2539

[10] Al-Khaiat, H., Haque, M.N., Effect of initial curing on early strength and physical properties of a lightweight concrete, Cement and Concrete Research, Vol. 28, 1998. pp 859-866.

[11] Sari, D., Paşamehmetoğlu, A.G., The effects of gradation and admixture on the pumice lightweight aggregate concrete, Cement and Concrete Research. Vol. 35, 2005. pp 936-942.

[12] Babu, K.G., Babu, D.S., Performance of fly ash concretes containing lightweight EPS aggregates, Cement & Concrete Composites. Vol. 26, 2004. pp 605-611.

[13] Uysal, H., Demirboğa, R., Şahin, R., Gül, R., The effects of different cement dosages, slumps, and pumice aggregate ratios on the thermal conductivity and density of concrete, Cement and Concrete Research. Vol. 34, 2004. pp 845–848.

[14] Kim, K.H., Jeon, S.E., Kim, J.K., Yang, S., An experimental study on thermal conductivity of concrete, Cement and Concrete Research. Vol. 33, 2003, pp 363–371.

[15] Al-Jabri, K.S., Hago, A.W., Al-Nuaimi, A.S., Al-Saidy, A.H., Concrete blocks for thermal insulation in hot climate, Cement and Concrete Research Vol. 35, 2005; 1472–9.

International Scientific Publications: Materials, Methods and Technology, Vol. 1
ISSN 1313-2539

TRANSFERING AND ADOPTATION OF TECHNOLOGY TO ACADEMIC ORGANIZATIONS: CASE STUDY OF KADIR HAS UNIVERSITY

Danaci Sakalar, Tugba
Kadir Has University, Faculty of Engineering, Industrial Engineering Department
tugbad@khas.edu.tr

Abstract

To be successful and competitive in the globalizing and rapidly changing world, most organizations are under pressure to effectively either develop or transfer technology. Technology transfer is a managed process of conveying a technology from a point of origin to its potential users. Transferring technology from universities to private sectors results in economic development and welfare improvement of the issued country. But, for a sustainable development, the universities should also transfer the available technology until they can be enough sufficient to develop it internally. Especially, new-established universities like the foundation those recently established in Turkey need to transfer the technology in order to become a potential technology developer as being other old and long-established ones. Therefore, this paper represents a case study of how to transfer and adopt the technology from a private sector to Kadir Has University, as a newly established private university, which should be rational on investment decisions. This study is a work of technology strategy development through positioning-based approach, and includes three sections as follows: in the first part, a SWOT analysis, the issues of technology scanning are presented, in the second part, the selection of technology transfer method is included, in the final part, the criterion are determined to have a successful technology transfer process.

Key words: *Technology strategy development, positioning-based approach, technology transfer, SWOT analysis*

1. INTRODUCTION

To be successful and competitive in the globalizing and rapidly changing world, most organizations are under pressure to effectively either develop or transfer technology. Technology transfer is a managed process of conveying a technology from a point of origin to its potential users. Transferring technology from universities to private sectors results in economic development and welfare improvement of the issued country. But, for a sustainable development, the universities should also transfer the available technology until they can be enough sufficient to develop it internally. Especially, new-established universities like the foundation those recently established in Turkey need to transfer the technology in order to become a potential technology developer as being other old and long-established ones.

In Turkey, there are 111 universities educating 2.242.995 student: 67 government, 30 foundation, 1 foundation vocational school, 5 military, 1 police academy, 5 in Turkish Republic of Northern Cyprus and 2 special status government schools [1]. To establish a university, there are rules made by a government agency called YOK. Since 1992, foundations have a chance to establish university. Kadir Has University (KHU) is one of the foundation universities and was founded in 1997, in Istanbul [2]. The mission of KHU is to educate bright individuals in international relations, technology, and culture. The school hopes to turn out students who have consciously assimilated Ataturk's principles and reforms and who have thus become better citizens. They will use the knowledge and experience that they have attained for the welfare of the country, nation and humanity. The university is composed of

ISSN 1313-2539

three campuses. The main campus is in the Cibali (Halic or Golden Horn) area. The English preparatory school and vocational schools are located at the Bahcelievler and Selimpasa campuses, respectively. The faculties and departments of the university are as follows:

- ✓ Faculty of Engineering offering BS degrees in Computer Engineering, Electronics Engineering and Industrial Engineering
- ✓ Faculty of Economics and Administrative Sciences offering BA degrees in Economics, Business Administration, International Relations, International Finance and Tourism Management
- ✓ Faculty of Arts and Sciences offering BA degrees in American Literature and Culture and the BS degree in Statistics and Computer Sciences
- ✓ Faculty of Communication offering BA degrees in Communication Design, Advertisement, Television and Cinema, Public Relations
- ✓ Faculty of Law offering the BA degree in Law
- ✓ Faculty of Fine Arts offering BA degrees in Industrial Design, Interior Design and Graphic Design
- ✓ Vocational Schools offering a pre-BA degree in Social Sciences and a pre-BS degree in Technical Sciences and Health Services
- ✓ Graduate Schools offering the MA degree in Social Sciences and MS degrees in Technical Sciences and Health Sciences

In order to be successful, a university should have some features like the quality and the quantity of teachers, laboratories, library, relationships with national or international universities and social medium.

In KHU, the number of teachers including from research assistant to professors is 205. On the other hand, KHU outsources professors, assistant professors and adjunct professors in the number of 105.

The Computer Technologies Center supports IT use for all members of the University. A total of 700 computers are in use by staff, all Internet connected. KHU has eight computer laboratories (two of them are Sun-Ray 1 Thin-client based) at the Cibali campus, two laboratories at Bahcelievler campus, and four laboratories at the Selimpasa campus. All laboratories are equipped with multimedia technology. All students at KHU receive their own internet access accounts for computers located in the laboratories and the entire KHU information system. Departments also have their special labs like chemistry, software, control, physics etc.

KHU library supplements its traditional services with several technological innovations like dedicated computers and up to date databases. It serves 225 users in over 1000 squares of meters of space in Cibali campus. Its collection consists of nearly 50000 published materials, over 1000 DVDs, 500 video tapes, 30 000 electronic books, and 13 online databases including more than 12 000 electronic journals.

KHU is a partner of ERASMUS program and has exchange or dual degree programs with USA universities. The USA universities are Wayne State College, Southern New Hampshire University, Virginia State University, Purdue University, Fordham University, Montana State University and Ball State University.

University student clubs help students to develop themselves, encouraging them to fill their spare time efficiently, to extend their knowledge and creavity. There are 38 clubs to total 3694 students. Clubs organize activities such as panels, conferences, forums organized with the participation of important scholars, businessmen, experts. On the other hand, KHU with 17 sport branches participating in

ISSN 1313-2539

official university leagues takes it very seriously to get its students improve themselves in sports in addition to their education.

When KHU is compared other universities in Turkey, it is seen that the number of the students in KHAS is %0. 16 of the total number [1]. In the rank of universities according to the number of publications per faculty member in SCI+ SSCI+ AHCI journals in 2006, the whole universities in Turkey has a ratio of 0,52 and KHU is 64th with 0,23 ratio.

This study is a work of technology strategy development in KHU. For technology strategy development there are 2 approaches: resource based approach and positioning based approach. Resource based approach assumes that the organization has its own competences and should make its competitive strategies based on the competences. It suggests that organizations compete and create value on the basis of resources that are unique, rare, valuable, and not easily imitable or substitutable [3, 4, 5]. Competencies develop when such resources are combined to create specific organizational abilities [6]. On the other hand positioning based approach is about where in the competitive environment, firm wants to see itself. Porter's generic strategies and strategy development phases are included in the approach [7].

As a new established university, KHU has no competences and wants to make technology investment in order to gain some tangible and intangible competences like choosing the right technology, applying that technology into its training process and to develop new technologies [8]. In the study, positioning-based approach is used.

2. POSITIONING BASED APPROACH METHOD:

In order to develop a technology strategy, firm should evaluate its environment, both internal and external. After taking the whole picture of the market, it should choose a strategy that will fulfill the hole of the market place and firm internal structure; and a technology to perform the strategy. The chosen technology can be get or develop inside the technology or outside.

ISSN 1313-2539

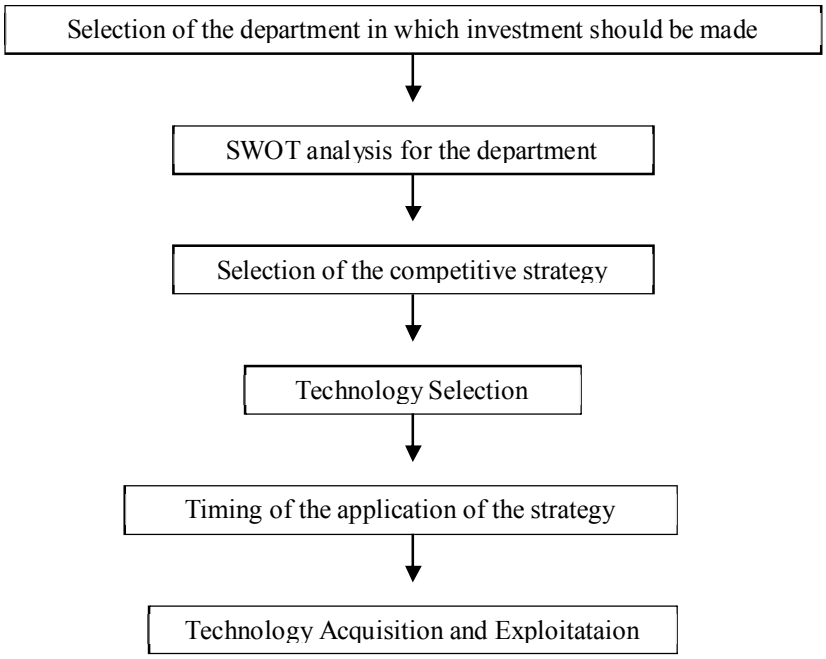

Figure1. Positioning based approach phases

2.1. Selection of Department

In order to determine to which department investment should be made Porter's 5 forces evaluation method is used [7].

2.1.1. Threats from Potential Entrants

To establish a university there are too many barriers in Turkey made by YOK the government agency. Capital requirement is so high. But established universities reserve only several rooms for their new faculty members because they've already provided necessary infrastructure such as laboratories. An enormous demand for university education has caused such an increase in the number of departments. Especially private universities start education in a specific department by recruiting several successful and experienced faculty members and the members necessary for other lectures are provided by recruiting part time faculty staff from state universities. They assure their need for research assistants again from the pool of doctorate and master students in state universities. Building departments in such a way is especially observed in departments such as industrial engineering and management which do not require too much investment on instrument and laboratory materials and are demanded highly by students.

2.1.2. Threat of Substitutes

Recently, many enterprises providing courses on management, industrial engineering and software, started in market. So the idea that people who do not get university education are not able to specialize and find a job is not valid anymore. People are able to specialize in certain areas in shorter time and with fewer prices by the help of courses provided by enterprises like Bilge Adam. Also increase in national income and easier access to abroad increase the potential number of foundation universities in our country. State universities are still a strong alternative because they provide cheaper education, more stable establishment and have a much longer history.

ISSN 1313-2539

2.1.3. Students Bargaining Power

The increased number of specialized courses and universities gives successful students the chance to bargain more strongly. All universities try establish legitimacy and to increase the quality of their education by offering scholarships to successful students. Especially private universities offer high scholarships. Another method to recruit successful students is to advertise connections with universities at abroad. Students, who have economical competency and have education in private universities without scholarship, are able to go abroad because the prices are almost same in foreign countries. The thought that US is advanced in management and industrial engineering, forces universities to make education in American style and make cooperation with US. Especially, 95% of math based students who participate in university presentations prefer industrial engineering.

2.1.4. Supplier Bargaining Power

Students, faculty members, business people and companies selling instruments can be considered as suppliers of universities. Demands of students are on in industrial engineering. Business people prefer more multi disciplinary education. The idea that engineering education is not enough by itself increases the demand for master and double major programs. Industrial engineering and management are most preferred areas in double major because they increase the chance to be a manager. System approach has caused an increase in demand for sonar industrial engineering. It's hard to find academics that are well educated and have a bright career. Especially in Turkey, the number is low. It's possible to observe transfers from state universities to private universities. The one who stay in state universities are satisfied with the student quality and infrastructure of state universities. Private universities generally recruit faculty members as part time staff. The cost of faculty members is high for universities because the number of qualified ones is low.

2.1.5. Competition among Universities

Industrial departments are built in all universities because of the demand from both students and industry. In these departments, business people can take courses in addition to students. Generally universities with established infrastructure, increase their rankings by advertisement and success stories. Not only students, but companies also prefer these universities as consultants. The amount of income from state depends on the student quality; this is another reason why scholarships are so high.

2.1.6. Evaluation Results

Continuous increase of demand to universities and industrial engineering to be a department to be preferred among students, low cost of infrastructure to build the department, demand by not only students but also companies for industrial engineering, increase of need for educated people in industrial engineering in industry, make industrial engineering one of the most preferred as a department to invest in. KHU must be one of the leading among its competitors and must educate its students adapted to recent advancements and requirements.

2.2. SWOT Analysis

In order to be a world class department in the university, industrial engineering department should make environment analysis to complete inefficiencies. The best method enabling the analysis of the environment and the organization itself is SWOT analysis. It is used for several reasons:

- ✓ Developing strategies
- ✓ Understanding relationship between internal and external issues
- ✓ Evaluate strategies

Determination strength and weakness includes determination of the main value added activities, determination of the requirements of customers, determination of the resources for each requirement, determination of competitors, evaluation of the rareness of each resource, and evaluation of the

ISSN 1313-2539

imitated possibility of each resource. Universities resources can be classified into three categories of physical capital, human resource and organizational resource:

- ✓ Capital is high.
- ✓ In faculty of engineering there are three departments; industrial, computer and electronic working together. So investment should be a kind of that all of them benefit from.
- ✓ There is no hierarchy in the faculty. Communication and decision taking speed are high.
- ✓ Campus is in the center of Istanbul.
- ✓ Lecturers who took education abroad are chosen.
- ✓ Because income level of students is high, they can get what is required easily.
- ✓ The faculty building is small, so small.
- ✓ Full time lecturers are only in number of 2; other required ones are supplied from other state universities.
- ✓ Nearly every university in Turkey has industrial engineering department. Competitors number of KHU Industrial Engineering department in Istanbul is 18 and only 6 of them are state universities [1]. On the other hand there are big and successful universities in other cities of Turkey like Ankara, Izmir.
- ✓ Competitors' industrial engineering departments have their specific hardware and software fixture.
- ✓ Students successful in the exam of OSS (student selection exam) do not prefer KHU.
- ✓ Because of its founder Kadir Has, KHU has an image of conservative and the image make KHU preferred by the families living in Anatolia.
- ✓ In the rank of industrial engineering departments according to the number of publications per department member in SCI+ SSCI+ AHCI journals in 2006, KHU is 2nd with 2,5 ratio.
- ✓ KHU industrial engineering department does not have a plant for manufacturing techniques like lathe, cutter etc.

In order to determine OT (opportunities and threats) PEST analysis is made which is abbreviation of political, economical, social and technical environment:

- ✓ Population and economic welfare increases and people give weight to their education much more than past.
- ✓ If the department wants to be a developer in the future, it should take care of current technologies forming basis for next generation technologies.
- ✓ Industry needs employees informed in ERP and statistics.
- ✓ Expectations of students from universities about practice education increase.
- ✓ Legislations are enacted about working conditions; so ergonomics should be understood not only by industrial engineers, but also every employee.
- ✓ Today to see and understand an industry with its suppliers and agencies is a necessity. So there should be simulation software packets for the integrity.
- ✓ Number of corporations other than universities giving education about CAD and ERP increases.
- ✓ YOK can impose restrictions and requirements for departments' education fixture.

ISSN 1313-2539

- ✓ Visual education makes students learn better.

2.3. Selection of Competitive Strategy

Porter has argued that a firm's strengths ultimately fall into one of two headings: cost advantage and differentiation [7]. By applying these strengths in either a broad or narrow scope, three generic strategies result: cost leadership, differentiation, and focus. Cost leadership generic strategy calls for being the low cost producer in an industry for a given level of quality. A differentiation strategy calls for the development of a product or service that offers unique attributes that are valued by customers and that customers perceive to be better than or different from the products of the competition. The focus strategy concentrates on a narrow segment and within that segment attempts to achieve either a cost advantage or differentiation. The premise is that the needs of the group can be better serviced by focusing entirely on it. A firm using a focus strategy often enjoys a high degree of customer loyalty, and this entrenched loyalty discourages other firms from competing directly.

The competitive strategy of KHU is both differentiation and cost leadership. By investing to the software and hardware which competitors have, cost leadership is aimed. By investing the software and hardware which competitors do not have and which are used in the industry, differentiation is aimed.

2.4. Technology Selection

All of the reasons listed above, university has decided to set up a laboratory special to industrial engineering department including ergonomics, CIM, ERP, optimization, simulation and statistics, and DVD about lectures.

ERP software is seen as the survivor of firms. Employee demand informed of ERP increases, so the number of corporations giving ERP education like Bilge Adam does. Research in the ERP Laboratory addresses both basic and applied research issues, including supply chain management, enterprise resource planning and optimization, production logistics, manufacturing systems modeling, business process reengineering, and manufacturing information systems. For business world ERP is in its key level on S curve of commitment and performance. In Istanbul because of the number of foundation universities is bigger than state ones, ERP implementation is higher than whole Turkey.

Computer-integrated manufacturing (CIM) is a method of manufacturing in which the entire production process is controlled by computer. Typically, it relies on closed-loop control processes, based on real-time input from sensors. It is also known as flexible design and manufacturing. The mission of the universities having CIM is to provide a facility where students and researchers can study manufacturing systems and develop tools for better decision-making throughout the product realization process, and to provide a place where students and researchers can discuss research, present research results, and demonstrate software.

To have an optimized decision, if the cost of wrong decision is high, the alternative solutions are simulated. Computer simulation has become a useful part of modeling many natural systems in physics, chemistry and biology, and human systems in economics and social science as well as in engineering to gain insight into the operation of those systems. Key issues in simulation include acquisition of valid source information about the referent, selection of key characteristics and behaviors, the use of simplifying approximations and assumptions within the simulation, and fidelity and validity of the simulation outcomes; in other words statistics knowledge. Nearly all of the universities are aware of the importance of simulation and optimization.

Ergonomics definition adopted by the International Ergonomics Association is the application of scientific information concerning objects, systems and environment for human use. Ergonomics is commonly thought of as how companies design tasks and work areas to maximize the efficiency and quality of their employees' work. Using special ergonomics software is new to both universities and business world.

ISSN 1313-2539

Radio-frequency identification (RFID) is an automatic identification method, relying on storing and remotely retrieving data using devices called RFID tags or transponders. A significant thrust in RFID use is in enterprise supply chain management, improving the efficiency of inventory tracking and management. However because it is a new technology, in business world its commitment and usage performance is low.

2.5. Timing of Application of the Strategy

KHU should apply its strategy about industrial engineering laboratory as soon as possible by thinking of learning curve effect and the impact of the laboratory to other engineering department education curriculum.

2.6. Technology Acquisition

Technology acquisition phases are scanning of technology and selection of technology transfer method.

2.6.1. Technology Scanning

Technology scanning areas are current& new technologies, competitors, common technologies and potential applications. Information can be found from two basic sources: "open to public" channels and "organizational" channels. Open to public channels are general channels like internet, newspaper and industrial channels like scientific publications, books, databases etc. Especially by using internet it is possible to reach every university's industrial engineering departments in the world. Organizational channels are internal reports. Firstly, competitors in Istanbul and Turkey are analyzed and their laboratory specifications are listed in Appendix A. There are 44 universities having industrial engineering department and 7 universities are on their establishment phase. 19 universities having the department locate in Istanbul and 63% of them are foundation universities. The second data resource is business world in order to understand which software is used and which can be used.

21 % of universities in Istanbul and only 23% of universities in Turkey have ERP laboratory: 40% SAP, % 40 IAS and %20 Oracle. But the problem is not nor can foundation or state use ERP efficiently. SAP is the most favorite ERP software in the business world and universities in Turkey. Although it has IAS/ CANIAS ERP package, KHU decided on SAP in order to reposition.

But because of its huge cost most of the universities do not have a manufacturing laboratory. In Turkey some of the universities like Istanbul Technical University have their own machine tool plant; and give their student a summer internship program. Some of the universities have CNC machines to be used in their manufacturing courses. But only 31% of universities in Istanbul and 39% of universities in Turkey have manufacturing laboratory. %83 of the universities in Istanbul has special CIM sets offering alternatives that software and hardware can be bought separately, made by COSIMIR or Intelitekt. At first hand, KHU decided to buy only software because of financial issues.

89% of universities in Istanbul and 82% of universities in Turkey have simulation and optimization laboratory. KHU has decided to buy some of the software that it does not have.

Only 43% of universities has ergonomics laboratory and 21% has software. But KHU not nor has hardware or software, and firstly it decided to buy some hardware that can be used in work study.

Universities have just realized RFID's opportunities and the necessity education of it. RFID is seen as an electronic engineering issue in Turkey and only 5% of universities industrial engineering department have it. Because KHU is in short supply of lecturer number and financial, it decided not to have RFID laboratory.

The technologies chosen for KHU laboratory is listed in Appendix B.

ISSN 1313-2539

2.6.2. Selection of Technology Transfer Method

As a new founded university it is impossible for KHAS to improve any of the selected technologies internally, so it has to transfer them. The investment's economic and physical nature [9] and, familiarity to the technology and market determine the transfer method. Current tools, human resource, capital resource and management support are some of the factors. In the majority of cases, technology is transferred not through formal search, but through some prior relationships among individuals [10].

From the list of technology transfer methods including joint venture, venture capital, internal venture, training agreement, licensing, company acquisition, research consortia, innovation network, external R&D; 3 of them are suitable for KHU:

- ✓ Licensing and Training Agreement
- ✓ Joint venture

A software license agreement is a memorandum of contract between a producer and a user of computer software which grants the user a software license. Most often, a software license agreement indicates the terms under which an end-user may utilize the licensed software, in which case the agreement is called an end-user license agreement. But licensing is not a whole solution because of short supply of is human resource. So KHU should make training agreement with the firms that software is licensed and with experienced teachers from other universities. The reason why teachers' selection is called as technology transfer is because technology transfer includes information transfer too.

The other method is joint venture. A joint venture is an entity formed between two or more parties to undertake economic activity together. The parties agree to create a new entity by both contributing equity, and they then share in the revenues, expenses, and control of the enterprise. New founded universities try to establish their infrastructure with a high capital cost, and generally they have to wait for years in order to implement their plans. On the other hand none of the universities use their infrastructure in 100% capacity. In order to use laboratory facility effectively and efficiently, KHU can make a joint venture with other universities not having laboratory. But this choice brings some problems along with itself like where to built laboratory, how to chose the university, how to make the laboratory in use of students, etc.

3. SUCCESS CRITERIA

Technology transfer should give know-how and know-why. It involves cooperation and communication between actors [10]. So the differences of situation, organization, society and culture should be eliminated [11]. To win the sufficiency in technology, technological, physical try and human resource is needed [12]. Characteristics of technology, transfer level and extent, modification, management experience, resource level and time management are other factors affecting the success of the transfer [13].

The first criterion for KHU's success depends on is human resource sufficiency. There should be 2 groups of people. First group is lecturers. The course curriculum should incline towards usage of the laboratory. There should be course projects and homework that make students really learn how to use software. The second group should be concentrated to use the software in university multidisciplinary and university- industry joint projects. The group should include students, research assistants and lecturers. The other problem is physical laboratory situation. As mentioned before in SWOT analysis, KHU building is small and it will be a problem for laboratory to have sufficient area.

ISSN 1313-2539

4. CONCLUSION

Technology transfer is a managed process of conveying a technology from a point of origin to its potential users. For a sustainable development, the universities should transfer the available technology until they can be enough sufficient to develop it internally. KHU a new established private university developed a technology strategy via positioning based approach. It decided to have an industrial engineering laboratory including CIM, ergonomics, ERP, simulation and optimization laboratories. To be successful in technology transfer process, the transfer method should be selected according to characteristics of technology, transfer level and extent, modification, management experience and resource level. There are 3 methods can be selected: licensing, training agreement and joint venture. But for the university the biggest barrier for its success is human resource and physical area insufficiency an. It can surmount difficulties by support of management.

REFERENCES

[1] www.yok.gov.tr

[2] www.khas.edu.tr

[3] Barney, J., 1991, "The resource-based model of the firm: origins, implications, and prospects", Journal of Management, Vol. 17, Iss. 1, 97–117.

[4] Conner, K.R., 1991, "A historical comparison of resource-based theory and five schools of thought within industrial organization economics: do we have a new theory of the firm?" Journal of Management, Vol. 17, Iss. 1, 121–154.

[5] Medcof, J., 2000, "The Resource-Based View and Transitional Technology Strategy", The Journal of High Technology Management Research, Vol. 11, 59-74.

[6] Teece, D.J., Pisano, G. & Shuen, A., 1997, "Dynamic capabilities and strategic management", Strategic Management Journal, Vol. 18, Iss. 7, 509–533.

[7] Porter, Michael E., Competitive Strategy: Techniques for Analyzing Industries and Competitors, 1980, Simon& Schuster Inc.

[8] Quazi, H. & Bartels, F., 1998, "Application of TQM Principles in the International Technology Transfer Process of Industrial Production Plants: A Conceptual Framework", British Journal of Management, Vol. 9, 289-300.

[9] Douglas, P. & Ziberman, D., 1993, "University technology transfers: Impacts on local and US economies", Complemantary Policy Issues, Vol. 11, Iss. 2; pg. 87, 13 pgs.

[10] Balthasar, A., Battig, C., Theirstein A. & Wilhelm, B., 2000, "Developers: key actors of the innovation process. Types of developers and their contacts to institutions involved in research and development, continuing education and training, and the transfer of the technology", Technovation, Vol. 20, 523-538

[11] Boulter, L. & Bendell, T., 2002, "Managing the Technology Transfer Process", IEEE, 643-650.

[12] McAdam, R., Koegh, W., Galbraith, B, & Laurie, D., 2005, "Defining and improving technology transfer business and management process in the university innovation centers", Technovation, Vol: 25, 1418-1429

[13] Levine, L., "Transactions Diffusion, Transfer and Implementation of Information Technologies", Proceedings of the IFIP TC8 Working Conference on Diffusion, Pittsburgh, PA, USA, 11–13 October, 1993

ISSN 1313-2539

6. APPENDIX A

University Name	Manufacturing facility	Simulation& Optimization	Ergonomics	ERP	RFID	Lecturer Number
Anadolu		●	●	SAP		20
Balıkesir		●				5
Boğaziçi	●	●	●			17
Çukurova		●	●	Oracle		8
Dokuz Eylül				IAS		13
Dumlupınar		●	●			4
Erciyes	●	●	●			
Eskişehir Osmangazi		●	●			12
Galatasaray	●	●				
Gazi	●	●	●			18
Gaziantep	●	●	●			6
Hacettepe		●				6
İstanbul		●				3
İstanbul Teknik	●	●	●		●	21
Kırıkkale	●	●	●			4
Kocaeli		●	●	SAP		10
Marmara		●				15
Ondokuz Mayıs						
Orta Doğu Teknik	●	●	●			20
Pamukkale						3
Sakarya				IAS		20
Selçuk		●				10
Süleyman Demirel						2
Uludağ	●	●	●			8
Yıldız Teknik		●		SAP		11
Atılım	●	●	●			8
Bahçeşehir	●	●				3
Başkent	●	●				10

ISSN 1313-2539

Bilkent	●	●	●			22
Çankaya	●	●				9
Doğuş		●				10
Haliç		●				2
Fatih	●	●	●			11
Işık		●				5
İstanbul Kültür		●		IAS		8
İstanbul Ticaret		●				3
Kadir Has		●		IAS		3
Koç		●				7
Maltepe						4
Okan						1
Sabancı	●	●	●	Oracle		11
Tobb						7
Yaşar	●	●	●	SAP	●	
Hava Harp Okulu		●	●			9

ISSN 1313-2539

7. APPENDIX B

KHU laboratory specifications

CIM	Ergonomics	ERP
FESTO "Digital Factory in iCIM" COSIMIR Factory	Accustudy 3.3 Testo 506 manometer Oregon Scientific SL888 Chronometer Thermometer Photometer Extech 407113 CFM wind meter Bicycle Ergonomics Lifecycle	IAS CANIAS ERP SAP R/3

Simulation, Optimization & Statistics	DVD Material
ARENA	Basic Hole making
Catia V	Basics of Grinding
CPLEX	Computer Numerical Control
Crystal Ball 2000.5	Ergonomic Safety
Expert Choice	Five S Factory Makeover
Expert Fit Professional	Flexible Material Handling
GAMS 22.3	Flexible Small Lot Production for JIT
LGO	Fundamental Manufacturing Processes Sampler
Lindo/ Lingo	Geometric Tolerance Program Sample
Matlab VI A	Introduction to Lean Manufacturing
MPL	Kanban Systems
Premium Solver	Metal forming Simulation
Promodel	Milling & Machining Center Basics
Quality Companion 2 by Minitab	Six Sigma
SPSS	Supply Chain Management
MS Project 2003	Toast Kaizen
C ++	Turning and Lathe Basics
	Work Measurement

ISSN 1313-2539

Contents

ISSN 1313-2539

ISSN 1313-2539